Exploring the structure-function relationship of Biotin Protein Ligase from *Staphylococcus aureus*: Implications for selective inhibitor design

by

Tatiana Pereira Soares da Costa

M.Sc. (Honours)

A thesis submitted to the University of Adelaide, South Australia in fulfilment of the requirements for the degree of Doctor of Philosophy

**Discipline of Biochemistry
School of Molecular and Biomedical Sciences
University of Adelaide
South Australia**

December, 2012

Table of Contents

Abbreviations

*Aa*BPL	*Aquifex aeolicus* biotin protein ligase
ACC	Acetyl-CoA carboxylase
AMP	Adenosine monophosphate
Apo	Unliganded enzyme
ATP	Adenosine triphosphate
AUC	Analytical ultracentrifugation
BC	Biotin carboxylase
BCCP	Biotin carboxyl carrier protein
bp	Base pair
BPL	Biotin protein ligase
BSA	Bovine serum albumin
^{o}C	Degrees Celsius
CA-MRSA	Community acquired methicillin resistant *Staphylococcus aureus*
CD	Circular dichroism
CT	Carboxyl transferase
Da	Dalton
DMSO	Dimethyl sulfoxide
DNA	Deoxyribonucleic acid
DTT	Dithiotheitol
*Ec*BPL	*Escherichia coli* biotin protein ligase

EDTA	Ethylenediaminetetraacetic acid
FDA	Food and Drug Administration
HA-MRSA	Hospital acquired methicillin resistant *Staphylococcus aureus*
HCS	Holocarboxylase synthetase
Holo	Ligand bound enzyme
HPLC	High-performance liquid chromatography
*Hs*BPL	*Homo sapiens* BPL
HTS	High-throughput screening
IC_{50}	Inhibition concentration at 50% enzyme activity
k_{cat}	Catalytic constant
k_d	Off-rate
K_D	Dissociation constant
K_m	Michaelis-Menten constant
K_i	Inhibition constant
M_w	Molecular weight
min	Minute
M	Molar
MCD	Multiple carboxylase deficiency
MIC	Minimal inhibitory concentration
MRSA	Methicillin resistant *Staphylococcus aureus*
MSSA	Methicillin sensitive *Staphylococcus aureus*
*Mt*BPL	*Mycobacterium tuberculosis* biotin protein ligase

NMR	Nuclear magnetic resonance
PAGE	Polyacrylamide gel electrophoresis
PC	Pyruvate carboxylase
PCR	Polymerase chain reaction
PDB	Protein data bank
*Ph*BPL	*Pyrococcus horikoshii* biotin protein ligase
rpm	Revolutions per minute
RNA	Ribonucleic acid
RU	Resonance units
s	Seconds
*Sa*BPL	*Staphylococcus aureus* biotin protein ligase
*Sa*PC	*Staphylococcus aureus* pyruvate carboxylase
*Sc*BPL	*Saccharomyces cerevisiae* biotin protein ligase
SAR	Structure-activity relationship
SDS	Sodium dodecyl sulphate
SPR	Surface plasmon resonance
Tris	2-amino-2-hydroxymethylpropane-1,3-diol
WT	Wild-type

Abstract

There is a well-documented need to replenish the antibiotic pipeline with new products to combat the rise of drug resistant bacteria, such as the superbug methicillin resistant *Staphylococcus aureus* (MRSA). One strategy to combat drug resistance is to identify new chemical classes with novel mechanisms of action and that are not subject to existing resistance mechanisms. As most of the obvious bacterial drug targets with no equivalents in mammals have been well explored, targets with a closely related human homologue represent a new frontier in antibiotic discovery. However, to avoid potential toxicity to the host, these inhibitors must have extremely high selectivity for the bacterial target over the human equivalent. This thesis is focused upon exploiting the ubiquitous enzyme biotin protein ligase (BPL), which is involved in the essential cellular process of attaching biotin onto biotin-dependent enzymes. Due to the pivotal metabolic roles played by biotin-dependent enzymes in bacteria, BPL has been proposed as a promising new antibiotic target. Hence, BPL inhibitors with selectivity for the bacterial isozyme over the human equivalent promise a new class of antibiotic to combat MRSA.

The aim of this project was to provide proof of concept data demonstrating that BPL from a pathogen could be selectively targeted for inhibition over the human equivalent. Here I employed a combination of structure-guided drug design and fragment-based approaches to discover novel BPL inhibitors. The X-ray crystal structure of *S. aureus* BPL (*Sa*BPL) shows two adjacent binding sites for the ligands biotin and ATP, making it an ideal candidate for a fragment-based approach to drug discovery. Although the residues at the biotin-binding site are highly conserved, the nucleotide pocket shows a high degree of variability that can be exploited to create compounds selective towards BPLs from pathogens. The biotin 1,2,3 triazole analogues identified in this work yielded our most potent and selective inhibitor (K_i = 90 nM) with >1100-fold selectivity for the *Sa*BPL over the human homologue (Chapter 2). The molecular basis for the selectivity was identified using mutagenesis studies with a key arginine residue in the BPL active site necessary for selective binding. Importantly, the biotin triazole inhibitors showed *in vivo* cytotoxicity against *S. aureus*, but not cultured mammalian cells (Chapter 2).

In an attempt to identify new chemical scaffolds with improved ligand efficiency for chemical development, a series of analogues based on the natural ligand biotin were also

designed and tested for enzyme inhibition and antimicrobial activities against clinically relevant strains of *S. aureus* (Chapter 3). This approach resulted in highly potent compounds (K_i < 100 nM) with antibacterial activity against MRSA strains (MIC = 2 - 16 µg/mL). Whilst only moderate selectivity over the human enzyme (10 - 20 fold) was observed, the biotin analogues provided a suitable chemical scaffold with high ligand efficiency for further chemical development. One of the compounds identified was biotin acetylene, which forms a long lived complex with *Sa*BPL and is a precursor for *in situ* click reactions. This target-guided approach to drug discovery relies on the ability of the enzyme to choose its own inhibitors from a range of acetylene and azide building blocks to form specific triazole products. Since a class of biotin-triazole molecules had already been identified as selective inhibitors of *Sa*BPL, we reasoned that this enzyme would provide an ideal candidate for performing *in situ* click approach to inhibitor discovery. In this work, a protocol for the BPL-catalyzed *in situ* click reaction was optimized to select the optimum triazole-based inhibitor using biotin acetylene as an anchor molecule to recruit complimentary fragments that could bind in the peripheral ATP pocket (Chapter 4). The *in situ* reaction was shown to be improved by the use of a *Sa*BPL mutant that promoted diffusion of the triazole product from the active site following synthesis. This novel approach improved efficiency and ease of detection (Chapter 4).

Apart from drug discovery, this thesis also focuses on enzymatic characterization of *Sa*BPL and highlighting the key differences between *Sa*BPL and the human homologue. The structure of human BPL is yet to be reported, so structure-function studies were performed to elucidate new information about the bacterial and human enzymes. The oligomeric state of *Sa*BPL was investigated using analytical ultracentrifugation in its apo form and in the presence of ligands (Chapter 5). Unlike human BPL, *Sa*BPL was shown to dimerize in solution. A single amino acid in *Sa*BPL, Phe123, was identified to have a dual key role in dimer formation and inhibitor binding (Chapter 5).

One of the major roadblocks to obtaining crystals of the full-length human enzyme is the low yield of protein obtained from recombinant expression and purification. In this thesis, an alternative approach is described that could be used to increase our chances of obtaining structural data about the human BPL. I created a 'humanized' chimeric protein in which all seven residues in the nucleotide pocket of *Sa*BPL that are not conserved with the human BPL were mutated to their human equivalents. This 'humanized' protein exhibited similar

kinetic and inhibition properties to the human enzyme (Chapter 6). Crystal trials have commenced to help direct future drug development efforts. Further studies on the human BPL enzyme will also be described, including the dissection of the binding mechanism using surface plasmon resonance (Chapter 7). The N-terminal domain of this enzyme was shown to play a role in stabilizing the complex between the enzyme and the biotin domain substrate, providing the first molecular explanation for human BPL-deficient patients that do not respond to biotin therapy.

In summary, this work demonstrates for the first time that BPL from the clinically important pathogen *Staphylococcus aureus* can be selectively inhibited. A provisional patent has been filed for the biotin 1,2,3 triazole molecules I have identified. These discoveries will enable further development of a new class of antibiotics.

Thesis layout:

The thesis will be presented as a series of manuscripts either published, submitted or to be submitted for publication. Each manuscript will be a chapter with its own references. A general introduction and discussion will also be included to link together all the research conducted during candidature. A publishing agreement with all co-authors involved with the work is also included.

Declaration for thesis containing published work and/ or work prepared for publication

This work contains no material which has been accepted for the award of any other degree or diploma in any university or other tertiary institution to Tatiana Pereira Soares da Costa and, to the best of my knowledge and belief, contains no material previously published or written by another person, except where due reference has been made in the text.

I give consent to this copy of my thesis when deposited in the University Library, being made available for loan and photocopying, subject to the provisions of the Copyright Act 1968.

The author acknowledges that copyright of published works contained within this thesis (as listed on the next page) resides with the copyright holder(s) of those works.

I also give permission for the digital version of my thesis to be made available on the web, via the University's digital research repository, the Library catalogue and also through web search engines, unless permission has been granted by the University to restrict access for a period of time.

……………………………………………   …………………..
    Tatiana Pereira Soares da Costa   Date

I acknowledge the copyright of published works contained within this thesis including:

Chapter 2:

Tatiana P. Soares da Costa, William Tieu, Min Y. Yap, Nicole R. Pendini, Steven W. Polyak, Daniel S. Pederson, Renato Morona, John D. Turnidge, John C. Wallace, Matthew C. J. Wilce, Grant W. Booker, Andrew D. Abell (2012) Selective inhibition of biotin protein ligase from *Staphylococcus aureus*. *Journal of Biological Chemistry.* 287 (21), 17823-17832.

Chapter 3:

Tatiana P. Soares da Costa, William Tieu, Min. Y. Yap, Ondrej Zvarec, Jan M. Bell, John D. Turnidge, John C. Wallace, Matthew C. J. Wilce, Grant W. Booker, Andrew D. Abell, Steven W. Polyak (2012) Biotin analogues with antibacterial activity are potent inhibitors of biotin protein ligase. *ACS Medicinal Chemistry Letters.* 3 (6), 509-514.

Chapter 4:

Tatiana P. Soares da Costa, William Tieu, Min. Y. Yap, Kelly K. Keeling, Matthew C. J. Wilce, Grant W. Booker, Steven W. Polyak, Andrew D. Abell (2012) Optimizing *in situ* click chemistry: The screening and identification of biotin protein ligase inhibitors. To be re-submitted to *Angwandte Chemie International Edition* for publication.

Chapter 5:

Tatiana P. Soares da Costa, Min. Y. Yap, Matthew Perugini, John C. Wallace, Andrew D. Abell, Matthew C. J. Wilce, Steven W. Polyak, Grant W. Booker (2012) A novel link between protein homodimerization and inhibitor binding to biotin protein ligase from *Staphylococcus aureus*. Submitted to *Journal of Biological Chemistry*, tracking number JBC/2012/439091.

Chapter 6:

<u>Tatiana P. Soares da Costa</u>, John C. Wallace, Steven W. Polyak, Grant W. Booker (2012) 'Humanized' biotin protein ligase provides clues about inhibitor selectivity. To be submitted to *Biochemistry* for publication.

Chapter 7:

Lungisa Mayende, Rachel D. Swift, Lisa M. Bailey, **<u>Tatiana P. Soares da Costa</u>**, John C. Wallace, Grant W. Booker, Steven W. Polyak (2012) A novel molecular mechanism to explain biotin-unresponsive holocarboxylase synthetase deficiency. *Journal of Molecular Medicine.* 90, 81-88.

Authorization to publish each paper has been given and provided in print for each chapter containing copyright and co-authored work, including acknowledgement of contribution to the work from each author.

Communications and Presentations

<u>T. P. Soares da Costa</u>, W. Tieu, M. Y. Yap, M. C. Wilce, A. R. Abell, S. W. Polyak, G. W. Booker (2012) Selective inhibition of biotin protein ligase from the superbug *Staphylococcus aureus. 13th FAOBMB Congress, Bangkok, Thailand.* **Awarded** YSP-travel fellowship by Australian Society of Biochemistry and Molecular Biology (ASBMB) to cover registration and flights. Oral presentation.

<u>T. P. Soares da Costa</u>, W. Tieu, M. Y. Yap, M. C. Wilce, A. R. Abell, S. W. Polyak, G. W. Booker (2012) Selective inhibition of biotin protein ligase from the superbug *Staphylococcus aureus. Young Scientist Forum, Bangkok, Thailand.* **Awarded** YSP-travel fellowship by ASBMB to cover registration, flights and accommodation. **Winner** of the best oral and poster presentation prizes.

<u>T. P. Soares da Costa</u>, W. Tieu, M. Y. Yap, M. C. Wilce, J. C. Wallace, A. R. Abell, S. W. Polyak, G. W. Booker (2012) A new approach to an old problem: The development of antibiotics against the superbug Golden Staph. *AusBiotech-GSK Conference, Melbourne, Australia.* Oral Presentation.

<u>T. P. Soares da Costa</u>, W. Tieu, M. Y. Yap, M. C. Wilce, J. C. Wallace, A. R. Abell, S. W. Polyak, G. W. Booker (2012) *In situ* click chemistry: Biotin protein ligase inhibitors made to their own specifications. *ComBio Conference, Adelaide, Australia.* Oral Presentation. **Awarded** student registration bursary of $350 by ASBMB.

<u>T. P. Soares da Costa</u>, W. Tieu, M. Y. Yap, M. C. Wilce, J. C. Wallace, A. R. Abell, S. W. Polyak, G. W. Booker (2012) The development of novel antibiotics against the superbug Golden Staph. *AusBiotech-GSK Student Excellence Award.* Oral Presentation, Adelaide, Australia. **State winner**. **Awarded** registration bursary of $350, flights to Melbourne and accommodation to attend the 2012 Ausbiotech-GSK Conference.

<u>T. P. Soares da Costa</u>, W. Tieu, M. Y. Yap, M. C. Wilce, J. C. Wallace, A. R. Abell, S. W. Polyak, G. W. Booker (2012) Selective inhibition of biotin protein ligase from the superbug *Staphylococcus aureus. Australian Society for Medical Research SA Division Scientific Meeting, Adelaide, Australia.* Oral Presentation.

T. P. Soares da Costa, W. Tieu, M. Y. Yap, M. C. Wilce, J. C. Wallace, A. R. Abell, S. W. Polyak, G. W. Booker (2012) Finding the Achilles' heel in the superbug MRSA Golden Staph. *School of Advanced Science – Computational Biology: Agrochemical and Drug Design Meeting, Sao Paulo, Brazil.* Poster Presentation. **Awarded** $4000 for registration, accommodation and flights to Brazil.

T. P. Soares da Costa, W. Tieu, M. Y. Yap, M. C. Wilce, J. C. Wallace, A. R. Abell, S. W. Polyak, G. W. Booker (2012) Finding the Achilles' heel in the superbug MRSA Golden Staph. *37th Lorne Proteins Conference, Lorne, Australia*. Poster Presentation. **Awarded** student registration of $295.

T. P. Soares da Costa, M. Y. Yap, W. Tieu, M. C. Wilce, S. W. Polyak , A. R. Abell, G. W. Booker (2011) Exploring the structure-function relationship of biotin protein ligase from *Staphylococcus aureus* to help the development of novel, highly potent and selective inhibitors. *ComBio Conference, Cairns, Australia.* Oral Presentation. **Awarded** student registration bursary of $330 by ASBMB.

T. P. Soares da Costa, M. Y. Yap, W. Tieu, M. C. Wilce, J. C. Wallace, A. R. Abell, S. W. Polyak, G. W. Booker (2011) First evidence of highly potent and selective inhibitors of MRSA biotin protein ligase. *Australian Society for Medical Research Meeting SA Division Scientific Meeting, Adelaide, Australia*. Oral Presentation.

T. P. Soares da Costa, M. Y. Yap, W. Tieu, M. C. Wilce, J. C. Wallace, A. R. Abell, S. W. Polyak, G. W. Booker (2011) Identification of novel and highly selective inhibitors of MRSA biotin protein ligase using a fragment-based approach to drug discovery. *Adelaide Protein Group Meeting, Adelaide, Australia.* Oral Presentation. **Awarded** $750 for best oral presentation.

T. P. Soares da Costa, W. Tieu, M. Y. Yap, M. C. Wilce, J. C. Wallace, A. R. Abell, S. W. Polyak, G. W. Booker (2010) Small molecule inhibitors for biotin protein ligase: Towards target specificity. *School of Molecular and Biomedical Sciences Research Symposia, Adelaide, Australia*. Poster Presentation.

T. P. Soares da Costa, W. Tieu, M. Y. Yap, R. Morona, M. C. Wilce, J. C. Wallace, A. R. Abell, S. W. Polyak, G. W. Booker (2010) Identifying novel antimicrobials using a fragment-based approach to drug discovery. *OzBio Conference, Melbourne, Australia.* Oral Presentation.

T. P. Soares da Costa (2010). Discovering new antibiotics against Golden Staph. *Three Minute Thesis Competition, Adelaide, Australia.* Oral Presentation. University of Adelaide **Finalist**. **Awarded** $100.

T. P. Soares da Costa, W. Tieu, M. Y. Yap, M. C. Wilce, J. C. Wallace, A. R. Abell, S. W. Polyak, G. W. Booker (2010). New drugs for bad bugs: Identifying novel and selective antimicrobials using a structure-based approach to drug discovery. *Australian Society for Medical Research SA Division Scientific Meeting, Adelaide, Australia.* Oral Presentation.

T. P. Soares da Costa, W. Tieu, M. Y. Yap, M. C. Wilce, J. C. Wallace, A. R. Abell, S. W. Polyak, G. W. Booker (2010) First evidence of differential inhibition between biotin protein ligase from *Staphylococcus aureus* and the human homologue. *Adelaide Protein Group Meeting, Adelaide. Australia.* Oral Presentation. **Finalist**.

T. P. Soares da Costa, W. Tieu, M. Y. Yap, M. C. Wilce, J. C. Wallace, A. R. Abell, S. W. Polyak, G. W. Booker (2010) Small molecule inhibitors for biotin protein ligase: Towards target specificity. *35th Lorne Proteins Conference, Lorne, Australia.* Poster Presentation. **Awarded** student travel grant of $100.

T. P. Soares da Costa, R. Dobson, S. Devenish, G. Jameson, J. Gerrard (2008) How essential is the 'essential' active site residue Lys161 in dihydrodipicolinate synthase? *33rd Lorne Proteins Conference, Lorne, Australia.* Poster Presentation. **Awarded** student travel grant of $400.

T. P. Soares da Costa, Dobson, S. Devenish, G. Jameson, J. Gerrard (2008) Probing the mechanism of dihydrodipicolinate synthase. *New Zealand Society of Molecular Biology and Biochemistry, Christchurch, New Zealand.* Oral Presentation.

Acknowledgements

Firstly, I would like to express my sincere gratitude to my supervisors Assoc. Prof. Grant Booker, Dr. Steven Polyak and Prof. Andrew Abell for the continuous support, patience, motivation, enthusiasm and immense knowledge.

Grant, thank you for giving me the opportunity to pursue my PhD studies in your lab and for helping me grow as a scientist. Steven, I'm so grateful that you invited me to visit the lab when I was still in New Zealand. Your extensive knowledge about BPL and all biotin-related things never cease to amaze me! You were always there for me with a big smile on your face and you were always happy to bounce ideas off. Thanks for introducing me to sparkling red wine and for providing so much entertainment every year at the School dinner☺. Andrew, thanks for helping me with all chemistry-related things and for always being so encouraging.

To Prof. John Wallace, you are an inspiration. Thanks for sharing your wisdom with me. You have always been so supportive. Thank you for all your helpful comments and for reading manuscripts.

A big thanks also goes to the present and past members of the lab. Lungisa, thanks for always being there for me, I'm so glad I got to share this experience with you! Big kudos to Ashleigh (the most photographic person I know☺), Martin (who owes me a year's supply of Nutella☺), Mike (a.k.a. the mini-prep king), Tony (who introduced me to Korean food), Angie (the award-winning baking queen), Kate (the cool mum☺), Karen, Al, Sushil, Connie and Ethan. Thanks also to the members of the BPL team in the Department of Chemistry for synthesizing compounds for me in record time, namely Dr. William Tieu, Dr. Ondrej Zvarec and Kelly Keeling.

Thanks to our collaborators Prof. Mathew Wilce and Min Yap at Monash University for providing us with beautiful crystal structures. I also would like to thank Assoc. Prof. Matthew Perugini for allowing me to come to his lab and learn about the wonderful world of analytical ultracentrifugation. Thanks also for the Perugini crew for making me feel so welcome during my stay in Melbourne.

Chapter 1:

Introduction

1.1 Need for new antibiotics

Antibiotic resistance is a major threat to public health worldwide. Most antibiotics available today target four major cellular processes: bacterial cell wall and membrane syntheses, protein synthesis, nucleic acid replication and folate-coenzyme biosynthesis (1). The majority of new drugs arising are next generation analogues of existing compounds that exert their effect on the same target. Thus one strategy to combat drug resistance is to discover new chemical classes that are not subject to current resistance mechanisms (2). Despite a desperate need for new antibiotics, there has been a decline in the rate of submission and introduction of new drug candidates, which provokes questions about the effectiveness of existing approaches to drug discovery. Most early stage antibiotic research and development is now carried out by academic and government laboratories (3). Many large pharmaceutical companies and biotechnology companies have terminated their early antibiotic research due to low return on investment, strict drug regulatory requirements and technical difficulty of developing a novel drug (3). Despite this, there are still commercial opportunities and unmet medical needs that must be addressed.

Staphylococcus aureus is a clinically important Gram-positive pathogen. It commonly colonizes the anterior nares, respiratory system and urinary tract of the host (4). *S. aureus* is implicated in a wide range of diseases including skin infections, pneumonia, meningitis and bacteraemia (5). The bacteria can also enter open wounds and is, thus, capable of causing life-threatening infections in humans (6). Bacteraemia caused by *S. aureus* has become increasingly difficult to treat due to resistance to existing antibiotics. The first case of antibiotic resistant *S. aureus* appeared in the 1940s after mass production of penicillin. Methicillin resistant *S. aureus* (MRSA) is a strain that has developed antibiotic resistance to most penicillin-based antibiotics, including methicillin (7). Two major variants of MRSA have been described: hospital acquired MRSA (HA-MRSA) and community acquired MRSA (CA-MRSA) (8,9). In Australia, MRSA bacteraemia accounts for 34% of hospital-onset and 18% of community-onset *S. aureus* infections (10). Currently, many available β-lactam antibiotics are ineffective against both HA-MRSA and CA-MRSA strains. Vancomycin has been seen as the last resort antibiotic for treating MRSA infections but reports of resistance emerged at a rapid rate (11). As a result, there has been an increase in the mortality rate by MRSA infections worldwide (12). In 2001, linezolid, which targets protein synthesis, became the first new class of antibiotic to receive FDA

approval in over 30 years. This was followed by daptomycin in 2003 and tygacycline in 2005. It is well recognized that more effort is required to stay ahead of drug resistance (2,13-15). One strategy to combat drug resistance in *S. aureus* is to develop new chemical entities against novel targets that are known to be essential for cell survival and which have no pre-existing target-based resistance. In this thesis, my focus is on the characterization of the enzyme biotin protein ligase (BPL) from *S. aureus* as a novel drug target. Here I have reviewed the literature on this enzyme and highlighted its critical role in bacteria. The techniques used to discover small molecule inhibitors of *S. aureus* BPL will also be discussed later in this chapter.

1.2   Biotin

Biotin, also known as vitamin H or B_7, was first discovered by Kogl and Tonis in 1934, while studying the growth requirements of yeast in synthetic media (16) and its structure was first determined in 1942 (17). Biotin is an important micronutrient in all living organisms but its synthesis is restricted to bacteria, plants and some fungi. Mammals must obtain biotin from either their diet or from intestinal bacteria, which can produce biotin *de novo* (18). The most well characterized and understood function of biotin is to act as a co-factor for biotin-dependent enzymes, which will be discussed in the next section.

1.3   Biotin-dependent enzymes and the biotin domain

All biotin-dependent enzymes require biotin as a co-factor to allow the transfer of carbon dioxide between organic acids in order to form cellular metabolites (19). The biotin-dependent enzymes are involved in carboxylase, decarboxylase and transcarboxylase reactions for the metabolism of carbohydrates, lipids and some amino acids, as well as having a role in ion transport (20,21). As these enzymes are degraded, biotin can be recycled by the hydrolysis of the degraded peptide fragments. In mammals, this occurs through the action of biotinidase. However, no bacterial equivalent has been reported (22). The focus of the rest of this section is on the biotin carboxylases, which are relevant to this study, and found in all kingdoms of life. They consist of three functionally distinct subunits: biotin domain, biotin carboxylase (BC) and carboxyl transferase (CT). BC catalyses the Mg^{2+} and ATP-dependent carboxylation of the biotin domain to produce the CO_2^- : biotin domain complex. The biotin domain then oscillates towards the second

partial reaction. CT catalyses the subsequent transfer of the carboxyl groups from the CO_2^- : biotin domain complex to the acceptor substrate, e.g. acetyl-CoA to form malonyl-CoA or pyruvate to form oxaloacetate (23).

Of particular significance to this thesis is the biotin domain. Sequence comparison of biotin domains between different species shows that these domains are highly conserved in amino acid composition and structure across species. A number of biotin domain structures have been solved with the first one being that of *E. coli* biotin carboxyl carrier protein (BCCP)-87 using both X-ray crystallography (24) and NMR (25). The structure contains two sets of four anti-parallel β-strands forming a β-sandwich (Figure 1.1). In recent years, more structures have become available (reviewed in (26)).

In all biotin domain structures, the biotin prosthetic group is found covalently attached to a lysine residue in a highly conserved Ala-Met-Lys-Met motif, which is located at the surface of a hairpin turn in one of the two β-sheets which make up the domain (27). The lysine is commonly found 35 residues from the C-terminus of the carboxylases (28). The correct positioning of the lysine residue is absolutely critical as moving it by just one position to the N- or C-terminal side results in the abolishment of biotinylation *in vitro* and *in vivo* (27). Several mutagenesis studies show that the flanking methionine residues are not essential for biotinylation (27,29-31), although they do affect carboxylation and carboxyl transfer reactions (32,33). The minimum requirement for BPL recognition of the biotin domains are the 35-40 residues on either side of the biotin attachment site (28,30). Further truncation or mutation of the residues that contribute to the hydrophobic core of the fold abolishes biotinylation (32-34).

(A)

(B)

Figure 1.1: *Crystal structure of apo (**A**) and holo (**B**) E. coli BCCP-87 in ribbon presentation. Target lysine 122 residing within the exposed hairpin loop of β-strands 4 and 5 is shown in the absence (**A**) and presence (**B**) of the biotin moiety, presented in ball and stick. Figure generated in USF Chimera using PDB 1DBO (24).*

1.4   Protein biotinylation is essential in bacteria

BPL is the enzyme responsible for the post-translational attachment of biotin onto the biotin domain of biotin-dependent enzymes (34). Due to its pivotal role in protein biotinylation in bacteria, BPL has been identified as a potential new antibacterial drug target, which has no pre-existing target-based resistance. Only one gene encoding biotin protein ligase is present in the genome of most bacteria, yeast and mammals, thus reducing the likelihood of resistance through redundancy. *Arabidopsis thaliana* and other plant species are a notable exception as they contain two *bpl* genes, one encoding a cytoplasmic enzyme and the other a chloroplast targeted enzyme (35). In addition, the low abundance of BPL in the cell suggests that chemical intervention can be effective in inhibiting this target.

All living organisms express at least one biotin-dependent enzyme. *S. aureus* expresses two, namely acetyl-CoA carboxylase (ACC) and pyruvate carboxylase (PC) (36). ACC catalyzes the first committed step in the fatty acid biosynthetic pathway, the carboxylation of acetyl-CoA into malonyl-CoA, that is essential for cell membrane maintenance and biogenesis (37). PC catalyzes the conversion of pyruvate to oxaloacetate, allowing the replenishment of the Krebs cycle, from which intermediates are withdrawn and used in a number of pathways such as lysine biosynthesis (38). Therefore, the debilitation of BPL in *S. aureus* interferes with the activity of its two biotin-dependent enzymes, ACC and PC.

The enzymes that belong to the fatty acid biosynthetic pathway provide an excellent source of new targets due to the essential nature of fatty acids in membrane structure (3,39-41). There is little doubt that fatty acid biosynthesis is essential in Gram-negative bacteria as there is no mechanism to allow fatty acid supplementation to form the lipid A core structure of outer membrane polysaccharides (42). Importantly, fatty acid synthesis has been shown to be essential in *S. aureus* because exogenous sources of fatty acids are not sufficient for bacterial survival (43). Recent studies have helped elucidate the importance of this pathway in Gram-positive bacteria and will be discussed in Chapter 8. Further validation comes from chemotherapeutic intervention of key enzymes in this pathway including the anti-tuberculosis drug isoniazid and antiseptic triclosan (44,45). In addition, ACC from grasses has been targeted for over 20 years through the use of herbicides aryloxophenoxypropanoic acid and cyclohexanedione (37). The clinical significance of these compounds has prompted the development of more inhibitors through

structure-based drug design that target drug resistant *S. aureus* infections (46,47). A recent study focused on biotin carboxylases as targets by using fragment-based drug discovery and virtual screening to develop inhibitors of the biotin carboxylase component that exhibit antibacterial activity (48). Natural products have also been identified that target ACC, the condensing enzymes or enoyl-acyl carrier protein reductase, also involved in fatty acid synthesis. A promising natural product is platensimycin, a secondary metabolite isolated from *Streptomyces platensis* with *in vivo* efficacy in murine *S. aureus* infection models and no reported toxicity (49). Two common problems associated with natural products are their poor pharmacokinetics and poor oral bioavailability. These problems can be overcome by identifying new chemical scaffolds as starting points for the development of fatty acid inhibitors.

In addition to ACC, *S. aureus* BPL also ligates biotin to PC, which plays an anaplerotic role in the Krebs cycle. Intermediates of this cycle are involved in biosynthesis including lysine synthesis. Supplies of lysine are required for bacterial peptidoglycan cell wall synthesis in both Gram-positive and Gram-negative bacteria (50). Lysine is also involved in modifying membrane lipids as a defense mechanism against the innate immune response and cationic glycopeptide antibiotics such as daptomycin (51). Furthermore, inhibition of lysine biosynthesis itself has been proposed as a novel antibacterial target (50).

Both ACC and BPL were previously identified by GlaxoSmith Kline as essential genes in *S. aureus* that could be potential targets for antibiotics (3). High-throughput screens were carried out against random compound libraries containing 260,000 to 530,000 compounds but no hits were identified. It was concluded that the quality of their small molecule libraries was not as high as required for this approach. Also the library contained poor molecular diversity (52). In section 1.11, high-throughput screening is discussed in detail and it will become clear why this was unlikely to succeed, therefore, new approaches to antibiotic discovery are required. The primary aim of this thesis is to understand the structure, function and structure-activity relationships (SARs) of *S. aureus* BPL (*Sa*BPL) with candidate inhibitors to facilitate the drug discovery process and potentially lead to the development of a new class of antibiotics against *S. aureus*.

1.5   BPL-catalyzed biotinylation reaction

Protein biotinylation is a post-translational modification of exquisite specificity, with only the biotin domains of the biotin-dependent enzymes serving as substrates *in vivo*. The BPL-catalyzed reaction proceeds through a conserved, two-step ordered reaction mechanism (Figure 1.2). In the first partial reaction, the reactive intermediate, biotinyl-5´-AMP, is produced from ATP and biotin. Subsequently, biotin is covalently attached to the ε-amino group of a specific lysine residue present in the biotin domain, resulting in the release of adenosine monophosphate (AMP) (31). The reaction mechanism is related to that of aminoacyl-tRNA synthetase (53) and lipoyl ligases (54), where an adenylated intermediate is formed, suggesting a common ancestry. Furthermore, BPL is interchangeable between organisms suggesting that the BPL: biotin domain interaction is highly conserved (28,32,34,55), although BPLs exhibit higher affinity towards their natural biotin domain substrate (31,56).

(1)

Biotin   **Biotinyl-5´-AMP**

(2)

Apo domain   **Holo domain**
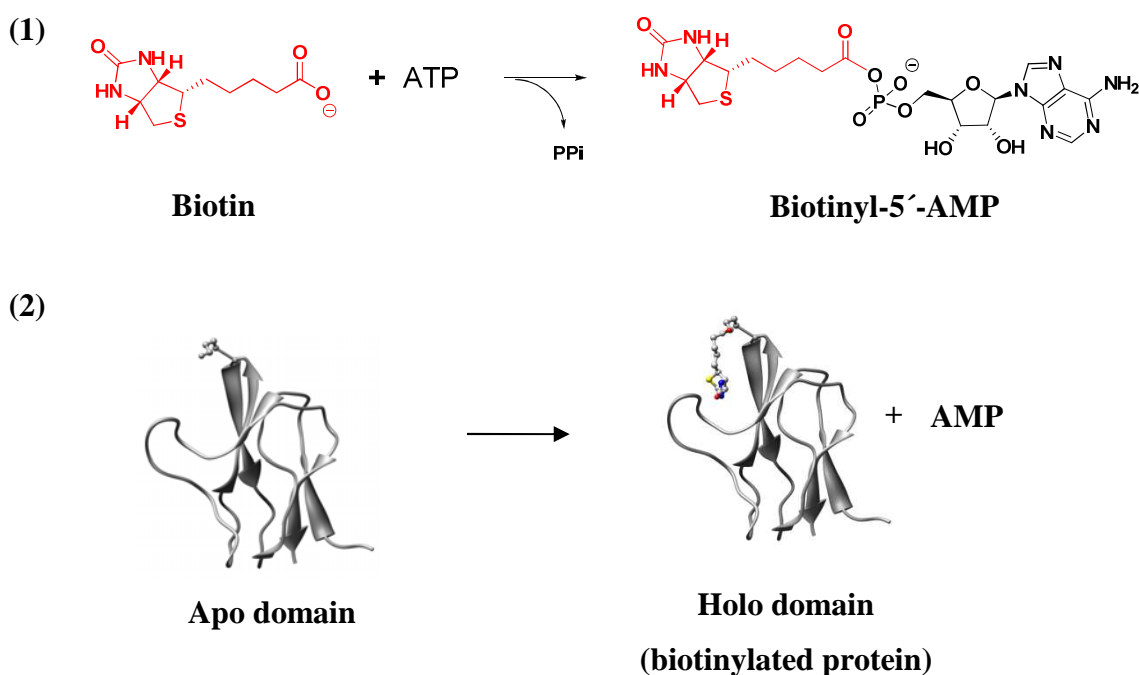   **(biotinylated protein)**

Figure 1.2:   *Two-step ordered BPL-catalyzed reaction.*

1.6   Classes of BPLs

BPLs can be divided into three structural classes (Figure 1.3) (26). All three classes share conserved C-terminal and catalytic domains that are central to the BPL enzymatic activity as represented by the blue and yellow bars respectively in Figure 1.3. Class I BPLs (e.g. *Pyrococcus horikoshii*, *Mycobacterium tuberculosis, Aquifex aeolicus*) consist of the C-terminal and catalytic domains only. Class II BPLs (e.g. *Escherichia coli*, *S. aureus*) contain an additional N-terminal helix-turn-helix domain required for DNA binding. This facilitates the BPL to function as a transcriptional repressor, which will be discussed in detail later in this section. Class III BPLs (e.g. *Homo sapiens* and *Saccharomyces cerevisiae*) have a large N-terminal extension that bears no resemblance to the DNA binding domain of Class II BPLs (26). Absence of a helix-turn-helix DNA binding domain in both Class I and III BPLs implies they do not have a transcriptional repressor function.
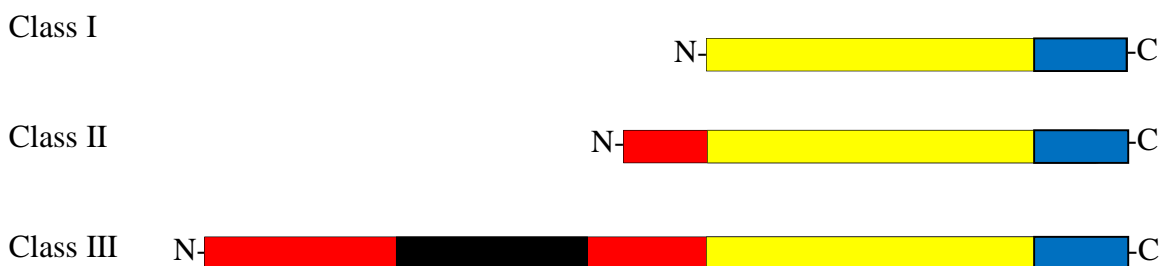
Class I

Class II

Class III

Figure 1.3:   *Schematic diagram of three classes of biotin protein ligase. Blue depicts the C-terminal domain. Yellow depicts the highly conserved catalytic domain. Red depicts the N-terminal domain. Black depicts the N-terminal cap region only found in Class III BPLs.*

A limited number of crystal structures of BPLs have been solved. From Class I, the structures from *P. horikoshii* (57), *M. tuberculosis* (58) and *A. aeolicus* (59) have been published. The structures of Class II BPLs from the Gram-positive bacterium *S. aureus* (60) and the Gram-negative bacterium *E. coli* (61-63) have also been deposited in the PDB. However, the structure of a Class III BPL has not yet been reported. One of the major roadblocks for obtaining crystals of the full-length human enzyme is the low yields from recombinant expression and purification. This enzyme also shares low sequence identity with the bacterial BPLs and diffraction quality crystals of this enzyme have not been reported. Despite a lack in structural information, a number of functional studies have been

carried out to try to elucidate how this enzyme works. This will be the focus of section 1.9 and Chapter 7.

The structures of the BPLs crystallized thus far show that the catalytic domain is highly conserved. This includes the presence of a biotin-binding loop and an adenylate-binding loop. However, these loops are absent in the apo crystal structures due to the high mobility of these regions, which effectively opens up the ligand binding sites to accept biotin and ATP moieties. Upon biotin and biotinyl-5´-AMP binding, a 'disorder-to order' transition of the biotin and adenylate-binding loops occur respectively. The ordering of the biotin-binding loop is characterized by the highly conserved GRGRX motif, where X can be any residue (64). Biotin is stabilized by hydrogen bond interactions with the hydrophilic interior of the biotin-binding pocket, whereas the biotin tail is stabilized via interactions with hydrophobic residues. The ATP-binding pocket lies adjacent to the biotin-binding pocket.

The oligomerization states of BPLs differ considerably regardless of their class. *M. tuberculosis* BPL (*Mt*BPL) and *A. aeolicus* BPL (*Aa*BPL) exist constitutively as monomers in apo, biotin and biotinyl-5´-AMP liganded forms (58,59). This implies that dimerization is not required for catalysis. This is in sharp contrast to *P. horikoshii* BPL (*Ph*BPL), also a class I BPL, which constitutively exists as a dimer regardless of its liganded state (65). Class II *E. coli BPL* (*Ec*BPL) is monomeric in solution, and forms a homodimer when biotin or biotinyl-5´-AMP is bound (63). The crystallized form of apo *Sa*BPL also suggests that this enzyme is a monomer, whereas the holo enzyme is a dimer (60). The oligomerization state in solution of *Sa*BPL in its apo and holo forms will be explored further in Chapter 5. Although *Ph*BPL and the Class II BPLs have the ability to dimerize, the interfaces for the protein: protein interaction are different. *Ph*BPL dimerizes via the N-terminal domain, while holo *Ec*BPL and *Sa*BPL dimerize via their catalytic domain (66). In addition, these enzymes dimerize for different purposes. The N-terminal domains of Class II BPLs allow them to act as transcriptional repressors. Homodimerization occurs in the presence of the co-repressor biotinyl-5´-AMP and the N-terminal domains bind to the operator sites of the biotin biosynthesis operon *bioO*, resulting in repression of biotin biosynthesis (67,68). Biotin has also been shown to induce dimerization (69). In the presence of a non-biotinylated biotin domain substrate, *Ec*BPL and *Sa*BPL behave as a biotin ligase. Thus Class II BPLs can serve as a cellular sensor of biotin demand and

supply. It also allows the cell to respond quickly to changes in intracellular biotin concentrations and switch between enzymatic catalysis and gene repression functions (70,71). However, as *Ph*BPL has no repressor function, the dimer formation is possibly required for thermostability in the hyperthermophilic organism (65). Both *H. sapiens* BPL (*Hs*BPL) and *S. cerevisiae* BPL (*Sc*BPL), which belong to Class III, have been shown to be monomeric (72,73).

Another key difference between BPLs is their substrate binding mechanisms. *Ec*BPL has an ordered reaction mechanism for substrate binding, with biotin binding first followed by ATP (74). The ordered reaction mechanism renders *Ec*BPL sensitive to changes in cellular biotin concentration, consistent with its function as a biotin sensor and transcriptional repressor. In contrast, Class I *Ph*BPL does not have an ordered binding mechanism, showing no co-operativity in binding between the substrates (66). Although *Aa*BPL can also bind biotin and ATP in a random order, the binding of one substrate is greatly enhanced by the presence of the other substrate (59). However, a study done of the Class I *Mt*BPL has shown that this enzyme must form a complex with biotin before ATP can bind (58). These differences may be explained by X-ray crystallography. The biotin-binding loop contains a highly conserved tryptophan residue. This is required for π-π stacking interaction with the purine ring system on ATP. The biotin-binding loop is pre-ordered in the apo structures of *Ph*BPL and *Aa*BPL, providing an explanation for their non-ordered binding mechanisms. In *Ec*BPL and *Mt*BPL, biotin-induced conformational changes are required to form the ATP binding site necessary for ATP binding. The substrate binding mechanism of *Sa*BPL is explored in Chapter 2.

1.7   Characterization of *Ec*BPL

*Ec*BPL is the best characterized BPL of all species. It is also the most closely related protein to *Sa*BPL, which is the focus of this thesis. It is encoded by the *birA* gene resulting in a polypeptide of 35.3 kDa in size (39). *Ec*BPL is a bifunctional enzyme that participates in both biotin attachment onto the biotin domain of ACC and also functions as a transcriptional repressor of the biotin biosynthetic operon. This enzyme is commonly referred to as 'biotin retention' (BirA). The X-ray crystal structures of apo *Ec*BPL (61) (Figure 1.4 A), *Ec*BPL in complex with biotin (62) (Figure 1.4 B) and *Ec*BPL in complex with the analogue biotinol-5´-AMP (63) have been reported. The monomeric apo structure solved to 2.3 Å resolution contains 3 domains characteristic of Class II BPLs. The N-

terminal 22-46 residues adopt a helix-turn-helix motif, a structure associated with DNA-binding proteins (61). The central domain consists of five α-helices, seven β-sheets and four poorly defined loops. The C-terminus consists of six strands which form a β-sandwich and has been implicated in the transfer of biotin onto the biotin domain (61,62,75) .

The crystal structure of *Ec*BPL in complex with biotin was resolved to 2.4 Å (62). As noted previously with other BPL structures, there are key conformational changes that occur upon biotin binding, resulting in the ordering of three loops in the catalytic domain. The only loop that remains unstructured consists of residues 212-233 (Figure 1.4) (76). The disordered-to-ordered transition has been proposed to be required for dimerization to occur (62). Ordering of the loops by biotin binding 1) encloses the active site and 2) forms the nucleotide binding site. Protein conformational changes induced by biotin and MgATP binding are believed to prime Class II BPLs for two competing protein: protein interactions (62). Firstly, heterodimerization with a biotin domain leads to the enzymatic attachment of biotin. Secondly, homodimerization leads to binding and sequence-specific transcriptional repression of the biotin biosynthetic operon (77,78).

Loop (i) in Figure 1.4 that becomes ordered upon ligand binding contains the highly conserved GRGRX motif, where X in this case is an arginine residue. Mutational analysis of this region showed reduced enzyme activity, highlighting the loop's importance (79). This region was originally proposed to be involved in nucleotide binding due to similarities with mononucleotide binding protein kinases (61). However, mutagenesis and kinetic studies have shown that this sequence is involved in biotin and biotinyl-5´-AMP binding, not ATP binding (79). Structural studies have also revealed that this region functions as a cap enclosing the biotin-binding pocket as well as the ATP-binding pocket.
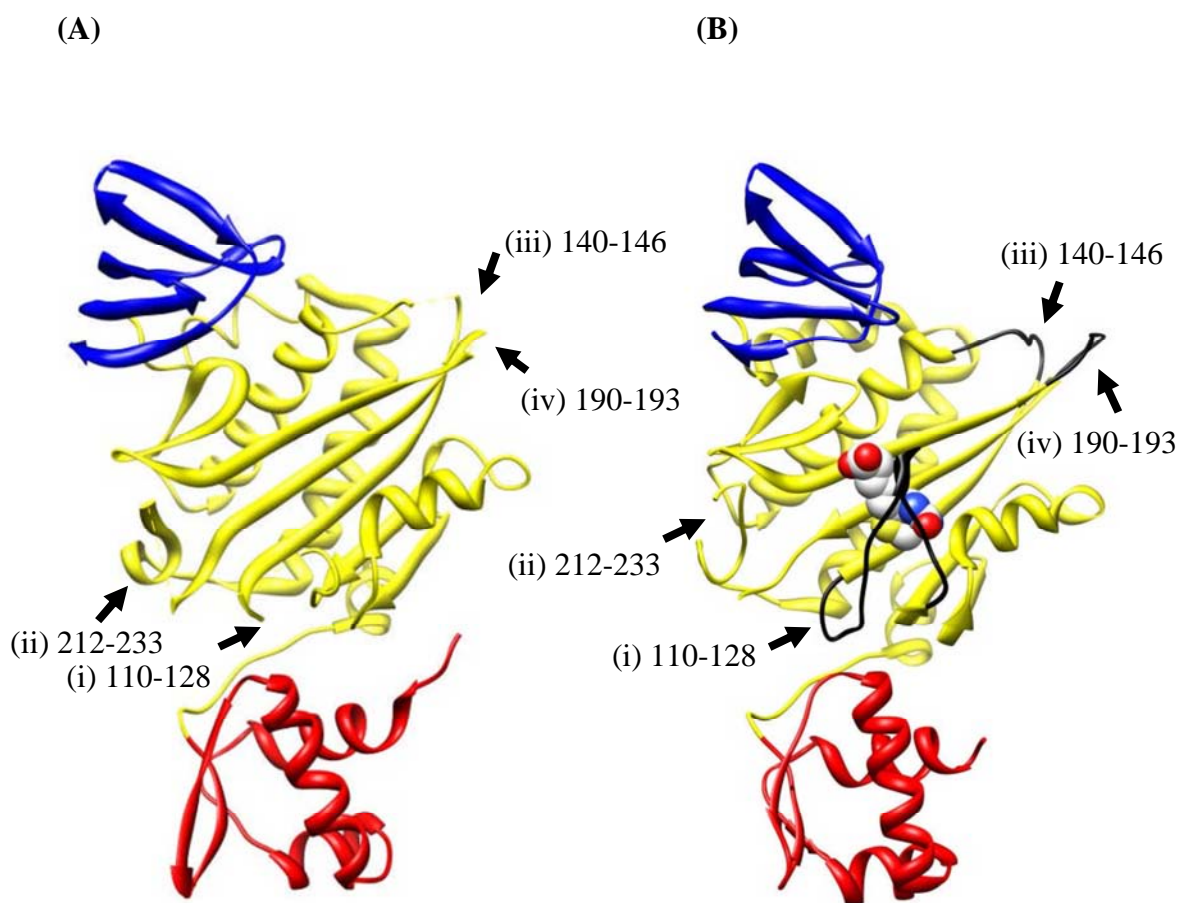
Figure 1.4: *The crystal structures of apo (A) and holo (B) EcBPL are shown in ribbon presentation. The three domains are depicted in different colours; the N-terminal domain in red, the catalytic domain in yellow and the C-terminal cap in blue. (A) Several surface loops, indicated by arrows with residue range, are presumed to be flexible. The figure was generated by UCSF Chimera using PBD 1BIA. (B) The holo structure of EcBPL in complex with biotin (viewed in sphere) showing the surface loops that became ordered upon biotin binding. Loop (i) is involved in ligand binding and is depicted in black, loops (iii) and (iv) form part of the dimerization interface and are also displayed in black, loop (ii) remained disordered. The figure was generated in UCSF Chimera using PBDID 1HXD (61).*

The crystal structure of *Ec*BPL in complex with a non-hydrolyzable analogue of the reaction intermediate provided the first evidence of the nucleotide binding site, which is

not observed in the apo structure (63). This structural data supports the argument that biotin binding in *Ec*BPL precedes ATP binding. The homodimer formed by biotinol-5´-AMP is also more tightly packed compared to that of *Ec*BPL: biotin complex. This is consistent with an increase in stability of 3.7 kcal/mol observed for *Ec*BPL: biotinyl-5´-AMP homodimer compared to *Ec*BPL: biotin homodimer from equilibrium ultracentrifugation analyses (67).

The N-terminal domain of *Ec*BPL is not directly involved in the catalytic mechanism as truncated *Ec*BPL mutants were still able to synthesize biotinyl-5´-AMP and transfer biotin onto the biotin domain. The N-terminal domain is, however, essential for DNA binding and regulation of the biotin biosynthetic operon. Synthesis of biotin is repressed by exogenous biotin concentrations greater than 40 nM (80). It is believed that two *Ec*BPL monomers in complex with biotinyl-5´-AMP bind co-operatively with the biotin operator (81) although biotin has been shown, to a lesser extent, to activate dimerization and DNA binding (69). The two holo monomers bind 12 bp apart, centre to centre at the ends of a pseudo-palindromic 40 bp operator sequence. There are two opposing views on the general model of *Ec*BPL transcription regulation. Beckett & Matthews proposed that Class II BPLs share the same surface for homodimerization and heterodimerization with the apo biotin domain (62). Thus, competing protein-protein interactions regulate the switch of the *bio* operon. Cronan *et al.* postulated that an extensive interaction is not required as the concentration of the co-repressor biotinyl-5´-AMP provides the switch (82).

Residues important for enzymatic and repressive function of *Ec*BPL have been identified. Arginine 118, found in the [115]GRGRR[119] motif of flexible loop (i) is of particular importance. Mutation of this residue to a glycine results in an enzyme unable to homodimerize (61,83). Further studies revealed that the *Ec*BPL-R118G mutant had dissociation constants for the intermediate biotinyl-5´-AMP that were ~400-fold greater than that of the wild-type enzyme, but the difference in dissociation rate for biotin was less drastic, with an increase of ~100-fold compared to wild-type *Ec*BPL (64). Results of this characterization indicate that Arg118 is required for binding of both biotin and the reaction intermediate. Choi-Ree *et al.* employed this observation and showed that since this mutant releases the highly reactive intermediate from the active site, it enables biotinylation of nearby proteins in a non-specific manner. This event was named 'promiscuous biotinylation' (84). The equivalent residue to Arg118 in other BPLs is proposed to have

similar properties. The characterization of the arginine residue at this position in *Sa*BPL is described in Chapter 4.

Another residue required for dimerization and repressor function in *Ec*BPL is Arg119, also present in the [115]GRGRR[119] motif. When this residue was mutated to a tryptophan, the protein was no longer able to homodimerize upon ligand binding, resulting in a decrease in affinity for the biotin operator site (64). However this mutation had little or no effect upon biotin, biotinyl-5´-AMP or ATP binding, suggesting that in *Ec*BPL, this residue does not make any contacts required for the post-translational addition of the substrates (64). The role of the equivalent residue in *Sa*BPL is described in Chapter 5.

1.8   *Sa*BPL structure

The unliganded, biotin-bound and biotinyl-5´-AMP structures have recently been solved for *Sa*BPL to resolutions of 2.1 Å, 3.2 Å and 2.6 Å respectively (60). Like Class II BPLs, the monomeric unit of *S. aureus* can be divided into three domains (Figure 1.5). The N-terminal domain (residues 1-60) consists of a winged helix-turn-helix motif consistent with DNA binding. The central catalytic domain (resides 68-274) forms an α-β domain and the C-terminal domain (residues 282-323) caps the active site upon ligand binding.

The apo structure crystallizes as a monomer with four disordered loops observed similar to *Ec*BPL. The *Sa*BPL: biotin complex is a dimer, where three of the loops become ordered. The biotin-binding loop is characterized by the highly conserved [119]GRGRX[123] motif (64). In *Ec*BPL, homodimerization leads to binding and sequence-specific transcriptional repression of *bioO* (77,78). This is also proposed to occur in *Sa*BPL, with the additional target gene *bioY* (85).

The biotinyl-5´-AMP structure shows that the intermediate binds in a tight 'U-shape' geometry in a relatively open binding pocket (Figure 1.6). The conformation positions the carbonyl carbon atom of biotin ready for nucleophilic attack by the target lysine residue of the biotin domain and may help the reaction by inducing strain in the bonds about this component of the ligand. The C-terminal and catalytic domains orientate themselves to make contact with the analogous residues on the other subunit. The N-terminal domains of the *Sa*BPL dimer come in contact with the catalytic core as observed in the *Ec*BPL dimer.

In *Ec*BPL, these contacts are important for binding to DNA, resulting in the repression of biotin biosynthetic operon. The main differences between the crystal structures of *Ec*BPL and *Sa*BPL dimers is the orientation of the N-terminal domains, with a 37.7^o rotation and a translation of 3.9 Å as depicted in Figure 1.7. The significance of this is unclear and may be an artifact of the crystallography.

C-terminal
cap domain

Catalytic
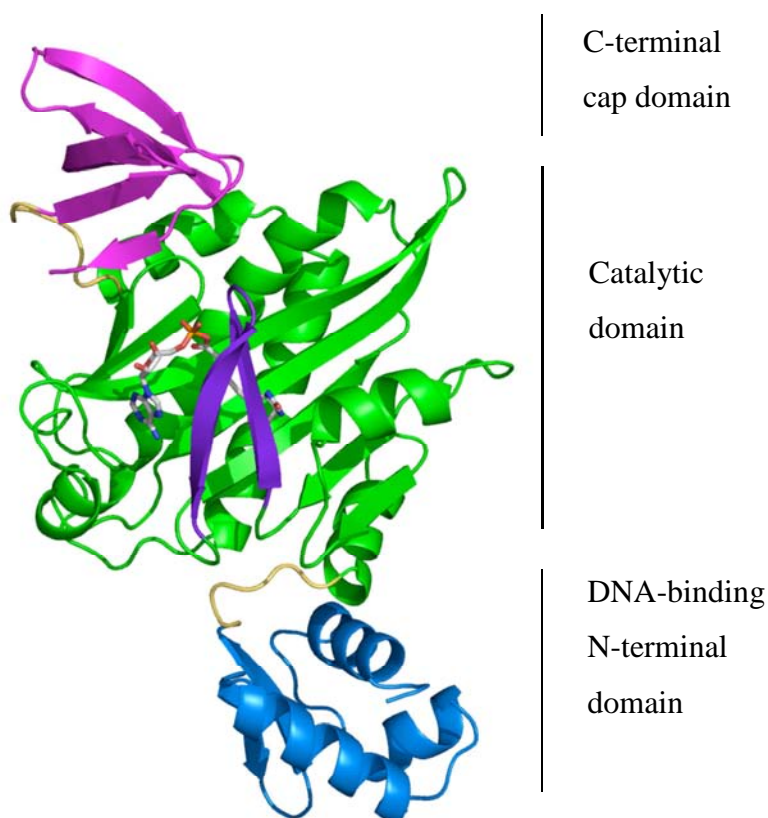domain

DNA-binding
N-terminal
domain

Figure 1.5:   *X-ray crystal structure of SaBPL in ribbon presentation. N-terminal domain residues 1-60 (blue), catalytic domain residues 68-274 (green) and C-terminal residues 282-323 (magenta). Linker regions 61-67 and 275-281 between these domains are shown in yellow. The reaction intermediate, biotinyl-5´-AMP, is shown by stick representation (71). The figure was generated in UCSF Chimera using PBDID 3RKW (61).*
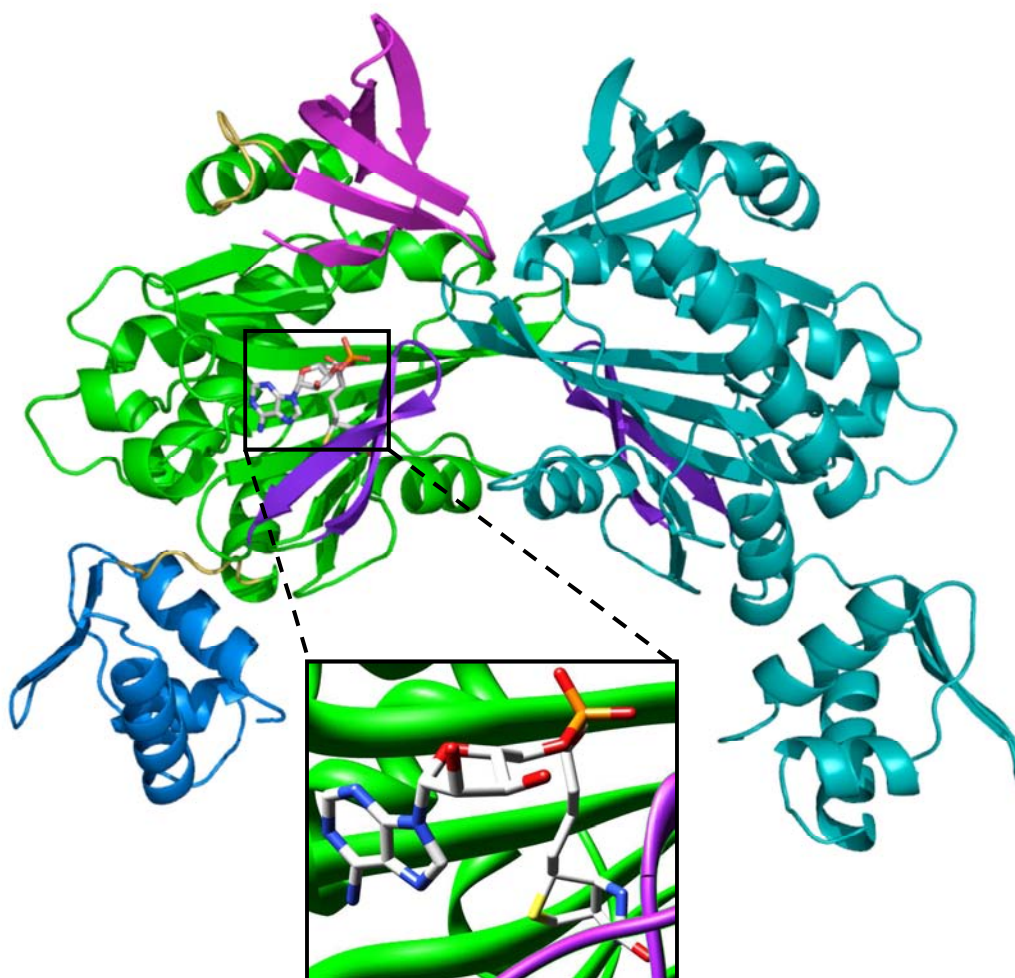
Figure 1.6: *X-ray crystal structure of dimer SaBPL in ribbon presentation with biotinyl-5´-AMP (71). The C-terminal domain of monomer A is shown in magenta, the catalytic domain in green, the N-terminal domain in blue and the linker regions in yellow in monomer A. Monomer B is shown in cyan. Inset shows 'U-shaped' geometry of the reaction intermediate biotinyl-5´-AMP. The figure was generated in UCSF Chimera using PBDID 3RKW (61).*
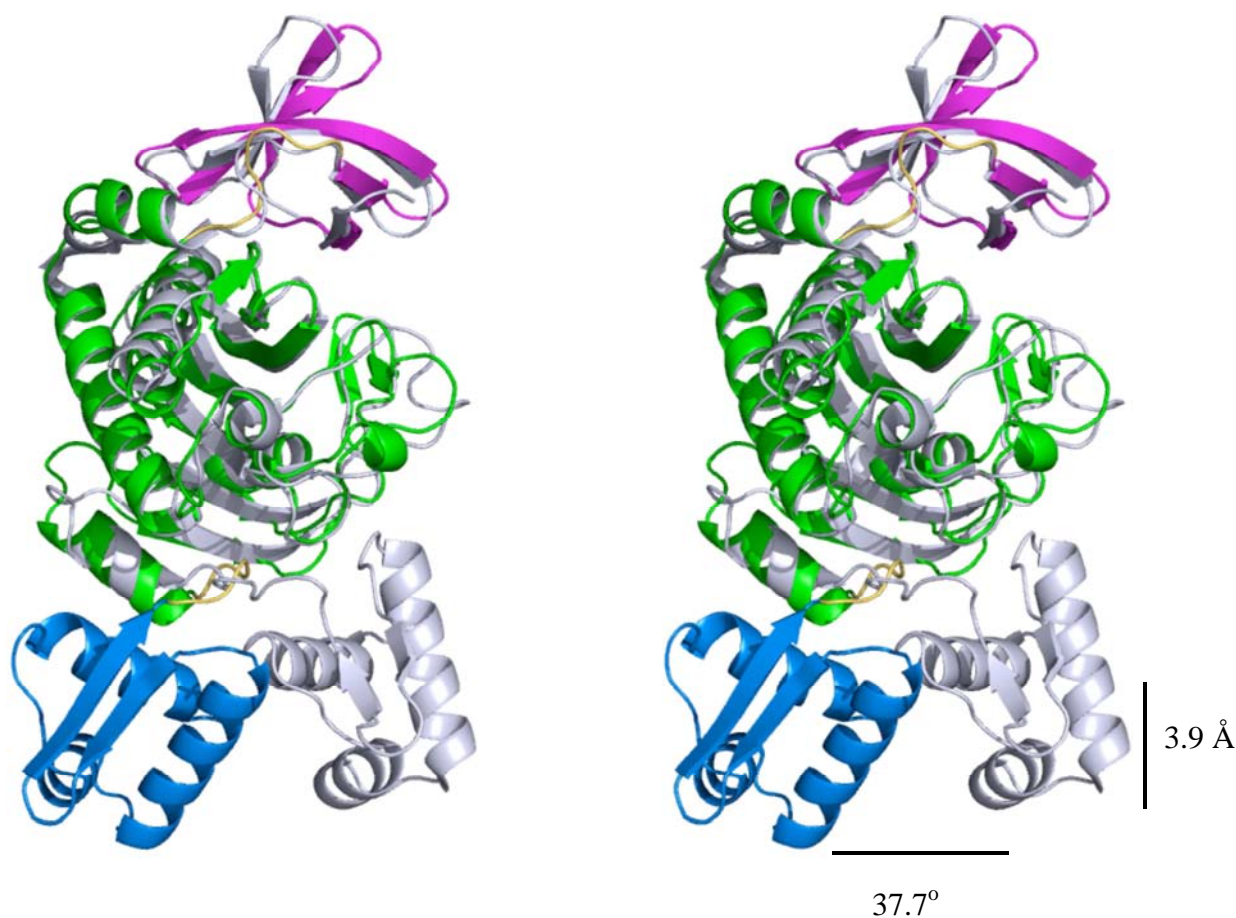
Figure 1.7: *Dimerization comparison of EcBPL (grey) and SaBPL (as coloured in Figure 1.6). Lines in black show large differences between the two structures in the positioning of the N-terminal domain. Adapted from Pendini et al. (2008) (71).*

1.9   Differences between *Sa*BPL and *Hs*BPL

As mentioned previously, targeting *Sa*BPL can lead to the debilitation of the function of both ACC and PC, impeding several pathways that are critical for cell survival. However, one of the biggest challenges in targeting *Sa*BPL is the existence of a human homologue. In order to avoid potential toxicity to the host, inhibitors of *Sa*BPL must have very high selectivity for the bacterial enzyme over the human equivalent. Therefore, a thorough understanding of the key differences between these enzymes is essential for the development of selective compounds. Selective inhibition has not previously been observed for any BPL. This area is the key focus of the work described in Chapters 2, 5 and 6.

Although all BPLs catalyze the same biotinylation reaction, not all BPLs exhibit DNA binding activity like the *S. aureus* and *E. coli* enzymes (33). This is consistent with the lack of repressor function for organisms that obtain biotin exogenously (86). The major difference between human and bacterial BPLs is the presence of an N-terminal extension, which shows no homology to any protein sequences in the literature (26,87). The X-ray crystal structure of *Hs*BPL has not been determined, therefore structure-function studies have been performed to elucidate some information. Campeau and Gravel (2001) postulated that the N-terminal domain region between Leu166 and Tyr266 functions in the biotinylation reaction or may be involved in substrate recognition as truncations in this region resulted in poor or no activity in a complementation assay in *E. coli*. Recent studies done in our laboratory show that the C-terminal and N-terminal domains in *Hs*BPL interact (88). The N-terminal region is implicated in the second partial reaction, i.e., the attachment of biotin into biotin-dependent enzymes. This work is described in Chapter 7. A mechanism where the N-terminal domain interacts with the catalytic domain was first proposed for yeast BPL (72), which also contains a large extended N-terminal domain characteristic of Class III BPLs.

Although the crystal structure of *Hs*BPL remains unsolved, our collaborators have generated a model of the human catalytic domain (26) (Figure 1.8) using the published *P. horikoshii* OT3 structure (65). In the absence of a crystal structure, the differences in the sequence between *Hs*BPL and *Sa*BPL provide clues about the main differences between the two enzymes. It is clear that there is a high degree of conservation in the residues making contact with the biotin pocket. In contrast, seven out of the nine residues that make contact with the nucleotide are different in *Sa*BPL compared to *Hs*BPL. The generation and characterization of a 'humanized' *Sa*BPL construct where all these seven residues are replaced by the equivalent residues in *Hs*BPL is the focus of Chapter 6.
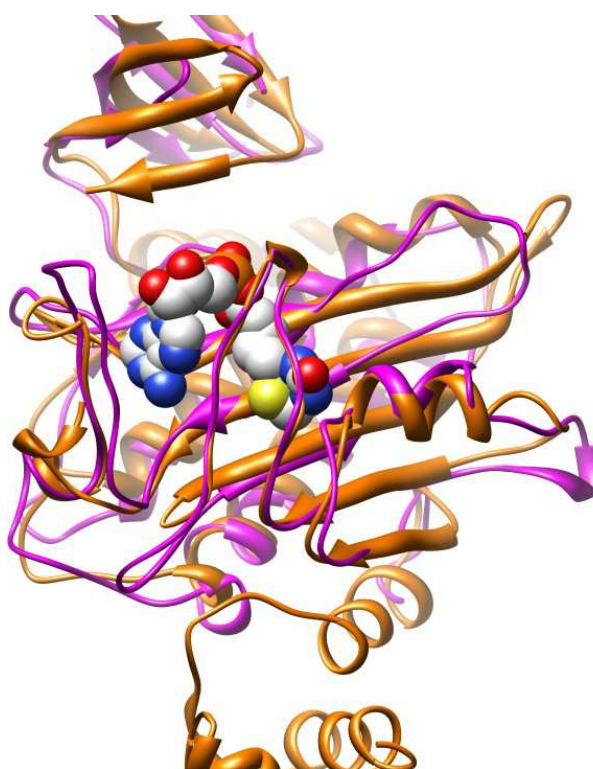
Figure 1.8: *Superimposition of the SaBPL (gold) and proposed catalytic domain model of the HsBPL (pink). The reaction intermediate biotinyl-5´-AMP is also shown. Adapted from Pendini et al. (2008) (26).*

1.10 BPL inhibitors

This chapter so far has highlighted the fundamental importance of *Sa*BPL in bacterial cell survival and maintenance. To date no therapeutics have been developed to target BPL and prior to this project there were precious few examples of small molecule inhibitors of BPL in the literature, none of which showed selectivity for any BPL. Biotinol-5´-AMP is one example of a known BPL inhibitor (Figure 1.9). This compound was designed to function as a non-hydrolyzable analogue of the BPL reaction intermediate (89). It lacks the carbonyl group on the biotin tether and is therefore stable to cleavage, preventing the attachment of biotin to the biotin domain. A similar approach has been employed to design inhibitors of aminoacyl-tRNA synthetase (90). As expected, this compound has been shown to inhibit BPLs from several species to a similar extent. The K_i values were determined to be 0.03 ± 0.01 µM for *Sa*BPL, 0.20 ± 0.03 µM for *Hs*BPL and 0.30 ± 0.06 µM for *Ec*BPL. This compound represents a valuable research tool but it is not selective enough to be a pre-clinical candidate. Additionally, the phosphate chemistry involved in the synthesis of this

compound is difficult to scale up. An important improvement on the structure would be to replace the phosphodiester linkage that connects the biotin and adenosine moieties with a more stable and selective linkage.
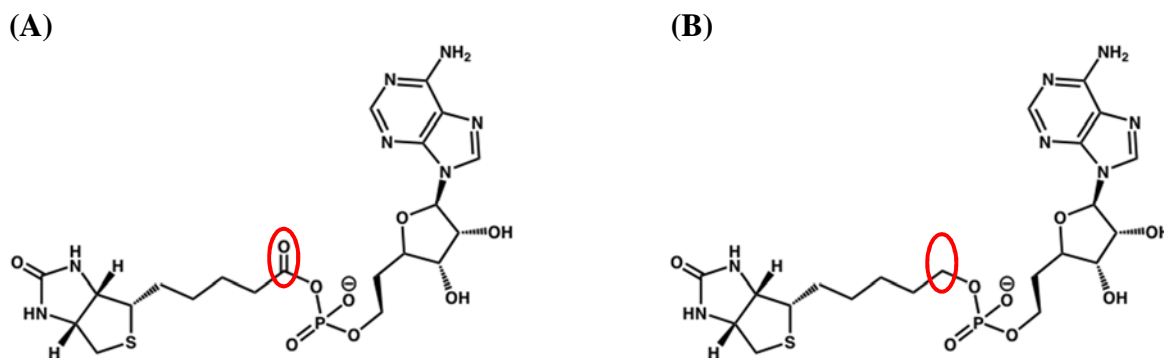
(A)   **(B)**

Figure 1.9: *Structure of the reaction intermediate biotinyl-5´-AMP (**A**) compared to the structure of the analogue biotinol-5´-AMP (**B**).*

1.11   Approaches to drug design

Rational drug design is a good starting point for hit generation when a wealth of information is known about the target-ligand interaction. This was the approach used to generate a series of biotin analogue inhibitors of *Sa*BPL, *Ec*BPL and *Hs*BPL described in Chapter 3. High-throughput screening (HTS) is a well-established approach within the pharmaceutical industry for hit identification. While the hits from such a screen result are usually highly potent, the success rate of developing these hits into pre-clinical candidates is low due to the size of the molecules and therefore their specificity for a particular site. The chemical space explored by HTS screening methods is also very small in regards to the complexity and size of each molecule tested. So despite many successes, the investment in these technologies has not yet reversed the downward trend in the number of new entities reaching the market and there is a need to find alternative approaches to hit discovery (91).

Fragment-based approaches offer a number of attractive features compared with HTS. First, the number of compounds typically screened is much lower because it is easier to find a fragment to match a particular binding site than a larger molecule. Second, a higher proportion of the atoms in a fragment hit are likely to be directly involved in the desired

protein-ligand interaction. It has been observed during chemical optimization that the binding affinity of compounds increases with their molecular weight (92). Hence the activity of fragment hits are usually measured in terms of 'ligand efficiency', which is defined as the binding energy per heavy (non-hydrogen) atom (93). Generally in HTS, larger and more potent compounds are identified, but the compounds have low ligand efficiency. Third, when the binding interaction is validated by structural biology, the subsequent chemical optimization of fragments benefits from design and synthesis of relatively few compounds. Finally, starting the chemical optimization stage with a low molecular mass fragment (generally less than 300 Da) is likely to produce smaller lead compounds (94). This is an advantage as medicinal chemists generally build upon a compound, therefore a small scaffold with good ligand efficiency is the preferred starting point.

The choice of fragment compound libraries is critical when screening for suitable hits. Many commercial libraries contain fragments that follow the 'Rule of Three': $M_w \leq 300$ Da, calculated logP ($c$logP) ≤ 3, hydrogen bond donors ≤ 3 and hydrogen bond acceptors ≤ 3 (94). The logP is the logarithm of the compound's partition coefficient between n-octanol and water and is a well-established measure of the hydrophilicity of a compound (92). The 'Rule of Three' was proposed initially after a careful review of all the successful attempts at drug discovery using the fragment-based drug discovery approach (92). This selection process ensures that the chemical diversity of the library is not compromised by the variation in drug-likeness of the fragments to be incorporated into a potential lead. In addition, fragments need to be tested at high concentrations to allow the detection of weak binding so solubility becomes critical. Hence, fragments with low $c$logP are generally chosen.

Two of the most commonly used biophysical techniques in fragment-based discovery are NMR and X-ray crystallography. While these approaches provide detailed structural information, they are low-throughput and may not be technically feasible. A relatively new approach now being used is surface plasmon resonance (SPR) that allows comprehensive protein: small molecule interaction analysis in real time. It has been proven to be a powerful tool for early drug discovery applications where hundreds to thousands of potential hit compounds must be investigated (95). In this approach, one of the interacting molecules, referred to as the ligand, is immobilized onto the surface of a sensor chip. A

potential interaction partner (analyte) is then injected in solution across the sensor surface. As an interaction partner binds to the immobilized molecule, refractive index at the surface alters in proportion to the change in mass. This results in a change in SPR signal (measured in resonance units RU) that is detected in real time (96). In this work, SPR is used extensively to study the interactions between BPLs, substrates and small molecule inhibitors. There are two potential problems associated with studying small molecule binding by SPR. Firstly, very high densities of the ligand must be immobilized in order to detect binding. A second problem is that with such small binding responses, refractive index effects become significant. The latter can be avoided by dissolving and/or diluting the analyte in the running buffer and using a control flow cell with very similar levels of immobilization. Improvements in the signal to noise ratios of BIAcore instruments have enabled binding to be detected of analytes with molecular weights as low as 180 Da (97).

Once hits have been found, it is crucial to validate their potential through chemical optimization. The key to optimization is to increase the potency of fragment hits while minimizing the reduction in ligand efficiency (98). The optimization of a fragment could be manipulated in two ways. Fragment growing involves the addition of functional groups onto the starting structure. This can be guided using structural data about the binding site. Alternatively, fragment linking involves combining fragments that bind to adjacent pockets. Successful experiments have shown improved affinity and specificity not only additively but synergistically. An appropriate linker needs to be found, however, that maintains the orientation and position of the fragment's key interactions (99). Ligand efficiency is not only useful in merging the initial hits, but also in guiding chemical optimization during drug development (100). An example of a fragment-based approach that is used in this work is *in situ* click chemistry, which will be described in detail in the next section.

1.12 *In situ* click chemistry, a novel approach to drug discovery

Target-guided synthesis is a fragment-based approach used in drug design, which relies on the ability of an enzyme to choose its own inhibitors from a range of building block reagents. It requires the binding of ligands simultaneously, which contain complementary functional groups that can connect once placed in close proximity. Rideout *et al.* pioneered this concept by proposing the self-assembly of cytotoxic hydrazones inside cells to explain

a marked synergism between the cytotoxic effects of decanal and *N*-amino-guanidines (101,102). A major problem with the target guided synthesis approach is the use of highly reactive reagents which are likely to react in undesired ways within biochemical systems.

To avoid this limitation, *in situ* click has been developed that employs the [1,3]-dipolar cycloaddition reaction between an acetylene and an azide to produce a triazole (Figure 1.10) (103). This reaction is slow at room temperature due to the high kinetic barrier for the cycloaddition reaction, despite exhibiting a large driving force that makes it irreversible. This allows the reaction to only take place when the reactants are brought into close proximity (e.g. catalyzed). The resulting triazole linkage cannot be cleaved hydrolytically or otherwise and unlike benzenoids and related aromatic heterocycles, they are almost impossible to oxidize or reduce (104). The triazoles are also capable of active participation in hydrogen bonding as well as dipole-dipole and π-π stacking interactions (105). Thus, *in situ* click can be used in conjunction with traditional methods for the discovery of novel hit compounds (106,107).
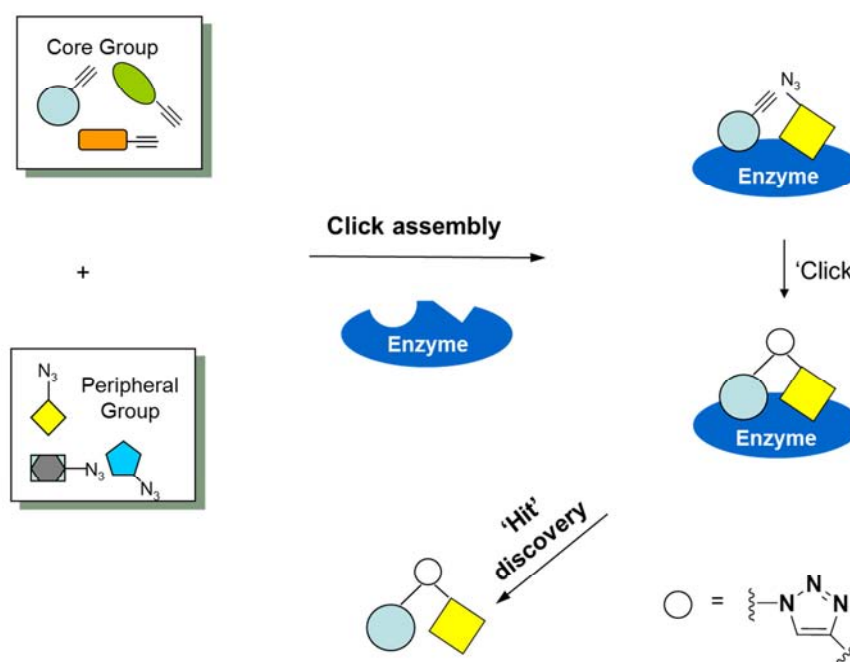

Figure 1.10: *Inhibitor discovery using in situ click chemistry.*

In situ click chemistry was first demonstrated by Mock *et al.* (1983), where the synthetic receptor cucurbituril was shown to accelerate the rate of cycloaddition between acetylene

and azide by 10^5-fold, leading to the exclusive irreversible production of the *anti*-triazole regioisomer (106). Since then, the efficacy of *in situ* click chemistry has been demonstrated by the discovery of novel, highly potent inhibitors of a small number of enzymes, *viz.* acetylcholinesterase (108,109), carbonic anhydrase II (110), chitinase (111) and HIV-protease (105). Whiting *et al.* (2006) showed that HIV-protease selectively formed an inhibitor from components that exhibited only weak binding to the target, demonstrating that this methodology can be applied to systems where high-affinity building blocks are not known.

The real power of *in situ* click chemistry lies in its ability to generate novel high affinity inhibitors that might not necessarily resemble known pharmacophores (104). Paradoxically, the ability to produce high-affinity products is also a limitation for this methodology. In particular, detection of triazole products by HPLC, NMR or mass spectrometry typically requires relative high concentrations of the products. However, tight-binding inhibitors often remain associated in the protein's active site, thereby preventing multiple rounds of catalysis and resulting in poor product yields. The work described in Chapter 4 resolves this problem by generating a 'leaky' mutant of the target enzyme, which results in a 40-fold increase in the rate of product formation relative to the wild-type enzyme. This allows this approach to be used to identify BPL inhibitors.

1.13 Aims of the project

It is imperative that we increase our efforts to develop novel antibiotic classes that are not subject to known resistance mechanisms. A new frontier for antibiotic research is to target essential enzymes that have mammalian equivalents. In this thesis, I highlight the importance of *Sa*BPL as a novel drug target. The challenge here will be to identify compounds with exquisite specificity towards the bacterial target.

While the first generation BPL inhibitor biotinol-5´-AMP represents a valuable research tool, there are limitations that hamper its selection as a pre-clinical candidate. As discussed in section 1.10, its *in vitro* selectivity for the pathogenic target requires optimization. Additionally, its synthesis is complex, not easily scalable and not amenable to derivatization, which has slowed down the progress of our *in vivo* studies. These are not trivial limitations in a chemical development programme. Therefore, we require a new pharmacophore with improved selectivity, while offering significant advances in ease of synthesis and derivatization in order to establish a possible clinical candidate against *Sa*BPL.

In this project, my aims were to enzymatically characterize *Sa*BPL, and to perform a combination of *in situ* click chemistry experiments, together with target-based drug discovery to allow the identification of novel inhibitors of *Sa*BPL. In addition, the differences between *Sa*BPL and HsBPL are explored in order to create selective compounds that do not target the human enzyme.

This thesis is divided into two main sections: inhibitor discovery and enzymology. The inhibitor discovery section consists of Chapters 2, 3 and 4. The enzymology section consists of Chapters 5, 6 and 7. Chapter 2 is a published paper in the *Journal of Biological Chemistry* entitled 'Selective inhibition of biotin protein ligase from *Staphylococcus aureus*' (60). This paper focuses on our most selective inhibitors, the biotin 1,2,3 triazole analogues. Importantly, the biotin triazole inhibitors show cytotoxicity against *S. aureus*, but not cultured mammalian cells. Chapter 3 is a published paper in *ACS Medicinal Chemistry Letters* entitled 'Biotin analogues with antibacterial activity are potent inhibitors of biotin protein ligase' (112). Here, the synthesis and characterization of a series of biotin analogues with activity against BPLs from *S. aureus*, *E. coli*, and *H. sapiens* are reported.

These compounds also have antibacterial activity against a panel of clinical isolates of *S. aureus* (MIC 2–16 μg/mL) and their mode of action is probed using SPR. Chapter 4 is a manuscript to be re-submitted to *Angewandte Chemie International Edition* entitled 'Optimizing *in situ* click chemistry: the screening and identification of biotin protein ligase inhibitors'. In this work, a protocol for the BPL-catalyzed *in situ* click reaction was optimized to select the optimum triazole-based inhibitor using a library of azides in a single experiment, with improved efficiency and ease of detection. Chapter 5 is a manuscript under review in the *Journal of Biological Chemistry* entitled 'A novel link between protein homodimerization and inhibitor binding to biotin protein ligase from *Staphylococcus aureus*'. In this work, the inhibitor biotin acetylene is used as a tool to study the effects of an inhibitor with a long life in the active site of *Sa*BPL on oligomerization. Chapter 6 is a draft of a manuscript entitled "'Humanized' biotin protein ligase provides clues about inhibitor selectivity" to be submitted to *Biochemistry*. Here I have created a chimeric protein where all 7 residues in *Sa*BPL that are different to those found in the nucleotide pocket of the human enzyme are replaced. This 'humanized' protein exhibits similar kinetic and inhibition properties to the human enzyme but has much higher yields from recombinant expression and purification, which has been one of the major roadblocks for obtaining protein crystals of the full-length human enzyme. Chapter 7 is a published manuscript in the *Journal of Molecular Medicine* entitled 'A novel molecular mechanism to explain biotin-unresponsive holocarboxylase synthetase deficiency' (88). My contribution to this work involved the dissection of the binding mechanism of human BPL using SPR. The data provides the first molecular explanation for BPL-deficient patients that do not respond to biotin therapy by demonstrating that these patients have mutations that reduce the affinity of the enzyme for the apo protein substrate through a >15-fold increase in dissociation rate. All the work that has been done in this thesis will establish a solid foundation for BPL inhibitor discovery in the future in our pursuit of novel antibiotics.

1.14 References

1. Bakheet, T., and Doig, A. (2010) *BMC Bioinformatics* **11**, 195

2. Boucher, H. W., Talbot, G. H., Bradley, J. S., Edwards, J. E., Gilbert, D., Rice, L. B., Scheld, M., Spellberg, B., and Bartlett, J. (2009) *Clinical Infectious Diseases* **48**, 1-12

3. Payne, D. J., Gwynn, M. N., Holmes, D. J., and Pompliano, D. L. (2007) *Nature Reviews Drug Discovery* **6**, 29-40

4. Archer, G. L. (1998) *Clinical Infectious Diseases* **26**, 1179-1181

5. Lowy, F. D. (1998) *New England Journal of Medicine* **339**, 520-532

6. Appelbaum, P. C. (2006) *Clinical Microbiology and Infection* **12**, 3-10

7. Chambers, H. F. (1988) *Clinical Microbiology Reviews* **1**, 173-186

8. Hand, W. L. (2000) *Adolescent Medicine (Philadelphia, Pa.)* **11**, 427-438

9. Weber, C. J. (2008) *Urologic Nursing : Official Journal of the American Urological Association Allied* **28**, 143-145

10. Turnidge, J. D., Kotsanas, D., Munckhof, W., Roberts, S., Bennet, C. M., Nimmo, G. R., Coombs, G. W., Murray, R. J., B., H., Johnson, P. D., and Dowling, K. (2009) *Medical Journal of Australia* **191**, 368-373

11. Weigel, L. M., Clewell, D. B., Gill, S. R., Clark, N. C., McDougal, L. K., Flannagan, S. E., Kolonay, J. F., Shetty, J., Killgore, G. E., and Tenover, F. C. (2003) *Science* **302**, 1569-1571

12. Klein, E., Smith, D. L., and Laxminarayan, R. (2007) *Emerging Infectious Diseases* **13**, 1840-1846

13. Walsh, C. (2003) *Nature Reviews Microbiology* **1**, 65-70

14. Tenover, F. (2006) *American Journal of Infection Control* **34**, S3 - S10

15. Moellering Jr, R. C., Graybill, J. R., McGowan Jr, J. E., and Corey, L. (2007) *American Journal of Infection Control* **35**, S1-S23

16. Kogl, F., and Tonnis, B. (1936) *Journal of Physiological Chemistry* **242**, 43

17. du Vigneaud, V., Melville, D. B., Folkers, K., Wolf, D. E., and Mozingo, R. (1942) *Journal of Biological Chemistry* **146**, 475-485

18. Wakil, S. J., Stoops, J. K., and Joshi, V. C. (1983) *Annual Review Biochemistry* **52**, 537-579

19. Knowles, J. R. (1989) *Annual Review of Biochemistry* **58**, 195-221

20. Buckel, W. (2001) *Biochimica et Biophysica Acta (BBA) - Bioenergetics* **1505**, 15-27

21. Tong, L. (2012) *Cellular and Molecular Life Sciences* **[Epub ahead of print]**

22. Chapman-Smith, A., and Cronan, J. E. (1999) *Journal of Nutrition* **129**, 477-484

23. Tong, L. (2005) *Cellular and Molecular Life Sciences* **62**, 1784-1803

24. Athappilly, F. K., and Hendrickson, W. A. (1995) *Structure* **3**, 1407-1419

25. Roberts, E. L., Shu, N. C., Howard, M. J., Broadhurst, R. W., Chapman-Smith, A., Wallace, J. C., Morris, T., Cronan, J. E., and Perham, R. N. (1999) *Biochemistry* **38**, 5045-5053

26. Pendini, N. R., Bailey, L. M., Booker, G., Wilce, M. C., Wallace, M. C., and Polyak, S. W. (2008) *Biochimica et Biophysica Acta* **1784**, 973-982

27. Reche, P., Li, Y. L., Fuller, C., Eichhorn, K., and Perham, R. N. (1998) *Biochemical Journal* **329**, 589-596

28. Cronan Jr, J. E. (1990) *Journal of Biological Chemistry* **265**, 10327-10333

29. Shenoy, B. C., and Wood, H. G. (1988) *FASEB Journal* **2**, 2396-2401

30. Shenoy, B. C., Xie, Y., Park, V. L., Kumar, G. K., Beegan, H., Wood, H. G., and Samols, D. (1992) *Journal of Biological Chemistry* **267**, 18407-18412

31. Polyak, S. W., Chapman-Smith, A., Mulhern, T. D., Cronan Jr, J. E., and Wallace, J. (2001) *Journal of Biological Chemistry* **276**, 3037-3045

32. Murtif, V. L., and Samols, D. (1987) *Journal of Biological Chemistry* **262**, 11813-11816

33. Leon-Del-Rio, A., and Gravel, R. A. (1994) *Journal of Biological Chemistry* **269**, 22964-22968

34. Chapman-Smith, A., and Cronan Jr, J. E. (1999) *Trends of Biochemical Sciences* **24**, 359-363

35. Tissot, G., Pepin, R., Job, D., Douce, R., and Alban, C. (1998) *European Journal of Biochemistry* **258**, 586-596

36. Pendini, N. R., Polyak, S. W., Booker, G. W., Wallace, J. C., and Wilce, M. C. (2008) *Acta Crystallographica Section D-Biological Crystallography* **64**, 520-523

37. Freiberg, C., Brunner, N. A., Schiffer, G., Lampe, T., Pohlmann, J., Brands, M., Raabe, M., Häbich, D., and Ziegelbauer, K. (2004) *Journal of Biological Chemistry* **279**, 26066-26073

38. Wallace, J. C., and Eastervrook-Smith, S. B. (1985) The structure of pyruvate carboxylase. in *Pyruvate carboxylase*, CRC Press, Boca Raton, FL. pp 66-108
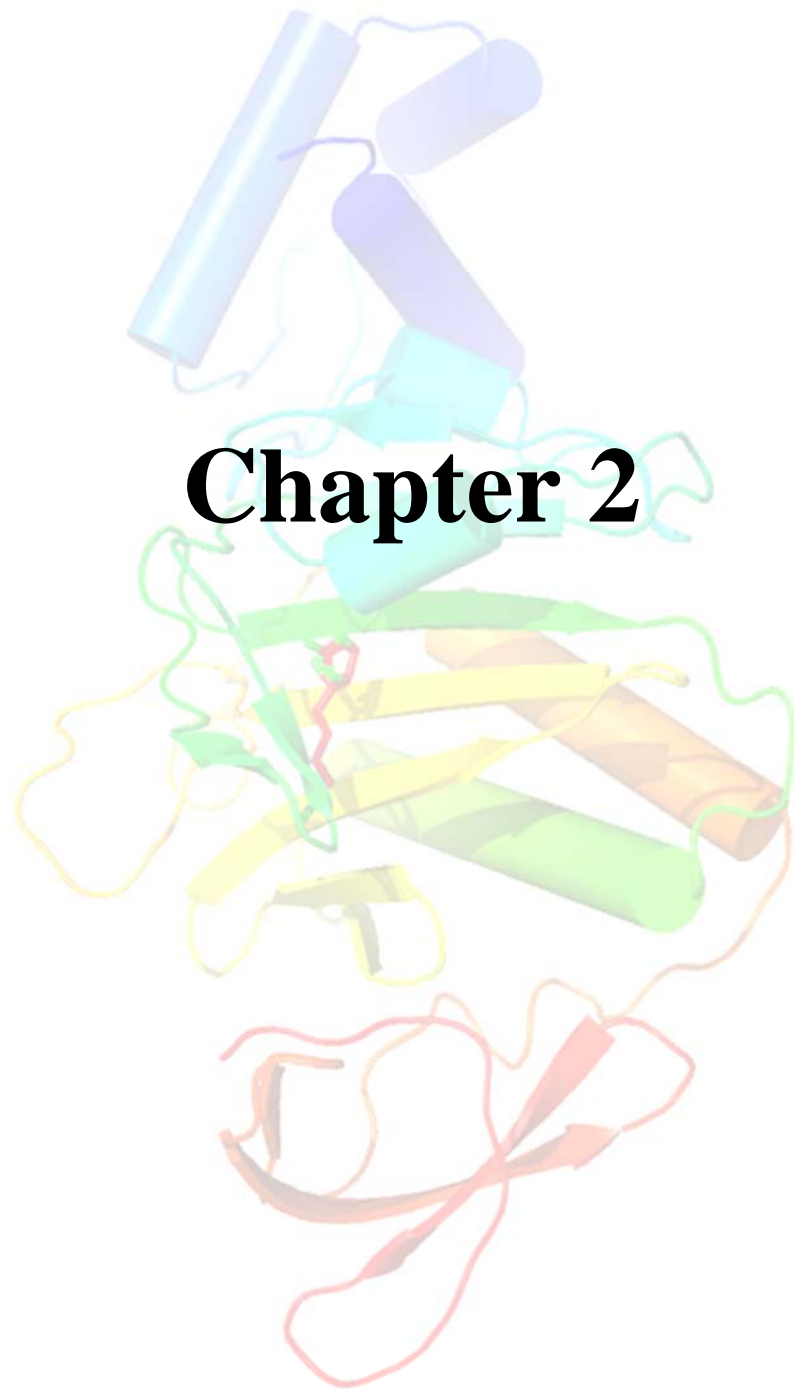
39.   Barker, D. F., and Campbell, A. M. (1981) *Journal of Molecular Biology* **146**, 451-467

40.   Thanassi, J. A., Hartman-Neumann, S. L., Dougherty, T. J., Dougherty, B. A., and Pucci, M. J. (2002) *Nucleic Acids Research* **30**, 3152-3162

41.   Gerdes, S. Y., Scholle, M. D., Campbell, J. W., Balazsi, G., Ravasz, E., Daugherty, M. D., Somera, A. L., Kyrpides, N. C., Anderson, I., Gelfand, M. S., Bhattacharya, A., Kapatral, V., D'Souza, M., Baev, M. V., Grechkin, Y., Mseeh, F., Fonstein, M. Y., Overbeek, R., Barabasi, A. L., Oltvai, Z. N., and Osterman, A. L. (2003) *Journal of Bacteriology* **185**, 5673-5684

42.   Parsons, J. B., and Rock, C. O. (2011) *Current Opinion in Microbiology* **14**, 544-549

43.   Parsons, J. B., Frank, M. W., Subramanian, C., Saenkham, P., and Rock, C. O. (2011) *Proceedings of the National Academy of Sciences* **108**, 15378-15383

44.   Campbell, J. W., and Cronan, J. E., Jr. (2001) *Annual Review of Microbiology* **55**, 305-332

45.   Wright, H. T., and Reynolds, K. A. (2007) *Current Opinions in Microbiology* **10**, 447-453

46.   Karlowsky, J. A., Kaplan, N., Hafkin, B., Hoban, D. J., and Zhanel, G. G. (2009) *Antimicrobial Agents and Chemotherapy* **53**, 3544-3548

47.   Bogdanovich, T., Clark, C., Kosowska-Shick, K., Dewasse, B., McGhee, P., and Appelbaum, P. C. (2007) *Antimicrobial Agents and Chemotherapy* **51**, 4191-4195

48.   Miller, J. R., Dunham, S., Mochalkin, I., Banotai, C., Bowman, M., Buist, S., Dunkle, B., Hanna, D., Harwood, H. J., Huband, M. D., Karnovsky, A., Kuhn, M., Limberakis, C., Liu, J. Y., Mehrens, S., Mueller, W. T., Narasimhan, L., Ogden, A., Ohren, J., Prasad, J. V. N. V., Shelly, J. A., Skerlos, L., Sulavik, M., Thomas, V. H., VanderRoest, S., Wang, L., Wang, Z., , Whitton, A., Zhu, T. , and Stover, C. K. (2009) *Proceedings of the National Academy of Sciences* **106**, 1737-1742

49.   Wang, J., Soisson, S. M., Young, K., Shoop, W., Kodali, S., Galgoci, A., Painter, R., Parthasarathy, G., Tang, Y. S., Cummings, R., Ha, S., Dorso, K., Motyl, M., Jayasuriya, H., Ondeyka, J., Herath, K., Zhang, C., Hernandez, L., Allocco, J., Basilio, Á., Tormo, J. R., Genilloud, O., Vicente, F., Pelaez, F., Colwell, L., Lee, S. H., Michael, B., Felcetto, T., Gill, C., Silver, L. L., Hermes, J. D., Bartizal, K., Barrett, J., Schmatz, D., Becker, J. W., Cully, D., and Singh, S. B. (2006) *Nature* **441**, 358-361

50. Hutton, C. A., Perugini, M. A., and Gerrard, J. A. (2007) *Molecular BioSystems* **3**, 458-465

51. Bae, T., Banger, A. K., Wallace, A., Glass, E. M., Aslund, F. M., Schneewind, O., and Missiakas, M. (2004) *Proceedings of the National Academy of Sciences* **101**, 12312-12317

52. Lipinski, C. A., Lombardo, F., Dominy, B. W., and Feeney, P. J. (1997) *Advanced Drug Delivery Review* **23**, 3-25

53. Artymiuk, P. J., Rice, D. W., Poirrette, A. R., and Willet, P. (1994) *Nature Structural Biology* **1**, 758-760

54. Reche, P. A. (2000) *Protein Science* **9**, 1922-1929

55. Reed, K. E., and Cronan Jr, J. E. (1991) *Journal of Biological Chemistry* **266**, 11425-11428

56. Sueda, S., Tanakaa, H., and Yamagishia, M. (2009) *Analytical Biochemistry* **393**, 189-195

57. Bagautdinov, B., Matsuura, Y., Bagautdinova, S., and Kunishima, N. (2008) *Journal of Biological Chemistry* **283**, 14739-14750

58. Purushothaman, S., Gupta, G., Srivastava, R., Ramu, V. G., and Surolia, A. (2008) *PLoS One* **3**, e2320

59. Tron, C. M., McNae, I. W., Nutley, M., Clarke1, D. J., Cooper, A., Walkinshaw, M. D., Baxter, R. L., and Campopiano, D. J. (2009) *Journal of Molecular Biology* **387**, 129-146

60. Soares da Costa, T. P., Tieu, W., Yap, M. Y., Pendini, N. R., Polyak, S. W., Sejer Pedersen, D., Morona, R., Turnidge, J. D., Wallace, J. C., Wilce, M. C., Booker, G. W., and Abell, A. D. (2012) *Journal of Biological Chemistry* **287**, 17823-17832

61. Wilson, K. P., Shewchuk, L. M., Brennan, R. G., Otsuka, A. J., and Matthews, B. W. (1992) *Proceedings of the National Academy of Sciences* **89**, 9257-9261

62. Weaver, L. H., Kwon, K., Beckett, D., and Matthews, B. W. (2001) *Proceedings of the National Academy of Sciences* **98**, 6045-6050

63. Wood, Z. A., Weaver, L. H., Brown, P. H., Beckett, D., and Matthews, B. W. (2006) *Journal of Molecular Biology* **357**, 509-523

64. Kwon, K., and Beckett, D. (2000) *Protein Science* **9**, 1530-1539

65. Bagautdinov, B., Kuroishi, C., Sugahara, M., and Kunishima, N. (2005) *Journal of Molecular Biology* **353**, 322-333

66. Daniels, K. G., and Beckett, D. (2010) *Biochemistry* **49**, 5358-5365

67.   Eisenstein, E., and Beckett, D. (1999) *Biochemistry* **38**, 9649-9656

68.   Streaker, E. D., Gupta, A., and Beckett, D. (2002) *Biochemistry* **41**, 14263-14271

69.   Prakash, O., and Eisenberg, M. A. (1979) *Proceedings of the National Academy of Sciences* **76**, 5592-5595

70.   Streaker, E. D., and Beckett, D. (2003) *Journal of Molecular Biology* **325**, 937-948

71.   Pendini, N. R. (2009) The structure and function of biotin protein ligase: a focus on *Staphylococcus aureus*, *Saccharomyces cerevisiae*, *Candida albicans* and *Homo sapiens*. in *School of Biomedical Science*, University of Adelaide, Adelaide

72.   Polyak, S. W., Chapman-Smith, A., Brautigan, P. J., and Wallace, J. C. (1999) *Journal of Biological Chemistry* **274**, 32847-32854

73.   Ingaramo, M., and Beckett, D. (2009) *Journal of Biological Chemistry* **284**, 30862-30870

74.   Xu, Y., and Beckett, D. (1994) *Biochemistry* **33**, 7354-7360

75.   Chapman-Smith, A., Mulhern, T. D., Whelan, F., Cronan, J. E., Jr., and Wallace, J. C. (2001) *Protein Science* **10**, 2608-2617

76.   Xu, Y., Nenortas, E., and Beckett, D. (1995) *Biochemistry* **34**, 16624-166231

77.   Beckett, D. (2007) *Annual Review of Genetics* **41**, 443-464

78.   Prakash, O., and Eisenberg, M. A. (1974) *Journal of Bacteriology* **120**, 785-791

79.   Kwon, K., Streaker, E. D., Ruparelia, S., and Beckett, D. (2000) *Journal of Molecular Biology* **304**, 821-833

80.   Eisenberg, M. A. (1973) *Advanced in Enzymology and Related Areas of Molecular Biology* **38**, 317-372

81.   Abbott, J., and Beckett, D. (1993) *Biochemistry* **32**, 9649-9656

82.   Solbiati, J., and Cronan, J. E. (2010) *Chemistry & Biology* **17**, 11-17

83.   Buoncristiani, M. R., Howard, P. K., and Otsuka, A. J. (1986) *Gene* **44**, 255-261

84.   Choi-Rhee, E., Schulman, H., and Cronan Jr, J. E. (2004) *Protein Science* **13**, 3043-3050

85.   Rodionov, D. A., Mironov, A. A., and Gelfand, M. S. (2002) *Genome Research* **12**, 1507-1516

86.   Chapman-Smith, A., and Cronan Jr, J. E. (1999) *Biomolecular Engineering* **16**, 119-125

87.   Campeau, E., and Gravel, R. A. (2001) *Journal of Biological Chemistry* **276**, 12310-12316

88.	Mayende, L., Swift, R. D., Bailey, L. M., Soares da Costa, T. P., Wallace, J. C., Booker, G. W., and Polyak, S. W. (2012) *Journal of Molecular Medicine* **90**, 81-88

89.	Brown, P. H., Cronan, J. E., Grotli, M., and Beckett, D. (2004) *Journal of Molecular Biology* **337**, 857-869

90.	Balg, C., Blais, S. P., Bernier, S., Huot, J. L., Couture, M., Lapointe, J., and Chenevert, R. (2007) *Bioorganic Medical Chemistry* **15**, 295-304

91.	Brown, D., and Superti-Furga, G. (2003) *Drug Discovery Today* **8**, 1067-1077

92.	Lipinski, C. A. (2000) *Journal of Pharmacological and Toxicological Methods* **44**, 235-249

93.	Hopkins, A. L., Groom, C. R., and Alex, A. (2004) *Drug Discovery Today* **9**, 430-431

94.	Congreve, M., Carr, R., Murray, C., and Jhoti, H. (2003) *Drug Discovery Today* **8**, 876-877

95.	Myszka, D. G., and Rich, R. L. (2000) *Pharmacy Science Technology Today* **3**, 310-317

96.	Biacore. (1998) *BIAapplications Handbook*, Pharmacia Biosencor AB, Uppsala

97.	Karlsson, R., and Stahlberg, R. (1995) *Analytical Biochemistry* **228**, 274-280

98.	Carr, R. A. E., Congreve, M., Murray, C. W., and Rees, D. C. (2005) *Drug Discovery Today* **10**, 987-992

99.	Foloppe, N. (2011) *Future Medicinal Chemistry* **3**, 1111-1115

100.	Hajduk, P. J., and Greer, J. (2007) *Nature Reviews Drug Discovery* **6**, 211-219

101.	Rideout, D. (1986) *Science* **233**, 561-563

102.	Rideout, D., Calogeropoulou, J., Jaworski, M., and McCarthy, M. (1990) *Biopolymer* **29**, 247-262

103.	Huisgen, R. (1984) *1,3-Dipolar cycloaddition chemistry*, Wiley, New York

104.	Kolb, H. C., and Sharpless, K. B. (2003) *Drugs Discovery Today* **8**, 1128-1137

105.	Whiting, M., Muldoon, J., Lin, Y.-C., Silverman, S. M., Lindstrom, W., Olson, A. J., Kolb, H. C., Fin, M. G., Sharpless, K. B., Elder, J. H., and Folkin, V. V. (2006) *Angewandte Chemie International Edition* **45**, 1435-1439

106.	Mock, W. L., Irra, T. A., Wepsiec, J. P., and Manimaran, T. L. (1983) *Journal of Organic Chemistry* **48**, 3619-3620

107.	Mock, W. L., A., I. T., P., W. J., and Adhyam, A. M. (1989) *Journal of Organic Chemistry* **54**, 5302-5308

108. Lewis, W. G., Green, L. G., Grynszpan, F., Radic, Z., Carlier, P. R., Taylor, P., Fin, M. G., and Sharpless, K. B. (2002) *Angewandte Chemie International Edition* **41**, 1053-1057

109. Krasiski, A., Radic, Z., Manetsch, R., Raushel, J., Taylor, P., Sharpless, K. B., and Kolb, H. C. (2005) *Journal of the American Chemical Society* **127**, 6686-6692

110. Mocharla, V. P., Colasson, B., Lee, L. V., Roper, S., Sharpless, K. B., Wong, C.-H., and Kolb, H. C. (2005) *Angewandte Chemie International Edition* **44**, 116-120

111. Hirose, T., Sunazuka, T., Sugawara, A., Endo, A., Iguchi, K., Yamamoto, T., Ui, H., Shiomi, K., Watanabe, T., Sharpless, K. B., and Omura, S. (2009) *The Journal of Antibiotics* **62**, 277-282

112. Soares da Costa, T. P., Tieu, W., Yap, M. Y., Zvarec, O., Bell, J. M., Turnidge, J. D., Wallace, J. C., Booker, G. W., Wilce, M. C. J., Abell, A. D., and Polyak, S. W. (2012) *ACS Medicinal Chemistry Letters* **3**, 509-514

Chapter 2

Statement of Authorship

Title of Paper	Selective inhibition of biotin protein ligase from *Staphylococcus aureus*.
Publication Status	⊙ Published ○ Accepted for Publication ○ Submitted for Publication ○ Publication Style
Publication Details	Soares da Costa, T. P., Tieu, W., Yap, M. Y., Pendini, N. R., Polyak, S. W., Pederson, D. S., Morona, R., Turnidge, J. D., Wallace, J. C., Wilce, M. C. J., Booker, G. W., Abell, A. D. (2012) Selective inhibition of biotin protein ligase from *Staphylococcus aureus*. *Journal of Biological Chemistry*, 287 (21), 17823-17832.

Author Contributions

By signing the Statement of Authorship, each author certifies that their stated contribution to the publication is accurate and that permission is granted for the publication to be included in the candidate's thesis.

Name of Principal Author (Candidate)	Tatiana P. Soares da Costa		
Contribution to the Paper	Primary role in performing biochemical testing and manuscript preparation. Performed protein expression, purification, kinetic analysis, surface plasmon resonance experiments, inhibition assays, antibacterial testing, cell culture toxicity assays, circular dichroism analysis and site-directed mutagenesis.		
Signature		Date	15/10/2012

Name of Co-Author	William Tieu		
Contribution to the Paper	Designed, synthesized and characterized all small molecule inhibitors.		
Signature		Date	15/10/12

Name of Co-Author	Min Y. Yap		
Contribution to the Paper	Solved crystal structures of *Sa*BPL in complex with inhibitors.		
Signature		Date	22/10/12

Name of Co-Author	Nicole R. Pendini		
Contribution to the Paper	Solved crystal structures of apo *Sa*BPL and in complex with substrates.		
Signature		Date	7/11/2012.

Name of Co-Author	Steven W. Polyak
Contribution to the Paper	Cloned SaBPL gene and developed protein purification and enzyme assays. Performed initial proof of concept experiments. Provided project direction and corresponding author on manuscript.
Signature	Date 16/10/2012

Name of Co-Author	Daniel S. Pederson
Contribution to the Paper	Provided direction in synthetic chemistry and small molecule design.
Signature	Date 15/11/2012

Name of Co-Author	Renato Morona
Contribution to the Paper	Directed the antibacterial testing experiments and provided bacterial strains.
Signature	Date 16/10/12

Name of Co-Author	John D. Turnidge
Contribution to the Paper	Provided direction in all aspects of antibacterial testing.
Signature	Date 19/10/12

Name of Co-Author	Matthew C. Wilce
Contribution to the Paper	Provided direction in all aspects of X-ray crystallography.
Signature	Date 5/11/2012

Name of Co-Author	Grant W. Booker
Contribution to the Paper	Provided direction and assistance in all aspects of protein chemistry.
Signature	Date 16/10/2012

Name of Co-Author	Andrew D. Abell
Contribution to the Paper	Provided direction in all aspects of synthetic chemistry and ligand design.
Signature	Date 15/10/2012

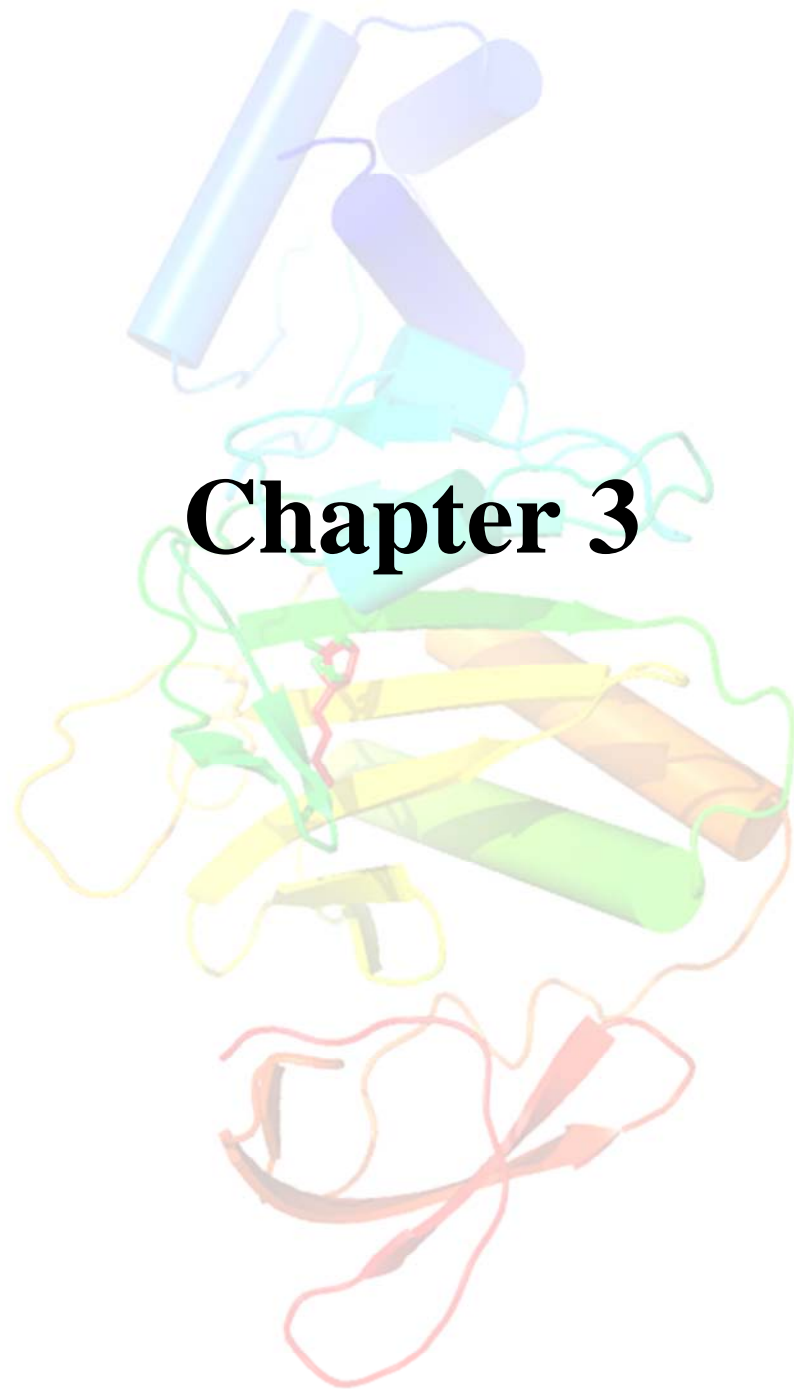| Name of Co-Author	John C. Wallace		
Contribution to the Paper	Provided intellectual discussion.		
Signature		Date	26/10/2012

Soares da Costa, T.P., Tieu, W., Yap, M.Y., Pendini, N.R., Polyak, S.W., Pederson, D.S., Morona, R., Turnbridge, J.D., Wallace, J.C., Wilce, M.C.J., Booker, G.W. & Abell, A.D. (2012) Selective inhibition of biotin protein ligase from *Staphylococcus aureus*. *Journal of Biological Chemistry, v. 287(21), pp. 17823-17832*

Chapter 3

Statement of Authorship

Title of Paper	Biotin analogues with antibacterial activity are potent inhibitors of biotin protein ligase.
Publication Status	⊙ Published ○ Accepted for Publication ○ Submitted for Publication ○ Publication Style
Publication Details	Soares da Costa, T. P., Tieu, W., Yap, M. Y., Zvarec, O., Bell, J. M., Turnidge, J. D., Wallace, J. C., Wilce, M. W., Booker, G. W., Abell, A. R., Polyak, S. W. (2012) Biotin analogues with antibacterial activity are potent inhibitors of biotin protein ligase. *ACS Medicinal Chemistry Letters*, 3 (6), 509-514.

Author Contributions

By signing the Statement of Authorship, each author certifies that their stated contribution to the publication is accurate and that permission is granted for the publication to be included in the candidate's thesis.

Name of Principal Author (Candidate)	Tatiana P. Soares da Costa		
Contribution to the Paper	Primary role in performing biochemical testing. Performed protein expression, purification, inhibition assays, surface plasmon resonance analysis, cell culture toxicity assays and mechanism of antibacterial activity testing. Assisted in manuscript preparation.		
Signature		Date	15/10/2012

Name of Co-Author	William Tieu		
Contribution to the Paper	Design, synthesis and characterization of small molecule inhibitors.		
Signature		Date	15/10/12

Name of Co-Author	Min Y. Yap		
Contribution to the Paper	Solved crystal structures of *Sa*BPL in complex with inhibitors.		
Signature		Date	22/10/12

Name of Co-Author	Ondrej Zvarec		
Contribution to the Paper	Synthesis of one small molecule inhibitor.		
Signature		Date	31/10/12

Name of Co-Author	Jan M. Bell		
Contribution to the Paper	Performed all antibacterial assays.		
Signature		Date	19/10/2012

Name of Co-Author	John D. Turnidge		
Contribution to the Paper	Provided direction for the antibacterial testing.		
Signature		Date	19/10/12

Name of Co-Author	John C. Wallace		
Contribution to the Paper	Provided intellectual discussion.		
Signature		Date	26/10/2012

Name of Co-Author	Matthew C. Wilce		
Contribution to the Paper	Provided direction in all aspects of X-ray crystallography.		
Signature		Date	5/11/2012

Name of Co-Author	Grant W. Booker		
Contribution to the Paper	Provided direction and assistance in all aspects of protein chemistry.		
Signature		Date	16/10/2012

Name of Co-Author	Andrew D. Abell		
Contribution to the Paper	Provided direction in all aspects of synthetic chemistry and manuscript preparation.		
Signature		Date	15/10/2012

Name of Co-Author	Steven. W. Polyak		
Contribution to the Paper	Primary responsibility in preparing the manuscript.		
Signature		Date	16/10/2012

Biotin Analogues with Antibacterial Activity Are Potent Inhibitors of Biotin Protein Ligase

Tatiana P. Soares da Costa,[†,#] William Tieu,[‡,#] Min Y. Yap,[§] Ondrej Zvarec,[‡,⊥] Jan M. Bell,[‖] John D. Turnidge,[†,‖] John C. Wallace,[†] Grant W. Booker,[†] Matthew C. J. Wilce,*[,§] Andrew D. Abell,*[,‡] and Steven W. Polyak*[,†]

[†]School of Molecular and Biomedical Science and [‡]School of Chemistry and Physics, University of Adelaide, South Australia 5005, Australia

[§]School of Biomedical Science, Monash University, Victoria, 3800, Australia

[‖]Microbiology and Infectious Diseases Directorate, SA Pathology, Women's and Children's Hospital, South Australia 5006, Australia

⑤ *Supporting Information*

ABSTRACT: There is a desperate need to develop new antibiotic agents to combat the rise of drug-resistant bacteria, such as clinically important *Staphylococcus aureus*. The essential multifunctional enzyme, biotin protein ligase (BPL), is one potential drug target for new antibiotics. We report the synthesis and characterization of a series of biotin analogues with activity against BPLs from *S. aureus*, *Escherichia coli*, and *Homo sapiens*. Two potent inhibitors with $K_i < 100$ nM were identified with antibacterial activity against a panel of clinical isolates of *S. aureus* (MIC 2–16 μg/mL). Compounds with high ligand efficiency and >20-fold selectivity between the isozymes were identified and characterized. The antibacterial mode of action was shown to be via inhibition of BPL. The bimolecular interactions between the BPL and the inhibitors were defined by surface plasmon resonance studies and X-ray crystallography. These findings pave the way for second-generation inhibitors and antibiotics with greater potency and selectivity.

KEYWORDS: *biotin protein ligase, enzyme, enzyme inhibitor, antibiotic, medicinal chemistry*
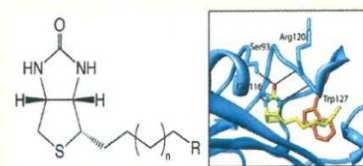
It is imperative that we identify new antibiotics to combat drug-resistant bacteria.[1] One clinically important pathogen, *Staphylococcus aureus* (*S. aureus*), is responsible for more than half of all life-threatening bloodstream infections. *S. aureus* is challenging to control as it has the ability to rapidly acquire drug-resistance mechanisms in both hospitals and the community, making treatment increasingly difficult and costly.[2,3] An important strategy to combat drug resistance is to develop novel antibiotic classes for which there are no pre-existing resistance mechanisms. This is becoming increasingly difficult, as most of the known chemical classes and obvious drug targets have been well explored, leaving the more challenging targets as a new frontier for antibacterial research. For example, little work has been done on essential bacterial enzymes that have mammalian paralogues due to perceived fears of possible toxicity.[4] For these targets, selective inhibition is critical.

The ubiquitous enzyme biotin protein ligase (BPL) is one potential antibacterial target that has not yet been comprehensively investigated.[5] BPL is responsible for the attachment of the cofactor biotin onto biotin-dependent enzymes. This proceeds in two partial reactions. Initially, the adenylated reaction intermediate biotinyl-5′-AMP is produced from biotin and ATP. Subsequently, the biotin moiety is covalently attached to the ε-amino group of a single target lysine residue present in the active site of biotin-dependent enzymes.[6] Here, biotin is required to facilitate the carboxylation of metabolites.

Without the attached cofactor, biotin-dependent enzymes are catalytically inactive and unable to fulfill their critical metabolic roles. As all organisms possess between one and five biotin-dependent enzymes, all organisms require a BPL, as there are no alternative enzymes to perform protein biotinylation. One important biotin-dependent enzyme is acetyl CoA carboxylase, which catalyzes the first committed step in the fatty acid biosynthetic pathway.[4] As this pathway is essential for bacterial cell membrane maintenance and biogenesis, they are a potential source of new antibiotic targets in certain Gram-positive bacteria such as *S. aureus*.[7] *S. aureus* expresses a second biotin-dependent enzyme, pyruvate carboxylase, which catalyzes the conversion of pyruvate to oxaloacetate, thereby replenishing the TCA cycle.[8] In addition to its biotin ligase activity, certain bacterial BPLs also function as transcriptional repressors, making them bifunctional proteins.[9] BPL recognition sites in the *S. aureus* genome suggest that *S. aureus* BPL regulates expression of the enzymes in the biotin biosynthesis operon, as well as the biotin transport protein BioY.[10] Thus, BPL is the master regulator protein of all biotin-mediated events in bacteria and, therefore, an attractive new antibiotic drug target.

In this paper, we present a novel series of biotin analogues with potent inhibitory activity against *Sa*BPL and antibacterial

activity against clinical strains of *S. aureus*. The mode of small molecule binding to *Sa*BPL was defined by X-ray crystallography and surface plasmon resonance studies. A few examples of biotin analogues with antibacterial activity do appear in the literature, including the natural product α-dehydrobiotin[11] and an analogue chemically modified at the N1 position required for binding carbon dioxide (Figure 1).[12] These function by first
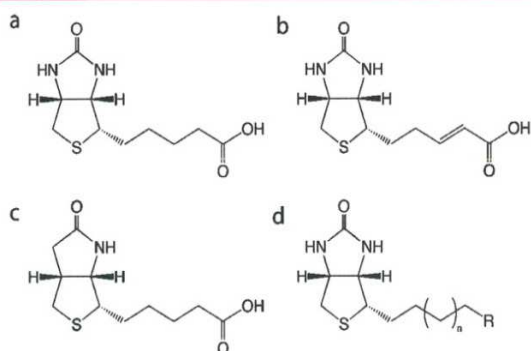

Figure 1. Chemical structures of (a) biotin **1** and its analogues (b) α-dehydrobiotin, (c) N1 substituted biotin, and (d) the pharmacophore investigated in this study.

being incorporated into a biotin-dependent enzyme where they abolish catalytic activity by preventing the binding or transfer of carbon dioxide.[13−15] Importantly, these analogues are either not specific or loose broad-spectrum antibacterial activity when assayed in rich growth media containing biotin.[11,14] Moreover, their activity has not been linked to the inhibition of BPL as they only transiently occupy the active site of this enzyme. A more effective approach for antibiotic discovery requires high-affinity inhibitors that bind directly and specifically to the bacterial BPL target, thereby preventing all protein biotinylation. A proof of concept for this approach to antibiotic discovery has been reported recently, targeting the BPLs from *Mycobacterium tuberculosis* and *S. aureus*.[5,16] In this current paper, we investigated biotin analogues with a view to

identifying BPL inhibitors with improved ligand efficiency (LE). Our findings provide new lead structures for further optimization, for example, **5** and **16**.

We began our search by screening analogues of biotin for their inhibitory properties. The compounds were assayed in an in vitro biotinylation assay measuring the incorporation of radiolabeled biotin into protein.[17] Purified recombinant BPLs from the Gram-positive bacterium *S. aureus* (*Sa*BPL[18]), the Gram-negative bacterium *Escherichia coli* (*Ec*BPL[19]), and *Homo sapiens* (*Hs*BPL[20]) were all assessed to investigate potency and species selectivity (Table 1). K_i values were calculated assuming that the mechanism of action was competitive with biotin, in agreement with Lineweaver−Burk analysis (Supporting Information, Figure S1).[21] This identified biotinol (**6**) as a pan inhibitor with K_i values of 3.4−4 μM for all three BPLs (Table 1). The binding mechanism was confirmed by solving the X-ray crystal structure of *Sa*BPL in complex with **6** (Figure 2a).
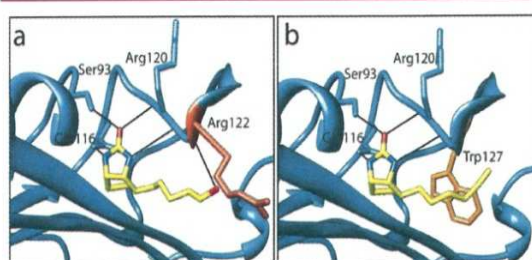

Figure 2. X-ray structures of inhibitors in complex with BPL. *S. aureus* BPL was crystallized in complex with biotin analogues alcohol **6** (a) and acetylene **14** (b). The hydrogen-bonding interactions with the inhibitors are shown.

Consistent with other BPL crystal structures that appear in the protein database, our data revealed the biotin-binding pocket of *Sa*BPL to be relatively small (187 Å³) with a hydrophobic cavity encasing the polar ureido and thiophene rings of biotin. This suggested limited opportunity for chemical modification of the biotin heterocycle in our inhibitor design. A narrow

Table 1. SAR Data for the Biotin Analogue Series[a]

			S. aureus		E. coli		H. sapiens	selectivity[c]
ID	n	R	K_i (μM)	LE[b]	K_i (μM)	LE[b]	K_i (μM)	Hs vs Sa/Ec vs Hs/Ec vs Sa
6	2	OH	3.37 ± 0.3	0.52	3.96 ± 0.4	0.51	3.85 ± 0.3	1.1/1.0/1.2
7	3	OH	>20	ND	>20	ND	>20	ND
3	1	NH$_2$	>20	ND	>20	ND	>20	ND
11	2	NH$_2$	>20	ND	>20	ND	>20	ND
16	1	CH$_3$	0.05 ± 0.01	0.69	1.10 ± 0.12	0.56	0.14 ± 0.02	2.8/7.9/22
17	2	CH$_3$	0.52 ± 0.06	0.56	7.30 ± 1.9	0.46	6.43 ± 1.4	12.4/1.1/14
5	1	C≡CH	0.08 ± 0.01	0.67	0.90 ± 0.1	0.57	0.2 ± 0.03	2.5/4.5/11.3
14	2	C≡CH	0.3 ± 0.05	0.58	7.33 ± 1.0	0.46	3.50 ± 0.5	11.7/2.1/24.4
15	3	C≡CH	2.40 ± 0.02	0.47	20.0 ± 0.3	0.39	12.0 ± 1.83	5/1.7/8.3

[a]A SAR series was investigated based upon the pharmacophore shown above. Compounds were assayed against BPLs from three species and where inhibition was observed K_i values are reported. Each K_i value is the mean (±standard error) of three independent experiments. [b]LE is ligand efficiency in kcal K^{-1} mol^{-1} per heavy atom. [c]Selectivity is expressed as ratios of K_i values. *Sa* is *S. aureus* BPL, *Ec* is *E. coli* BPL, and *Hs* is *H. sapiens* BPL.

Scheme 1[a]
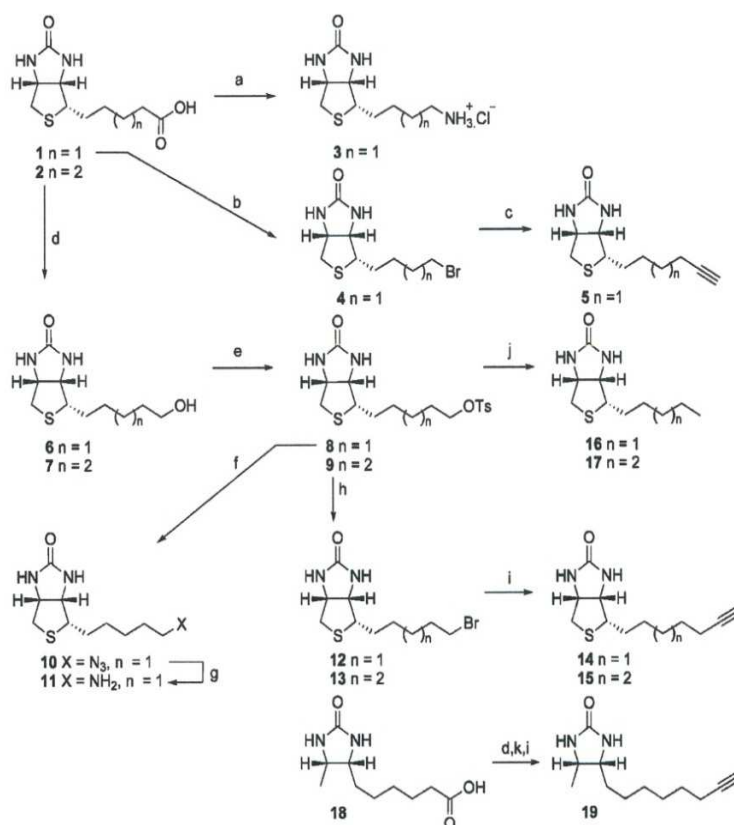
[a]Conditions and reagents: (a) (i) DPPA, Et$_3$N, THF; (ii) 6 N HCl. (b) (i) (COCl)$_2$, DCM (ii) 2-pyrithione, 1:9 (BrCCl$_3$:DMF), 80 °C. (c) Li-acetylide EDA complex, DMSO, 15 °C. (d) (i) SOCl$_2$, MeOH; (ii) LiAlH$_4$, THF. (e) TsCl, py. (f) NaN$_3$, DMF. (g) (i) PPh$_3$, THF; (ii) H$_2$O. (h) LiBr, 2-butanone. (i) Li-acetylide EDA complex, DMSO, 15 °C. (j) LiAlH$_4$, THF.

hydrophobic tunnel accommodates the valeric acid side chain with the carboxyl group being solvent exposed to provide a prime target for derivitisation. The protein:ligand interaction is stabilized through hydrogen bonding between the hydroxyl group (present on biotin and alcohol **6**) and an NH backbone amide of Arg 122 (Figure 2a). A series of analogues were proposed to further explore inhibition of BPL as a route to novel antibacterial agents. Our hypothesis was that derivatization of the carboxyl moiety of biotin would produce tight-binding inhibitors with increased potency and selectivity. Thus, to establish optimal binding, modifications of biotin were investigated that either replaced the carboxyl functionality with motifs capable of forming direct contacts with BPL as in compounds **3**, **16**, and **5**, and/or modified the length of the carbon chain (compounds **7**, **11**, **17**, **14**, and **15**).

The syntheses of all of the derivatives are shown in Scheme 1. Biotin **1** and homobiotin **2**[5] were first esterified, and the resulting methyl esters reduced with LiAlH$_4$ to give the alcohols **6** and **7**, respectively. Tosylation followed by bromination then gave **12** and **13**, respectively, which were separately reacted with lithium-acetylide EDA complex to give the two acetylenes **14** and **15**.[5] The tosylate **8** was also reacted with NaN$_3$ to give the azide **10**, which then gave the amine **11** using Staudinger reduction with PPh$_3$ followed by hydrolysis of the aza-ylide intermediate. The two tosylates **8** and **9** were also reduced with LiAlH$_4$ to give the alkyl derivatives **16** and **17**, respectively. Curtius rearrangement of biotin **1**, on reaction with diphenylphosphoryl azide in *tert*-butanol, followed by treatment

with 6 N aqueous HCl, gave amine **3**.[22] Finally, bromide **4** was prepared by Barton decarboxylation of **1** using 2-pyrithione, which on treatment with lithium-acetylide EDA complex gave acetylene **5**.[5]

The biotin derivatives were tested against the three BPLs using an in vitro biotinylation assay (Table 1) to reveal potent and selective inhibitors of *Sa*BPL. Interestingly, increasing the chain length of **6** by one carbon resulted in an inactive compound (**7**). The crystallographic data for *Sa*BPL bound to **6** as discussed earlier supports this observation, where the key hydrogen bond between the hydroxyl group of **6** and the enzyme is incompatible with the longer chain length. Replacement of the hydroxyl group of **6** with an amine, as in **3** and **11**, removed all inhibitory activity. This was somewhat surprising given that the amine would be expected to have similar polarity and hydrogen-bonding properties to the hydroxyl group of **6**. This observation may simply reflect the relative pK_a values of the two groups. We also assayed the synthetic intermediate bromides (**4**, **12**, and **13**), and these were all devoid of activity, presumably due to the steric bulk of the halids.

We next investigated hydrophobic groups (alkyl and acetylene) at the terminus of the carbon chain of biotin (see **5** and **14**–**17**) that we anticipated might be accommodated by the hydrophobic nature of the biotin pocket. Most notably **5**, **14**, **16**, and **17** exhibited up to a 20-fold selectivity for *Sa*BPL over *Ec*BPL and *Hs*BPL. Interestingly, removal of the tetrahydrothiophane ring in **14** removed all activity (see **18**
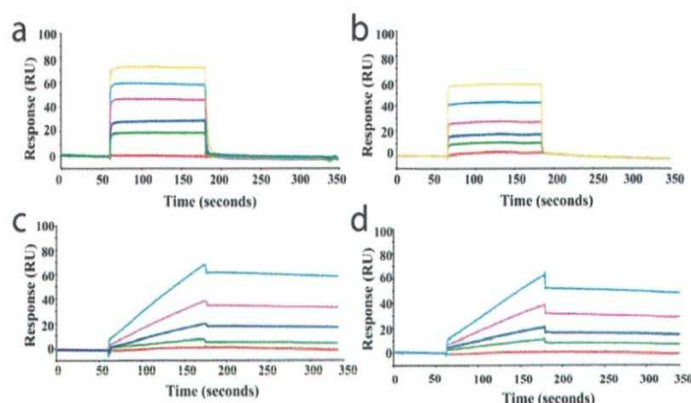
63

Figure 3. SPR analysis of BPL inhibitor binding. Surface plasmon resonance sensorgrams are shown for the binding of (a) biotin, (b) **6**, (c) **16**, and (d) **5** to immobilized *S. aureus* BPL. Varying concentrations of the inhibitors were included in the running buffer, and analysis was performed as described in the Supporting Information.

and **19**), highlighting the importance of the fused bicyclic ring of biotin. In the alkyl series, **16** was the most potent inhibitor for all three enzymes (*Sa*BPL, $K_i = 0.05 \ \mu M$) and displayed the greatest LE (0.69 kcal K^{-1} mol^{-1} per heavy atom). Again, a longer chain length (see **17**) decreased potency by ≈10-fold for the two bacterial enzymes and by 45-fold for the human enzyme. However, significant improvement in selectivity was apparent (see Table 1). The most potent compound in the acetylene series was again that with the shortest carbon chain (see **5**, $K_i = 0.08 \ \mu M$ and LE 0.67 kcal K^{-1} mol^{-1} per heavy atom for *Sa*BPL) with an observed decrease in potency and LE on increasing the chain length from $n = 1$ to 3 (see compounds **14** and **15** in Table 1). Once again, the most selective compound was where $n = 2$ (see **14**; with 20- and 10-fold selectivity for *Sa*BPL against *E. coli* and *H. sapiens* BPL, respectively). The acetylene **5** retained significant potency against the target *Sa*BPL with a $K_i = 0.30 \ \mu M$. The structure of biotin acetylene (**14**) in complex with *Sa*BPL was determined to confirm both the mode of binding and our proposal that substitution of the carboxyl group of biotin with hydrophobic functionalities would promote binding to the target. In agreement with the hypothesis, the complex was stabilized through a direct hydrophobic interaction between the acetylene and the Trp 127 (Figure 2b). Given that we observed selectivity in this series, we propose that this interaction should be further explored in inhibitor design. Our data strongly suggest that the biotin pockets of the three BPLs are not as structurally conserved as previously proposed, and this could be explored to improve potency and selectivity.

Ideally, our antibacterial compounds should have a relatively high affinity for BPL through slow dissociation from the binding pocket. To study this, *Sa*BPL was immobilized on a sensor chip for subsequent binding studies by surface plasmon resonance. Biotin and analogues **6**, **16**, and **5** were then separately passed across the surface, providing quantitative analysis of association and dissociation rates. The binding of biotin to *Sa*BPL (Figure 3a) was found to exhibit rapid on and off rates outside the range for quantitative evaluation. Hence, the K_D (9.2 ± 1.4 μM) was calculated using steady-state affinity. This observation is consistent with a two-step binding mechanism that has been reported for *E. coli* BPL.[23] Initially, the enzyme and biotin rapidly form a "collision complex" that is followed by a slower conformational change to BPL that is both rate-limiting in the binding mechanism and necessary to stablize the enzyme−biotin complex. Alcohol analogue **6** showed similar kinetics of binding as biotin (Figure 3b, $K_D = 2.5 ± 0.3 \ \mu M$), representative of a dynamic equilibrium between the free enzyme and the collision complex but unable to overcome the rate-limiting conformational change. In contrast, **16** and **5** displayed slower association ($k_a = 43.2 ± 2.3 × 10^3$ M^{-1} s^{-1} and 41.2 ± 2.3 × 10^3 M^{-1} s^{-1}, respectively) and dissociation rates relative to both biotin and **6** (**16** $k_d = 2.80 ± 0.20 × 10^{-3}$ s^{-1} and **5** 3.40 ± 0.30 × 10^{-3} s^{-1}), thereby contributing to their significantly higher affinities (**16** $K_D = 0.06 ± 0.01 \ \mu M$, Figure 3c, and **5** $K_D = 0.08 ± 0.01$, Figure 3d). The different association and dissociation kinetics displayed by **16** and **5** as compared to biotin and **6** imply that the modes of binding are mechanistically different. We propose that unlike biotin, **16** and **5** do indeed induce the conformational changes to *Sa*BPL that are necessary to retard the inhibitors from vacating their binding pockets. For antibacterial discovery, inhibitors that possess high occupancy rates on their bacterial targets are desirable.

Finally, the antibacterial activity of the most potent biotin analogues was determined using antimicrobial growth assays. These studies revealed significant bacteriostatic activity against both Gram-positive and Gram-negative bacteria. Compounds **16** and **5** were the most potent against clinical isolates of *S. aureus* with MICs in the range of 2−16 μg/mL, including methicillin-susceptible and -resistant strains (Table 2). This is consistent with the fact that these two derivatives were the most potent inhibitors of *Sa*BPL (Table 1). Derivative **17**, containing an extra carbon in the side chain relative to **16**, was less active against MSSA and MRSA, but interestingly, it was weakly active against vancomycin-resistant *Enterococcus* (MIC 32 μg/mL).

Table 2. Antibacterial Susceptibility Testing[a]

strain	range (μg/mL)	MIC$_{50}$ (μg/mL)		MIC$_{90}$ (μg/mL)	
		16	5	16	5
MSSA ($n = 8$)	4−16	8	8	16	16
MRSA ($n = 8$)	4−16	8	8	16	16
coagulase negative *Staphylococci* ($n = 7$)	2−>64	2	4	8	8

[a]MICs are shown for a library of *S. aureus* clinical isolates of coagulase negative and positive strains, including methicillin-sensitive (MSSA) and -resistant (MRSA) subtypes.

64

Compounds **16** and **5** were also active against coagulase negative *Staphylococci* strains. The mechanism of antibacterial action was assessed with a complementation assay using **5** with an *E. coli K12* strain engineered to overexpress the BPL target. Bacterial growth was monitored over 14 h in the absence or presence of **5** at 32 μg/mL (Figure S2 in the Supporting Information). Overexpression of *Ec*BPL completely alleviated antibacterial activity, strongly implying that the drug target is indeed BPL. Finally, the toxicity of the compounds was addressed in a mammalian cell culture model using HepG2 cells. These studies showed that the metabolic activity of the cells was uneffected when treated with 64 μg/mL of **7**, **16**, **17**, **5**, **14**, and **15**.

Here, we report new data that supports the hypothesis that BPL is a druggable antibacterial target in vitro. Our data demonstrate that BPL inhibitors with favorable in vitro properties also show significant antibacterial activity against clinical isolates of methicillin-sensitive and -resistant *S. aureus*. It is noteworthy that there was a positive correlation between slow enzyme:inhibitor dissociation kinetics and potent antibacterial activity. The quantitative data reported here help to define the target product profile necessary for future chemical optimization. Our biotin alkyl and acetylene series represent new chemical scaffolds with high LE for chemical development toward new antibacterial agents, a point that we have begun to address as reported in our earlier publication.[5]

ASSOCIATED CONTENT

Supporting Information

Assay and synthetic procedures and data for selected compounds. This material is available free of charge via the Internet at http://pubs.acs.org.

AUTHOR INFORMATION

Corresponding Author

*Tel: +61 3 9902 9244. E-mail matthew.wilce@monash. edu(M.C.J.W.). Tel: +61 8 8313 5652. Fax: +61 8 8313 4358. E-mail: andrew.abell@adelaide.edu.au (A.D.A.). Tel: +61 8 8313 5289. Fax: +61 8 8313 6042. E-mail: steven.polyak@ adelaide.edu.au (S.W.P.).

Present Address

[⊥]School of Materials Science and Engineering, Nanyang Technological University, Singapore. E-mail: OJZVAREC@ ntu.edu.sg.

Author Contributions

[#]These authors contributed equally. The manuscript was written through contributions of all authors. All authors have given approval to the final version of the manuscript.

Notes

The authors declare no competing financial interest.
M.C.J.W. is a National Health and Medical Research Council Senior Research Fellow.

ACKNOWLEDGMENTS

ABBREVIATIONS

BPL, biotin protein ligase; *Ec*, *Escherichia coli*; *Hs*, *Homo sapiens*; LE, ligand efficiency; MIC, minimal inhibitory concentration; *Sa*, *Staphylococcus aureus*

REFERENCES

(1) Cooper, M. A.; Shlaes, D. Fix the antibiotics pipeline. *Nature* **2011**, *472* (7341), 32.
(2) Allegranzi, B.; Bagheri Nejad, S.; Combescure, C.; Graafmans, W.; Attar, H.; Donaldson, L.; Pittet, D. Burden of endemic health-care-associated infection in developing countries: Systematic review and meta-analysis. *Lancet* **2011**, *377* (9761), 228–241.
(3) Jean, S. S.; Hsueh, P. R. High burden of antimicrobial resistance in Asia. *Int. J. Antimicrob. Agents* **2011**, *37* (4), 291–295.
(4) Polyak, S. W.; Abell, A. D.; Wilce, M. C.; Zhang, L.; Booker, G. W. Structure, function and selective inhibition of bacterial acetyl-CoA carboxylase. *Appl. Microbiol. Biotechnol.* **2012**, *93* (3), 983–992.
(5) Soares da Costa, T. P.; Tieu, W.; Yap, M. Y.; Pendini, N. R.; Polyak, S. W.; Sejer Pedersen, D.; Morona, R.; Turnidge, J. D.; Wallace, J. C.; Wilce, M. C.; Booker, G. W.; Abell, A. D. Selective inhibition of biotin protein ligase from *Staphylococcus aureus*. *J. Biol. Chem.* **2012**, *287*, 17823–17832.
(6) Pendini, N. R.; Bailey, L. M.; Booker, G. W.; Wilce, M. C.; Wallace, J. C.; Polyak, S. W. Microbial biotin protein ligases aid in understanding holocarboxylase synthetase deficiency. *Biochim. Biophys. Acta* **2008**, *1784* (7–8), 973–982.
(7) Parsons, J. B.; Rock, C. O. Is bacterial fatty acid synthesis a valid target for antibacterial drug discovery? *Curr. Opin. Microbiol.* **2011**, *14* (5), 544–549.
(8) Jitrapakdee, S.; St. Maurice, M.; Rayment, I.; Cleland, W. W.; Wallace, J. C.; Attwood, P. V. Structure, mechanism and regulation of pyruvate carboxylase. *Biochem. J.* **2008**, *413* (3), 369–387.
(9) Beckett, D. Biotin sensing at the molecular level. *J. Nutr.* **2009**, *139* (1), 167–170.
(10) Rodionov, D. A.; Mironov, A. A.; Gelfand, M. S. Conservation of the biotin regulon and the BirA regulatory signal in Eubacteria and Archaea. *Genome Res.* **2002**, *12* (10), 1507–1516.
(11) Hanka, L. J.; Bergy, M. E.; Kelly, R. B. Naturally occurring antimetabolite antibiotic related to biotin. *Science* **1966**, *154* (757), 1667–1668.
(12) Amspacher, D. R.; Blanchard, C. Z.; Fronczek, F. R.; Saraiva, M. C.; Waldrop, G. L.; Strongin, R. M. Synthesis of a reaction intermediate analogue of biotin-dependent carboxylases via a selective derivatization of biotin. *Org. Lett.* **1999**, *1* (1), 99–102.
(13) Blanchard, C. Z.; Amspacher, D.; Strongin, R.; Waldrop, G. L. Inhibition of biotin carboxylase by a reaction intermediate analog: Implications for the kinetic mechanism. *Biochem. Biophys. Res. Commun.* **1999**, *266* (2), 466–471.
(14) Levert, K. L.; Waldrop, G. L.; Stephens, J. M. A biotin analog inhibits acetyl-CoA carboxylase activity and adipogenesis. *J. Biol. Chem.* **2002**, *277* (19), 16347–16350.
(15) Piffeteau, A.; Dufour, M. N.; Zamboni, M.; Gaudry, M.; Marquet, A. Mechanism of the antibiotic action of alpha-dehydrobiotin. *Biochemistry* **1980**, *19* (13), 3069–3073.
(16) Duckworth, B. P.; Geders, T. W.; Tiwari, D.; Boshoff, H. I.; Sibbald, P. A.; Barry, C. E., 3rd; Schnappinger, D.; Finzel, B. C.; Aldrich, C. C. Bisubstrate adenylation inhibitors of biotin protein ligase from *Mycobacterium tuberculosis*. *Chem. Biol.* **2011**, *18* (11), 1432–1441.
(17) Polyak, S. W.; Chapman-Smith, A.; Brautigan, P. J.; Wallace, J. C. Biotin protein ligase from *Saccharomyces cerevisiae*. The N-terminal domain is required for complete activity. *J. Biol. Chem.* **1999**, *274* (46), 32847–32854.
(18) Pendini, N. R.; Polyak, S. W.; Booker, G. W.; Wallace, J. C.; Wilce, M. C. Purification, crystallization and preliminary crystallographic analysis of biotin protein ligase from *Staphylococcus aureus*. *Acta Crystallogr., Sect. F: Struct. Biol. Cryst. Commun.* **2008**, *64* (Part 6), 520–523.

513 dx.doi.org/10.1021/ml300106p | *ACS Med. Chem. Lett.* 2012, 3, 509–514

65

(19) Chapman-Smith, A.; Mulhern, T. D.; Whelan, F.; Cronan, J. E., Jr.; Wallace, J. C. The C-terminal domain of biotin protein ligase from *E. coli* is required for catalytic activity. *Protein Sci.* **2001**, *10* (12), 2608−2617.

(20) Mayende, L.; Swift, R. D.; Bailey, L. M.; Soares da Costa, T. P.; Wallace, J. C.; Booker, G. W.; Polyak, S. W. A novel molecular mechanism to explain biotin-unresponsive holocarboxylase synthetase deficiency. *J. Mol. Med. (Berlin)* **2012**, *90* (1), 81−88.

(21) Cleland, W. W. Steady State Kinetics. *The Enzymes* **1970**, *2*, 1.

(22) Szalecki, W. Synthesis of norbiotinamine and its derivatives. *Bioconjugate Chem.* **1996**, *7* (2), 271−273.

(23) Xu, Y.; Nenortas, E.; Beckett, D. Evidence for distinct ligand-bound conformational states of the multifunctional *Escherichia coli* repressor of biotin biosynthesis. *Biochemistry* **1995**, *34* (51), 16624−16631.

66

BIOTIN ANALOGUES WITH ANTIBACTERIAL ACTIVITY ARE POTENT INHIBITORS OF BIOTIN PROTEIN LIGASE

Tatiana P. Soares da Costa †, William Tieu ‡, Min Y. Yap ", Ondrej Zvarec ‡ , Jan Bell §, John D. Turnidge †§, John C. Wallace †, Grant W. Booker †, Matthew C. J. Wilce ", Andrew D. Abell ‡ , Steven W. Polyak †.

† School of Molecular and Biomedical Science, University of Adelaide, South Australia 5005, Australia.

‡ School of Chemistry and Physics, University of Adelaide, South Australia 5005, Australia.

" School of Biomedical Science, Monash University, Victoria, Australia.

§ Microbiology and Infectious Diseases Directorate, SA Pathology, Women's and Children's Hospital, South Australia 5006, Australia.

Supporting information

Contents

Supporting Experimental Methods

General synthetic chemistry methods

All reagents were from standard commercial sources and of reagent grade or as specified. Solvents were from standard commercial sources and used without further treatment, except for anhydrous THF and anhydrous dichloromethane that were dried and distilled according to reported procedures. [1] Reactions were monitored by ascending TLC using precoated plates (silica gel 60 F_{254}, 250 µm, Merck, Darmstadt, Germany), spots were visualised under ultraviolet light at 254 nm and with basic potassium permanganate dip. Column chromatography was performed with silica gel (40-63 µm 60 Å, Davisil, Grace, Germany). RP-HPLC was performed on HP Series 1100 with Phenomenex Gemini C18 5 µM (250 x 4.60 mm). ^{1}H and ^{13}C NMR spectra were recorded on a Varian Gemini 2000 (300 MHz) or a Varian Inova 600 MHz. Chemical shifts are given in ppm (δ) relative to the residue signals (DMSO-d_6 was 2.50 ppm for ^{1}H and 39.55 ppm for ^{13}C and CDCl$_3$ was 7.26 ppm for ^{1}H and 77.23 ppm for ^{13}C. High-resolution mass spectra (HRMS) were recorded on a Thermo Fisher Scientific LTQ orbitrap FT MS equipment (Δ < 2 ppm) at Adelaide Proteomics Centre, the University of Adelaide. Purity of biologically assayed compounds were determined using ^{1}H NMR or analytical RP-HPLC (>90%). Compounds **2 – 7** and **12 - 15** were synthesized as previously reported. [2-4]

Specific chemical synthesis and characterisation methods

(3a*S*,6a*R*)-4-(5-Azidopentyl)-1,3,3a,4,6,6a-hexahydrothieno[3,4-*d*]imidazol-2-one (Compound 10).

To a solution of biotin tosylate **8** [5] (151 mg, 0.39 mmol) in DMF (2 mL) was added sodium azide (32 mg, 0.48 mmol) and solution was stirred overnight under nitrogen atmosphere. The reaction mixture was poured into water (20 mL) and extracted with dichloromethane (3 x 25 mL). The organic layers were pooled and washed with brine (1 x 75 mL), dried over Na$_2$SO$_4$, filtered and concentrated *in vacuo*. The residue was purified by silica gel chromatography eluting with 5% methanol in dichloromethane

to give a white solid (86 mg, 86%). ^{1}**H NMR** (300 MHz, CDCl$_3$): 6.57 (1H, bs), 6.46 (1H, bs), 4.38-4.42 (1H, m), 4.20-4.24 (1H, m), 3.40 (2H, t, J = 6.9 Hz), 3.16-3.22 (1H, m), 2.91 (1H, dd, J = 5.1, 12.6 Hz), 2.66 (1H, d, J = 12.6 Hz), 1.37-1.78 (8H, m); ^{13}**C NMR** (300 MHz, DMSO-d$_6$): δ 164.30, 62.31, 60.35, 55.91, 51.56, 40.62, 28.93, 28.87, 28.71, 26.85.

(3a*S*,6a*R*)-4-(5-Aminopentyl)-1,3,3a,4,6,6a-hexahydrothieno[3,4-*d*]imidazol-2-one (Compound 11)

To a solution of biotin azide **10** [6] (80 mg, 0.31 mmol) in THF (2 mL) was added triphenylphosphine (106 mg, 0.41 mmol) and the solution was stirred at ambient temperature for 1 h, followed by addition of water (2 mL) and stirred for a further 3 h at 60 °C. The reaction mixture was filtered and the filtrand was diluted with water (20 mL) and extracted with dichloromethane (3 x 25 mL). The organic layer were pooled, dried over Na$_2$SO$_4$, filtered and concentrated *in vacuo*. The residue was purified by silica gel chromatography eluting with 10% methanol in dichloromethane to give a white solid (13 mg, 18%). ^{1}**H NMR** (300 MHz, CDCl$_3$): 6.51 (0.5H, bs, C(O)NH), 6.41 (0.5H, bs), 4.33-4.38 (1H, m), 4.15-4.20 (1H, m), 3.59 (2H, bs), 3.14-3.16 (1H, m), 2.87 (1H, dd, J = 7.5, 12.6 Hz), 2.56-2.64 (3H, m), 1.25-1.74 (8H, m); ^{13}**C NMR** (300 MHz, DMSO-d$_6$): 163.14, 79.61, 61.47, 59.64, 55.94, 41.35, 32.35, 28.87, 28.70, 26.74. **HRMS** calcd. for (M$^+$ + H) C$_{11}$H$_{20}$N$_2$OSNa: requires 230.1322, found 230.1319.

(3a*S*,6a*R*)-4-Hexyl-1,3,3a,4,6,6a-hexahydrothieno[3,4-*d*]imidazol-2-one (Compound 16)

To a solution of biotin tosylate **8** [5] (52 mg, 0.14 mmol) in anhydrous THF (2 mL) was added lithium aluminium hydride (15 mg, 0.41 mmol) and the solution was stirred under reflux for 3 h. The reaction mixture was cooled to ambient temperature and were added methanol (1 mL) and saturated aqueous sodium sulphate (2 mL), followed by concentration *in vacuo* and dissolving with 1:1 dichloromethane and methanol (15 mL) and stirring for 30 min. The solution was filtered and the filtrate was concentrated *in vacuo* and purified by silica gel chromatography eluting with 3%

methanol in dichloromethane to give an off white solid (16 mg, 56%). **^{1}H NMR** (300 MHz, CDCl$_3$): δ 5.27 (1H, bs), 5.16 (1H, bs), 4.49-4.53 (1H, m); 4.29-4.33 (1H, m), 3.14-3.20 (1H, m), 2.94 (1H, dd, J = 4.8, 12.6 Hz), 2.73(1H, d, J = 12.6 Hz), 1.62-1.70 (2H, m), 1.28-1.45 (4H, m), 0.89 (3H, t, J = 6.6 Hz); **^{13}C NMR** (300 MHz, DMSO-d$_6$): δ 163.16, 62.23, 60.41, 55.81, 40.92, 31.93, 29.52, 29.34, 28.98, 22.90, 14.39. **HRMS** calcd. for (M + H) C$_{10}$H$_{19}$N$_2$OS: requires 215.1218, found 215.1217.

(3aS,6aR)-4-Heptyl-1,3,3a,4,6,6a-hexahydrothieno[3,4-d]imidazol-2-one (Compound 17)

To a solution of homobiotin tosylate **9** [3] (5 mg, 0.013mmol) in anhydrous THF (1 mL) was added lithium aluminium hydride (3 mg, 0.079 mmol) and the solution was stirred under reflux for 3 h. The reaction mixture was cooled to ambient temperature and were added methanol (1 mL) and saturated aqueous sodium sulphate (2 mL), followed by concentration *in vacuo* and dissolving with 1:1 dichloromethane and methanol (15 mL) and stirring for 30 min. The solution was filtered and the filtrate was concentrated *in vacuo* and purified by silica gel chromatography eluting with 3% methanol in dichloromethane to give an off white solid (2 mg, 69%).**^{1}H NMR** (300 MHz, CDCl$_3$): δ 4.93 (1H, bs), 4.86 (1H, bs,), 4.50-4.54 (1H, m); 4.32 (1H, ddd, J = 1.5, 4.5, 7.5 Hz), 3.19 (1H, dt, J = 4.5, 7.5 Hz), 2.94 (1H, dd, J = 5.1, 12.9 Hz), 2.73 (1H, d, J = 12.9 Hz), 1.63-1.68 (2H, m), 1.26-1.45 (6H, m), 0.89 (3H, t, J = 6.9 Hz); **^{13}C NMR** (75 MHz, DMSO-d$_6$): δ 163.16, 62.23, 60.41, 55.81, 40.92, 31.93, 29.52, 29.34, 28.98, 22.90, 14.39. **HRMS** calcd. for (M + H) C$_{11}$H$_{21}$N$_2$OS: requires 229.1374 found 229.1369.

(4*S*,5*R*)-4-methyl-5-(oct-7-ynyl)imidazolidin-2-one (Compound 19)

18a   18b   18c

19
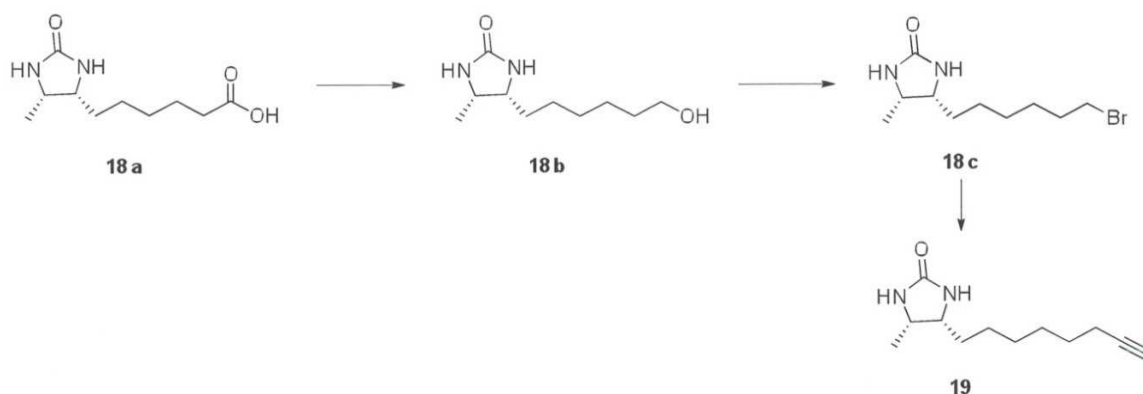
Compound **18b** was prepared from desthiobiotin **18a** (200 mg, 0.93 mmol) and according to the procedure outlined for compound **7**. [3] Yield (153 mg, 82%); **^{1}H NMR** (300 MHz, CDCl$_3$): δ 1.33 (3H, d, *J* = 6.6 Hz), 1.25-1.77 (11H, m), 3.62-3.71 (3H, m), 3.84 (1H, ddd, *J* = 13.5, 6.6, 6.6 Hz), 4.69 (1H, s), 5.11 (1H, s); **^{13}C NMR** (75 MHz, DMSO-d$_6$): δ 163.47, 62.65, 56.00, 51.38, 32.45, 29.50, 29.09, 26.38, 25.52, 15.74; **HRMS** calcd. for (M + Na) C$_{10}$H$_{20}$O$_2$N$_2$Na: requires 223.1422, found 223.1432.

To a stirred solution of triphenylphosphine (152 mg, 0.58 mmol) and 2,3-dichloro-5,6-dicyano-*p*-benzoquinone (DDQ) (130 mg, 0.58 mmol) in dry dichloromethane (10 mL) under a stream of nitrogen at ambient temperature was added tetrabutylammonium bromide (186 mg, 0.58 mmol) followed by addition of the compound **18b** (97 mg, 0.48 mmol) and stirred for 1 h. Volatiles where removed *in vacuo* and the crude residue purified by silica gel chromatography to give compound **18c** as an orange powder (113 mg, 89%).**^{1}H NMR** (300 MHz, CDCl$_3$): δ 1.46 (3H, d, *J* = 6.3 Hz), 1.29-1.47 (8H, m), 1.86 (2H, ddd, *J* = 14.25, 6.9, 6.9 Hz), 3.41 (1H, t, *J* = 6.9 Hz), 3.67-3.74 (1H, m), 3.86 (1H, ddd, *J* = 13.65, 6.6, 6.6 Hz), 4.44 (1H, s), 4.64 (1H, s); **^{13}C NMR** (300 MHz, DMSO-d$_6$): δ 163.06, 56.27, 51.37, 33.78, 32.58, 29.57, 28.71, 27.95, 26.34, 15.77; **HRMS** calcd. for (M + Na) C$_{10}$H$_{19}$O$_2$N$_2$Na: requires 285.0578, found 285.0584.

Compound **18c** (86 mg, 0.32 mmol) was reacted according to the procedure outlined for compound **14**. [3] The residue was purified by silica gel chromatography eluting with 5% methanol in dichloromethane to give the title compound (**19**) as an orange

powder (34 mg, 50%) **¹H NMR** (300 MHz, CDCl₃): δ 1.14 (3H, d, J = 6.3 Hz), 1.25-1.59 (10H, m), 1.95 (1H, dt, J = 2.55, 0.9 Hz), 2.19 (1H, ddd, J = 6.9, 6.9, 2.7 Hz), 3.67-3.73 (1H, m), 3.85 (1H, ddd, J = 13.8, 6.6, 6.6 Hz), 4.36 (1H, s), 4.54 (1H, s); **¹³C NMR** (300 MHz, DMSO-d₆): δ 163.75, 84.45, 68.16, 55.96, 51.23, 40.77, 29.52, 28.93, 28.36, 28.17, 26.20, 18.19, 15.57; **HRMS** calcd. for (M + Na) $C_{12}H_{20}ON_2Na$: requires 231.1473, found 231.1470.

Protein expression and purification

The expression and purification of recombinant *Sa*BPL [7], *Ec*BPL [8] and *Hs*BPL [9] were performed as previously described.

Nucleic acid manipulation

To generate a construct for over-expression of *Ec*BPL in *E. coli*, the *bir*A gene was placed under control of the IPTG-inducible, strong tac promoter. The gene was amplified by PCR using oligonucleotides B130 [5′-TCATGAAGGATAACACCGTGCCAC-3′] and B131 [5′-AAGCTTAATGATGATGATGATGATGTCCTTTTTCTGCACTACGCAGGG-3′] upon template pCY216 containing the *bir*A. [10] The resulting PCR product was digested with *BspH*1 and *Hind*111 and ligated into *Nco*1 and *Hind*111 treated pC104 [11], a derivative of pK223-3 (Amersham). This yielded the vector pK(*Ec*BPL-H6) that was confirmed by DNA sequence analysis (DNA Sequencing Service, SA Pathology, South Australia). *E. coli* K12 was transformed with pK (*Ec*BPL-H6) to address the mechanism of antibiotic action.

X-ray crystallography

Apo-*Sa*BPL was buffer exchanged into 50 mM Tris HCl pH 7.5, 50 mM NaCl, 1 mM DTT and 5% (v/v) glycerol, and concentrated to 5 mg/mL. Each compound was then added to BPL in a 10:1 molar ratio. The complex was crystallized using the hanging drop method at 4°C in 8 – 12% Peg 8000 in 0.1 M Tris pH 7.5 or 8.0, and 10% (v/v) glycerol as the reservoir. A single crystal was picked using a Hampton cryo-loop (Hampton Research, USA) and streaked through cryo-protectant containing 25% (v/v) glycerol in the reservoir buffer prior to cryo-cooling. X-ray diffraction data was collected using the macromolecular crystallography beamline (MX1) at the Australian Synchrotron using an ADSC Quantum 210r Detector. 90 images were collected with a 1 second exposure each and an oscillation angle of 1° for each frame. Data was integrated and scaled using XDS. [12] PDB and cif files for the compounds were obtained using the PRODRG web interface. [13] The co-ordinates from the *Sa*BPL –

biotinol-5-AMP (PDBID = 4DQ2)[3], with all water and ligands removed were used as a starting model. After rigid body refinement using REFMAC,[14] the models were built using cycles of manual modelling using COOT[15] and refinement with REFMAC.[14] The electron density clearly defined the positions of the ligands. The quality of the final models was evaluated using MOLPROBITY.[16] Data collection and refinement statistics are summarized in Supplementary Table S1.

In vitro biotinylation assays

Quantitation of BPL catalysed ^{3}H-biotin incorporation into the biotin domain substrate was performed as previously described[11, 17]. Briefly, the reaction mixture contained: 50 mM Tris HCl pH 8.0, 3 mM ATP, 4.5 µM biotin, 0.5 µM ^{3}H-biotin, 5.5 mM MgCl$_2$, 100 mM KCl, 0.1 mg/mL BSA and 10 µM biotin domain of *S. aureus* pyruvate carboxylase. The reaction was initiated by the addition of BPL to a final concentration of 4 nM. After 20 minutes at 37° C, 4 µL aliquots of the reaction were spotted onto Whatman paper pre-treated with biotin and trichloroacetic acid. The filters were washed twice with 10% v/v ice-cold trichloroacetic acid and once with ethanol before air-drying. Quantitation of protein-bound radiolabelled biotin was performed by liquid scintillation. One unit of enzyme activity was defined by the amount of BPL required to incorporate 1 nmol of biotin per minute. The IC_{50} value of each compound was determined from a dose-response curve by varying the concentration of the inhibitor under the same enzyme concentration. The data was analysed with GraphPad Prism using a non-linear fit of $\log_{10}$ (inhibitor) vs. normalized response. The K_i, the absolute inhibition constant for a compound, was determined using Eq 1:[18]

Eq 1. $$K_i = \frac{IC_{50}}{1 + \dfrac{[S]}{K_m}}$$

where [S] is the substrate concentration ([biotin] =5 µM) and K_m is the affinity of the enzyme for biotin (*S. aureus* BPL =1 µM[3], *E. coli* BPL = 0.3 µM[8] and human BPL = 1 µM[19]). The mode of inhibition was investigated by varying the concentrations of inhibitor alongside varying the concentrations of ^{3}H-biotin. The data was plotted as

double reciprocal plots and assessed using Lineweaver-Burk analysis. Ligand efficiency was calculated using Eq2: [20]

Eq 2. $LE = - RT \ln K_i$ / number of heavy atoms

where R is the gas constant and T is the temperature (^{o}Kelvin).

Surface Plasmon Resonance

SPR was performed using a Biacore™ T100 (GE Healthcare). BPL was immobilised on a CM5 sensor chip following the manufacturer's instructions. Typically, 6500 resonance units of *Sa*BPL were immobilised on the sensor chip. One channel was left blank which was subtracted from sample channel to allow analysis methods to distinguish between actual and non-specific binding. All experiments were conducted at 25°C at a flow rate of 30 µL/minute with running buffer containing 10 mM HEPES pH 7.4, 150 mM NaCl, 3 mM EDTA and 0.005% (v/v) surfactant. Regeneration of the surface was carried out by injecting 10 mM sodium acetate pH 5.8 at a flow rate of 30 µL/minute for 10 seconds. Zero concentration samples were used as blanks. Biotin and compound **6** showed fast on and off rates outside the range of kinetic quantification hence only K_D values could be estimated from equilibrium responses using compounds of different concentrations. In contrast, the association and dissociate rate constants for compounds **16** and **5** could be determined from the sensorgrams. The data were fitted to a 1:1 ligand binding model using the Biacore™ evaluation software. Buffers for experiments conducted with non-water soluble compounds contained 4% (v/v) DMSO.

The sensorgrams for the SPR experiments are shown in Figure 3. The concentrations of ligands employed were as follows: For biotin (Figure 1a) the concentrations used were 0 (-), 0.98 (-) , 3.9 (-), 7.8 (-), 31.3 (-), 62.5 (-) and 125 µM. For compound **6** (Figure 1b), the concentrations used were: 0 (-), 0.68 (-), 2.7 (-), 5.5 (-), 10.9 (-) and 43.8 (-) µM. For compounds **16** and **5** (Figure 1c and d), the concentrations used were: 0 (-), 0.4 (-), 0.8 (-), 1.6 (-) and 3.2 (-) µM.

Antibacterial Activity Evaluation

Minimal Inhibitory Concentrations (MICs) were determined by a microdilution broth method as recommended by the CLSI (Clinical and Laboratory Standards Institute, Document M07-A8, 2009, Wayne, Pa.) with cation-adjusted Mueller-Hinton broth (Trek Diagnostics Systems, U.K.). Compounds were dissolved using DMSO. Serial two-fold dilutions of each compound were made using DMSO as the diluent. Trays were inoculated with 5 x 10^4 CFU of each strain in a volume of 100 μL (final concentration of DMSO was 5% (v/v)), and incubated at 35° C for 16-20 hours when MICs were determined.

To address the antibiotic mechanism of action, a complementation assay was performed using *E. coli* K12 cells. Cells harbouring the *Ec*BPL over-expression vector pK(*Ec*BPL-H6) was employed. Bacteria, 5 x 10^4 CFU, were seeded in each well of a 96-well plate and treated either with compound **16** (final concentration 32 μg/mL) or DMSO control (final concentration 3.2% (v/v)) for 20 hours at 37° C. The final optical density of the culture was measured on a Thermo Multiskan Acsent plate reader at 620 nm.

Assay of cytotoxicity

HepG2 cells were suspended in Dulbecco-modified Eagle's medium containing 10% fetal bovine serum, and then seeded in 96-well tissue culture plates at either 5 000, 10 000 or 20 000 cells per well. After 24 hours, cells were treated with varying concentrations of compound, such that the DMSO concentration was consistent at 4% (v/v) in all wells. After treatment for 24 or 48 hours, WST-1 cell proliferation reagent (Roche) was added to each well and incubated for 0.5 hours at 37° C. The WST-1 assay quantitatively monitors the metabolic activity of cells by measuring the hydrolysis of the WST-1 reagent, the products of which are detectable at absorbance 450 nm.

Supporting References

1. Armarego, W. L. F.; Perrin, D. D., *Purification of laboratory chemicals.* 1997; Vol. 4, p 529.

2. Liu, F.-T.; Leonard, N. J., Avidin-biotin interaction. Synthesis, oxidation and spectroscopic properties of linked models. *J. Am. Chem. Soc.* **1979,** *101* (4), 996 - 1005.

3. Soares da Costa, T. P.; Tieu, W.; Yap, M. Y.; Pendini, N. R.; Polyak, S. W.; Sejer Pedersen, D.; Morona, R.; Turnidge, J. D.; Wallace, J. C.; Wilce, M. C.; Booker, G. W.; Abell, A. D., Selective inhibition of Biotin Protein Ligase from Staphylococcus aureus. *J Biol Chem* **2012**.

4. Szalecki, W., Synthesis of norbiotinamine and its derivatives. *Bioconjug Chem* **1996,** *7* (2), 271-3.

5. Corona, C.; Bryant, B. K.; Arterburn, J. B., Synthesis of a biotin-derived alkyne for pd-catalyzed coupling reactions. *Org Lett* **2006,** *8* (9), 1883-6.

6. Umeda, N.; Ueno, T.; Pohlmeyer, C.; Nagano, T.; Inoue, T., A photocleavable rapamycin conjugate for spatiotemporal control of small GTPase activity. *J Am Chem Soc* **2010,** *133* (1), 12-4.

7. Pendini, N. R.; Polyak, S. W.; Booker, G. W.; Wallace, J. C.; Wilce, M. C., Purification, crystallization and preliminary crystallographic analysis of biotin protein ligase from Staphylococcus aureus. *Acta Crystallogr Sect F Struct Biol Cryst Commun* **2008,** *64* (Pt 6), 520-3.

8. Chapman-Smith, A.; Mulhern, T. D.; Whelan, F.; Cronan, J. E., Jr.; Wallace, J. C., The C-terminal domain of biotin protein ligase from E. coli is required for catalytic activity. *Protein Sci* **2001,** *10* (12), 2608-17.

9. Mayende, L.; Swift, R. D.; Bailey, L. M.; Soares da Costa, T. P.; Wallace, J. C.; Booker, G. W.; Polyak, S. W., A novel molecular mechanism to explain biotin-unresponsive holocarboxylase synthetase deficiency. *J Mol Med (Berl)* **2012,** *90* (1), 81-8.

10. Chapman-Smith, A.; Turner, D. L.; Cronan, J. E.; Morris, T. W.; Wallace, J. C., Expression, biotinylation and purification of a biotin-domain peptide from the biotin carboxy carrier protein of Escherichia coli acetyl-CoA carboxylase. *Biochem. J.* **1994,** *302* (3), 881-887.

11. Polyak, S. W.; Chapman-Smith, A.; Mulhern, T. D.; Cronan, J. E., Jr.; Wallace, J. C., Mutational analysis of protein substrate presentation in the post-translational attachment of biotin to biotin domains. *J Biol Chem* **2001,** *276* (5), 3037-45.

12. Kabsch, W., Xds. *Acta Crystallogr D Biol Crystallogr* **2010,** *66* (Pt 2), 125-32.

13. Schuttelkopf, A. W.; van Aalten, D. M., PRODRG: a tool for high-throughput crystallography of protein-ligand complexes. *Acta Crystallogr D Biol Crystallogr* **2004,** *60* (Pt 8), 1355-63.

14. Winn, M. D.; Murshudov, G. N.; Papiz, M. Z., Macromolecular TLS refinement in REFMAC at moderate resolutions. *Methods Enzymol* **2003,** *374*, 300-21.

15. Emsley, P.; Cowtan, K., Coot: model-building tools for molecular graphics. *Acta Crystallogr D Biol Crystallogr* **2004,** *60* (Pt 12 Pt 1), 2126-32.

16.   Chen, V. B.; Arendall, W. B., 3rd; Headd, J. J.; Keedy, D. A.; Immormino, R. M.; Kapral, G. J.; Murray, L. W.; Richardson, J. S.; Richardson, D. C., MolProbity: all-atom structure validation for macromolecular crystallography. *Acta Crystallogr D Biol Crystallogr* **2010,** *66* (Pt 1), 12-21.

17.   Polyak, S. W.; Chapman-Smith, A.; Brautigan, P. J.; Wallace, J. C., Biotin protein ligase from Saccharomyces cerevisiae. The N-terminal domain is required for complete activity. *J Biol Chem* **1999,** *274* (46), 32847-54.

18.   Cheng, Y.; Prusoff, W. H., Relationship between the inhibition constant (K1) and the concentration of inhibitor which causes 50 per cent inhibition (I50) of an enzymatic reaction. *Biochem Pharmacol* **1973,** *22* (23), 3099-108.

19.   Bailey, L. M.; Ivanov, R. A.; Jitrapakdee, S.; Wilson, C. J.; Wallace, J. C.; Polyak, S. W., Reduced half-life of holocarboxylase synthetase from patients with severe multiple carboxylase deficiency. *Hum Mutat* **2008,** *29* (6), E47-57.

20.   Kuntz, I. D.; Chen, K.; Sharp, K. A.; Kollman, P. A., The maximal affinity of ligands. *Proc Natl Acad Sci U S A* **1999,** *96* (18), 9997-10002.

21.   Weiss, M. S., Global indicators of X-ray quality. *Journal of Applied Crystallography* **2001,** *34* (2), 130-135.
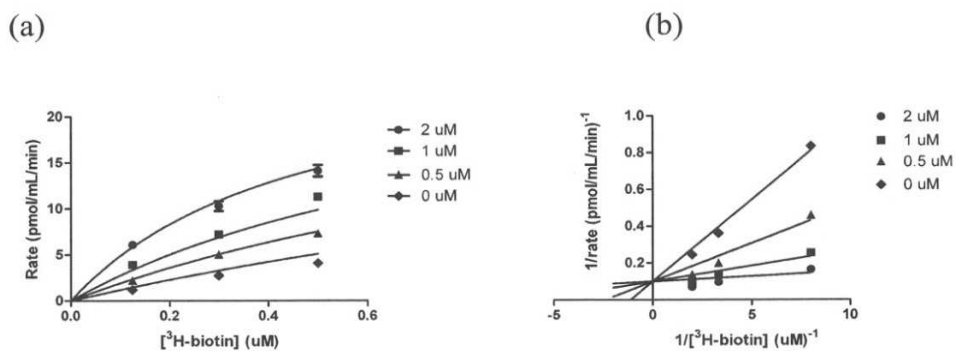
(a) (b)

Figure S1. Mechanism of inhibition is via competition with biotin.

Concentration dependent inhibition of *S. aureus* BPL by compound **16** and associated double reciprocal Lineweaver-Burk plot show that this compound is a competitive inhibitor of biotin. (a) Rate plot with different fixed concentrations of inhibitor and varying concentrations of ^{3}H-biotin, b) Double reciprocal Lineweaver-Burke plot of initial velocity curves against varying concentrations of ^{3}H-biotin.
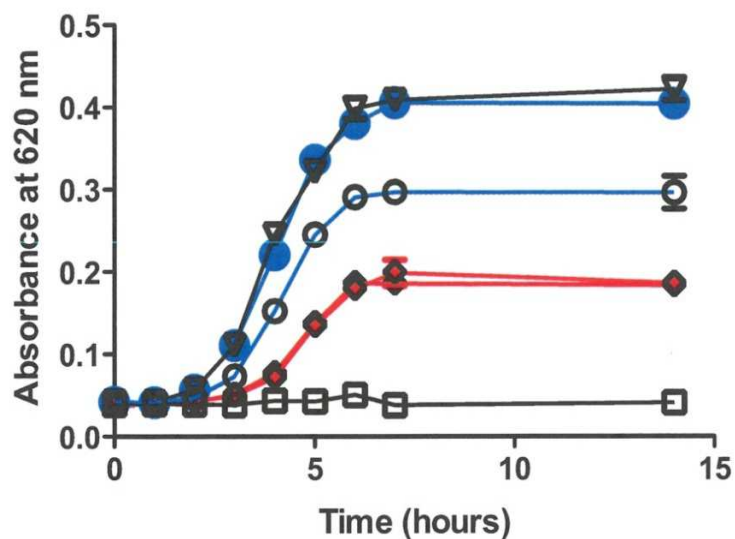
Figure S2. Mechanism of antibacterial activity is via inhibition of BPL.

E. coli K12 cells were transformed with either the parent vector pKK-223-3 (diamonds with red lines) or pK(*Ec*BPL-H6) (circles with blue lines) for the over-expression of *E. coli* BPL. Cells were the grown for 14 hours at 37°C in the presence or absence of 32 μg/ml compound **5** when the absorbance of the culture was measured at 600 nm. Protein expression was induced by the addition of IPTG into the growth media (solid symbols contain IPTG vs open symbols with no IPTG). A control with no compound was included (▽), as was a control with no bacteria (□).

Supporting Table S1. X-ray data collection and refinement. Data collection and refinement statistics for holo SaBPL structures with compounds **6** and **14** bound.

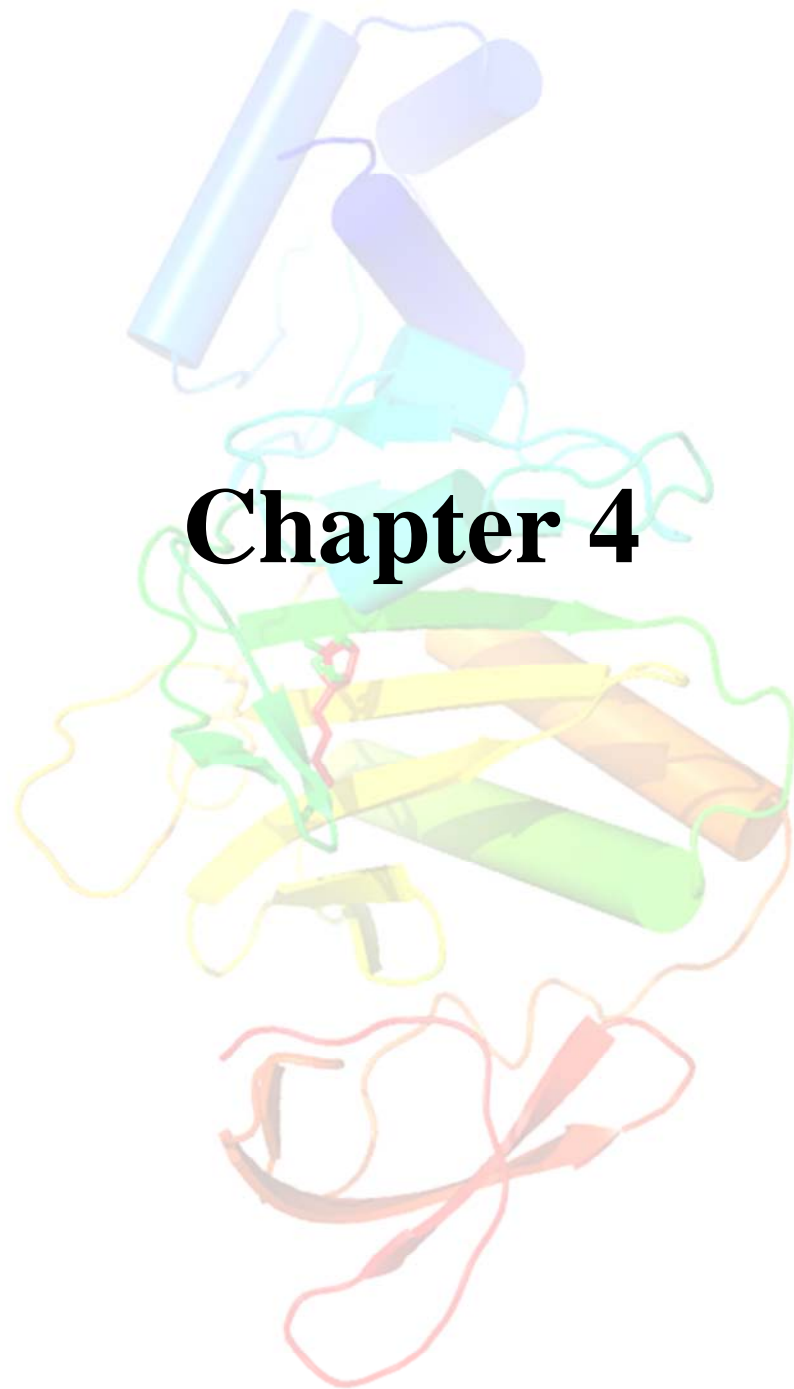|	Compound 6	Compound 14
Data collection		
Space group	$P4_22_12$	$P4_22_12$
Unit cell (*a,b,c*)	93.6, 93.6, 130.4	93.1, 93.1, 129.9
Resolution	50.00 -2.60 (2.67- 2.60)	50.00 - 2.65 (2.72-2.65)
Number of unique reflections	18454 (1329)	17103 (1234)
Multiplicity	6.9 (7.1)	5.4 (5.6)
Completeness	99.3% (99.6%)	99.3% (97.4%)
I/σ	13.9 (4.5)	17.4 (2.5)
R_{merge}	12.5% (70.5%)	8.1% (83.1%)
R_{pim}	2.8% (26.4%)	2.2 % (27.0%)
Refinement		
R_{factor}	19.7	19.7
R_{free}	26.8	24.2
r.m.s. deviations		
Bond lengths	0.022	0.022
Bond angles	1.96	2.05
Ramachandran plot		
Allowed regions	99.4%	98.7%
Outliers	0.7%	1.3%

[a] Values in parentheses refer to the highest resolution shell.

[b] $R_{merge} = \sum |I - <I>|/\sum<I>$ where I is the intensity of individual reflections.

[c] $R_{pim} = \sum[1/(N-1)]^{1/2}\sum |I - <I>|/\sum<I>$ [21]

[d] $R_{factor} = \sum_h|F_o - F_c|/ \sum_h|F_o|$, where F_o and F_c are the observed and calculated structure-factor amplitudes for each reflection "h".

[e] R_{free} was calculated with 5% of the diffraction data selected randomly and excluded from refinement.

Chapter 4

Statement of Authorship

Title of Paper	Optimising *in situ* click chemistry: The screening and identification of biotin protein ligase inhibitors.
Publication Status	○ Published ○ Accepted for Publication ● Submitted for Publication ○ Publication Style
Publication Details	Soares da Costa, T. P., Tieu, W., Yap, M. Y., Keeling, K. K., Wilce, M. C. J., Booker, G. W., Polyak, S. W., Abell, A. D. (2012) Optimising *in situ* click chemistry: The screening and identification of biotin protein ligase inhibitors. *Angwandte Chemie International Edition.* Manuscript under review.

Author Contributions

By signing the Statement of Authorship, each author certifies that their stated contribution to the publication is accurate and that permission is granted for the publication to be included in the candidate's thesis.

Name of Principal Author (Candidate)	Tatiana P. Soares da Costa		
Contribution to the Paper	Primary role in performing the *in situ* click experiments and analysis by HPLC. Performed protein expression, purification, kinetic analysis, inhibition assays, surface plasmon resonance studies, circular dichroism and western blot analyses. Assisted in manuscript preparation.		
Signature		Date	29/10/2012

Name of Co-Author	William Tieu		
Contribution to the Paper	Design, synthesis and chemical characterisation of most small molecules used in this study. Performed LC/MS. Assisted in manuscript preparation.		
Signature		Date	30/ʀ/12

Name of Co-Author	Min Y. Yap		
Contribution to the Paper	Solved crystal structures of *Sa*BPL in complex with inhibitors.		
Signature		Date	1/11/2012

Name of Co-Author	Kelly K. Keeling
Contribution to the Paper	Synthesis of small molecule inhibitors.
Signature		Date	4 /12 /2012.

Name of Co-Author	Matthew C. Wilce
Contribution to the Paper	Provided direction in all aspects of X-ray crystallography.
Signature		Date	5/11/2012

Name of Co-Author	Grant W. Booker
Contribution to the Paper	Provided direction and assistance in all aspects of protein chemistry.
Signature		Date	14/11/2012

Name of Co-Author	Steven W. Polyak
Contribution to the Paper	Performed site directed mutagenesis on SaBPL. Provided direction in all aspects of enzymology.
Signature		Date	1/11/2012

Name of Co-Author	Andrew D. Abell
Contribution to the Paper	Provided direction in all aspects of synthetic chemistry and involved in manuscript preparation.
Signature		Date	3/12/2012

Optimising *in situ* click chemistry: the screening and identification of biotin protein ligase inhibitors

Tatiana P. Soares da Costa, William Tieu, Min Y. Yap, Kelly L. Keeling, Matthew C. J. Wilce, John C. Wallace, Grant W. Booker, Steven W. Polyak, Andrew D. Abell*

The Huisgen cycloaddition of an alkyne and an azide can, in special cases, be catalysed by an enzyme in what is referred to as *in situ* click chemistry.[1-8] This then provides the basis of an elegant approach for identifying enzyme inhibitors, where the target enzyme is used to select and assemble the optimum combination of an azide and alkyne from a library of each.[4,8,9,10] However, this methodology is limited to situations where the target enzyme has binding pockets capable of bringing the two fragments together for subsequent Huisgen cycloaddition. The goal of producing high-affinity inhibitors can also be a limitation of this methodology, since tight-binding inhibitors often remain associated in the protein's active site, thereby preventing multiple rounds of catalysis. Here we present an example of *in situ* click chemistry that overcomes these inherent limitations, whereby the target enzyme (biotin protein ligase, BPL) is specifically engineered to promote efficient catalytic turnover and hence Huisgen cycloaddition.

Ms. T. P. Soares da Costa, A/Prof. G. W. Booker, Dr. S. W. Polyak, Prof J. C. Wallace
School of Molecular and Biomedical Science
University of Adelaide
Adelaide, South Australia, 5005, Australia

Dr. W. Tieu, Ms. K. L. Keeling, Prof. A. D. Abell
School of Chemistry and Physics
University of Adelaide
Adelaide, South Australia, 5005, Australia
Fax: (+61) 883035652
E-mail: Andrew.abell@adelaide.edu.au

Ms. M. Y. Yap, A/Prof. M. C. J. Wilce
School of Biomedical Science
Monash University
Victoria, 3800, Australia

Our choice of target enzyme for this study was motivated by our recent report that triazoles (e.g. **1**, see Scheme 1) are potent and selective inhibitors of BPL from the clinically important bacterial pathogen *Staphylococcus aureus* (*Sa*).[12] BPL catalyses the stepwise formation of biotinyl-5′-AMP (which the triazoles mimic) from biotin and ATP, see Scheme 1. Biotinyl-5′-AMP then enables biotinylation of enzymes central to fatty acid biosynthesis[13] and the tricarboxylic acid cycle[14]. Examples of the triazoles inhibit the growth of these bacteria and as such they represent an important new lead for antibiotic development.[12,15,16] The triazoles are prepared by Huisgen cycloaddition of biotin alkyne **2** and adenosine azide **3** fragments as depicted in Scheme 1.[12]

We deemed *Sa*BPL to be an ideal candidate for *in situ* click chemistry since its active site has two well-defined pockets. Initial binding of biotin to pocket one defines a biotin-binding loop, consisting of residues T117–K131, which locks biotin in place while also defining a second pocket for the subsequent binding of ATP for reaction with biotin to give biotinyl-5′-AMP.[12,17] Our X-ray crystal structures of *Sa*BPL show that these biotin and ATP-binding sites are juxtaposed, with the phosphoanhydride linkage in biotinyl-5′-AMP residing between the two pockets.[12] The enzyme thus functions much like the Cu(I) catalyst used in the chemical preparation of **1**, where the biotin and ATP species are co-located for specific reaction in both cases.
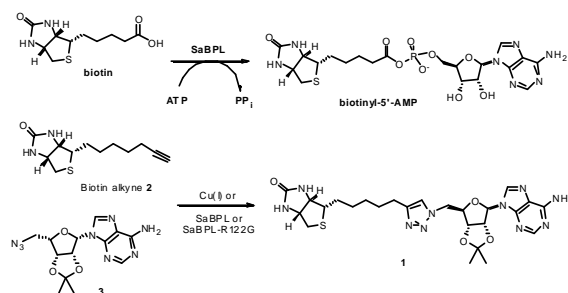
Scheme 1. *Sa*BPL catalysed reaction of biotin and ATP (top) and synthesis of 1,4-triazole **1** from biotin alkyne **2** and azide **3** (bottom).

We thus attempted an *in situ* experiment using wild-type *Sa*BPL as a template to bind and catalyse Huisgen cycloaddition of alkyne **2** (*Sa*BPL $K_i = 0.30 \pm 0.03$ μM)[18] with azide **3**, see Scheme 1. Analysis of the crude product by reverse phase HPLC (see Figure 1a) indicated 1.07 ± 0.1 mol of triazole formed per mol of enzyme (see supporting data for detail). The product formed is presumed to be the 1,4-triazole **1** ($K_i = 1.83 \pm 0.33$ μM)[12], given that the alternative 1,5-isomer is inactive and hence unable to bind. For comparison, *in situ* click catalysis by acetylcholinesterase gives a similarly low conversion (2 ± 1 moles of the triazole product for every mole of active enzyme).[2] Encouragingly, the triazole **1** was not formed in the absence of BPL, or using bovine serum albumin, such that the observed chemical ligation is template guided (Figure 1c and d).

Given this preliminary success an *in situ* experiment was attempted using the alkyne **2** and a small library of azides **3-7**, see Scheme in Figure 2. The azide **3** was used as a reference, while **4-7** were used to probe the importance of the furanose ring and the length of the azide spacer with regards to potency. However, in this case triazole products were not detected by HPLC (see Figure 2a), nor LC/MS-SIM above the level of background that was observed on reaction in the absence of enzyme, see Figure 2c (compare red and blue traces) for triazole **8**. We reasoned that this lack of success reflected a low turnover rate for the wild-type BPL, an inherent limitation of BPL (and presumably other enzymes) for use of *in situ* chemistry.
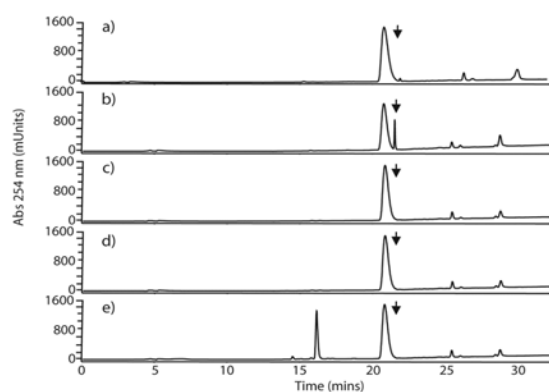

Figure 1. HPLC traces from the *in situ* click reactions of **2** and **3** as measured at 254 nm (a) In the presence of wild-type *Sa*BPL, (b) In the presence of *Sa*BPL-R122G, (c) In the absence of enzyme, (d) In the presence of bovine serum albumin instead of BPL, (e) In the presence of *Sa*BPL-R122G and biotinol-5′-AMP (Rt 16.7 mins). The arrow indicates the retention time of triazole **1**.

Attention was therefore focussed on improving the catalytic efficiency of the target enzyme, *Sa*BPL. We suspected that the before mentioned biotin-binding loop, might be closing over the active site to prevent diffusion of the synthesized triazole from the active site and thereby preventing efficient turnover. This loop is maintained in this 'closed' conformation, primarily due to an interaction between R122 in the biotin-binding loop and D180 that resides in the C-terminal domain (see later and Figure 3b). We reasoned that an engineered variant of *Sa*BPL, with R122 substituted by glycine, would improve production of triazole **1** by increasing the enzyme's turnover rate. In support, studies with *Escherichia coli* BPL have demonstrated that mutation of the equivalent residue (R118) results in enhanced dissociation rates for both biotin and biotinyl-5′-AMP.[19]

Encouragingly, SPR and kinetic data demonstrated that the affinities for the substrates biotin and MgATP were not compromised by the amino acid substitution (Table 1 & supporting information Figure S1 and Table S1). Likewise, circular dichroism spectra for the wild-type and R122G mutant were super-imposable, demonstrating secondary structural conservation of the two proteins (supporting information Figure S2). However, the R122G

mutant did possess unique properties not observed in the wild-type protein that were favourable for this study. Only *Sa*BPL-R122G was able to promiscuously biotinylate non-target bacterial proteins when recombinantly expressed in *E. coli*, the result of increased diffusion of the reactive biotinyl-5′-AMP intermediate from the enzyme (supporting information Figure S3). This 'leaky' phenotype was likewise confirmed by SPR studies as outlined in supporting information Figure S4. The equilibrium dissociation constant for triazole **1** and **8** with *Sa*BPL-R122G was determined to be >40-fold higher than with the wild-type enzyme (Table 1) due to an increased dissociation rate. Thus, the R122G mutant is an ideal candidate for the discovery of BPL inhibitors using *in situ* click chemistry.
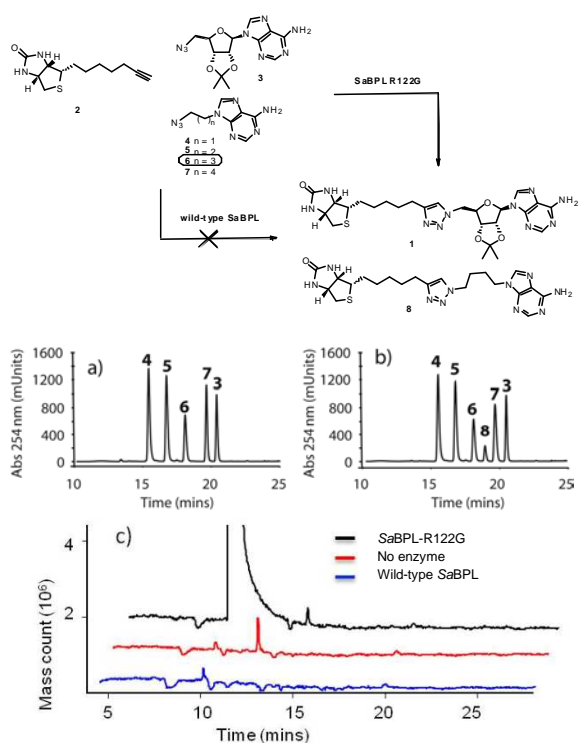

Figure 2. Analysis of BPL templated *in situ* click reactions of alkyne **2** with azides **3-7**. a) in the presence of wild-type *Sa*BPL, HPLC (detection at 254 nm); b) in the presence of *Sa*BPL-R122G, HPLC (detection at 254 nm) and c) overlay of LC/MS-SIM traces for *Sa*BPL-R122G (black, off scale), BPL (blue) and control (red) with detection at *m/z* 471 for triazole **8** evident at 10.1 min.

Table 1. Equilibrium dissociation kinetics for binding of biotin, AMP and triazole compounds to *Sa*BPL and *Sa*BPL-R122G analysed by SPR. [a]Data were fitted to either a steady-state affinity model or 1:1 ligand binding model.

*Sa*BPL	K_D (µM)			
	Biotin	AMP	Triazole **1**	Triazole **8**
Wild-type	9.2±1.4	900±80	0.11±0.01	0.06±0.01
R122G	8.7±0.9	920±80	9.83±0.04	2.96±0.11

[a] see supplementary methods for details

Significantly, an *in situ* click reaction of biotin alkyne **2** (500 μM) and azide **3** (500 μM) with *Sa*BPL-R122G (2 μM) gave vastly improved formation of triazole (11.9 ± 0.7 moles per mol of enzyme (*n* = 3) by HPLC, see Figure 1b. Triazole product was not observed when *Sa*BPL R122G was incubated with **2** and **3** in the presence of a competitive BPL inhibitor, biotinol-5′-AMP (K_i = 0.03 ± 0.01 μM) (Figure 1e). This clearly demonstrates that the mutant enzyme *Sa*BPL-R122G provides a template for cycloaddition, with an increased turnover rate compared to the wild-type enzyme. The 'leaky' mutant thus provides much improved efficiency of reaction and sensitivity of detection.

The library experiment using biotin alkyne **2** (160 μM) and azides **3-7** (320 μM each) was repeated using our 'leaky' mutant as depicted in Figure 2. Analysis of the product mixture by HPLC and LC/MS-SIM revealed efficient formation of 1,4-triazole **8** (see Figure 2b and black trace in Figure 2c, respectively). Interestingly, a trace of the 1,4-triazole **1** (or its 1,5-triazole regioisomer) was also detected at a level slightly above background by MS (see supporting information Figure S5(F)) and LC/MS-SIM (see supporting information Figure S6), but not by HPLC (see Figure 2b). None of the other possible triazole products were detected. As before, the addition of biotinol-5′-AMP, to the *in situ* experiment inhibited the formation of triazole product (supporting information Figure S5 (E)). As expected, control experiments in the absence of BPL, or with bovine serum albumin in place of *Sa*BPL-R122G (supporting information Figure S4), failed to produce any triazole product.

The 10 possible triazoles from the reaction of biotin alkyne **2** with the azide library (**3-7**) were independently synthesised and characterised to confirm that *Sa*BPL-R122G had indeed selected and synthesised the most potent inhibitors of the wild-type *Sa*BPL, see supporting information Table S2. Each compound was separately assayed against wild-type *Sa*BPL in an *in vitro* biotinylation assay to reveal that the 1,4-triazoles **1** and **8** were the only active triazoles, with **8** being the most potent (K_i = 0.66 ± 0.05 μM c.f. 1.83 ± 0.33 μM for **1**). This potency profile matches the results from the *in situ* click experiment, where **8** was the predominant product formed along with a trace amount of **1**. Neither of the 1,5-triazole regioisomers of **1** and **8** were active, highlighting selectivity of binding to *Sa*BPL and hence *in situ* synthesis of the 1,4-isomers. Additionally, SPR analysis as presented in supporting information Figure S4, indicated both triazoles **1** and **8** had faster dissociation kinetics with *Sa*BPL-R122G compared to the wild-type enzyme. This is in agreement with our hypothesis that the mutant encourages multiple catalytic cycles through release of the triazole products.

An *in situ* reaction of biotin alkyne **2** with a new azide **S9** was also undertaken in the presence of both wild-type and 'leaky' mutant *Sa*BPL in order to further explore its potential, see supporting data. Again, the 'leaky' mutant catalysed the efficient formation of triazole **S10**, whilst the wild-type was ineffective as depicted in supporting information Figure S7. The product triazole (K_i = 0.09 ± 0.01 μM)[12] proved to be significantly more active than the acetylene fragment (K_i = 0.30 ± 0.03 μM) and it is as such an important lead for ongoing antibiotic development.[12,18,20]

Finally, the X-ray crystal structure of **8** bound to *Sa*BPL (PDB = 1V7R) was solved to define its mode of binding, particularly with regards the role of the key R122 residue, see Figure 3. Significantly, R122 does not hydrogen bond or otherwise interact with the biotin or adenine component, *i.e.* R122 is not necessary for binding. While R122 forms a hydrogen bond with N3 of the 1,4-triazole, it does so through its backbone amide, which is conserved in the mutant. These observations, together with the kinetic analyses described in Table 1, suggests that the mutant is a good model for the wild-type enzyme and hence for screening inhibitors. The guanidinium group of R122 does hydrogen bond with D180 and D320 (see Figure 3b), which are thought to stabilise the key flexible biotin-binding loop. The X-ray structure also reveals that both the adenine and biotin components of **8** bind into their respective pockets with a number of key interactions. The ureido ring of biotin hydrogen bonds with S93, T94 and E116, where these residues are reported to be instrumental in anchoring the biotin within the active site. The adenine ring is ideally positioned in the ATP pocket for π- π stacking interaction with W127 and also hydrogen bonding with N212. The 1,4-triazole ring adopts key hydrogen bonds with R122, R125 and D180 and also an apparent edge to face π-π interaction with W127 (Figure 3b). The absence of a ribose group, present in the natural substrate biotinyl-5′-AMP and our lead inhibitor **1**, is clearly accommodated with an appropriate linker length (n = 3 as in triazole **8** and its precursor azide **6**, Scheme 2).
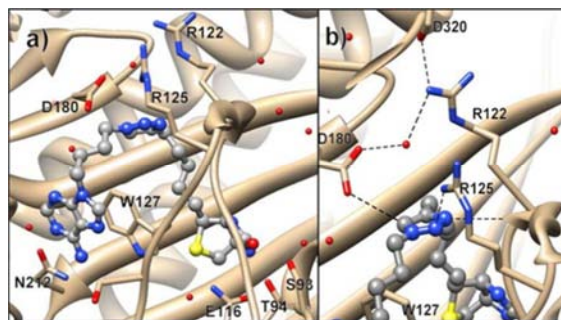

Figure 3. X-ray crystal structure of 1,4-triazole **8** bound to wild-type *Sa*BPL. a) A close up view of the active site with W127 partitioning the two binding pockets. b) Detailed hydrogen bonding interactions between *Sa*BPL and the 1,2,3-triazole ring (black dashes), specifically between R122, H_2O, D180 and D320. Distances summarised in supporting information Figure 6. Graphics performed with UCSF chimera 1.6.1

In summary, we use a 'leaky' mutant (*Sa*BPL-R122G) of wild- type *Sa*BPL to enhance the turnover rate for the reaction of biotin alkyne with an azide to give a triazole. This allows the enzyme to select the optimum triazole-based inhibitor using a library of such azides in a single experiment, with improved efficiency and sensitivity of detection, difficulties that can restrict the

general utility of a multi-component *in situ* click approach to ligand optimisation. The leaky mutant has a 40-fold enhanced rate of product dissociation relative to the target enzyme (*Sa*BPL). Importantly, the overwhelming major product (**8**) identified in this library-based experiment was the most potent inhibitor. Our study also clearly shows that the ribose sugar present in our lead inhibitors (**1** and biotinol-5′-AMP) and in the natural intermediate (biotinyl-5′-AMP)[12, 18] is not required for activity, with incorporation of the appropriate linker length between the triazole and adenine groups as in **8**.

Improving the efficiency of the target enzyme (as reported here for BPL) presents one approach to improving the generality and utility of multi-component *in situ* click beyond the few examples reported to date. Such an approach provides a means to enhance sensitivity of detection, to allow improved identification of weak inhibitors or even an extended population of inhibitors resulting from a large library of precursor fragments.
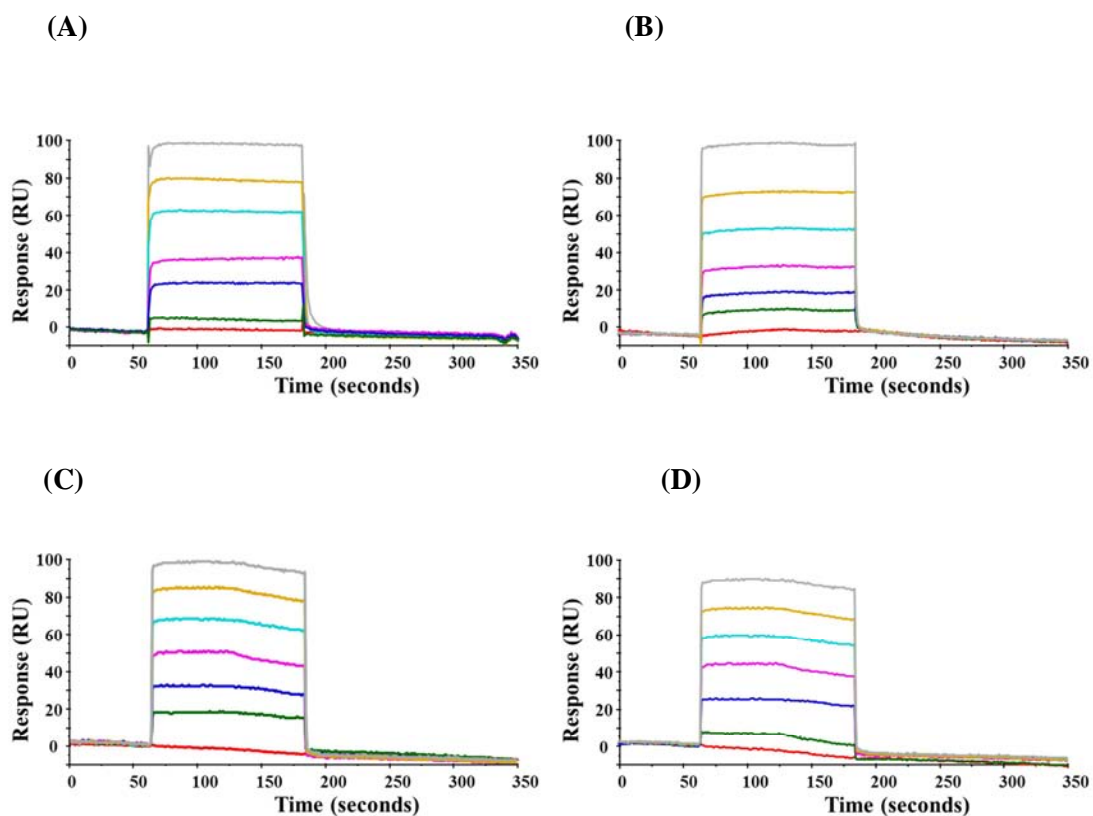
[1] S. K. Mamidyala, M. G. Finn, *Chemical Society Reviews* **2010**, *39*, 1252-1261.

[2] W. G. Lewis, L. G. Green, F. Grynszpan, Z. Radić, P. R. Carlier, P. Taylor, M. G. Finn, K. B. Sharpless, *Angewandte Chemie International Edition* **2002**, *41*, 1053-1057.

[3] V. P. Mocharla, B. Colasson, L. V. Lee, S. Röper, K. B. Sharpless, C.-H. Wong, H. C. Kolb, *Angewandte Chemie International Edition* **2005**, *44*, 116-120.

[4] M. Whiting, J. Muldoon, Y.-C. Lin, S. M. Silverman, W. Lindstrom, A. J. Olson, H. C. Kolb, M. G. Finn, K. B. Sharpless, J. H. Elder, V. V. Fokin, *Angewandte Chemie International Edition* **2006**, *45*, 1435-1439.

[5] T. Hirose, T. Sunazuka, A. Sugawara, A. Endo, K. Iguchi, T. Yamamoto, H. Ui, K. Shiomi, T. Watanabe, K. B. Sharpless, S. Omura, *The Journal of Antibiotics* **2009**, *62*, 277-282.

[6] H. D. Agnew, R. D. Rohde, S. W. Millward, A. Nag, W.-S. Yeo, J. E. Hein, S. M. Pitram, A. A. Tariq, V. M. Burns, R. J. Krom, V. V. Fokin, K. B. Sharpless, J. R. Heath, *Angewandte Chemie International Edition* **2009**, *48*, 4944-4948.

[7] S. W. Millward, R. K. Henning, G. A. Kwong, S. Pitram, H. D. Agnew, K. M. Deyle, A. Nag, J. Hein, S. S. Lee, J. Lim, J. A. Pfeilsticker, K. B. Sharpless, J. R. Heath, *Journal of the American Chemical Society* **2011**, *133*, 18280-18288.

[8] N. P. Grimster, B. Stump, J. R. Fotsing, T. Weide, T. T. Talley, J. G. Yamauchi, Á. Nemecz, C. Kim, K.-Y. Ho, K. B. Sharpless, P. Taylor, V. V. Fokin, *Journal of the American Chemical Society* **2012**, *134*, 6732-6740.

[9] A. Krasiński, Z. Radić, R. Manetsch, J. Raushel, P. Taylor, K. B. Sharpless, H. C. Kolb, *Journal of the American Chemical Society* **2005**, *127*, 6686-6692.

[10] R. Manetsch, A. Krasiński, Z. Radić, J. Raushel, P. Taylor, K. B. Sharpless, H. C. Kolb, *Journal of the American Chemical Society* **2004**, *126*, 12809-12818.

[11] J. G. Yamauchi, K. Gomez, N. Grimster, M. Dufouil, Á. Nemecz, J. R. Fotsing, K.-Y. Ho, T. T. Talley, K. B. Sharpless, V. V. Fokin, P. Taylor, *Molecular Pharmacology* **2012**, *82*, 687-699.

[12] T. P. Soares da Costa, W. Tieu, M. Y. Yap, N. R. Pendini, S. W. Polyak, D. Sejer Pedersen, R. Morona, J. D. Turnidge, J. C. Wallace, M. C. J. Wilce, G. W. Booker, A. D. Abell, *Journal of Biological Chemistry* **2012**.

[13] N. R. Pendini, L. M. Bailey, G. W. Booker, M. C. Wilce, J. C. Wallace, S. W. Polyak, *Biochimica et Biophysica Acta (BBA) - Proteins and Proteomics* **2008**, *1784*, 973-982.

[14] S. Jitrapakdee, M. St maurice, I. Rayment, W. W. Cleland, J. C. Wallace, P. V. Attwood, *Biochemical Journal* **2008**, *413*, 369-387.

[15] D. J. Payne, M. N. Gwynn, D. J. Holmes, D. L. Pompliano, *Nature Reviews Drug Discovery* **2007**, *6*, 29-40.

[16] Benjamin P. Duckworth, Todd W. Geders, D. Tiwari, Helena I. Boshoff, Paul A. Sibbald, Clifton E. Barry Iii, D. Schnappinger, Barry C. Finzel, Courtney C. Aldrich, *Chemistry & Biology* **2011**, *18*, 1432-1441.

[17] Also observed in other clinically relevant bacteria, see: Z. A. Wood, L. H. Weaver, P. H. Brown, D. Beckett, B. W. Matthews, *Journal of Molecular Biology* **2006**, *357*, 509-523; B. Bagautdinov, C. Kuroishi, M. Sugahara, N. Kunishima, *Journal of Molecular Biology* **2005**, *353*, 322-333; C. M. Tron, I. W. McNae, M. Nutley, D. J. Clarke, A. Cooper, M. D. Walkinshaw, R. L. Baxter, D. J. Campopiano, *Journal of Molecular Biology* **2009**, *387*, 129-146; V. Gupta, R. K. Gupta, G. Khare, D. M. Salunke, A. Surolia, A. K. Tyagi, *PLoS ONE* **2010**, *5*, e9222.

[18] T. P. Soares da Costa, W. Tieu, M. Y. Yap, O. Zvarec, J. M. Bell, J. D. Turnidge, J. C. Wallace, G. W. Booker, M. C. J. Wilce, A. D. Abell, S. W. Polyak, *ACS Medicinal Chemistry Letters* **2012**, *3*, 509-514.

[19] K. Kwon, E. D. Streaker, D. Beckett, *Protein Science* **2002**, *11*, 558-570.

[20] PCT/AU2012/001138.

Supporting Information

Table S1. Kinetic characterisation of wild-type *Sa*BPL and *Sa*BPL-R122G.

	Biotin			MgATP		
	k_{cat} (s^{-1}) x 10^3	K_m (mM)	k_{cat}/K_m (s^{-1} M^{-1}) x 10^4	k_{cat} (s^{-1}) x 10^3	K_m (mM)	k_{cat}/K_m (s^{-1} M^{-1}) x 10^4
Wild-type *Sa*BPL	450±90	1.01±0.16	4500±190	360±70	0.18±0.03	20±0.2
*Sa*BPL-R122G	0.20±0.01	1.68±0.24	1.70±0.10	0.15±0.01	0.18±0.03	0.08±0.01

Figure S1. SPR analysis of biotin and AMP binding. Sensorgrams showing binding of various concentrations of biotin[a] to either wild-type *Sa*BPL (A) or *Sa*BPL-R122G (B). Sensorgrams showing binding of various concentrations of AMP[b] to either wild-type *Sa*BPL (C) or *Sa*BPL-R122G (D). AMP binding was measured after injection of saturating concentrations of biotin alkyne (100 µM) to pre-charge the BPLs. Enzymes were immobilised onto the same CM5 chip using standard amine coupling chemistry. One channel was left blank to detect non-specific binding to the sensor chip.

(A)

(B)

(C)

(D)

[a] Concentration of biotin: 500 µM (grey), 125 µM (yellow), 31.3 µM (cyan), 7.8 µM (magenta), 0.98 µM (blue), 0.24 µM (green), 0 µM (red).

[b] Concentration of AMP: 10 µM (grey), 5 µM (yellow), 2.5 µM (cyan), 1.25 µM (magenta), 0.6 µM (blue), 0.15 µM (green), 0 µM (red).

Figure S2. Overlaid CD spectra of wild-type *Sa*BPL (red) and *Sa*BPL-R122G (blue), demonstrating that the amino acid substitution at position 122 had no discernible effect upon the enzyme's secondary structure.
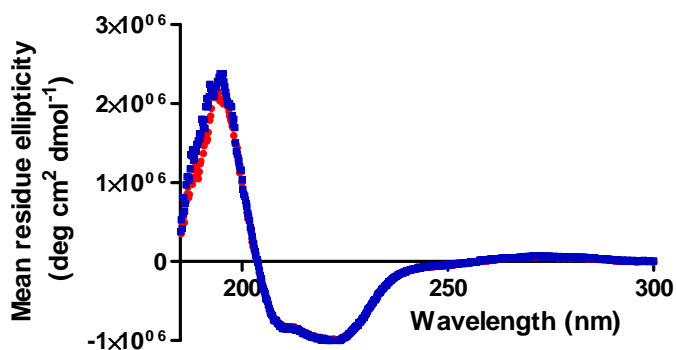
Figure S3. Streptavidin western blot analysis of soluble whole cell lysates. The lysates were separated by 12% SDS-PAGE and analysed by western blotting with streptavidin conjugated to Alexa488. Lane 1, Empty vector control; Lane 2, *Ec*BPL; Lane 3, *Ec*BPL-R118G; Lane 4, *Sa*BPL; Lane 5, *Sa*BPL-R122G. The arrows indicate the bands corresponding to biotin protein ligase (BPL) and the endogenous biotinylated protein in *E. coli*, the biotin carboxyl carrier protein (BCCP) subunit from acetyl-CoA carboxylase. The streptavidin blot shows 'promiscuous biotinylation' of non-target bacterial proteins caused by over-expression of the *Ec*BPL-R118G and *Sa*BPL-R122G mutants but not their wild-type equivalents. The promiscuous biotinylation phenotype is indicative of enhanced dissociation of biotinyl-5′-AMP from the enzyme where it can chemically modify non-target proteins.
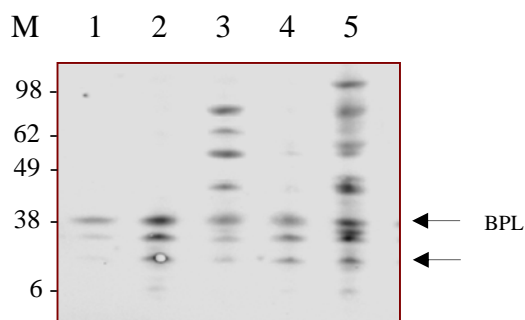
Figure S4. SPR profiles of different concentrations[a] of 1 binding to wild-type *Sa*BPL (A) and *Sa*BPL-R122G (C) and compound 8 binding to wild-type *Sa*BPL (B) and *Sa*BPL-R122G (D). Both enzymes were immobilised onto the same CM5 chip using standard amine coupling chemistry, leaving one channel (red) blank. Although compounds show similar association rates with both enzymes, the compounds dissociate more rapidly when arginine 122 is mutated to a glycine residue.

(A)

(B)

(C)

(D)
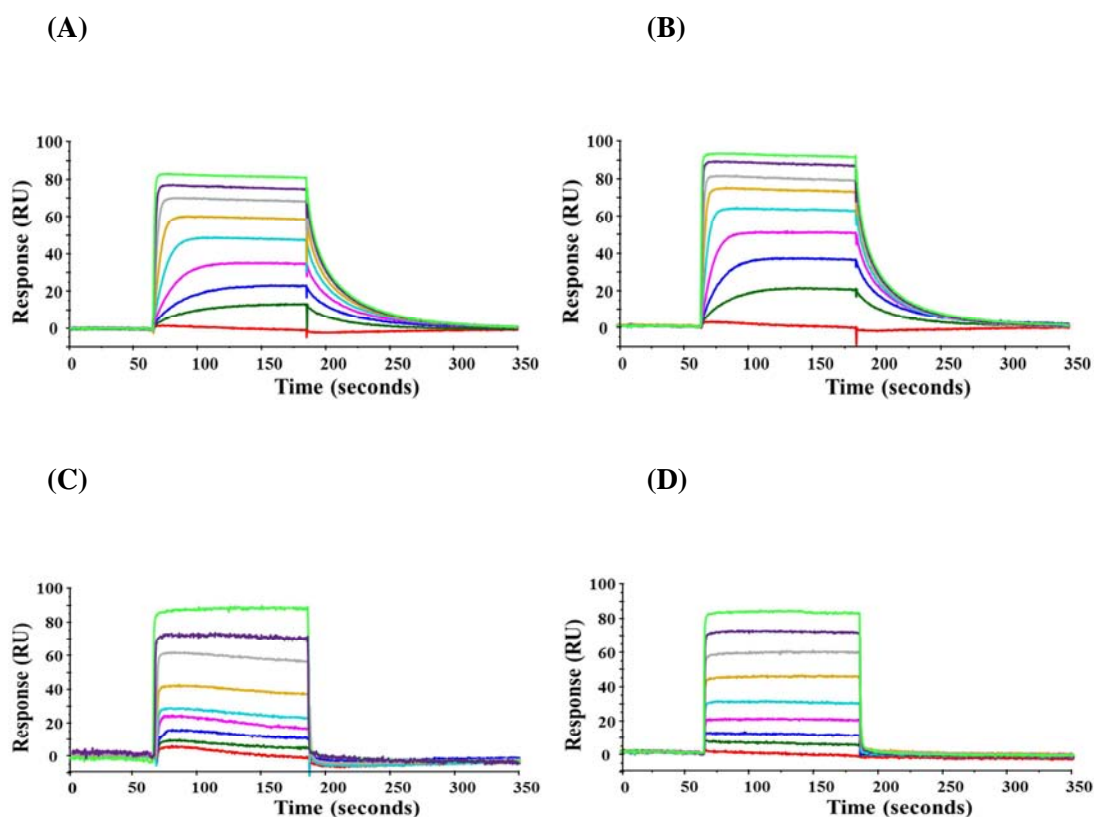
[a] Concentration of compound **1** or **8**: 5 µM (light green), 2.5 µM (purple), 1.25 µM (grey), 0.625 µM (yellow), 0.31 µM (cyan), 0.15 µM (magenta), 0.075 µM (blue), 0.036 µM (dark green), 0 µM (red).

Figure S5. Analysis of products from *in situ* click reaction of alkyne 2 with azides **3**–**7** by HPLC (measured at 254 nm) and mass spectrometry. (A) In the presence of wild-type *Sa*BPL, (B) In the presence of *Sa*BPL-R122G showing triazole **8** at ~18 min, (C) In the absence of enzyme, (D) In the presence of bovine serum albumin instead of BPL, (E) In the presence of *Sa*BPL-R122G and biotinol-5´-AMP, which is evident at 16.7 min (F) Mass spectrum of sample giving rise to (B) revealing triazole **8** (470.4 Da) and a trace of triazole 1 (570.3 Da).

(A)
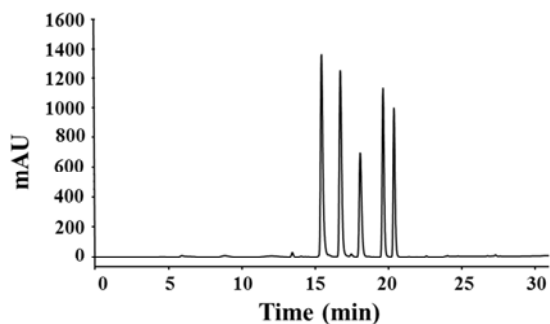
(B)
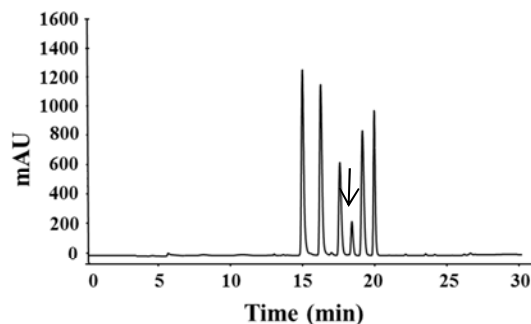
(C)
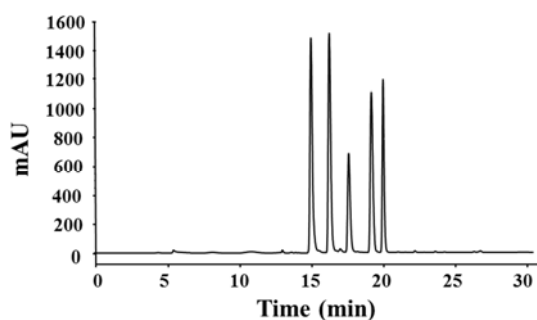
(D)
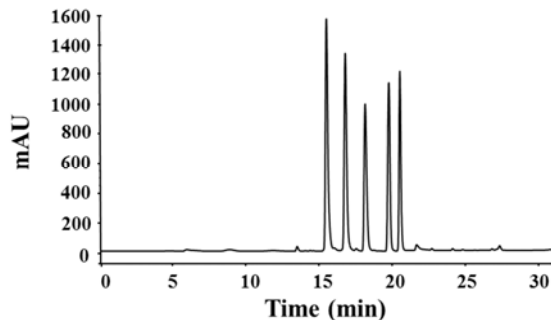
(E)
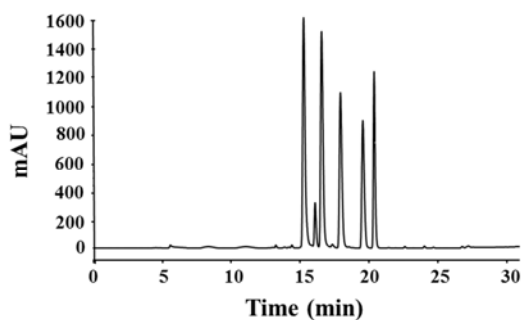
(F)
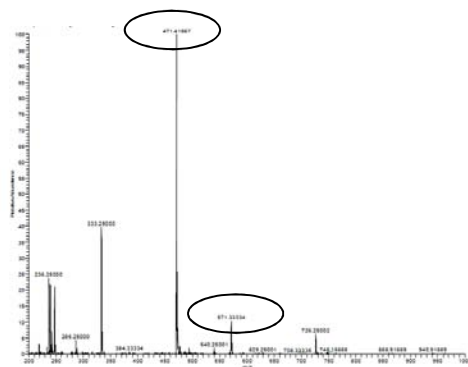
Figure S6.   LC/MS-SIM analysis of triazole **1**, with detection at 571 mass units. A) Authentic sample of **1** at 0.35 µM, synthesised by Cu catalysis of alkyne **2** and azide **3**. B) Products of reaction of alkyne **2** with azides **3** – **7** in (i) PBS buffer solution (Red), (ii) the presence of *Sa*BPL-R122G (Black) and (iii) the presence of wild-type *Sa*BPL (Blue). Y-axes of chromatograms A) and B) are not to scale. Triazole **1** eluted at 11.6 min.
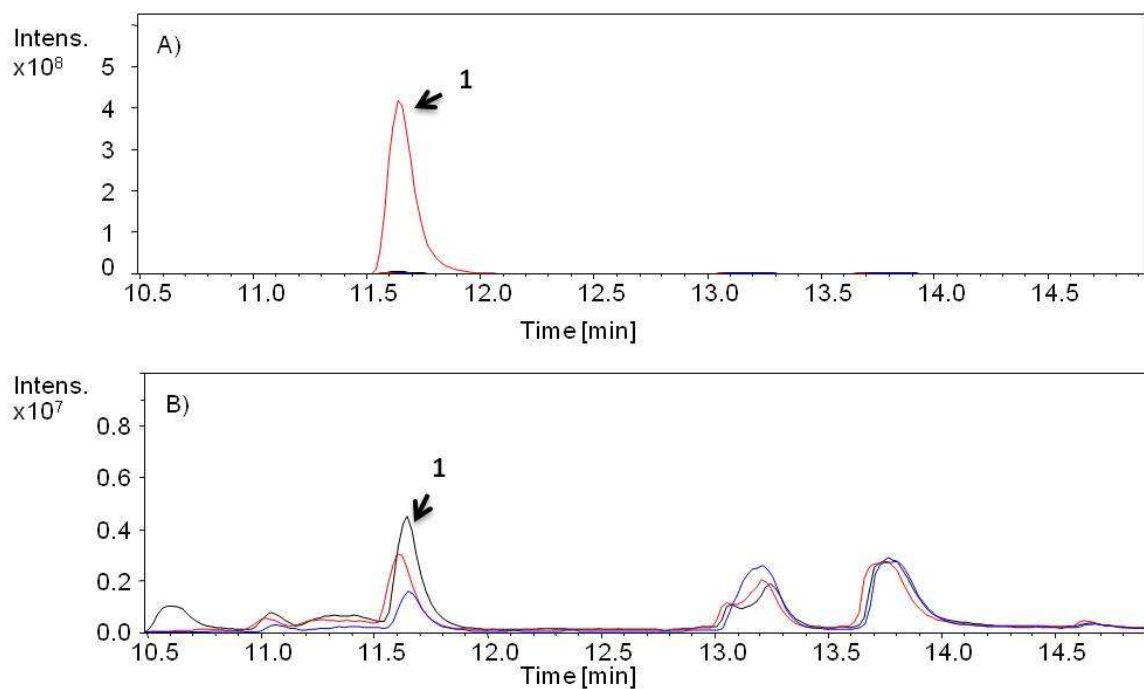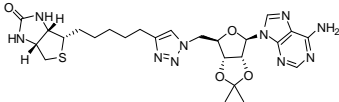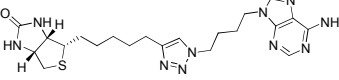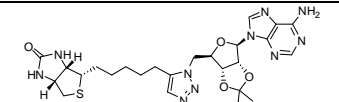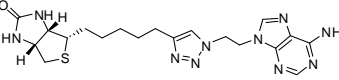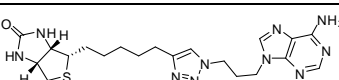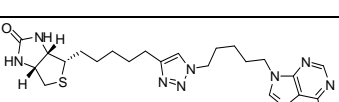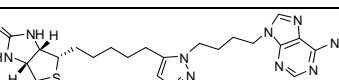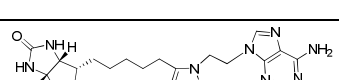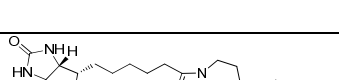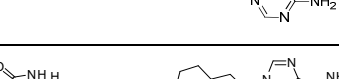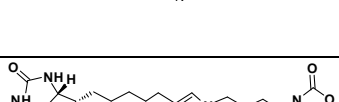
Table S2. HPLC retention times (R_t) and K_i values for synthetic **1**, **S1–S8**, **8**.

	Compound	HPLC R_t (min)[a]	SaBPL K_i (µM)[b]
1		20.1	1.83 ± 0.33
8		18.5	0.66 ± 0.05
S1		20.1	>10
S2		17.8	>10
S3		18.0	>10
S4		19.0	>10
S5		18.2	>10
S6		17.5	>10
S7		18.4	>10
S8		19.0	>10
S10		24.5	0.09 ± 0.01

[a] Compounds were detected on an RP-C18 column (4.6 mm x 250 mm), using eluents A (0.1% TFA in water) and B (0.08% TFA in 80% acetonitrile) at a flow rate of 0.5 mL/min. The gradient increased from 20% acetonitrile to 80% acetonitrile over 20 min followed by a 1 min 100% acetonitrile wash.
[b] K_i values were determined as described in Supplementary Methods.

Figure S7. HPLC analysis of *in situ* click formation of triazole **S10** from biotin alkyne **2** and azide **S9**. a) In PBS buffer. b) In the presence of 2.5 µM wild-type *Sa*BPL. c) In the presence of 25 µM wild-type *Sa*BPL. d) In the presence of 2.5 µM mutant *Sa*BPL-R122G. f) In the presence of 25 µM mutant *Sa*BPL-R122G. The black arrows denote observed peaks that correspond to the retention time of an authentic sample of triazole **S10**.
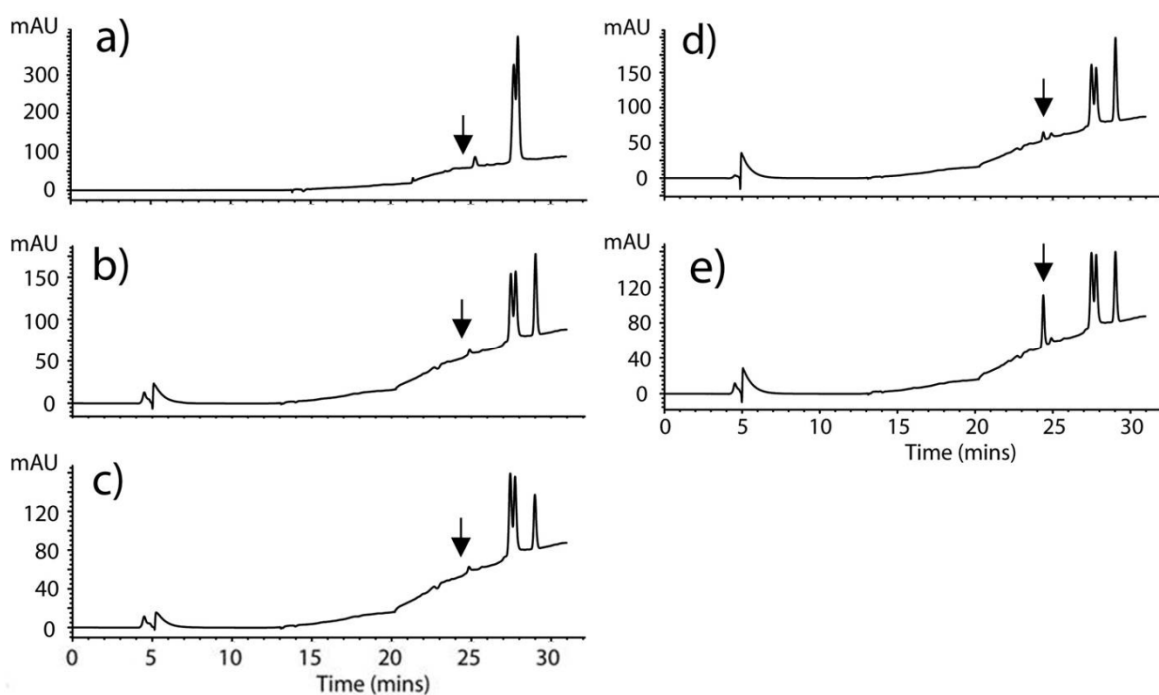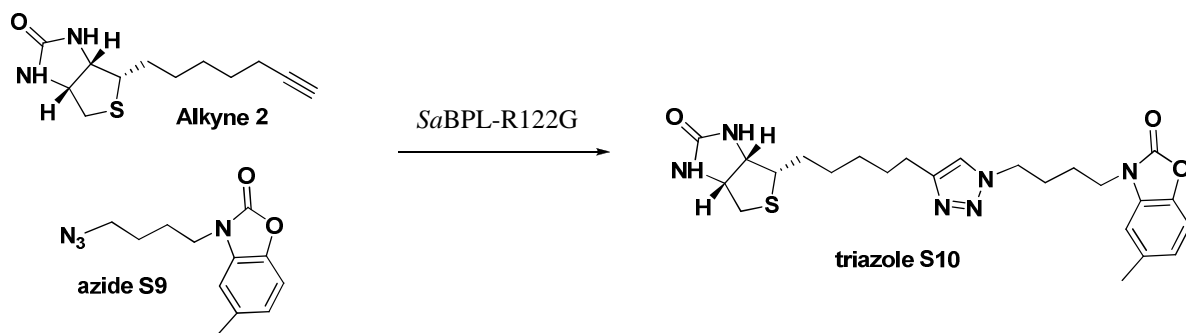
Table S3. X-ray data collection and refinement. Data collection and refinement statistics for holo *Sa*BPL structures with compound **8** bound.

	*Sa*BPL with 8
Data collection[a]	
Space group	P 4(2) 2(1) 2
Cell dimensions	
a, b, c (Å)	94.6, 94.6, 130.7
α, β, γ (°)	90, 90, 90
Resolution (Å)	50.00 - 2.61 (2.68-2.61)
R_{sym} or R_{merge}	0.06 (0.40)
$I/\sigma I$	15.3 (3.54)
Completeness (%)	99.0 (94.3)
Redundancy	2.46 (2.47)
Refinement	
Resolution (Å)	50 - 2.60
No. reflections	125676
R_{work} / R_{free}	20.65/25.77
No. atoms	
Protein	2613
Ligand/ion	32
Water	147
B-factors	
Protein	52.4
Ligand/ion	37.9
Water	57.7
R.m.s. deviations	
Bond lengths (Å)	0.02
Bond angles (°)	1.9

[a] Values in parentheses refer to the highest resolution shell.

[b] $R_{merge} = \sum |I - <I>|/\sum<I>$ where I is the intensity of individual reflections.

[c] $R_{pim} = \sum[1/(N-1)]^{1/2}\sum |I - <I>|/\sum<I>^{1}$

[d] $R_{factor} = \sum_h|F_o - F_c|/ \sum_h|F_o|$, where F_o and F_c are the observed and calculated structure-factor amplitudes for each reflection "h".

[e] R_{free} was calculated with 5% of the diffraction data selected randomly and excluded from refinement.

Protein Methods

In situ click experiment A: Preparation of triazole 1

The *in situ click* reaction of biotin alkyne **1** with azide **2** was performed at 37° C for 48 hours in PBS (137 mM NaCl, 2.7 mM KCl, 8 mM Na_2HPO_4, 1.46 mM KH_2PO_4, pH 7.4) using either wild-type or mutant *Sa*BPL (final enzyme concentration 2 µM). Control experiments were performed in parallel using either no enzyme or BSA in place of *Sa*BPL. Additionally, 500 µM of competitive inhibitor biotinol-5′-AMP was added to another control experiment with *Sa*BPL-R122G to address the specificity of the template guided reaction. The alkyne **2** and azide **3** were first solubilised in DMSO then added to all reactions to a final concentration of 500 µM each (final DMSO concentration 4% (v/v)). Aliquots of the reactions (50 µL) were diluted in 0.1% TFA (50 µL) and subjected to HPLC analysis. The analytes were fractionated using an analytical C18 reverse phase column (dimensions 4.6 mm x 250 mm), using eluents A (0.1% TFA in water) and B (0.08% TFA in 80% acetonitrile) at a flow rate of 0.5 mL/min. The gradient increased from 20% acetonitrile to 80% acetonitrile over 20 minutes followed by a 1 minute 100% acetonitrile wash. The system was set up for batch injections of 90 µL. Before each injection, the column was equilibrated with 100% Buffer A for 15 minutes. A duplicate sample was analysed using Orbitrap mass spectroscopy (Adelaide Proteomics Centre). To quantitate the yield of triazole product formed, the area under the peak on the UV trace was measured and compared against a standard curve established using known amounts of the synthesised triazole product.

In situ click experiment B: Library experiments

The *in situ* click reaction was performed essentially as described above with alkyne **2** (160 µM) reacted with a mixture azides **3–7** (final concentration of DMSO 4% (v/v)). HPLC of the reactions were performed as described above. LC-MS analysis was performed on an Agilent 1100 LC/MSD with a Bruker HCTultra PTM Discovery System (ES) eluting on a Agilent Poroshell 120 SB-C18

reverse-phase column (2.1 mm x 50 mm, 2.7 μm); 5 μL of sample was injected per run; flow rate at 0.2 mL/min; gradient elution (H_2O + 0.05% TFA)/(90% aqueous MeCN + 0.05% TFA) from 95:5 to 0:100 over 20 min followed by a wash of 5 min with 20:80 and a post-run time of 5 min using the starting solvent ratio. Detection was by electrospray ionization with positive selected-ion monitoring tuned to the molecular masses of triazole **8** and **1** (M+H = 471 and M+H = 571 respectively). The cycloaddition products were identified by comparison of its retention time with those determined from analysis of the copper-catalyzed reaction and by its molecular weight.

In situ click experiment C: Preparation of Triazole S10

The *in situ click* reaction was performed at 37° C for 48 hours in PBS (137 mM NaCl, 2.7 mM KCl, 8 mM Na_2HPO_4, 1.46 mM KH_2PO_4, pH 7.4) using either wild-type or mutant *Sa*BPL (at final enzyme concentrations 2.5 μM). A second set of *in situ* click reactions were performed under the same conditions, except using 25 μM final concentrations of either wild type or mutant *SaBPL*. The alkyne **2** and azide **S9** were first solubilised in DMSO then added to all reactions to a final concentration of 500 μM each (final DMSO concentration 4% (v/v)). Control experiments were performed in parallel and as detailed in '*in situ* click experiment 1'. Aliquots of the reactions (50 μL) were diluted in 0.1% TFA (50 μL) and subjected to HPLC analysis following the conditions described in '*in situ* click experiment 1'. The cycloaddition product **S10** was identified by comparing its retention time with that of an authentic sample of **S10**. Duplicate samples were analysed using Orbitrap mass spectroscopy (Adelaide Proteomics Centre). Detection of triazole **S10** was confirmed with mutant *Sa*BPL at 25 μM concentration (found: 485.23 m/z, expected (M+H): 485.23), whilst triazole **S10** was not detected by mass spectroscopy in samples containing wild-type enzyme and negative controls.

Protein expression and purification

DNA constructs required for recombinant expression of *Sa*BPL-H$_6$ in *E. coli* were described previously[2]. The R122G mutation was obtained using the QuikChange^{TM} mutagenesis kit (Stratagene) with plasmid pGEM-(*Sa*BPL-H6)[2] and oligonucleotides B227 (5′-CGAAAGGTCGTGGT**GGT**TTTAATAGACATTGG-3′) and B228 (5′-CCAATGTCTATTAAA**ACC**ACCACGACCTTTCG-3′). The expression and purification of wild-type and the *Sa*BPL-H$_6$ mutant R122G were performed using the same strategy as previously described by Pendini[2].

Surface plasmon resonance

SPR was performed using a Biacore^{TM} T100 instrument (GE Healthcare). BPL was immobilised on a CM5 sensor chip by standard amine coupling chemistry. The carboxymethyl groups on the chip were activated by the addition of *N*-ethyl-*N*´-(3-diethylamino-propyl) carbodiimide and *N*-hydroxysuccinimide. BPL (120 µg/mL) in 10 mM sodium acetate buffer (pH 5.8) was coupled onto the surface, and 1 M ethanolamine hydrochloride was injected to block any unreacted sites. Typically, 6,500 resonance units of BPL were immobilised on the sensor chip. One channel was left blank which was subtracted from sample channel(s) to allow analysis methods to distinguish between actual and non-specific binding. Experiment was conducted at 25° C at a flow rate of 30 µL/minute with a running buffer containing 10 mM HEPES pH 7.4, 150 mM NaCl. Zero concentration samples were used as blanks. The results for binding of biotin and AMP to both wild-type enzyme and *Sa*BPL-R122G showed fast on and off-rates outside the range of kinetic quantification, so K_D values were estimated using steady-state affinity. A binding curve for AMP was obtained by injecting saturating concentrations of biotin alkyne **1** (100 µM) prior to injection of AMP. Binding of compounds to wild-type *Sa*BPL were fitted to a 1:1 ligand binding model. K_D values for binding of compounds to *Sa*BPL-R122G were estimated using steady-state affinity. Buffers for experiments conducted with non-water soluble compounds contained 4% (v/v) DMSO.

Circular dichroism analysis

Far–UV CD spectra were recorded at 20° C using a Jasco CD J-185 spectrophotometer. Purified wild-type and mutant *Sa*BPL were dialysed overnight against the assay buffer (10 mM NaPO$_4$ pH 8.0) at 4° C prior to analysis. Final concentrations of the proteins used were 0.25 mg/mL (6.5 µM). CD spectra were recorded from 185 nm to 300 nm at 0.2 nm increments, using a 1 mm path length quartz cell. The reported spectra are the average of five scans that were corrected for buffer blanks.

In vitro biotinylation assays

Quantitation of BPL catalysed ^{3}H-biotin incorporation into the biotin domain substrate was performed as previously described[3,4]. The *IC*$_{50}$ value of each compound was determined from a dose-response curve by varying the concentration of the inhibitor under the same enzyme concentration. The data was analysed with GraphPad Prism software using a non-linear fit of log$_{10}$ (inhibitor) vs. normalized response. The *K*$_i$, the absolute inhibition constant for a compound, was determined using Eq1[5]:

$$\text{Eq1.} \quad K_i = IC_{50} / (1 + [S] / K_m)$$

where K_m is the affinity of the substrate for the enzyme ([biotin] =1.01 µM, Supplementary Table S2) and [S] is the substrate concentration ([biotin] =5 µM). The mode of inhibition was investigated by varying the concentrations of inhibitor alongside varying the concentrations of ^{3}H-biotin. The data was plotted as double reciprocal plots and assessed using Lineweaver-Burk analysis. Data reported here are the means of three independent assays (*n* = 3) ± standard error of the mean. Statistical analysis between two data sets was performed using a two-tailed unpaired *t* test using GraphPad Prism. See Supplementary Table S2 for enzyme inhibition results of **1**, **S1 – S8**, **8**).

X-ray crystallography

Apo-*Sa*BPL was buffer exchanged into 50 mM Tris HCl pH 7.5, 50 mM NaCl, 1 mM DTT and 5% (v/v) glycerol, and concentrated to 5 mg/mL. Each compound was then added to BPL in a 10:1 molar ratio. The complex was crystallised using the hanging drop method at 4° C in 8 – 12% Peg 8000 in 0.1 M Tris pH 7.5 or 8.0, and 10% (v/v) glycerol as the reservoir. A single crystal was picked using a Hampton cryo-loop and streaked through cryo-protectant containing 25% (v/v) glycerol in the reservoir buffer prior to data collection. X-ray diffraction data was collected at the macromolecular crystallography beamline at the Australian Synchrotron using an ADSC Quantum 315r Detector. 90 images were collected for 1 second each at an oscillation angle of 1° for each frame. Data was integrated using XDS, and refined using the CCP4 suite of programs. PDB and cif files for the compounds were obtained using the PRODRG web interface. The models were built using cycles of manual modelling using COOT and refinement with REFMAC. The quality of the final models was evaluated using MOLPROBITY. Composite omit maps were inspected for each crystal structure and statistics for the data and refinement reported (supporting information Table S3).

Synthetic chemistry methods

All reagents were from standard commercial sources and of reagent grade or as specified. Solvents were from standard commercial sources. Reactions were monitored by ascending TLC using precoated plates (silica gel 60 F_{254}, 250 µm, Merck, Darmstadt, Germany), spots were visualised under ultraviolet light at 254 nm and with either sulphuric acid-vanillin spray, potassium permanganate dip or Hanessian's stain. Column chromatography was performed with silica gel (40-63 µm 60 Å, Davisil, Grace, Germany). Melting points were recorded uncorrected on a Reichert Thermovar Kofler microscope. ^{1}H and ^{13}C NMR spectra were recorded on a Varian Gemini 2000 (300 MHz) or a Varian Inova 600 MHz. Chemical shifts are given in ppm (δ) relative to the residue signals, which in the case of DMSO-d_6 were 2.50 ppm for ^{1}H and 39.50 ppm for ^{13}C, CDCl$_3$ were 7.26 ppm for ^{1}H and 77.23 ppm for ^{13}C. Structural assignment was confirmed with COSY, ROESY, HMQC and HMBC. High-resolution mass spectra (HRMS) were recorded on a Thermo Fisher Scientific LTQ orbitrap FT MS equipment (Δ < 2 ppm) and Brucker micrO TOF-Q. Compounds **1 – 3**[6], **S1**[6], **S9**[6], **S10**[6] and Cp*Ru(PPh$_3$)$_2$[7] catalyst were synthesised according to literature procedures.

Synthetic scheme for triazoles 8 and S2 – S8
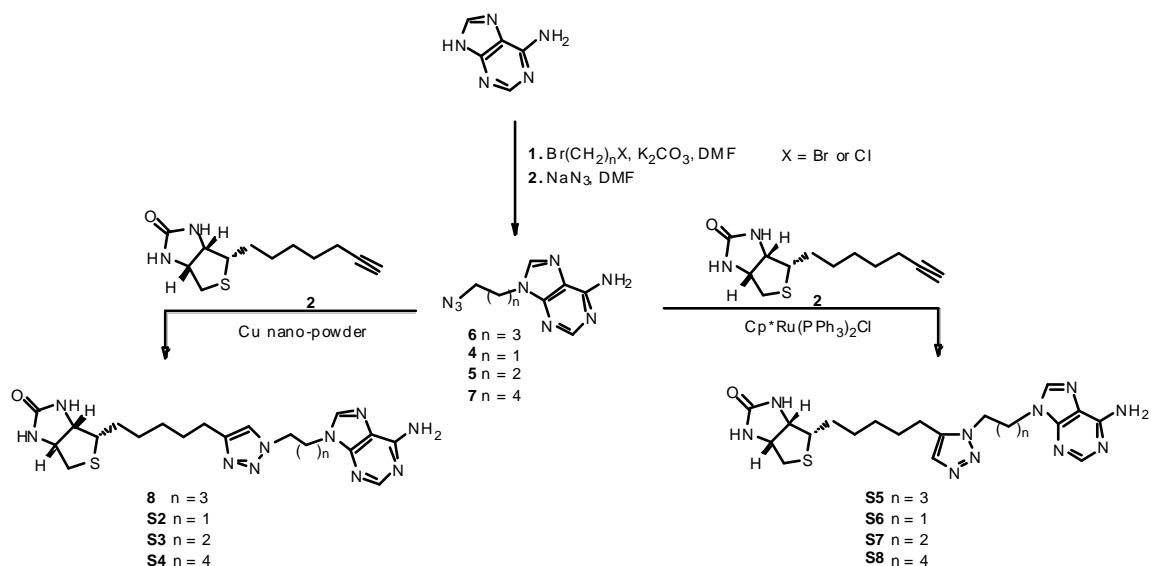
Supplementary References

(1)   Weiss, M. S. *Journal of Applied Crystallography* **2001**, *34*, 130.

(2)   Pendini, N. R.; Polyak, S. W.; Booker, G. W.; Wallace, J. C.; Wilce, M. C. J. *Acta Crystallographica Section F* **2008**, *64*, 520.

(3)   Polyak, S. W.; Chapman-Smith, A.; Brautigan, P. J.; Wallace, J. C. *Journal of Biological Chemistry* **1999**, *274*, 32847.

(4)   Polyak, S. W.; Chapman-Smith, A.; Mulhern, T. D.; Cronan, J. E., Jr.; Wallace, J. C. *Journal of Biological Chemistry* **2001**, *276*, 3037.

(5)   Cheng, Y.; Prusoff, W. H. *Biochemical Pharmacology* **1973**, *22*, 3099.

(6)   Soares da Costa, T. P.; Tieu, W.; Yap, M. Y.; Pendini, N. R.; Polyak, S. W.; Sejer Pedersen, D.; Morona, R.; Turnidge, J. D.; Wallace, J. C.; Wilce, M. C. J.; Booker, G. W.; Abell, A. D. *Journal of Biological Chemistry* **2012**, *287*, 17823.

(7)   Boren, B. C.; Narayan, S.; Rasmussen, L. K.; Zhang, L.; Zhao, H.; Lin, Z.; Jia, G.; Fokin, V. V. *Journal of the American Chemical Society* **2008**, *130*, 8923.

Chapter 5

Statement of Authorship

Title of Paper	A novel link between protein homodimerization and inhibitor binding to biotin protein ligase from *Staphylococcus aureus*
Publication Status	○ Published ○ Accepted for Publication ● Submitted for Publication ○ Publication Style
Publication Details	Soares da Costa, T.P., Yap, M. Y., Perugini, M., Wallace, J. C., Abell, A. D., Wilce, M. C., Polyak, S. W., Booker, G. W. (2012) A novel link between protein homodimerization and inhibitor binding to biotin protein ligase from *Staphylococcus aureus*. *Journal of Biological Chemistry*. Manuscript under review.

Author Contributions

By signing the Statement of Authorship, each author certifies that their stated contribution to the publication is accurate and that permission is granted for the publication to be included in the candidate's thesis.

Name of Principal Author (Candidate)	Tatiana P. Soares da Costa		
Contribution to the Paper	Primary role in performing most experiments and preparing the manuscript. Performed protein expression, purification, site-directed mutagenesis, analytical ultracentrifugation experiments, inhibition assays, surface plasmon resonance and circular dichroism analyses.		
Signature		Date	29/10/2012

Name of Co-Author	Min Y. Yap		
Contribution to the Paper	Performed electrophoretic mobility shift assays and structural analysis.		
Signature		Date	1/11/2012

Name of Co-Author	Matthew Perugini		
Contribution to the Paper	Provided direction in all aspects of analytical ultracentrifugation experiments and data analysis.		
Signature		Date	22/11/2012

Name of Co-Author	John C. Wallace		
Contribution to the Paper	Provided intellectual discussion.		
Signature		Date	29/11/2011

Name of Co-Author	Andrew D. Abell		
Contribution to the Paper	Provided intellectual discussion and research support.		
Signature		Date	3/12/2012

Name of Co-Author	Matthew C. Wilce		
Contribution to the Paper	rovided direction in structural and DNA binding studies.		
Signature		Date	5/11/2012

Name of Co-Author	Steven W. Polyak		
Contribution to the Paper	Provided direction in all aspects of enzymology and assisted in manuscript preparation.		
Signature		Date	1/11/2012

Name of Co-Author	Grant W. Booker		
Contribution to the Paper	Provided direction in all aspects of protein chemistry.		
Signature		Date	14/11/2012.

A novel link between protein homodimerization and inhibitor binding to biotin protein ligase from *Staphylococcus aureus*

Tatiana P. Soares da Costa[1]**, Min Y. Yap**[2]**, Matthew A. Perugini**[3]**, John C. Wallace**[1]**, Andrew D. Abell**[4]**, Matthew C. J. Wilce**[2]**, Steven W. Polyak**[1*]** and Grant W. Booker**[1]**.**

[1] School of Molecular and Biomedical Science, University of Adelaide, South Australia 5005, Australia.
[2] School of Biomedical Science, Monash University, Victoria 3800, Australia.
[3] Department of Biochemistry, La Trobe Institute for Molecular Science, La Trobe University, Victoria 3086, Australia.
[4] School of Chemistry and Physics, University of Adelaide, South Australia 5005, Australia.

Running title: Biotin protein ligase from *Staphylococcus aureus*

*To whom correspondence should be addressed: Steven W. Polyak, Department of Biochemistry, School of Molecular and Biomedical Sciences, University of Adelaide, Adelaide, SA 5005, Australia, Tel: 61-8-8303-5289; Fax: 61-8-8303-4362; E-mail: steven.polyak@adelaide.edu.au.

Background: Class II biotin protein ligases (BPL) are bifunctional proteins with enzymatic and DNA binding activities.
Results: BPL from *Staphylococcus aureus* exists in a dimer-monomer equilibrium.
Conclusion: F123 in *S. aureus* BPL plays dual roles in dimerization and potent inhibitor binding.
Significance: *S. aureus* may have an additional level of BPL-regulated transcriptional control that is important during pathogenesis.

SUMMARY

The essential process of attaching the cofactor biotin onto specific target enzymes is catalyzed by biotin protein ligase (BPL). The most extensively characterized BPL is from the prototypic bacteria *Escherichia coli* where it functions as both a biotin ligase and as a transcriptional repressor. Here we characterize another example of a bifunctional BPL (*Sa*BPL) from the clinically important bacteria *Staphylococcus aureus*. Analytical ultracentrifugation studies, alongside size exclusion chromatography and multi-angle light scattering analyses demonstrated that unliganded *Sa*BPL exists in a dimer-monomer equilibrium in solution at low micromolar concentrations. This is in stark contrast to the *E. coli* BPL (*Ec*BPL) that exists as a monomer under the same conditions. The dimer-monomer dissociation constant for *Sa*BPL is 6-fold tighter in the presence of an inhibitor (biotin acetylene), but unchanged in the presence of the natural substrate biotin. F123, located in the dimer interface, is shown to play a critical role in homodimerization. Inhibition studies together with surface plasmon resonance analysis revealed a strong correlation between inhibitor potency and slow dissociation kinetics. A 24-fold difference in K_i values for these two enzymes was explained by differences in enzyme: inhibitor dissociation rates. Substitution of F123 in *Sa*BPL and R119 in *Ec*BPL altered both inhibitor potency and dissociation rates. Hence, F123 in *Sa*BPL has novel roles in both protein dimerization and ligand-binding that have not been reported in *Ec*BPL. We propose a new model that facilitates rapid switching between repressor and ligase activities, thereby providing *S. aureus* and other clinically important bacteria significant advantages during pathogenesis.

Biotin protein ligase (BPL) is an important metabolic enzyme that catalyzes the ubiquitous and essential process of attaching biotin onto biotin-dependent enzymes; a family of enzymes that play key roles in various metabolic pathways (1). Protein biotinylation proceeds through a conserved, two-step ordered reaction

mechanism. In the first partial reaction, the intermediate biotinyl-5′-AMP is produced from biotin and ATP. Subsequently, the biotinyl moiety is transferred onto the ε-amino group of a specific lysine residue present in the biotin domain of all biotin-dependent enzymes, with the release of AMP. BPLs can be divided into three structural classes (reviewed (2)). All three classes share a highly conserved catalytic module that is central to enzymatic biotinylation. Class I enzymes consist solely of this catalytic module, which is a fusion of an SH2-like domain with an SH3-like domain (3,4). X-ray crystal structures have been reported for the Class I enzymes from *Pyrococcus horikoshii* (3), *Aquifex aeolicus* (5) and *Mycobacterium tuberculosis* (6,7). Class II BPLs contain the conserved catalytic module with an additional helix-turn-helix domain at the N-terminus that facilitates DNA binding and allows them to also function as transcriptional repressors. Thus, the Class II enzymes are truly bifunctional proteins. The most studied Class II isozyme is from the prototypical bacteria *Escherichia coli* (4,8,9), with the X-ray crystal structure of a second example from *Staphylococcus aureus* recently being reported (10). In contrast, Class III BPLs from mammals and fungi are more complex with a larger N-terminal extension that bears no homology to the DNA binding domains present in Class II enzymes, nor any other protein yet identified in the protein database (11). An X-ray crystal structure for a Class III enzyme has not been reported. Primary structure alignments, in combination with the available structural data on the simpler BPLs, reveal a common biotin-binding loop that undergoes a disordered-to-ordered transition upon the binding of biotin. Within this loop resides a GRGRX motif, where X is divergent between homologs. Amino acids in this motif play key roles in stabilizing the BPL: biotinyl-5′-AMP complex (12). However, the role of the divergent residue X has not been extensively investigated.

An interesting observation from crystallography, size exclusion chromatography analysis, and analytical ultracentrifugation experiments is the difference in oligomerization states amongst all BPLs. *M. tuberculosis* BPL exists predominately as monomers in its apo, biotin and biotinyl-5′-AMP liganded forms (13). This is in sharp contrast to *P. horikoshii*

BPL that constitutively exists as a dimer, regardless of its liganded state (3). *E. coli* BPL (*Ec*BPL) undergoes a more complex transition from essentially monomer in its apo form to homodimer in the presence of biotin or biotinyl-5′-AMP. In *Ec*BPL, amino acids within the GRGRX motif are located in the dimer interface and contribute to the network of hydrogen bonds and ionic interactions that stabilize the protein-protein interaction (8,9). Dimerization orients the two N-terminal domains such that they are receptive to binding specific DNA recognition sequences in the promoter of the biotin biosynthesis operon *bioO*, resulting in repression of biotin biosynthesis (14,15). It has been proposed that *Ec*BPL utilizes the same protein surface for homodimerization and heterodimerization with the apo biotin domain substrates (8). Hence, competing protein-protein interactions are proposed to regulate the switch between transcriptional repressor and biotin protein ligase activities (8,16). This switch mechanism allows *Ec*BPL to serve as a cellular sensor of biotin demand and regulator of its *de novo* synthesis. The oligomerization state(s) of other Class II BPLs have not been investigated so it is unclear whether or not the same intricate mechanisms occur in other bacteria, such as *S. aureus*. Class III *Homo sapiens* and *Saccharomyces cerevisiae* BPLs have been shown to be monomeric in solution (17,18) and not subject to the same dynamic processes as the Class II counterparts.

In a recent report, we described a series of biotin analogues as BPL inhibitors that possess antibacterial activity against clinical isolates of *S. aureus* (MIC$_{50}$ 2 – 4 μg/mL) (19). These compounds serve as valuable tools for chemical biology studies and leads for a new class of antibiotic. We observed unexpected selectivity between the BPLs from *S. aureus*, *E. coli* and *H. sapiens*. The most selective compound was biotin acetylene (K_i = 0.30 ± 0.03 μM), with a 24-fold greater affinity for *S. aureus* BPL (*Sa*BPL) compared to the *E. coli* equivalent. X-ray crystallography revealed that biotin acetylene induced the same conformational changes in *Sa*BPL as biotin, especially those in the biotin-binding loop (RMSD 0.30 Å overall between the two structures) (19). A key difference between the two structures is that the BPL: biotin acetylene complex is stabilized through a direct hydrophobic interaction

between the acetylene moiety and W127 that also resides in the biotin-binding loop (19). This is in contrast to the BPL: biotin interaction that is stabilized through hydrogen bonding between the hydroxyl group on biotin and an NH backbone amide of R122 (10). As W127 is invariant amongst all BPLs, preferential binding cannot simply be rationalized by interactions involving this amino acid alone. Surface plasmon resonance (SPR) studies on SaBPL helped to dissect the binding mechanism in further detail. In particular, biotin acetylene forms a long-lived complex with SaBPL due to its slow dissociation kinetics ($k_d = 3.40 \pm 0.30 \times 10^{-6}$ s^{-1}). A slow off-rate is similarly observed between the reaction intermediate biotinyl-5´-AMP for both SaBPL (10) and EcBPL (20). This is in sharp contrast to the fast off-rate observed with biotin alone (19). In EcBPL, the dissociation of the enzyme-biotin complex is 1000-fold faster than dissociation of the enzyme-intermediate complex (20). Biotin binding has been linked to a considerably greater loss in entropy than binding of the reaction intermediate due to more induced conformational changes to the protein (21). The enthalpy cost of the intermediate binding is 'off set' by the enthalpy that would have otherwise been realized from the formation of non-covalent bonds between the ligand and the repressor monomer (22). A stable BPL: biotinyl-5´-AMP complex is of importance since the adenylate serves both as the activated intermediate in transfer of biotin to the biotin domain (i.e. ligase activity - monomeric BPL) and as the co-repressor in site-specific DNA binding (transcriptional repressor activity - i.e. dimeric BPL) (23,24).

In this work, the oligomeric state of SaBPL is investigated using analytical ultracentrifugation and size exclusion chromatography coupled to multi-angle light scattering in order to define the mechanisms that govern the switch between ligase and repressor functions. In addition, biotin acetylene is employed to study the effects on oligomerization of a long-lived inhibitor in the active site. The explanation for the higher affinity of biotin acetylene for SaBPL compared to EcBPL was also pursued. We report that a single amino acid in SaBPL, F123, plays dual roles in dimer formation as well as stabilizing inhibitor binding. These findings provide new insights into the indispensable metabolic activities performed by the bifunctional BPL from $S. aureus$ that are likely to also exist in other clinically important bacterial pathogens.

EXPERIMENTAL PROCEDURES

Materials: Chemicals were purchased (unless otherwise stated) from Sigma-Aldrich Pty Ltd (Castle Hill, Australia). Protein concentration was measured using the Bradford assay (25). All enzymes were stored in 50 mM Tris HCl pH 8.0, 1 mM DTT, 5 mM EDTA and 5% (v/v) glycerol at -80° C.

Nucleic acid manipulations: Cloning of the $S. aureus$ gene with a C-terminal His6-tag, and construction of the recombinant expression vector, are described in Pendini *et al.* 2008 (26). A hexahistidine tag was similarly engineered onto the C-terminus of EcBPL to facilitate purification. Site-directed mutagenesis was performed using a QuikChange® Mutagenesis Kit (Stratagene). All oligonucleotides used in this study were purchased from Geneworks (Adelaide, Australia) and are shown in supplemental Table S1. Mutant plasmids were confirmed through DNA sequencing (SA Pathology, Adelaide, Australia).

Protein methods: The production of hexahistidine-tagged SaBPL and EcBPL enzymes was performed essentially as described (26) and in supplemental Methods. Samples were further purified by size exclusion chromatography on a Superdex 75 column, eluting with a buffer containing 50 mM Tris HCl pH 8.0, 1 mM DTT, 5 mM EDTA and 5% (v/v) glycerol. BPL activity was measured using an *in vitro* biotinylation assay (17), and inhibition by biotin acetylene was performed as described (10). Circular dichroism (CD) spectroscopy (10) and SPR (19) were also performed as previously reported. The data for biotin acetylene binding to SaBPL were fitted to a 1:1 binding model. The electromobility shift assay is described in supplemental Experimental Procedures.

Analytical ultracentrifugation (AUC): Sedimentation velocity and sedimentation equilibrium studies were performed using an XL-I analytical ultracentrifuge (Beckman-

Coulter) with an 8-hole An-50-Ti rotor. Double sector centrifuge cells with quartz windows were loaded with 380 µL of sample and 400 µL of reference buffer (20 mM Tris, 150 mM NaCl, pH 8.0) for sedimentation velocity experiments or 100 µL sample and 120 µL reference for sedimentation equilibrium experiments. Initial scans were carried out at 3,000 rpm to determine the optimum wavelength and radial range for the experiments. For sedimentation velocity analyses, absorbance versus radial profiles were measured in continuous mode using a step size of 0.003 cm at a single wavelength (280 nm) every 6 minutes employing a rotor speed of 40,000 rpm at a temperature of 20° C for enzyme concentrations of 26.0, 11.7 and 3.9 µM. Sedimentation equilibrium scans were also performed at 20° C but in step mode with a step size of 0.001 cm with 10 averages using rotor speeds of 13,000 and 19,000 rpm for enzyme concentrations of 11.7, 7.8 and 3.9 µM. The partial specific volume of SaBPL and mutants (0.7332 mL/g), buffer density (1.00499 g/mL) and viscosity (1.0214 cp) were calculated using the program SEDNTERP (27). Sedimentation velocity data were fitted to a continuous sedimentation coefficient [$c(s)$] distribution model using the programme SEDFIT (28-31). Sedimentation equilibrium data were fitted to various self-associating models using the program SEDPHAT (32-34).

RESULTS

Oligomeric state of SaBPL in the absence and in the presence of ligands: The high degree of variability in oligomeric states of BPLs between species prompted us to carry out absorbance-detected sedimentation velocity in the analytical ultracentrifuge to determine the quaternary structure of SaBPL in solution. Protein was first purified using a His-Trap column as described in the Experimental Procedures. We used two alternative biotinyl-transferase assays to show that no biotinyl-5′-AMP was co-purified with the enzyme and, hence, it was in its apo form (supplemental Fig. S1). The Ni-NTA purified material was then loaded onto a Superdex 75 size exclusion column at 26 µM. Two peaks were observed corresponding to the molecular sizes of the monomer and dimer of SaBPL respectively. Protein contained in the monomeric peak was collected for subsequent

analysis. AUC was performed with this material at three different protein concentrations. The apo enzyme existed in a reversible self-association at these low micromolar concentrations with standardized sedimentation coefficients ($s_{20,w}$) of 2.5 S and 3.8 S at both 26 µM (Fig. 1A) and 11.7 µM (Fig. 1B). At 3.9 µM, only one peak was observed with a $s_{20,w}$ value of 2.5 S (Fig. 1C). Therefore, the oligomerization state is concentration dependent. The [$c(M)$] distribution yielded apparent molecular masses of around 38 and 76 kDa, which are consistent with the predicted molecular masses of SaBPL monomer and dimer respectively (Table 1). This effect was subsequently quantified using sedimentation equilibrium analysis of SaBPL. Samples containing 11.7 µM, 7.8 µM and 3.9 µM were centrifuged at 13,000 and 19,000 rpm until sedimentation equilibrium was achieved at each speed. The data were fitted to a range of models including monomer-dimer, monomer-trimer and monomer-tetramer association. The model that yielded the best global nonlinear least-squares fit (Reduced ψ^2 = 0.06) was the monomer-dimer association model, resulting in a K_D^{2-1} of 29 µM in the absence of ligand. This was consistent with SEC-MALS analysis of this protein sample at 26 µM, which showed that the apo protein was indeed primarily dimeric (supplemental Fig. S2A). Self-association of the class II EcBPL in the apo state has not been observed previously at these low protein concentrations (15,35,36). Thus SaBPL represents the first example of a Class II BPL able to self-associate at physiologically relevant concentrations.

The effect of ligand binding on the oligomerization of SaBPL was then quantitated using sedimentation velocity experiments. Interestingly, in the presence of 100 µM biotin (i.e. $100 \times K_m$), the equilibrium did not shift towards the dimer even at the highest protein concentration of 26 µM (Fig. 2). However, in the presence of 100 µM biotin acetylene the equilibrium shifted significantly in favour of the 3.8 S species (Fig. 2). These results indicate that tight-binding biotin acetylene effectively induces dimer formation. This effect was subsequently quantified using sedimentation equilibrium analysis with the same conditions as reported above. Once again, the data were fitted to a number of models, with the monomer-dimer model yielding the best global

nonlinear least squares fit (Reduced $\psi^2 = 0.06$). The dissociation constant was 5.0 µM in the presence of biotin acetylene, which is ~ 6-fold tighter compared with the unliganded enzyme.

We next confirmed that the *Sa*BPL dimer assembled into a conformation that was competent to bind DNA, and therefore biologically relevant for assessing repressor activity. This was performed using an electromobility shift assay. Here, double stranded 44-mer oligonucleotides with the *bioO* operator sequence from *S. aureus* were employed (37). Importantly both the apo and holo enzymes bound the DNA, with the holo enzyme possessing a 7.4-fold higher affinity than the apo protein (K_D apo 630.8 ± 69 nM; holo 85.0 ± 10.6 nM; p < 0.01 apo *vs.* holo) (Figure 3). The difference observed in the EMSA was consistent with the 6-fold difference observed between the apo enzyme and the biotin acetylene-induced dimer observed above, suggesting that the apo dimer is likely to be pre-assembled in solution prior to DNA binding. This represents a key difference between the *S. aureus* and *E. coli* BPLs. Non-related DNA probes failed to bind either enzyme, demonstrating the specificity of the DNA: protein interaction. Together, these data highlight that the *Sa*BPL dimer exists in form competent to bind DNA at protein concentrations that are biologically relevant.

Characterization of SaBPL-F123G, SaBPL-F123R and EcBPL-R119F: The *Sa*BPL dimer was further investigated using mutagenesis studies. We examined the X-ray crystal structure of the *Sa*BPL dimer enzyme in complex with a chemical analogue of the reaction intermediate (PDB ID 4DQ2 (10)) for amino acids located in the protein: protein interface and, thus, potentially required for dimerization. The interaction surface covers 1020 Å^2 of solvent accessible surface area and contains an extensive network of hydrogen and ionic bonds (supplemental Fig. S3). The C-terminal and catalytic domains orientate themselves to make contact with appropriate amino acid residues on the other subunit. Importantly, two intersubunit bonding interactions at the dimer interface were observed that are not present in the *Ec*BPL dimer. Notably R122 and F123 both contact the side chain of D200 on the partner subunit: R122 through hydrogen bonding and F123

through a hydrophobic interaction with the γ-carbon (Fig. 4). Therefore, we proposed a potential role for the phenylalanine in the GRGRF[123] motif for protein dimerization. Previous studies on *Ec*BPL have shown that the introduction of an aromatic amino acid at the equivalent position (R119W) had no effect upon ligand binding or enzyme activity (12) but did significantly impede protein dimerization and transcriptional repressor activities (36,38). Given the findings on the *Ec*BPL-R119W mutant, it was intriguing that the equivalent position in native *Sa*BPL should also be an aromatic amino acid. To define a possible function for F123 in protein oligomerization, a series of mutant proteins was generated. The side chain of F123 was removed via a glycine substitution (F123G). Additionally, an arginine substitution was generated (F123R) as this is the equivalent residue in the *E. coli* enzyme. The reverse mutant *Ec*BPL-R119F was also generated and characterized. CD spectra confirmed that all mutant proteins fold similarly in solution compared to their wild-type counterparts (supplemental Fig. S4). Therefore, any changes in catalytic efficiency, or substrate binding, are not attributable to gross perturbations in the secondary structure upon mutation.

Phe123 involvement in dimerization: AUC and SEC-MALS were again employed to determine the oligomeric state of the two *Sa*BPL mutant proteins. AUC sedimentation velocity experiments were performed using a protein concentration of 26 µM. Data were fitted to a continuous sedimentation coefficient [$c(s)$] distribution model, which revealed a single peak at 2.5 S for both proteins (Fig. 5 & Table 1), indicative of a monomer. SEC-MALS analysis confirmed the AUC results, showing a single peak for both apo *Sa*BPL-F123G and *Sa*BPL-F123R (26 µM enzyme concentration) at retention times corresponding to monomeric species (35 ± 4 kDa and 37 ± 4 kDa respectively; supplemental Fig. S2 B and C). Interestingly, neither biotin nor biotin acetylene induced the formation of a dimer for either mutant protein (Fig. 6). These results indicate that substitution of F123 abolished dimerization of *Sa*BPL. To confirm the importance of the phenylalanine residue in the dimerization of the apo protein, the *Ec*BPL proteins were analyzed using SEC-MALS. Whilst the wild-type enzyme was monomeric, *Ec*BPL-R119F eluted

primarily as a dimer (supplemental Fig. S2 D and E, respectively). These findings highlight that an aromatic amino acid at position X in the GRGRX motif plays a novel role in the dimerization of SaBPL.

Analysis of inhibitor binding by enzyme kinetics: A comparison of the kinetic parameters for the mutant enzymes with the corresponding wild-type enzymes is shown in supplemental Table S2. The kinetic constants for biotin and MgATP were determined by steady-state kinetics (10). Kinetic analyses of wild-type SaBPL and EcBPL were in agreement with published values (10,39). As has been observed previously with EcBPL-R119W (12), the F123G and F123R substitutions in SaBPL had minimal effect upon the K_m for MgATP and biotin. Also, the R119F substitution in EcBPL had no effect on the enzyme's turnover rates (k_{cat}). In contrast, the k_{cat} for biotin and MgATP were significantly compromised for both SaBPL mutant proteins to ~10% that of wild-type enzyme. These results suggested a previously unknown role for the phenylalanine residue in the catalytic mechanism of SaBPL.

Inhibition studies were performed to quantitate the effect of biotin acetylene on the activities of mutant BPLs (Table 2). We have previously reported biotin acetylene to be a potent inhibitor of both *S. aureus* and *E. coli* BPLs with a 24-fold higher affinity for SaBPL (19). The F123R substitution resulted in K_i = 7.2 ± 0.9 µM. Interestingly, the inhibition constant observed for SaBPL-F123R was in excellent agreement with the value obtained for wild-type EcBPL (7.3 ± 1.0 µM, p < 0.01 EcBPL *vs.* SaBPL-F123R; Fig. 6A). Thus, a single, non-conserved amino acid at position 123 in SaBPL was sufficient to account for the higher affinity of SaBPL for biotin acetylene. In support of this observation, substitution of the EcBPL R119 residue to a phenylalanine yielded a mutant that was equally sensitive to biotin acetylene as the wild-type *S. aureus* enzyme (K_i = 0.37 ± 0.03 µM, p < 0.01 EcBPL-R119F *vs.* SaBPL; Fig. 6B). This data suggested that EcBPL-R119F had the same properties as wild-type SaBPL. The mutation of F123 to a glycine resulted in an 11-fold increase in K_i value compared to the wild-type enzyme.

Analysis of inhibitor binding by SPR: To further dissect the bimolecular interaction between BPL and the biotin acetylene inhibitor, SPR studies were employed. Apo BPLs were applied to activated surfaces of a CM5 sensor chip for protein immobilization at a concentration known to represent primarily monomeric protein (i.e. 3.9 µM, > 5-fold less than K_D^{2-1}). The wild-type SaBPL, SaBPL-F123G, SaBPL-F123R, wild-type EcBPL and EcBPL-R119F were all investigated, with one channel left blank in each experiment as a reference and to take into account changes in refractive index associated with the buffer. Varying concentrations of biotin acetylene (0 to 6.4 µM) were injected over the immobilized proteins for 120 seconds, followed by a 200 second dissociation phase. Data were fitted to a 1:1 ligand-binding model and the association and dissociation rates (k_d) determined (Table 2). The association rates were less than 2-fold different for all enzymes (Fig. 7). However, the greatest variance between the proteins was observed in the dissociation rates with excellent correlation between the relative k_d values and the *in vitro* potency of the biotin acetylene inhibitor. A 29-fold increase in the relative dissociation rates between inhibitor and wild-type SaBPL versus SaBPL-F123R was observed (Table 2). This agreed with the 24-fold difference in K_i values observed between these proteins. Additionally, both EcBPL and SaBPL-F123R displayed indistinguishable dissociation kinetics (p > 0.05). Likewise, the binding curves for EcBPL-R119F were superimposable with those obtained for wild-type SaBPL, indicating a 29-fold decrease in dissociation rate upon mutation of arginine 119 to a phenylalanine. Together the data demonstrate that a phenylalanine residue at position 123 in SaBPL plays dual roles in both protein dimerization and ligand binding. These represent key differences between SaBPL and the well-characterized EcBPL.

DISCUSSION

SaBPL and EcBPL belong to the same class of BPLs that function as both biotin ligases and transcriptional repressors. EcBPL is the best-characterized example, and we reasoned that the large volume of genetic, structural, kinetic and mutagenic data about this enzyme would provide valuable information to assist in

the design of inhibitors against *Sa*BPL. Surprisingly, we discovered unexpected differences between the two enzymes despite the high degree of conservation in enzyme mechanism, as well as primary and tertiary structures. Importantly, our studies have revealed novel roles for an aromatic residue at position X in the GRGRX motif in both protein dimerization and selective binding of the inhibitor. This is important since other clinically important bacteria also contain BPLs with a phenylalanine at this position and are likely to be subject to the mechanisms described here for *S. aureus*. These include *Streptococci*, *Enterococci* and *Legionella sp.* Through this work we made the unexpected discovery that *Sa*BPL exists in an apparent equilibrium between two oligomeric states, monomer and dimer, at low micromolar concentrations. This is in sharp contrast to the *Ec*BPL that exists as a monomer in solution under similar conditions, but can dimerize at low millimolar concentrations (15,35,36). Here, sedimentation velocity experiments showed that biotin acetylene significantly shifted the equilibrium in favour of the *Sa*BPL dimer formation in solution. The X-ray crystal structure of biotin acetylene bound to *Sa*BPL showed the ordering of loops, especially the biotin-binding loop, located in the interface between the two monomers (19). The organization of the structure is believed to be a pre-requisite for dimerization and DNA binding. Interestingly, biotin itself did not induce dimerization of *Sa*BPL. This could be explained by the rapid dissociation kinetics observed in SPR experiments (19). The on and off-rates for biotin binding were so fast that the K_D could only be estimated using a steady-state affinity model (19). Hence, a stable enzyme: ligand complex is required to drive the monomer-dimer transition.

X-ray crystallography was used to identify key differences between the dimer interfaces of *Sa*BPL [PDB ID 4DQ2 (10)] and *Ec*BPL [PDB ID 2EWN (9)]. We reasoned this analysis would provide molecular clues to explain the difference in the stability of the two apo BPL dimers and further understand the mechanism of DNA binding and subsequent regulation of gene expression. Of particular importance were two residues in the biotin-binding loop of *Sa*BPL, namely R122 and F123. Both amino acid residues form inter-subunit contacts with

D200 on the partnering subunit. Our AUC and SEC-MALS analysis clearly demonstrate the importance of the F123 in stabilizing the dimer as substitution with either glycine or arginine abolished dimerization. This is different to *Ec*BPL where R118 forms intra-subunit contacts with D176 and the backbone oxygen of I187. R118 also hydrogen bonds with the phosphate group of biotinyl-5′-AMP through its side chain and a backbone amine (9). Conversely, the guanidinium side chain of R119 forms hydrogen-bonding interactions with E140 side chain and backbone oxygen of G196 on the partner subunit (9). This explains why a tryptophan substitution at R119 had a dramatic effect upon *Ec*BPL dimerization (12,38). Interestingly, SEC-MALS analysis of the *Ec*BPL-R119F mutant also showed a propensity to dimerize that was similar to *Sa*BPL. It is likely the R119F mutation introduces an analogous hydrophobic interaction between the two *Ec*BPL subunits, as observed in *Sa*BPL, possibly involving D197 (distance between the two β-carbons = 7 Å).

Our data also demonstrate that F123 in *Sa*BPL has a previously unknown role in ligand binding. To eliminate the possibility that the differences in binding affinity (K_i) observed with biotin acetylene was a direct cause of dimerization, we designed SPR experiments such that the BPLs were immobilized onto the sensor chip at a concentration where the proteins were predominantly monomeric. Hence, we reasoned that these experiments would dissect the bimolecular interaction between monomeric *Sa*BPL and biotin acetylene. Here we observed a strong correlation between the dissociation rates and inhibitor potency. Logically, those BPLs that form a tight-binding complex with biotin acetylene, characterized by slow dissociation kinetics, were also most susceptible to inhibition. Unexpectedly, the inhibition and SPR analysis identified a role for F123 in the selective binding mechanism. X-ray crystal structures have shown that the side chain of F123 does not bind directly to the inhibitor (19). We propose that the role of this amino acid is to help stabilize the biotin-binding loop, thereby preventing the dissociation of the biotin analogue from its binding site. Understanding the disordered-to-ordered conformational change performed by the biotin-binding loop, and the forces that stabilize this transition, will

114

be essential considerations for the future design of BPL inhibitors.

What is the biological significance of these findings? Class II BPLs are positioned as the master regulator of all biotin related activities in bacteria. Having both biotin ligase and transcriptional activities linked together in one protein provides the bacteria with a mechanism to both sense cellular demand for the enzyme cofactor and facilitate its supply through *de novo* synthesis. *E. coli* is a comparatively simple system with one biotin-dependent enzyme (i.e. acetyl-CoA carboxylase) and one known target for the transcriptional repressor (i.e. the biotin biosynthesis operon). *S. aureus*, however, is more complex with two biotin-dependent enzymes (acetyl-CoA carboxylase and pyruvate carboxylase) and at least two proposed transcriptional targets (i.e. the biotin biosynthesis operon and the biotin import protein BioY (37)). The pre-existing apo BPL dimer in *S. aureus* may provide the cell with more stringent control over gene expression, thereby allowing the *S. aureus* to rapidly respond to environmental conditions such as the availability of micronutrients. This is particularly important during pathogenesis when rapid adaptation to niche microenvironments is critical for survival and avoiding the host immune system. Specifically, biotin has been identified as a key micronutrient for several bacterial species, including *Francisella* (40) and *Mycobacterium* (41). We propose that our findings here provide certain bacteria with a more refined genetic switch between competing BPL activities than has been previously reported in the prototypical bacteria *E. coli*. These findings also extend our understanding of molecular mechanisms that regulate metabolic adaptation in clinically important bacteria, such as *S. aureus*, with the view to provide new avenues for the discovery of treatments to combat infection.

ACKNOWLEDGEMENTS

REFERENCES

1.   Polyak, S. W., Bailey, L. M., Azhar, A., and Booker, G. W. (2012) Biotin. in *Micronutrients: Source, properties and health benefits* (Betancourt, A. I., and Gaitan, H. F. eds.), Nova Science Publishers. pp 65-94

2.   Pendini, N. R., Bailey, L. M., Booker, G. W., Wilce, M. C., Wallace, M. C., and Polyak, S. W. (2008) Microbial biotin protein ligase aid in understanding holocarboxylase synthetase deficiency *Biochim. Biophys. Acta* **1784**, 973-982

3.   Bagautdinov, B., Kuroishi, C., Sugahara, M., and Kunishima, N. (2005) Crystal structures of biotin protein ligase from *Pyrococcus horikoshii* OT3 and complexes: structural basis of biotin activation *J. Mol. Biol.* **353**, 322-333

4.   Wilson, K. P., Shewchuk, L. M., Brennan, R. G., Otsuka, A. J., and Matthews, B. W. (1992) *Escherichia coli* biotin holoenzyme synthetase/bio repressor crystal structure delineates the biotin- and DNA-binding domains. *Proc. Natl. Acad. Sci. USA.* **89**, 9257-9261

5.   Tron, C. M., McNae, I. W., Nutley, M., Clarke1, D. J., Cooper, A., Walkinshaw, M. D., Baxter, R. L., and Campopiano, D. J. (2009) Structural and functional studies of the biotin protein ligase from *Aquifex aeolicus* reveal a critical role for a conserved residue in target specificity *J. Mol. Biol.* **387**, 129-146

6.   Duckworth, B. P., Geders, T. W., Tiwari, D., Boshoff, H. I., Sibbald, P. A., Barry, C. E., 3rd, Schnappinger, D., Finzel, B. C., and Aldrich, C. C. (2011) Bisubstrate adenylation inhibitors of biotin protein ligase from *Mycobacterium tuberculosis Chem. Biol.* **18**, 1432-1441

7.   Gupta, V., Gupta, R. K., Khare, G., Salunke, D. M., Surolia, A., and Tyagi, A. K. (2010) Structural ordering of disordered ligand-binding loops of biotin protein ligase into active conformations as a consequence of dehydration *PLoS One* **5**, e9222

8.   Weaver, L. H., Kwon, K., Beckett, D., and Matthews, B. W. (2001) Corepressor-induced organization and assembly of the biotin repressor: a model for allosteric activation of a transcriptional regulator *Proc. Natl. Acad. Sci. USA.* **98**, 6045-6050

9.   Wood, Z. A., Weaver, L. H., Brown, P. H., Beckett, D., and Matthews, B. W. (2006) Co-repressor induced order and biotin repressor dimerization: A case for divergent followed by convergent evolution *J. Mol. Biol.* **357**, 509-523

10.   Soares da Costa, T. P., Tieu, W., Yap, M. Y., Pendini, N. R., Polyak, S. W., Sejer Pedersen, D., Morona, R., Turnidge, J. D., Wallace, J. C., Wilce, M. C., Booker, G. W., and Abell, A. D. (2012) Selective inhibition of biotin protein ligase from *Staphylococcus aureus J. Biol. Chem.* **287**, 17823-17832

11.   Mayende, L., Swift, R. D., Bailey, L. M., Soares da Costa, T. P., Wallace, J. C., Booker, G. W., and Polyak, S. W. (2012) A novel molecular mechanism to explain biotin-unresponsive holocarboxylase synthetase deficiency *J. Mol. Med.* **90**, 81-88

12.   Kwon, K., and Beckett, D. (2000) Function of a conserved sequence motif in biotin holoenzyme synthetases *Prot. Sci.* **9**, 1530-1539

13.   Purushothaman, S., Gupta, G., Srivastava, R., Ramu, V. G., and Surolia, A. (2008) Ligand specificity of Group I biotin protein ligase of *Mycobacterium tuberculosis PLoS One* **3**, e2320

14.   Eisenstein, E., and Beckett, D. (1999) Dimerization of the *Escherichia coli* biotin repressor: Corepressor function in protein assembly *Biochemistry* **38**, 9649-9656

15.   Streaker, E. D., Gupta, A., and Beckett, D. (2002) The biotin repressor: Thermodynamic coupling of corepressor binding, protein assembly, and sequence-specific DNA binding *Biochemistry* **41**, 14263-14271

16.   Streaker, E. D., and Beckett, D. (2003) Coupling of protein aseembly and DNA binding: Biotin repressor dimerization precedes biotin operator binding *J. Mol. Biol.* **325**, 937-948

17.   Polyak, S. W., Chapman-Smith, A., Brautigan, P. J., and Wallace, J. C. (1999) Biotin protein ligase from *Saccharomyces cerevisiae.* The N-terminal domain is required for complete activity *J. Biol. Chem.* **274**, 32847-32854

18.   Ingaramo, M., and Beckett, D. (2009) Distinct amino termini of two human HCS isoforms influence biotin acceptor substrate recognition *J. Biol. Chem.* **284**, 30862-30870

19.   Soares da Costa, T. P., Tieu, W., Yap, M. Y., Zvarec, O., Bell, J. M., Turnidge, J. D., Wallace, J. C., Booker, G. W., Wilce, M. C. J., Abell, A. D., and Polyak, S. W. (2012) Biotin analogues with antibacterial activity are potent inhibitors of biotin protein ligase *ACS Med. Chem. Letts.* **3**, 509-514

20.   Xu, Y., and Beckett, D. (1994) Kinetics of biotinyl-5'-adenylate synthesis catalyzed by the *Escherichia coli* repressor of biotin biosynthesis and the stability of the enzyme-product complex *Biochemistry* **33**, 7354-7360

21.   Xu, Y., and Beckett, D. (1996) Evidence for interdomain interaction in the *E. coli* repressor of biotin biosynthesis from the studies of an N-terminal domain deletion mutant *Biochemistry* **35**, 1783-1792

22.   Brown, P. H., Cronan, J. E., Grotli, M., and Beckett, D. (2004) The biotin repressor: Modulation of allostery by corepressor analogs *J. Mol. Biol.* **337**, 857-869

23.   Chakravartty, V., and Cronan, J. E. (2012) Altered regulation of *Escherichia coli* biotin biosynthesis in BirA superrepressor mutant strains *J. Bacteriol.* **194**, 1113-1126

24.   Solbiati, J., and Cronan, J. E. (2010) The switch regulating transcription of the *Escherichia coli* biotin operon does not require extensive protein-protein interactions *Chem. Biol.* **17**, 11-17

25.   Bradford, M. (1976) A rapid and sensitive method for the quantification of microgram quantities of protein utilizing the principle of protein-dye binding *Anal. Biochem.* **72**, 248-254

26.   Pendini, N. R., Polyak, S. W., Booker, G. W., Wallace, J. C., and Wilce, M. C. (2008) Purification, crystallization and preliminary crystallographic analysis of biotin protein ligase from *Staphylococcus aureus Acta Crystallogr. Sect. F Struct. Biol. Cryst. Commun.* **64**, 520-523

27.   Laue, T. M., Shah, B. D., Ridgeway, T. M., and Pelletier, S. L. (1992) *Analytical Untracentrifugation in Biochemistry and Polymer Science*, Cambridge, UK

28.   Schuck, P. (2000) Size-distribution analysis of macromolecules by sedimentation velocity ultracentrifugation and lamm equation modelling *Biophys. J.* **78**, 1606-1619

29.   Perugini, M. A., Schuck, P. & Howlett, G.J. . (2000) Self-association of human apolipoprotein E3 and E4 in the presence and absence of phospholipid. *J. Biol. Chem.* **275**, 36758-36765

30.   Perugini, M. A., Schuck, P. & Howlett, G.J. (2002) Differences in the binding capacity of human apolipoprotein E3 and E4 to size-fractioned lipid emulsions. *Euro. J. Biochem.* **269**, 5939-5949

31.   Schuck, P., Perugini, M. A., Gonzales, N. R., Howlett, G. J., and Schubert, D. (2002) Size-distribution analysis of proteins by analytical ultracentrifugation: strategies and application to model systems. *Biophys. J.* **82**, 1096-1111

32.   Vistica, J., Dam, J., Balbo, A., Yikilmaz, E., Mariuzza, R. A., Rouault, T. A., and Schuck, P. (2004) Sedimentation equilibrium analysis of protein interactions with global implicit mass conservation constraints and systematic noise decomposition *Anal. Biochem.* **326**, 234-256

33.   Burgess, B. R., Dobson, R. C. J., Bailey, M. F., Atkinson, S. C., Griffin, M. D. W., Jameson, G. B., Parker, M. W., Gerrard, J. A., and Perugini, M. A. (2008) Structure and evolution of a novel dimeric enzyme from a clinically-important bacterial pathogen *J. Biol. Chem.* **283**, 27598-27603

34.   Voss, J. E., Scally, S. W., Taylor, N. L., Atkinson, S. C., Griffin, M. D. W., Hutton, C. A., Parker, M. W., Alderton, M. R., Gerrard, J. A., Dobson, R. C. J., Dogovski, C., and Perugini, M. A. (2010) Substrate-mediated stabilization of a tetrameric drug target reveals Achilles heel in anthrax *J. Biol. Chem.* **285**, 5788-5195

35.   Kwon, K., Streaker, E. D., Ruparelia, S., and Beckett, D. (2000) Multiple disordered loops function in co-repressor induced dimerization of the biotin repressor. *J. Mol. Biol.* **304**, 821-833

36.   Zhao, H., Naganathan, S., and Beckett, D. (2009) Thermodynamic and structural investigation of bispecificity in protein-protein interactions *J. Mol. Biol.* **389**, 336-348

37.   Rodionov, D. A., Mironov, A. A., and Gelfand, M. S. (2002) Conservation of the biotin regulon and the BirA regulatory signal in Eubacteria and Archaea *Genome Res.* **12**, 1507-1516

38.   Barker, D. F., and Campbell, A. M. (1981) The *birA* gene of *Escherichia coli* encodes a biotin holoenzyme synthetase *J. Mol. Biol.* **146**, 451-467

39.   Chapman-Smith, A., Mulhern, T. D., Whelan, F., Cronan, J. E., Jr., and Wallace, J. C. (2001) The C-terminal domain of biotin protein ligase from *E. coli* is required for catalytic activity *Prot. Sci.* **10**, 2608-2617

40.   Napier, B. A., Meyer, L., Bina, J. E., Miller, M. A., Sjostedt, A., and Weiss, D. S. (2012) Link between intraphagosomal biotin and rapid phagosomal escape in *Francisella Proc. Natl. Acad. Sci. USA*. **109**, 18084-18089

41.   Salaemae, W., Azhar, A., Booker, G. W., and Polyak, S. W. (2011) Biotin biosynthesis in *Mycobacterium tuberculosis*: physiology, biochemistry and molecular intervention *Protein Cell* **2**, 691-695

FOOTNOTES

Abbreviations

AUC – analytical ultracentrifugation; BPL – biotin protein ligase, SEC-MALS – Size exclusion chromatography coupled to multi-angle light scattering; SPR – surface plasmon resonance

FIGURES

Figure legends

Fig 1. Concentration dependent dimerization of *S. aureus* BPL.
Analytical ultracentrifugation analyses were performed and $c(s)$ plotted as a function of $s_{20,w}$ (S) for apo *Sa*BPL at (A) 26 μM, (B) 11.7 μM and (C) 3.9 μM. Residuals resulting from the $c(s)$ distribution best fits are shown as a function of radius from the axis of rotation.

Fig. 2. Inhibitor induced dimerization of *S. aureus* BPL.
Analytical ultracentrifugation analyses were performed and $c(s)$ plotted as a function of $s_{20,w}$ (S) for 26 μM apo *Sa*BPL in the presence of either no ligand (black curve), 100 μM biotin (blue curve) or biotin acetylene (red curve). A representative residuals plot resulting from one of the $c(s)$ distribution best fits is shown as a function of radius from the axis of rotation.

Fig 3. Electromobility shift assays.
Binding curves for (A) apo and (B) holo forms of *Sa*BPL.

Fig 4. *S. aureus* BPL dimer.
*Sa*BPL in complex with biotinol-5′-AMP (yellow stick) is shown in its dimeric form, with one monomer coloured tan and the other cyan. The biotin-binding loop is highlighted in magenta. Enlarged in box are key amino acids required for dimerization. Figure was prepared using USCF Chimera with PDB 4DQ2 (10).

Fig 5. Mutation of F123 abolishes inhibitor induced dimerization of *S. aureus* BPL.
Analytical ultracentrifugation analyses were pre-formed and $c(s)$ plotted as a function of $s_{20,w}$ (S) for *Sa*BPL-F123G (A) and *Sa*BPL-F123R (B) at 26.0 μM in the absence (black) and presence of biotin (blue) and biotin acetylene (red).

Fig 6. Inhibition of BPL activity by biotin acetylene.
The activity of BPLs from *S. aureus* (red curves) and *E. coli* (green curves) were measured in the presence of varying concentrations of biotin acetylene. The inhibitory activities of the two wild-type BPLs were compared against (A) *Ec*BPL-R119F mutant (black curve) and (B) the *Sa*BPL-F123R mutant (orange curve). Inhibition constants from these analyses are shown in Table 2.

Fig 7. SPR binding of biotin acetylene.
SPR sensorgrams measuring biotin acetylene binding to either (A) wild-type *Sa*BPL, (B) *Sa*BPL-F123G, (C) *Sa*BPL-F123R, (D) wild-type *Ec*BPL and (E) *Ec*BPL-R119F. All enzymes were immobilized onto a CM5 sensor chip and data subtracted from a blank reference cell contained no enzyme. Concentrations of biotin acetylene injected were 0 (red), 1.6 μM (green), 3.2 μM (blue) and 6.4 μM (pink).

Fig.1
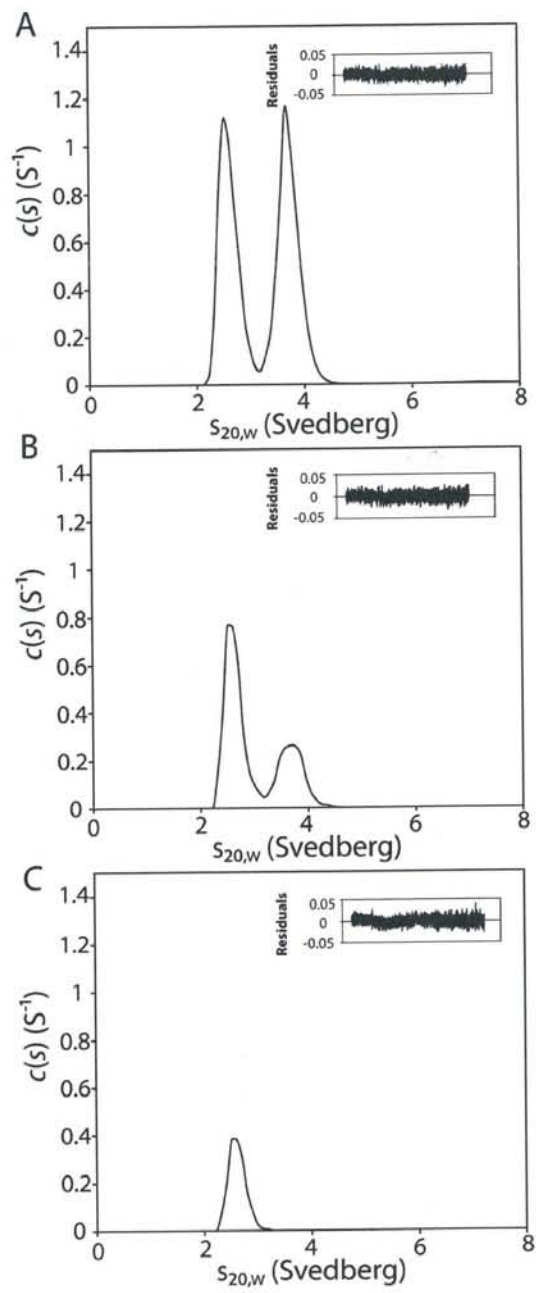
Fig. 2
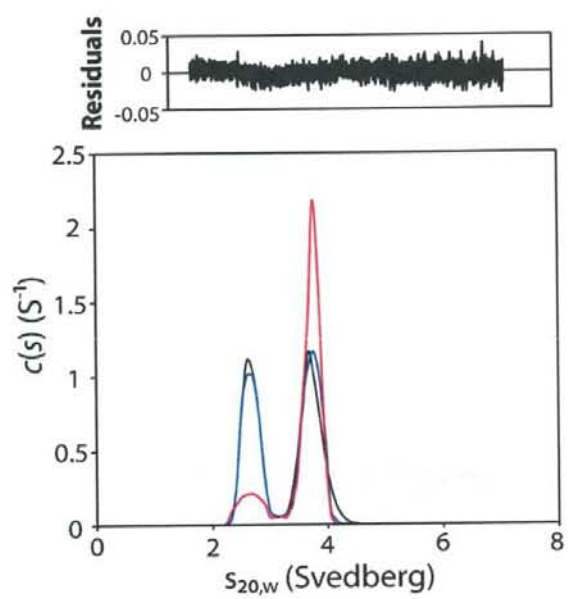
Fig. 3
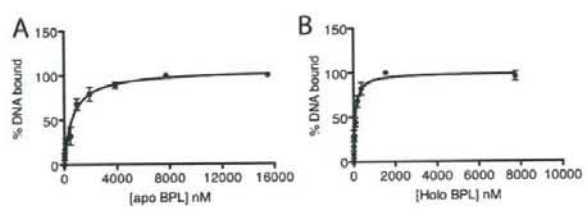
Fig. 4
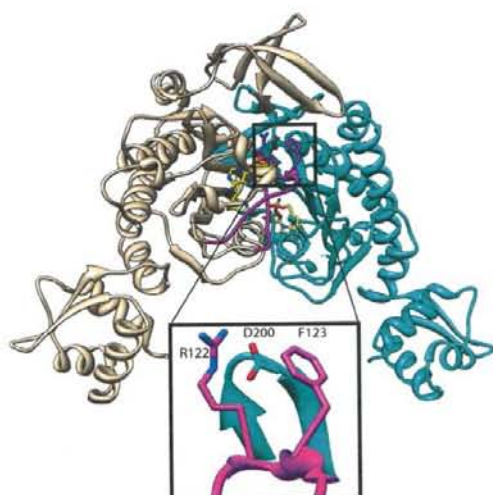
Fig. 5
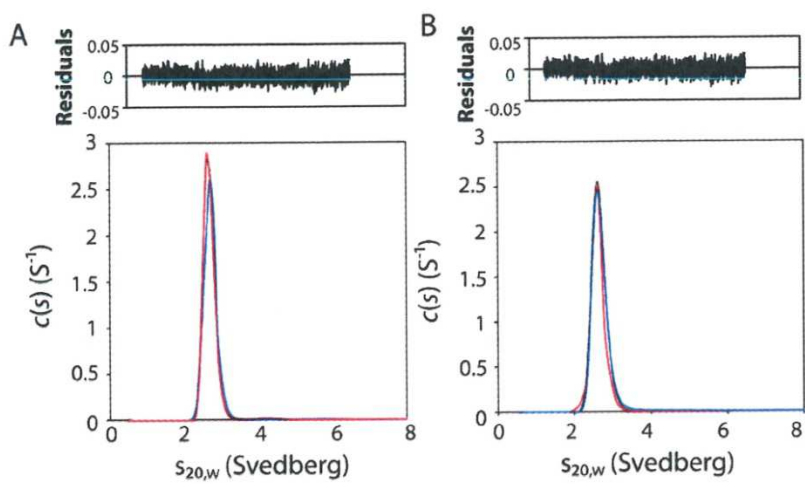
Fig. 6
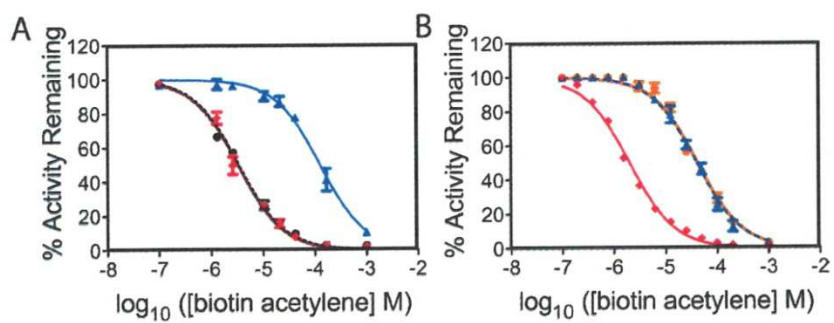
Fig. 7
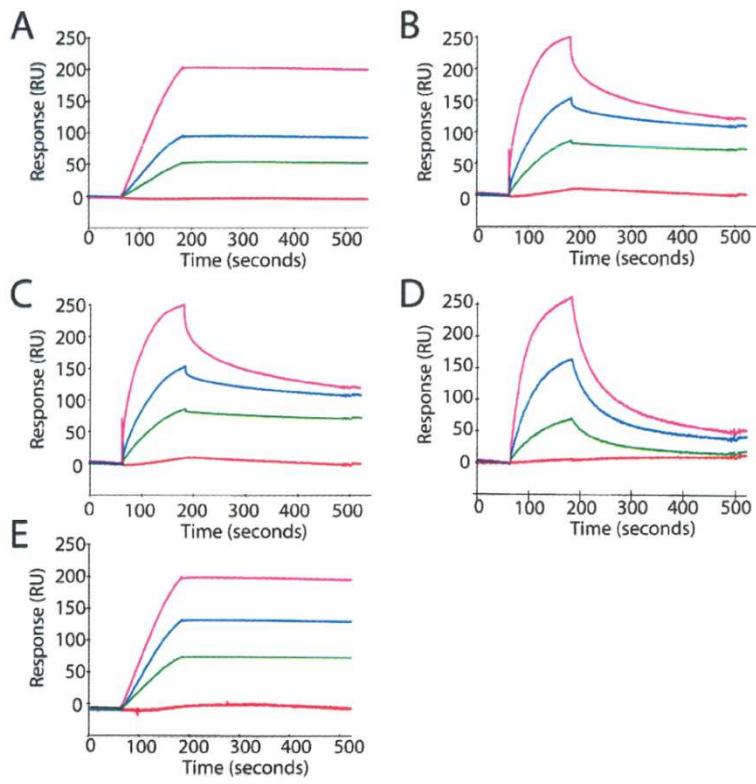
Supplemental data

A novel link between protein homodimerization and inhibitor binding to biotin protein ligase from *Staphylococcus aureus*

Tatiana P. Soares da Costa[1]**, Min Y. Yap**[2]**, Matthew A. Perugini**[3]**, John C. Wallace**[1]**, Andrew D. Abell**[4]**, Matthew C. J. Wilce**[2]**, Steven W. Polyak**[1*]** and Grant W. Booker**[1]**.**

[1] School of Molecular and Biomedical Science, University of Adelaide, South Australia 5005, Australia.

[2] School of Biomedical Science, Monash University, Victoria 3800, Australia.

[3] Department of Biochemistry, La Trobe Institute for Molecular Science, La Trobe University, Victoria 3086, Australia.

[4] School of Chemistry and Physics, University of Adelaide, South Australia 5005, Australia.

Table of Contents

1

Supplemental Experimental Procedures

Nucleic acid manipulations

The genomic DNA sequence for the methicillin-resistant *S. aureus* strain N315, used to design oligonucleotides for PCR and mutagenesis (shown in Table S1), was from GenBank (Genbank accession no. NC002745). Here the biotin domain from pyruvate carboxylase from *S. aureus* (*Sa*PC90) was employed as a substrate in all BPL assays. The DNA encoding *Sa*PC90 was obtained by genomic PCR using oligonucleotides *SaPC90 forward* and *SaPC90 reverse*. PCR products were digested with *Bam*HI and *Eco*RI restriction endonucleases and ligated into similarly treated pGEX-4T-2 (GE Healthcare), yielding pGEX-*Sa*PC90. All recombinant DNA constructs were confirmed by DNA sequencing (Institute of Medical and Veterinary Science, Adelaide).

Purification of apo **Sa*PC90***

Expression of the biotin domain from *S. aureus* pyruvate carboxylase (*Sa*PC90) was performed in the *bir*A85⁻ *E. coli* strain BM4062 (2) containing a temperature sensitive mutation in the endogenous *bpl* gene that renders the enzyme inactive at $42°C$, thereby facilitating the production of the non-biotinylated protein. The biotin domains were expressed as GST fusion proteins permitting high-level expression and rapid purification by affinity chromatography. Cells were grown in LB media supplemented with 200 µg/ml ampicillin and 10 µM biotin at $30°C$ to OD_{600} ~0.8, then moved to $42°C$ for another 30 minutes before 3 hours induction with 200 µg/ml IPTG. Cells were disrupted by three passages through a M110L homogenizer (Microfluidics, USA) prior to affinity chromatography. The filtered lysate was passed over a 40 ml glutathione-agarose resin (Scientifix, Australia) at a flow rate of 2 ml/min. Unbound material was removed by washing with 3 column volumes of TBS pH 8.5, then 1 column volume of TBS pH 8.5 containing 2.5 mM $CaCl_2$. The GST fusion proteins were cleaved on the column for 2 hours at $37°C$ with thrombin (≈3U thrombin/mg protein) then *Sa*PC90 washed off with TBS pH 8.5. Fractions were analysed by SDS-PAGE and fractions containing the biotin domain were pooled, concentrated with a 3000 molecular weight cut-off protein concentrator (GE Healthcare) and dialysed overnight at $4°C$ against 2 mM ammonium acetate. Protein purity was assessed by SDS-PAGE. The concentrations of

biotin domains were estimated using a BCA assay (Pierce Biotechnology) following the manufacturer's instructions.

Purification of apo BPL enzymes

The production of *Sa*BPL and *Ec*BPL enzymes was performed essentially as described (1) with the following modifications. To remove any biotinyl-5'-AMP that may have co-purified with the *Sa*BPL, whole cell lysates were first incubated at 37°C for 1 hour with 100 mg of GST-*Sa*PC90 protein to accept the biotinyl moiety. Whole cell extracts were then fractionated using a 5 mL His-Trap HP column (GE Healthcare) that had been equilibrated with 10 column volumes of 50 mM KH_2PO_4 pH 8.0, 300 mM KCl and 5 mM imidazole. The column was first washed with 10 column volumes of the same buffer followed by a wash with 50 mM KH_2PO_4 pH 8.0, 300 mM KCl and 10 mM imidazole. The protein was eluted with 50 mM KH_2PO_4 pH 8.0, 300 mM KCl and 250 mM imidazole before buffer exchange into a enzyme storage buffer (50 mM Tris-HCl, 100 mM KCl, 5% (v/v) glycerol, 1 mM dithiothreitol). Aliquots of the enzyme were stored at -80°C.

Biotinyl-transferase assays.

To confirm that no biotinyl-5-AMP had co-purified with *Sa*BPL, and thus the sample was truly in its apo state, two alternative biotinyl-transferase assays were employed. Both assays used streptavidin-based methodologies to measure the incorporation of biotin onto an acceptor substrate. Firstly, 5 ng of the substrate *Sa*PC90 was immobilized onto the surface of each well of a white 96-well plate as previously described (2). The enzyme assay was then performed on the plate using BPL assay buffer (50 mM Tris pH 8.0, 100 mM KCl, 3 mM ATP, 5.5 mM $MgCl_2$, 0.1 μM dithiothreitol). Reactions were performed in the absence or presence of 5 μM biotin at 37°C for 2 hours with varying concentrations of *Sa*BPL. The plates were then washed, probed with Europium-labelled streptavidin and biotinylated protein detected using time resolved fluorescence as previously described (2). A standard curve of biotinylated *Sa*PC90 was included to allow quantitation of the amount of biotinylated product produced during the reaction. Alternatively, the biotinyl-transferase assay was performed in a solution-based assay using *Sa*PC90. Here *Sa*BPL was incubated in reaction buffer (50 mM Tris-HCl pH 7.5, 50 mM NaCl, 10 mM $MgCl_2$, 1 mM ATP and 10 % glyercol) together with

a 5-fold molar excess of *Sa*PC90. After 1 hour at 37°C, the products were fractionated by SDS-PAGE before Western transfer onto nitrocellulose. The resulting blot was subsequently probed with a Streptavidin-horse radish peroxidase conjugate to detect biotinylated protein.

Size exclusion chromatography with multi-angle light scattering (SEC-MALS):

The instrument set-up used consisted of a Superdex 200 10/300 GL column (Amersham Biosciences) connected in series with a miniDAWN TREOS light-scattering detector (Wyatt Technology) and an OPTILAB rEX interferometric refractometer detector (Wyatt Technology). Analytical size-exclusion chromatography was performed at 20° C using a mobile phase containing 50 mM Tris.HCl pH 8.0, 150 mM NaCl and 0.1 mM EDTA. 100 μL of purified *Sa*BPL at 26 μM was injected into the column and eluted at a flow rate of 0.25 mL/min. Detector outputs were acquired using Astra software (Wyatt Technology).

Electromobility shift assay

The region of the *bioO* repressor bound by *Sa*BPL was delineated bioinformatically by Rodionov et al (3). Extension of this sequence allows for an imperfect inverted repeat: 5′-CCTTAAATGTAAACTTATTAATTATAAAAGTTTACATTTAAGG-3′ and 5'-AATCCAAATGTAAACTTTTATAATTAATAAGTTTACATTTAAGG-3'. Single stranded DNA was ordered from Geneworks, and annealed together at 97°C for 5 minutes before allowed to cool down slowly to room temperature. The resulting double stranded DNA was labelled with a 3′ digoxigenin-11-ddUTP tag using the DIG-labelling kit (Roche). Apo or biotinyl-5′-AMP holo *Sa*BPL were incubated with the DIG-labeled DNA in the presence of 50 mM Tris-HCl pH 7.5, 50 mM NaCl, 5% (v/v) glycerol and 10 mM $MgCl_2$ for half an hour on ice. The resulting protein-complex was fractionated on a 8% polyacrylamide-TBE gel for 20 minutes at 200 V, and then transferred onto a positively charged Nylon membrane (Roche). Detection of DIG-labelled DNA bands was performed according to manufacturers instructions. Quantitation of bands was carried out with ImageJ, and the percentage of unbound DNA was determined by comparing the intensity of the unbound DNA band with the total intensity of the unbound and bound DNA in each lane.

4

Supplemental Results

Fig S1: *Sa*BPL was purified in its apo form.

Two alternative biotinyl-transferase assays were performed to confirm biotinyl-5′-AMP did not co-purify with apo *Sa*BPL, as described in supplemental Experimental Procedures. The biotinylated products from the reaction were detected by using either A) time-resolved fluorescence with Europium-labelled streptavidin or B) Western-blot analysis with streptavidin-horse radish peroxidase conjugate. A) The biotinyl-transferase assay was performed in the presence (black bars) or absence (white bars) of additional biotin with varying concentrations of *Sa*BPL. B) The biotinyl-transferase assay was performed with 1) apo *Sa*BPL alone, 2) holo *Sa*BPL alone, 3) non-biotinylated *Sa*PC90 alone, 4) biotinylated *Sa*PC90 alone, 5) apo SaBPL with *Sa*PC90 and 6) holo *Sa*BPL with *Sa*PC90.
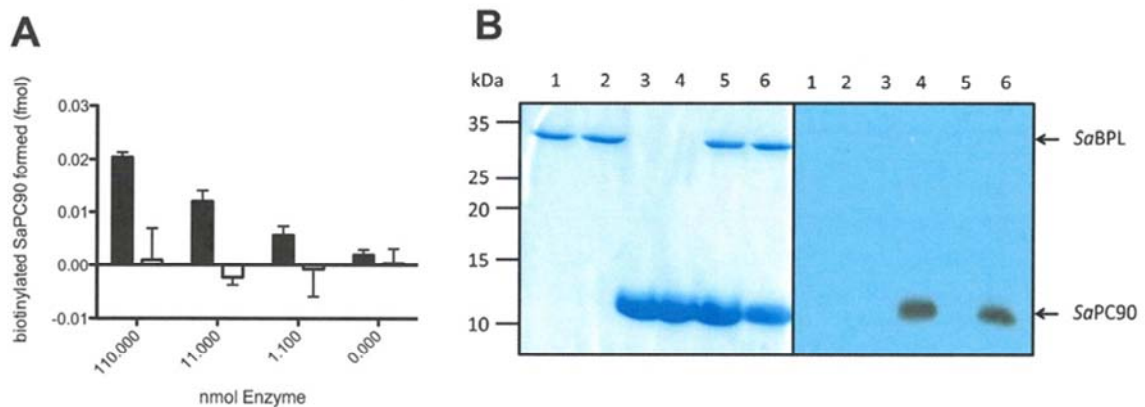
Fig S2: SEC-MALS spectra for (A) wild-type *Sa*BPL, (B) *Sa*BPL-F123G, (C) *Sa*BPL-F123R, (D) Wild-type *Ec*BPL and (E) *Ec*BPL-R119F.

Fig 3. DimPlot of *Sa*BPL homodimer surface.

Key

- Residues of first surface
- Residues of second surface
- Hydrogen bond and its length

His 53 — Residues involved in hydrophobic contact(s)

Corresponding atoms involved in hydrophobic contact(s)
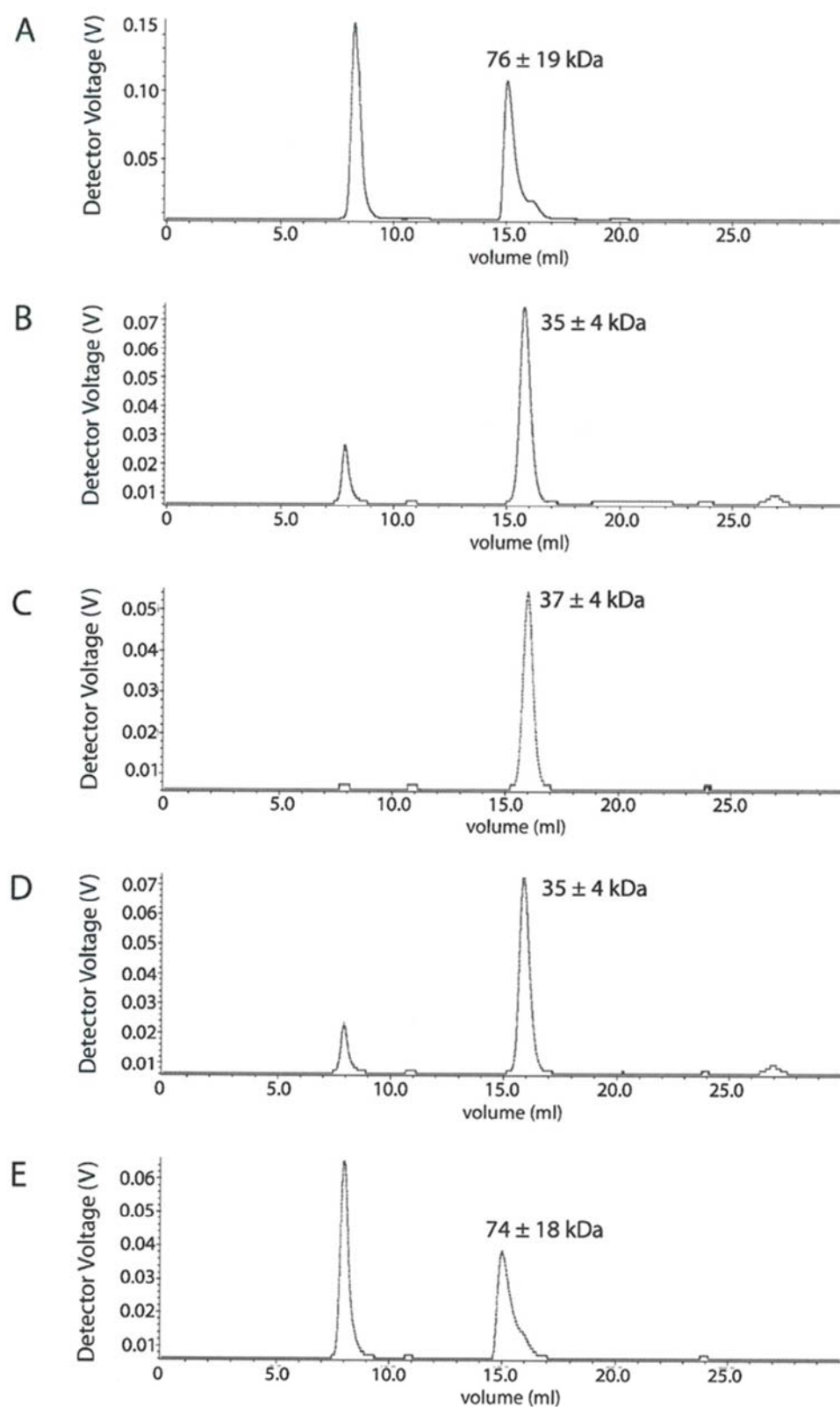
Fig S4. Overlaid circular dichroism spectra. (A) Wild-type *Sa*BPL (red), *Sa*BPL-F123G (black), *Sa*BPL-F123R (blue). (B) Wild-type *Ec*BPL (red) and *Ec*BPL-R119F (blue).

(A)

(B)
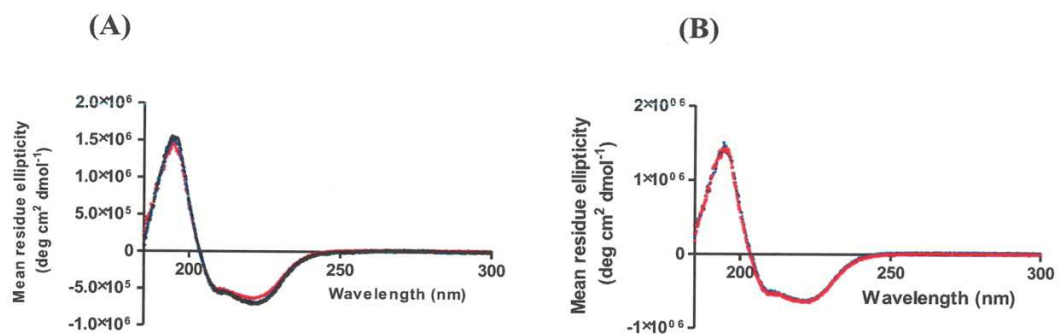
Supplemental Tables

Table S1: Oligonucleotides employed in this study, with the mutated codons underlined. Numbers in superscript designate position in the target gene sequence.

Construct	Forward primer
SaPC90 (forward)	5' ATCTAC<u>GGATCC</u>^{3181}AATGTGCATACAAATGCGAACGTTAAGC^{3208} 3'
SaPC90 (reverse)	5' ATCTAC<u>GAATTCA</u>^{3451}GTCAGTTGCTTTTTCAATTTCG^{3429} 3'
*Sa*BPL-F123G	5'-CGAAAGGTCGTGGTCGA<u>CGT</u>AATAGACATTGGAG-3'
*Sa*BPL-F123R	5'- CGAAAGGTCGTGGTCGA<u>GGT</u>AATAGACATTGGAG -3'
*Ec*BPL-FOR	5'- TCATGAAGGATAACACCGTGCCAC-3'
*Ec*BPL-REV (His6-tag)	5'- AAGCTTA<u>ATGATGATGATGATGATG</u>TCCTTTTTCTGCAC-3'
*Ec*BPL-R119F	5'-GGCCGTGGTCGC<u>TTC</u>GGTCGGAAATGG-3'

Table S2

	Biotin			MgATP		
BPL	k_{cat} (s^{-1})	K_m (μM)	k_{cat}/K_m (s^{-1} M^{-1}) x 10^3	k_{cat} (s^{-1})	K_m (mM)	k_{cat}/K_m (s^{-1} M^{-1}) x 10^3
WT *Sa*BPL	0.45±0.09	1.01±0.16	450±14	0.36±0.07	0.18±0.03	2.00±0.20
*Sa*BPL-F123G	0.04±0.01	3.06±0.30	13.4±1.0	0.04±0.003	0.24±0.04	0.15±0.01
*Sa*BPL-F123R	0.04±0.01	3.11±0.39	11.6±0.8	0.03±0.01	0.26±0.04	0.12±0.01
WT *Ec*BPL	0.34±0.08	0.31±0.04	1100±24	0.29±0.06	0.42±0.04	690±17
*Ec*BPL-R119F	0.27±0.08	0.35±0.04	770±20	0.24±0.06	0.22±0.02	1090±26

9

Supplemental References

1. Pendini, N. R., Polyak, S. W., Booker, G. W., Wallace, J. C., and Wilce, M. C. (2008) *Acta Crystallogr. Sect. F Struct. Biol. Cryst. Commun.* **64**, 520-523
2. Pendini, N. R., Bailey, L., Booker, G., Wilce, M. C., Wallace, J., and Polyak, S. W. (2008) *Archives of Biochemistry and Biophysics* **479**, 163-169
3. Rodionov, D. A., Mironov, A. A., and Gelfand, M. S. (2002) *Genome Res.* **12**, 1507-1516

10

Chapter 6
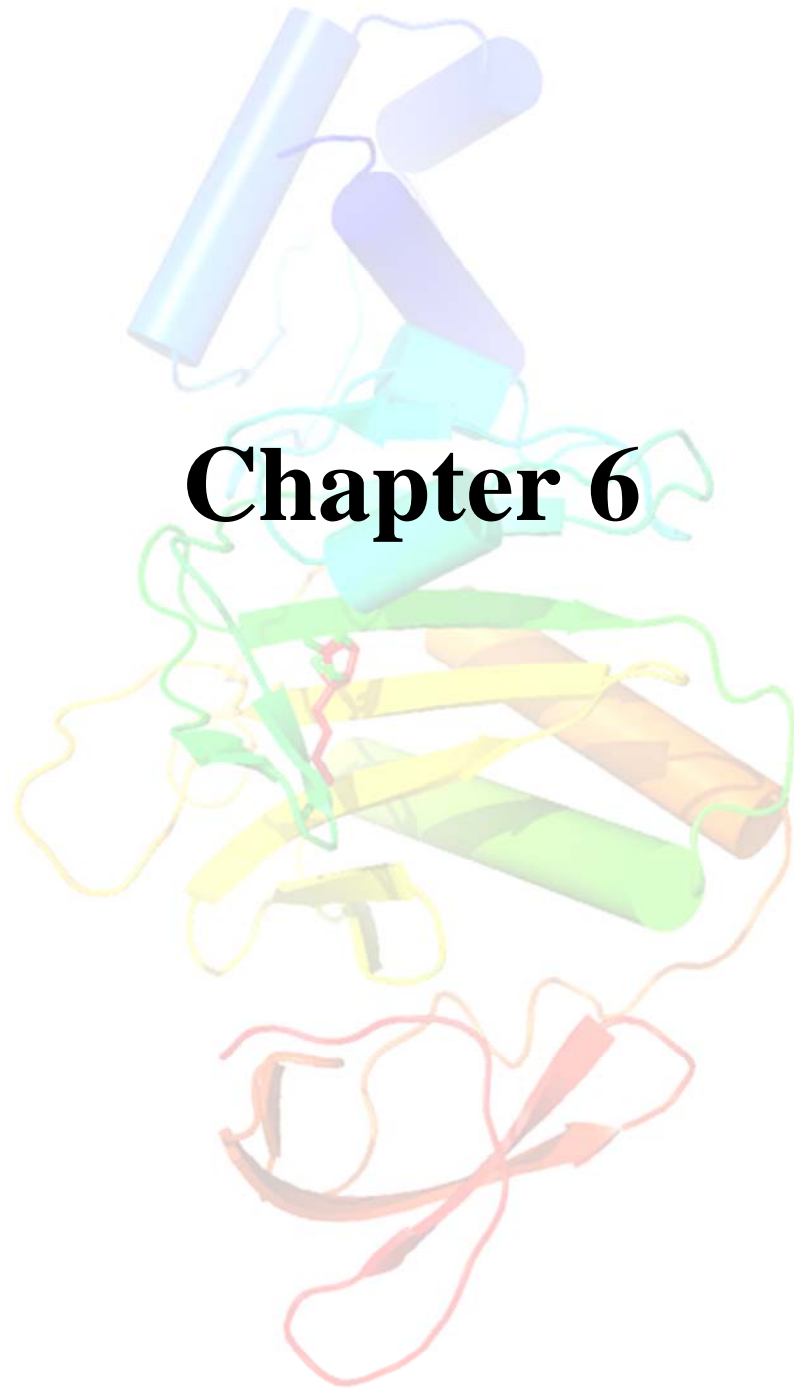
Statement of Authorship

Title of Paper	'Humanized' biotin protein ligase provides clues about inhibitor selectivity.
Publication Status	◯ Published ◯ Accepted for Publication ◯ Submitted for Publication ⦿ Publication Style
Publication Details	N/A

Author Contributions

By signing the Statement of Authorship, each author certifies that their stated contribution to the publication is accurate and that permission is granted for the publication to be included in the candidate's thesis.

Name of Principal Author (Candidate)	Tatiana P. Soares da Costa		
Contribution to the Paper	Primary role in performing all experiments and preparing the manuscript. Performed protein expression, purification, kinetic analysis, inhibition assays, surface plasmon resonance analysis and circular dichroism analysis.		
Signature		Date	16/11/2012

Name of Co-Author	John. C. Wallace		
Contribution to the Paper	Provided intellectual discussion.		
Signature		Date	29/11/2012

Name of Co-Author	Grant W. Booker		
Contribution to the Paper	Provided direction and assistance in all aspects of protein chemistry.		
Signature		Date	28/11/2012

Name of Co-Author	Steven W. Polyak		
Contribution to the Paper	Provided direction on all aspects of enzymology and design of the construct.		
Signature		Date	29/11/2012

'HUMANIZED' BIOTIN PROTEIN LIGASE PROVIDES CLUES ABOUT INHIBITOR SELECTIVITY

Tatiana P. Soares da Costa, John C. Wallace, Steven W. Polyak, Grant W. Booker*

School of Molecular and Biomedical Science, University of Adelaide, SA, Australia

* Address correspondence to: Grant W. Booker, Molecular Life Science Building, Department of Biochemistry, University of Adelaide, South Australia, Australia, 5005, Tel. 61-8-8313-3090; Fax: 61-8-8303-4362; E-mail: grant.booker@adelaide.edu.au

Biotin protein ligase (BPL) is a ubiquitous enzyme involved in the attachment of biotin onto biotin-dependent enzymes. Due to the pivotal role of biotin-dependent enzymes in important metabolic pathways in bacteria, BPL has been proposed as a novel antibiotic target. Bacterial drug targets that have a closely related human homologue such as BPL represent a new frontier in antibiotic discovery. However, to avoid potential toxicity to the host these inhibitors must have very high selectivity for the bacterial enzyme. A triazole-based class of compounds has recently been shown to inhibit *Staphylococcus aureus* BPL (*Sa*BPL) but not the human enzyme. A number of BPL crystal structures have been published but the structure of human BPL (*Hs*BPL), which would be useful in understanding the molecular explanation for selectivity, is yet to be reported. Although the amino acid residues in the biotin-binding site are highly conserved, the nucleotide pocket shows a high degree of variability that can be exploited to create selective compounds towards BPLs from pathogens. Here, we converted the seven variable amino acids in the nucleotide binding site of *Sa*BPL to the corresponding equivalents in human BPL. The resulting 'humanized' enzyme has similar kinetic and inhibitory properties to *Hs*BPL but importantly, can be purified at >20-fold greater yield. Crystal trials of this chimeric protein have commenced as this structure may help us design species selective compounds in future drug discovery efforts.

Antibiotic resistant bacteria have become a major health problem worldwide (1). It is imperative that we increase our efforts to develop novel antibiotic classes that are not subject to known resistance mechanisms. A new frontier for antibiotic research is to target essential enzymes that have mammalian equivalents. The challenge here will be to identify compounds with exquisite specificity towards the bacterial target. Biotin protein ligase (BPL) is one such example. BPL is responsible for the attachment of biotin onto the biotin-dependent enzymes, which often play important roles in essential metabolic pathways. Protein biotinylation is carried out in two steps (Scheme 1.0). In the first step, the biotinyl-5´-AMP reaction intermediate is formed from biotin and ATP. In the second step, the biotin moiety is covalently attached to the ε-amino group of a specific lysine residue present in the conserved biotin domain of all biotin-dependent enzymes, resulting in the release of adenosine monophosphate (AMP) (2). In many bacteria and other organisms, protein biotinylation is essential for the activation of the biotin-dependent enzyme acetyl-CoA carboxylase, which catalyzes the first committed step in fatty acid biosynthesis. Genetic and pharmacological studies have shown that this metabolic pathway provides a number of attractive drug targets for new antibiotics (1,3-8). Therefore BPL inhibitors provide a new approach to the discovery of novel antibiotic classes required to combat drug resistance.
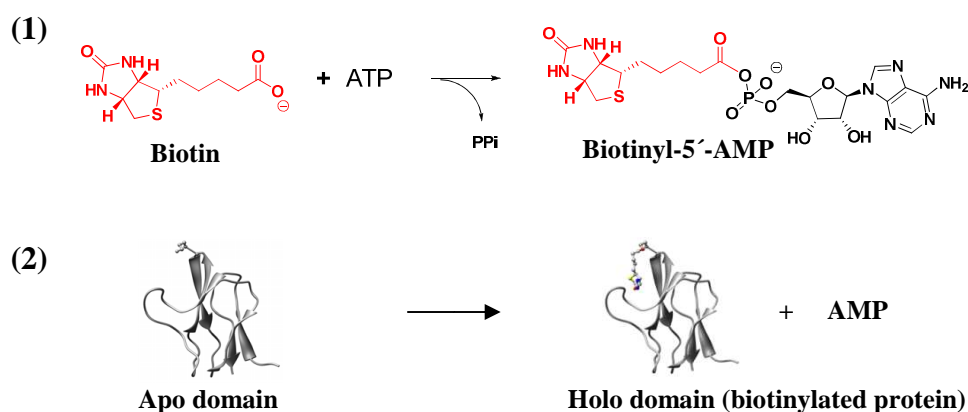
Scheme 1.0: *Two-step ordered BPL-catalyzed reaction.*

BPLs can be divided into three structural classes (9). Class I enzymes (e.g. *Pyrococcus horikoshii*, *Mycobacterium tuberculosis*) have a two domain structure consisting solely of the C-terminal and the catalytic domains. Class II BPLs (e.g. *Escherichia coli*, *Staphylococcus aureus*) contain an additional N-terminal domain required for DNA

binding. Class III BPLs (e.g. *Homo sapiens* and *Candida albicans*) have a large N-terminal extension that bears no resemblance to any other protein sequence in the literature (9,10). Deletion studies have shown that the minimal region required for *H. sapiens* BPL (*Hs*BPL) function consists of the C-terminal 349 residues (10). Although not essential for activity, an N-terminal deletion of the first 165 residues resulted in protein instability (10). It has since been shown that the region of the N-terminal domain between Leu166 and Tyr266 is involved in recognition of the biotin domain substrate through an interaction with the catalytic domain (10,11). This has been previously proposed for the Class III yeast BPL (12). Thus it is speculated that the N-terminal region possesses 'proof-reading activity' that allows it to differentiate between various biotin-dependent enzymes and is involved in stabilizing the enzyme: biotin domain complex.

Despite the high degree of similarity in the catalytic domain between BPLs, we have recently identified a series of biotin-triazole molecules with selective inhibitory activity against *S. aureus* BPL (*Sa*BPL) over the human equivalent (13). The biotin triazoles are the first example of highly selective BPL inhibitors to be reported. The most potent compound against *Sa*BPL from this series is BPL-068 (Figure 1B), resulting in a K_i value against *Sa*BPL of   0.09 ± 0.01 µM and displaying >1100-fold selectivity for the *Sa*BPL over the human homologue (13). Importantly, the biotin triazole inhibitors showed cytotoxicity against *S. aureus*, but not cultured mammalian cells. The structure of the *Sa*BPL: BPL-068 complex reveals that the inhibitor adopts a 'U-shaped' geometry similar to the intermediate biotinyl-5´-AMP. The triazole linker is stabilized by hydrogen bond interactions with Arg125 and the highly conserved residues Arg122 and Asp180. Arg125 has been shown to be a key determinant in the selectivity observed for BPL-068. Mutation of Arg125 to an alanine or asparagine, the equivalent residue in *Hs*BPL, results in a decrease in affinity for *Sa*BPL by 50-fold (13). BPL-068 also makes a key π- π stacking interaction with the highly conserved Trp127 residue, which is pre-required for molecules to bind in the ATP pocket. The benzoxazolone ring in the nucleotide pocket is accommodated by the hydrophobic region created by the *Sa*BPL amino acid residues Phe220, Ile224 and Ala228. Phe220 and Ala228 are non-conserved between the *Sa*BPL and *Hs*BPL enzymes. The biotin-triazole molecules provide a novel pharmacophore for future medicinal chemistry programmes to develop this new antibiotic class (Figure 1A).

(A)   **(B)**
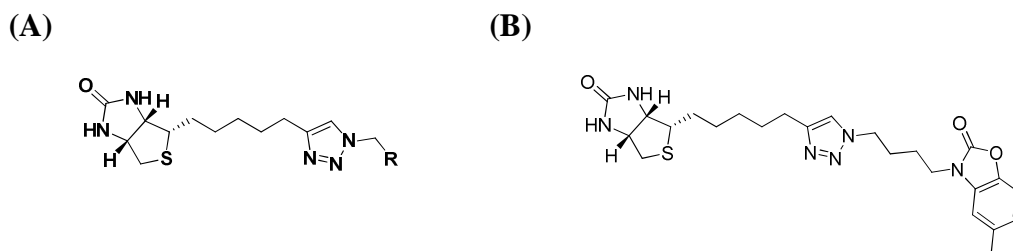
Figure 1: *(A) Pharmacophore representing the biotin-triazole moiety, (B) Structure of compound BPL-068.*

A number of functional studies have been done on *Hs*BPL (10,11,14-19), but its structure is yet to be reported. One of the major roadblocks to obtaining crystals of the full-length human enzyme is the low yield of protein from recombinant expression/purification. A molecular model of the catalytic domain of *Hs*BPL has been proposed (9) using the published *P. horikoshii* OT3 structure (20), with which it shares a 23% sequence identity. A structure-based sequence alignment revealed the variant amino acids involved in substrate binding between *Sa*BPL and *Hs* BPL (Figure 2A). It is clear that there is a high degree of conservation in the residues making contact with biotin. The biotin pocket is relatively small and hydrophobic, which is required to accommodate the ureido and thiophene rings of biotin. In contrast, the amino acid residues in the ATP binding site of BPLs are divergent. Seven out of the nine residues that make contact with the nucleotide are different in *Sa*BPL compared to *Hs*BPL: Arg125, His126, Ser128, Gln215, Phe220, Arg227, Ala228 (highlighted in Figure 2B) are replaced by, respectively, Asn, Val, Leu, Asn, Ile, Leu and Ile in *Hs*BPL.

Here we describe an alternative approach that could be used to increase our chances of obtaining structural data about *Hs*BPL. We have created a 'humanized' protein in which all seven residues in *Sa*BPL that are different to those found in the nucleotide pocket of the human enzyme are replaced. Specifically, we have produced a 'humanized' *Sa*BPL (h*Sa*BPL) with the following mutations introduced to the *Sa*BPL protein: R125N, H126V, S128L, G215N, F220I, R227L and A228I. This 'humanized' protein exhibits similar kinetic and inhibitory properties to the human enzyme and is readily purified.

(A)


```
SaBPL     -----------------------------------MSKYSQDVLQLLYKNKPNYISG-  22
HsBPL     EVRSVLADCVDIDSYILYHLLEDSALRDPWTDNCLLLVIATRESIPEDLYQKFMAYLSQG 240

SaBPL     ----------------------QSIAESLNISRTAVKKVIDQLKLEGCKIDS-------  52
HsBPL     GKVLGLSSSFTFGGFQVTSKGALHKTVQNLVFSKADQSEVKLSVLSSGCRYQEGPVRLSP 300

SaBPL     ------------------------------------------------------------
HsBPL     GRLQGHLENEDKDRMIVHVPFGTRGGEAVLCQVHLELPPSSNIVQTPEDFNLLKSSNFRR 360

SaBPL     ----------------------------------------------VNHKGHLLQQLPDI  66
HsBPL     YEVLREILTTLGLSCDMKQVPALTPLYLLSAAEEIRDPLMQWLGKHVDSEGEIKSGQLSL 420

                                                          BB
SaBPL     WYQG--------------IIDQYTKSSALFDFSEVYDSIDSTQLAAKKSLVGNQSS---  108
HsBPL     RFVSSYVSEVEITPSCIPVVTNMEAFSSEHFNLEIYRQNLQTKQLGKVILFAEVTPTTMR 480

                              B         BBA  AACA
SaBPL     --------------FFILSDEQTKGRGRFNRHWSSSKGQGLWMSVVLRPN-----VAFSM 149
HsBPL     LLDGLMFQTPQEMGLIVIAARQTEGKGRGGNVWLSPVGCALSTLLISIPLRSQLGQRIPF 540

                                                    C  B
SaBPL     ISKFNLFIALGIRDAIQHFSQDEVKVKWPNDIYIDNGKVCG--FLTEMVANNDGIEAIIC 207
HsBPL     VQHLMSVAVVEAVRSIPKYQDINLRVKWPNDIYYSDLMKIGGVLVNSTLMGETFYILIGC 600

          B B   A   A    A        AA
SaBPL     GIGINLTQQLENFDESIRHRATSIQLHDKNKLDRYQFLERLLQEIEKRYNQFLTLPFSEI 267
HsBPL     GFNVTNSNPTICINDLITEYNKQHKAELKP-LRADYLIARVVTVLEKLIKEFQDKGPNSV 659

SaBPL     REEYIAASNIWNRTLLFTENDKQFKGQAIDLDYDGYLIVRDEAGESHRLISADID----- 322
HsBPL     LPLYYRYWVHSGQQVHLG-SAEGPKVSIVGLDDSGFLQVHQEGGEVVTVHPDGNSFDMLR 718

SaBPL     --------
HsBPL     NLILPKRR                                                     726
```

(B)

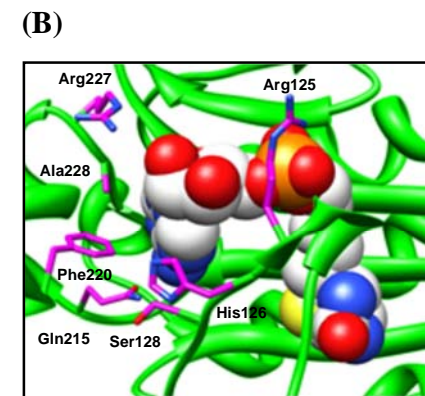**Figure 2:** *(A) Sequence alignment between SaBPL and HsBPL.* **B** *denotes residues that come into contact with biotin,* **A** *are residues that come into contact with the nucleotide and* **C** *are those that make contact with both ligands. (B) The structure of SaBPL: biotinyl-5´-AMP complex, highlighting the position of the non-conserved residues between SaBPL and HsBPL that make contact with the nucleotide.*

Experimental Procedures

Generation of hSaBPL: The DNA encoding h*Sa*BPL was custom synthesized with codon optimization for *E. coli* expression at Invitrogen (Australia). For overexpression of recombinant h*Sa*BPL in *E. coli*, the 1 kbp fragment liberated from pMK (h*Sa*BPL) upon digestion with *Pci*I and *Hin*dIII was ligated into *Nco*I- and *Hin*dIII-treated pET16b (Novagen). The resulting plasmid, pET (h*Sa*BPL), was transformed into *E. coli* BL21 (DE3) for recombinant protein expression. The resulting construct was confirmed by DNA sequencing (SA Pathology, Adelaide, Australia).

Expression of SaBPL, hSaBPL and HsBPL: The expression of recombinant BPLs from *S. aureus* (21) and *H. sapiens* (11) were performed in *E. coli* as previously described. The h*Sa*BPL was treated in the same manner as the wild-type *Sa*BPL protein. All proteins were engineered with a C-terminal hexa-histidine tag to facilitate protein purification.

Protein purification: All proteins were purified using immobilized metal ion chromatography. The crude extract was loaded onto a 5 mL His-Trap HP column (GE Healthcare) that had been equilibrated with 10 column volumes of 50 mM KH_2PO_4 pH 8.0, 300 mM KCl and 5 mM imidazole. The column was first washed with 10 column volumes of the same buffer followed by a wash with 50 mM KH_2PO_4 pH 8.0, 300 mM KCl and 10 mM imidazole. The protein was eluted with 50 mM KH_2PO_4 pH 8.0, 300 mM KCl and 250 mM imidazole. The eluted protein was then applied onto a HiTrap de-salting column (GE Healthcare) that had been equilibrated with the storage buffer (50 mM Tris HCl pH 8.0, 1 mM DTT, 5 mM EDTA, 5% (v/v) glycerol) and routinely stored at -80° C. Protein concentrations were determined using the Bradford assay using bovine serum albumin as standards (22).

In vitro biotinylation assays: Quantitation of BPL-catalyzed ^{3}H-biotin incorporation into the biotin domain substrate was performed as previously described (13).

Circular dichroism (CD) spectroscopy: Far–UV CD spectra were recorded at 20° C using a Jasco CD J-185 spectrophotometer as described by Soares da Costa *et al.* (2012) (13). Thermal unfolding of wild-type *Sa*BPL, h*Sa*BPL and *Hs*BPL was also monitored by CD spectroscopy. Melting curves were recorded at 222 nm between 20° C and 90° C, collecting data every 1° C and using a ramp rate of 2° C/min.

Size exclusion chromatography with multi-angle light scattering (SEC-MALS): The instrument set-up used consisted of a Superdex 200 10/300 GL column (Amersham Biosciences) connected in series with a miniDAWN TREOS light-scattering detector (Wyatt Technology) and an OPTILAB rEX interferometric refractometer detector (Wyatt Technology). Analytical size-exclusion chromatography was performed at 20° C using a mobile phase containing 50 mM Tris HCl pH 8.0, 150 mM NaCl and 0.1 mM EDTA. 100 µL of purified h*Sa*BPL at 26 µM was injected into the column and eluted at a flow rate of 0.25 mL/min. Detector outputs were acquired using Astra software (Wyatt Technology).

Surface Plasmon Resonance (SPR): SPR was performed using a BIAcore[TM] T100 instrument (GE Healthcare) as described by Soares da Costa *et al.* (2012) (23).

Results and Discussion

Characterization of hSaBPL:

Wild-type *Sa*BPL, *Hs*BPL and h*Sa*BPL were recombinantly expressed in *E. coli.* Each was cloned with a C-terminal hexa-histidine tag to facilitate purification by a single metal ion chromatography step as described in Experimental Procedures. The final yields of h*Sa*BPL and wild-type *Sa*BPL were comparable: 20 mg of protein per litre of culture (Figure 3A). This was >20-fold greater than the amount of full-length *Hs*BPL that was purified, 0.75 mg per litre of culture, which is comparable to yields previously observed (11). CD spectra confirmed that *Sa*BPL, *Hs*BPL and h*Sa*BPL fold similarly in solution (Figure 3B). All spectra are comprised of double minima at 208 nm and 222 nm, which is characteristic of a predominantly α-helical structure and they confirm there are no gross perturbations in the secondary structure of the h*Sa*BPL. To examine the differences in stabilities between the three enzymes in solution, thermal denaturation experiments monitored by CD spectroscopy were conducted over the temperature range of 20-90° C (Figure 3C). All three melting curves superimpose, indicating that all three proteins have similar melting temperatures (~50° C).
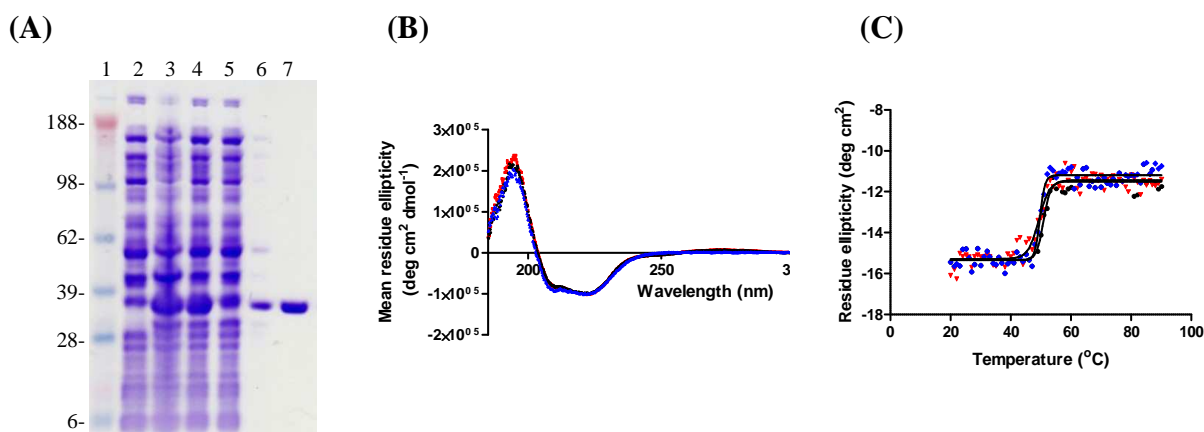
Figure 3. *(A) SDS-PAGE following the purification of hSaBPL. Lanes: 1, Sigmamarker; 2, uninduced sample; 3, induced sample; 4, crude cell extract; 5, unbound fraction; 6, eluant at 10 mM imidazole; 7, eluant at 250mM imidazole. Overlaid CD spectroscopy (**B**) and thermal denaturation (**C**) chromatographs for wild-type SaBPL (black), hSaBPL (blue) and HsBPL (red).*

The 'humanized' construct was analyzed using SEC-MALS to confirm its oligomeric structure. A single peak corresponding to a molecular weight of 38,240 ± 70 Da was detected (Figure 4), confirming that this enzyme exists as a monomer in solution (expected monomeric mass of 38,260 Da). This is in agreement with the oligomeric state of human BPL (14). Interestingly, wild-type *Sa*BPL has been shown to exist in a monomer-dimer equilibrium using analytical ultracentrifugation and SEC-MALS (Chapter 5). The seven mutations introduced in the enzyme have abolished its ability to dimerize. Phe123 in *Sa*BPL has been shown to be a key amino acid involved in dimerization (Chapter 5). However, this residue is still present in the 'humanized' construct so it cannot account for this observation. These results imply that amino acids making contact with the nucleotide pocket are also involved in oligomerization.
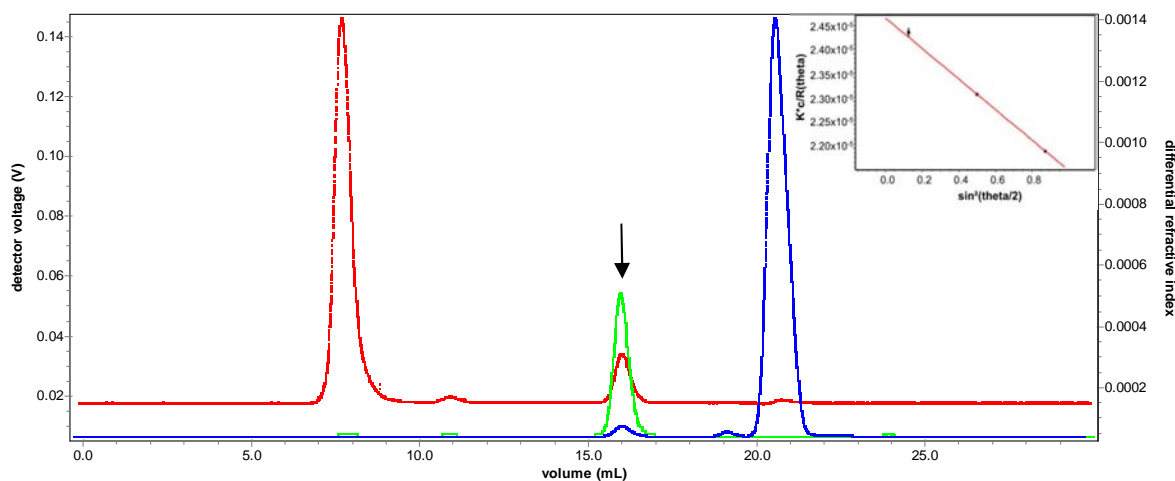
Figure 4. *SEC-MALS spectra of hSaBPL injected at 26 µM. Red corresponds to the 90° light scattering profile, green corresponds to the UV absorbance data at 280 nm and blue corresponds to the differential refractive index data. The arrow indicates the peak corresponding to hSaBPL. Debye plot of K*c/R(u) versus sin2(u/2) from a single SEC/MALS analysis of hSaBPL is also included. Plot shows information from one data slice within the designated peak boundaries. Plotted points correspond to the three light scattering detectors. The y-intercept of the weighted regression line provides an estimate of the reciprocal of the molecular weight for this protein.*

The kinetic constants for biotin and MgATP were determined by steady-state kinetics using tritium-labelled biotin and apo *S. aureus* pyruvate carboxylase as the biotin domain substrate. A comparison of the kinetic parameters for the 'humanized' construct with the wild-type *Sa*BPL and *Hs*BPL enzymes is shown in Table I. For h*Sa*BPL, the turnover rates (k_{cat}) for both biotin and MgATP are ~0.1% of those obtained for wild-type *Sa*BPL and *Hs*BPL. Consistent with the high degree of conservation observed in the biotin-binding pocket, all three enzymes had similar K_m values for biotin. However, the K_m for MgATP was 3-fold lower for human BPL compared with wild-type *Sa*BPL enzyme (*Hs*BPL 56 ± 9 µM vs. *Sa*BPL 180 ± 30 µM). Interestingly, the K_m for this substrate for the 'humanized' construct was strikingly similar to the value for *Hs*BPL (62 ± 11 µM, p > 0.05). This kinetic characterization shows that *h*SaBPL and *Hs*BPL have the same affinity for both biotin and MgATP, despite the decreased catalytic activity of the mutant. These results indicate that mutating the seven residues in contact with ATP in *Sa*BPL to those found in *Hs*BPL yields an enzyme that has the same binding properties as the human enzyme, highlighting that the key differences in ligand binding comes from the variation in the nucleotide pocket.

144

Table I: *Kinetic characterization of wild-type SaBPL, hSaBPL and HsBPL.*

	Biotin		MgATP	
	k_{cat} (s^{-1})	K_m (µM)	k_{cat} (s^{-1})	K_m (µM)
*Sa*BPL	0.45±0.09	1.01 ± 0.16	0.36±0.07	180 ± 30
h*Sa*BPL	0.00039±0.00003	1.16 ± 0.22	0.00042±0.00003	62 ± 11
*Hs*BPL	0.35±0.08	1.08 ± 0.14	0.32±0.08	56 ± 9

Inhibition studies:

To evaluate the inhibitory sensitivity of h*Sa*BPL, the enzyme was tested against our lead inhibitor, compound BPL-068, alongside *Sa*BPL and *Hs*BPL. As mentioned previously, this compound does not inhibit *Hs*BPL at 200 µM. Arg125 has been shown to play a key role in the selective inhibition by this compound and other biotin triazoles, with its substitution to alanine or asparagine (the equivalent residue in *Hs*BPL) resulting in an increase in K_i value by 50-fold (13). Whilst Arg125 is a key determinant of selectivity, it cannot fully explain the >1100-fold selectivity for *Sa*BPL over *Hs*BPL observed with compound BPL-068. In order to highlight the contribution from the R group of BPL-068 to the potency, not only Arg125, *Sa*BPL-R125N was also tested against this compound.

Our hypothesis is that the selectivity observed comes from the differences in the residues in contact with the compound in the nucleotide pocket. Interestingly, the X-ray crystal structure of *Sa*BPL in complex with BPL-068 shows that the R group does not many any hydrogen bond contacts with the protein. However, it makes a number of hydrophobic contacts with non-conserved residues in the *Sa*BPL ATP pocket including Phe220, Ile224 and Ala228. Phe220 and Ala228 were replaced by isoleucine residues in the 'humanized' protein. The inhibition assay results in a K_i values of 0.10 ± 0.02 µM and 4.5 ± 0.80 µM for wild-type *Sa*BPL and *Sa*BPL-R125N respectively, which are in agreement with previously reported values (13) (Figure 5). The mutation of all seven residues in the *Sa*BPL nucleotide pocket to those found in *Hs*BPL completely abolished inhibition by compound BPL-068 (Figure 5). This was consistent with the data obtained with *Hs*BPL.
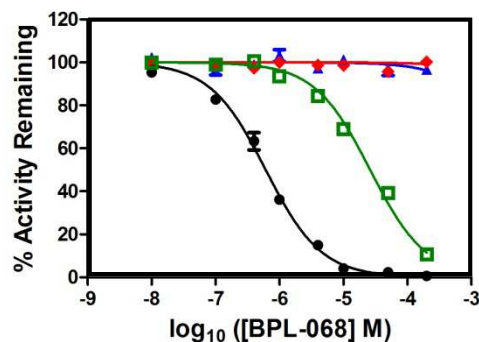
Figure 5. *Inhibition assays. BPL activity was measured in vitro with varying concentrations of BPL-068. The assays were performed using recombinant BPL from S. aureus (black), SaBPL-R125N (green), H. sapiens (red) and 'humanized' S. aureus (blue). Percentage activity is based on 100% activity with no inhibitor.*

Surface plasmon resonance studies:

SPR was subsequently used to further probe the bimolecular interaction between BPL-068 and the enzyme. All three BPLs were immobilized onto discrete channels of the same CM5 chip using standard amine coupling chemistry, leaving one channel blank to take into account non-specific binding. The concentration of BPL-068 injected across the surface was 10 μM (~100 x K_i). This resulted in similar association rates for all three enzymes (Figure 6). However, the most noticeable differences were observed with the dissociation rates. BPL-068 dissociated slowly from wild-type *Sa*BPL. This allowed the curve to be fitted to a 1:1 ligand binding model, resulting in a k_d value of 2.6 x 10^{-4} s^{-1}. In contrast, rapid off-rates were observed for both h*Sa*BPL and *Hs*BPL that were outside the range for quantitative evaluation. Interestingly, the curves for binding of BPL-068 to *Hs*BPL and h*Sa*BPL are superimposable (Figure 6), and are consistent with the observation that both enzymes were not subject to inhibition by the compound. High occupancy rates for inhibitors on bacterial targets are a desirable property for antibacterial discovery.
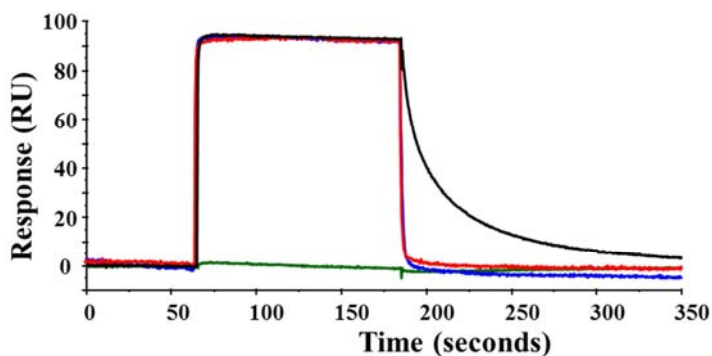
Figure 6. *SPR profiles of 10 µM of BPL-068 binding to wild-type SaBPL (black), hSaBPL (blue) and HsBPL (red). The buffer only control is shown in green.*

Conclusions

Compound BPL-068, which displays >1100-fold selectivity for *Sa*BPL over *Hs*BPL, shows that targeting the more divergent ATP pocket of BPLs could provide a way to improve selectivity over the human enzyme. A number of attempts to purify suitable amounts of full-length human enzyme by recombinant expression in bacteria and in yeast resulted in low yields of soluble protein and proteolytically degraded products. Shortened protein forms of the predicted structural domains have also resulted in insoluble protein. Here, we created a 'humanized' BPL enzyme by introducing seven mutations in the *Sa*BPL enzyme. The chimeric BPL protein was characterized using SPR, CD, SEC-MALS, kinetic and inhibition studies. Interestingly, the mutations resulted in a decrease in K_m for MgATP to 62 ± 11 µM and no inhibition by BPL-068, which is consistent with what is observed with *Hs*BPL. Importantly, the chimeric protein yields >20-fold more protein from recombinant expression than the full-length human enzyme. Crystallization trials are now underway in the laboratory of our collaborators. The crystal structure of the 'humanized' *Sa*BPL enzyme may help us understand the molecular mechanism of binding and selectivity of the biotin-triazole molecules. A similar approach of using an enzyme from a surrogate system has proven invaluable for structure-based drug design of human acetyl-CoA carboxylase inhibitors (24). The structure of h*Sa*BPL could also be a valuable tool in docking studies to identify novel moieties that can bind selectively in the *Sa*BPL ATP site to allow further optimization of the biotin-triazole pharmacophore.

References

1. Payne, D. J., Gwynn, M. N., Holmes, D. J., and Pompliano, D. L. (2007) *Nature Reviews Drug Discovery* **6**, 29-40

2. Polyak, S. W., Chapman-Smith, A., Mulhern, T. D., Cronan Jr, J. E., and Wallace, J. (2001) *Journal of Biological Chemistry* **276**, 3037-3045

3. Thanassi, J. A., Hartman-Neumann, S. L., Dougherty, T. J., Dougherty, B. A., and Pucci, M. J. (2002) *Nucleic Acids Research* **30**, 3152-3162

4. Gerdes, S. Y., Scholle, M. D., Campbell, J. W., Balazsi, G., Ravasz, E., Daugherty, M. D., Somera, A. L., Kyrpides, N. C., Anderson, I., Gelfand, M. S., Bhattacharya, A., Kapatral, V., D'Souza, M., Baev, M. V., Grechkin, Y., Mseeh, F., Fonstein, M. Y., Overbeek, R., Barabasi, A. L., Oltvai, Z. N., and Osterman, A. L. (2003) *Journal of Bacteriology* **185**, 5673-5684

5. Bogdanovich, T., Clark, C., Kosowska-Shick, K., Dewasse, B., McGhee, P., and Appelbaum, P. C. (2007) *Antimicrobial Agents and Chemotherapy* **51**, 4191-4195

6. Karlowsky, J. A., Kaplan, N., Hafkin, B., Hoban, D. J., and Zhanel, G. G. (2009) *Antimicrobial Agents and Chemotherapy* **53**, 3544-3548

7. Miller, J. R., Dunham, S., Mochalkin, I., Banotai, C., Bowman, M., Buist, S., Dunkle, B., Hanna, D., Harwood, H. J., Huband, M. D., Karnovsky, A., Kuhn, M., Limberakis, C., Liu, J. Y., Mehrens, S., Mueller, W. T., Narasimhan, L., Ogden, A., Ohren, J., Prasad, J. V. N. V., Shelly, J. A., Skerlos, L., Sulavik, M., Thomas, V. H., VanderRoest, S., Wang, L., Wang, Z., , Whitton, A., Zhu, T. , and Stover, C. K. (2009) *Proceedings of the National Academy of Sciences* **106**, 1737– 1742

8. Parsons, J. B., and Rock, C. O. (2011) *Current Opinion in Microbiology* **14**, 544-549

9. Pendini, N. R., Bailey, L. M., Booker, G., Wilce, M. C., Wallace, M. C., and Polyak, S. W. (2008) *Biochimica et Biophysica Acta* **1784**, 973-982

10. Campeau, E., and Gravel, R. A. (2001) *Journal of Biological Chemistry* **276**, 12310-12316

11. Mayende, L., Swift, R. D., Bailey, L. M., Soares da Costa, T. P., Wallace, J. C., Booker, G. W., and Polyak, S. W. (2012) *Journal of Molecular Medicine* **90**, 81-88

12. Polyak, S. W., Chapman-Smith, A., Brautigan, P. J., and Wallace, J. C. (1999) *Journal of Biological Chemistry* **274**, 32847-32854

13. Soares da Costa, T. P., Tieu, W., Yap, M. Y., Pendini, N. R., Polyak, S. W., Sejer Pedersen, D., Morona, R., Turnidge, J. D., Wallace, J. C., Wilce, M. C., Booker, G. W., and Abell, A. D. (2012) *Journal of Biological Chemistry* **287**, 17823-17832

14. Ingaramo, M., and Beckett, D. (2009) *Journal of Biological Chemistry* **284**, 30862-30870

15. Hassan, Y. I., Moriyama, H., and Zempleni, J. (2010) *Archives of Biochemistry and Biophysics* **495**, 35-41

16. Lee, C. K., Cheong, C., and Jeon, Y. H. (2010) *FEBS Letters* **584**, 675-680

17. Lee, C. K., Cheong, C., and Jeon, Y. H. (2010) *Biochemical and Biophysical Research Communications* **391**, 455-460

18. Bao, B., Wijeratne, S. S., Rodriguez-Melendez, R., and Zempleni, J. (2011) *Biochemical and Biophysical Research Communications* **412**, 115-120

19. Ingaramo, M., and Beckett, D. (2012) *Journal of Biological Chemistry* **287**, 1813-1822

20. Bagautdinov, B., Kuroishi, C., Sugahara, M., and Kunishima, N. (2005) *Journal of Molecular Biology* **353**, 322-333

21. Pendini, N. R., Polyak, S. W., Booker, G. W., Wallace, J. C., and Wilce, M. C. (2008) *Acta Crystallographica Section D-Biological Crystallography* **64**, 520-523

22. Bradford, M. (1976) *Analytical Biochemistry* **72**, 248-254

23. Soares da Costa, T. P., Tieu, W., Yap, M. Y., Zvarec, O., Bell, J. M., Turnidge, J. D., Wallace, J. C., Booker, G. W., Wilce, M. C. J., Abell, A. D., and Polyak, S. W. (2012) *ACS Medicinal Chemistry Letters* **3**, 509-514

24. Rajamohan, F., Marr, E., Reyes, A. R., Landro, J. A., Anderson, M. D., Corbett, J. W., Dirico, K. J., Harwood, J. H., Tu, M., and Vajdos, F. F. (2011) *Journal of Biological Chemistry* **286**, 41510-41519.

Chapter 7
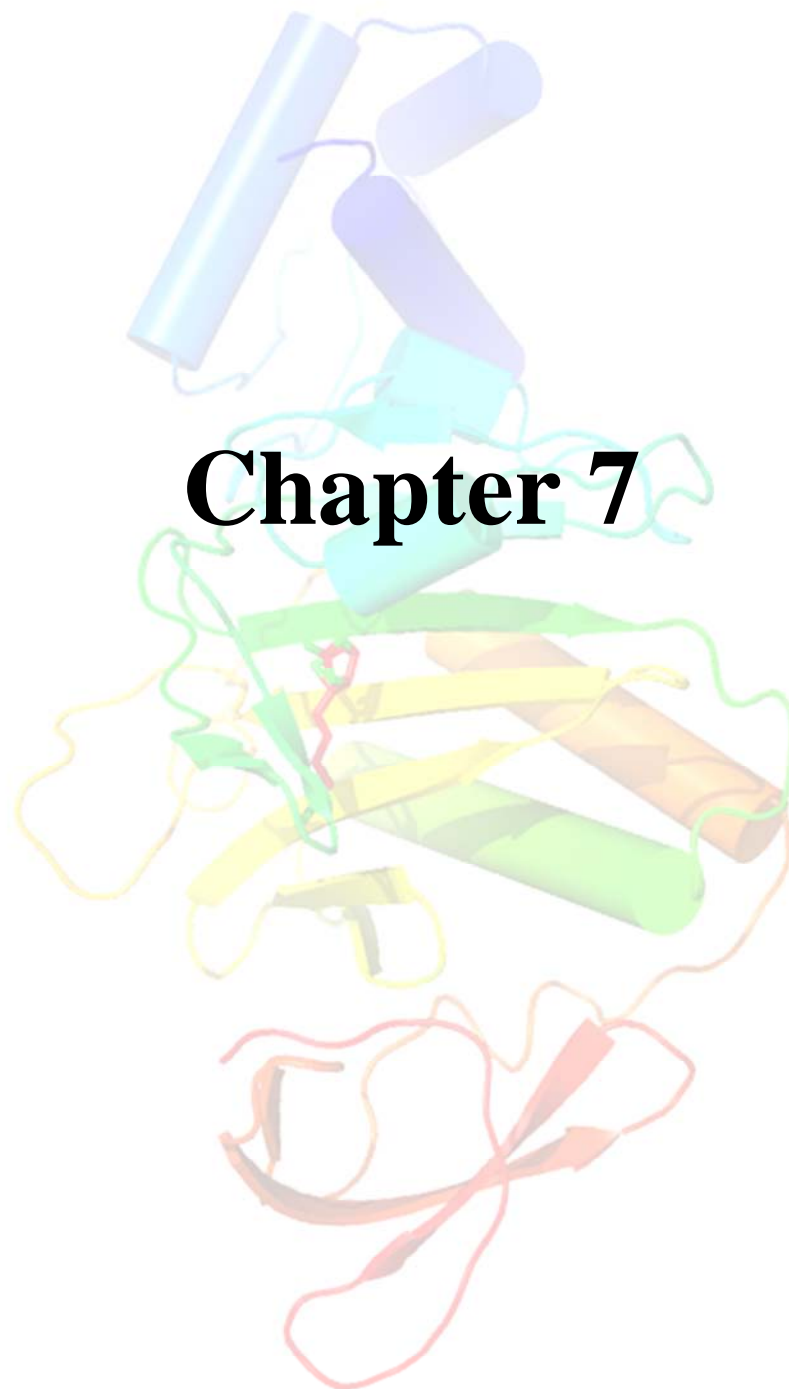
Statement of Authorship

Title of Paper	A novel molecular mechanism to explain biotin-unresponsive holocarboxylase synthetase deficiency.
Publication Status	⦿ Published ○ Accepted for Publication ○ Submitted for Publication ○ Publication Style
Publication Details	Mayende, L., Swift, R. D., Bailey, L.M., Soares da Costa, T. P., Wallace, J. C., Booker, G. W., Polyak, S. W. (2012) A novel molecular mechanism to explain biotin-unresponsive holocarboxylase synthetase deficiency. *Journal of Molecular Medicine*, 90, 81-88.

Author Contributions

By signing the Statement of Authorship, each author certifies that their stated contribution to the publication is accurate and that permission is granted for the publication to be included in the candidate's thesis.

Name of Principal Author	Lungisa Mayende		
Contribution to the Paper	Performed yeast two hyrid assays, enzyme purification and analysis. Also was responsible for random mutagenesis and subcloning experiments. Assisted with manuscript preparation.		
Signature		Date	08/10/12

Name of Co-Author	Rachel D. Swift		
Contribution to the Paper	Performed all limited proteolysis experiments.		
Signature		Date	27/11/12

Name of Co-Author	Lisa M. Bailey		
Contribution to the Paper	Produced DNA constructs for yeast two hybrid analysis.		
Signature		Date	25/10/12

Name of Co-Author (Candidate)	Tatiana P. Soares da Costa		
Contribution to the Paper	Optimised surface plasmon resonance protocol and assisted with the binding assays.		
Signature		Date	08/10/2012

Name of Co-Author	John C. Wallace		
Contribution to the Paper	Provided intellectual discussion.		
Signature		Date	29/11/2012

Name of Co-Author	Grant W. Booker		
Contribution to the Paper	Provided direction in all aspects of protein chemistry.		
Signature		Date	3/12/2012

Name of Co-Author	Steven W. Polyak		
Contribution to the Paper	Provided direction in all the overall project and primary responsibility for manuscript preparation.		
Signature		Date	16/10/2012

Mayende, L., Swift, R.D., Bailey, L.M., Soares da Costa, T.P., Wallace, J.C., Booker, G.W. & Polyak, S.W. (2011) A novel molecular mechanism to explain biotin-unresponsive holocarboxylase synthetase deficiency.
Journal of Molecular Medicine, v. 90(1), pp. 81-88
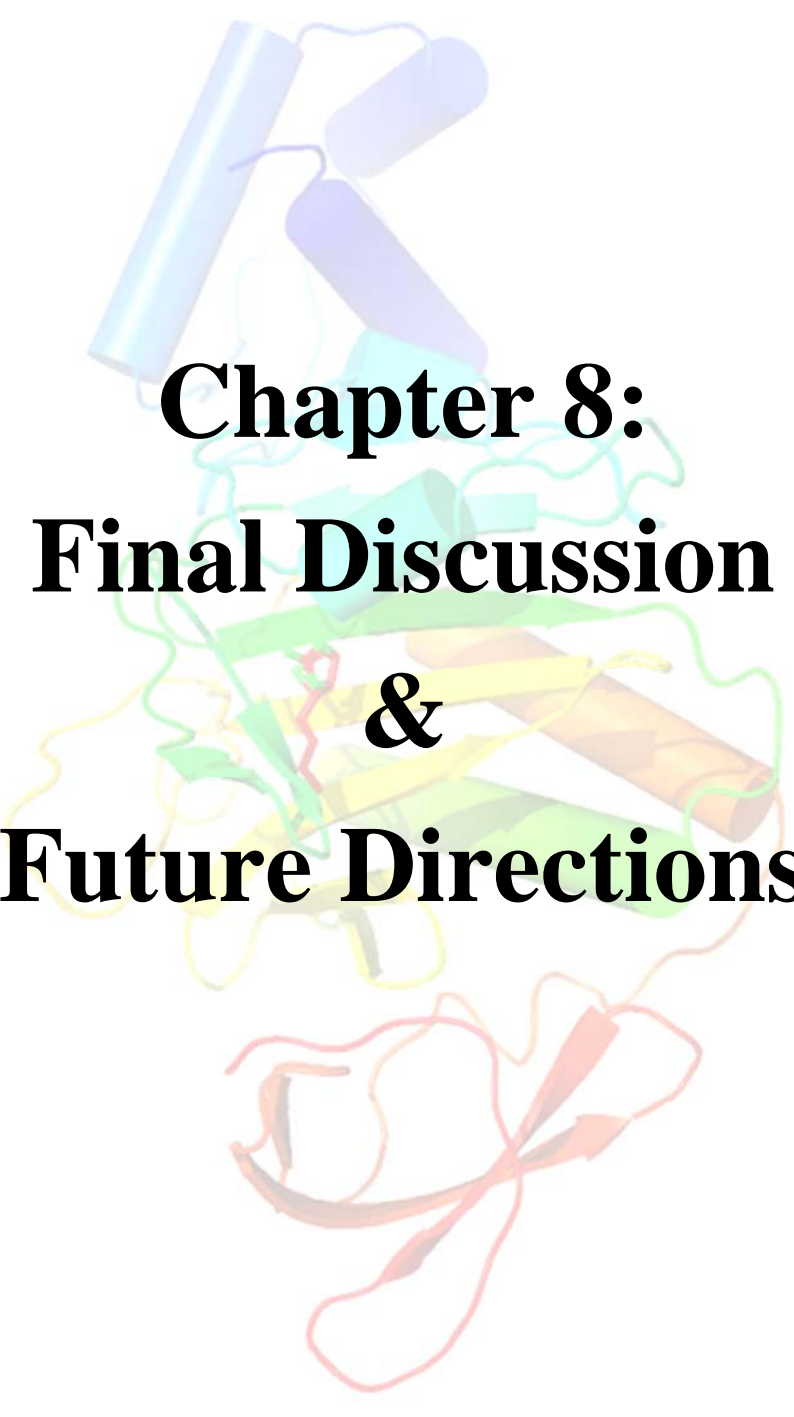
Chapter 8:
Final Discussion
&
Future Directions

8.1   Final discussion

In this section, a summary of the biophysical, mutagenic and kinetic analyses described in the experimental chapters is included and how this information can provide insights into the differences between BPLs and thus help the development of potent and selective inhibitors. I will also highlight recently published work with relevance to my findings and discuss future directions that might be useful in elucidating some unanswered questions.

8.1.1   Understanding the differences between BPLs

A number of studies have recently been published highlighting the differences in the mechanism of self-association of BPLs. Class I BPLs from *M. tuberculosis* (*Mt*BPL) and *A. aeolicus* (*Aa*BPL) exist as monomers in apo, biotin and biotinyl-5´-AMP liganded forms (1,2). *P. horikoshii* BPL (*Ph*BPL), also a class I BPL, constitutively exists as a dimer regardless of its liganded state (3,4). Class II *E. coli* BPL (*Ec*BPL) only forms a dimer upon ligand binding (5). Class III BPLs from *S. cerevisiae* (*Sc*BPL) and *H. sapiens* (*Hs*BPL) have been reported to be monomeric (6,7). Dimerization is not a pre-requisite for enzymatic activity but it is required for repressor function of the Class II transcriptional repressor BPLs (8,9) and for thermal stability as proposed for *Ph*BPL and other thermophiles (3,10). Interestingly, analytical ultracentrifugation experiments on *S. aureus* BPL (*Sa*BPL) suggest that this enzyme exists in a protein concentration dependent monomer-dimer equilibrium in its apo form at low micromolar concentrations. This has not been observed for any other Class II isozymes (Chapter 5). The existence of apo dimeric *Sa*BPL might be due to its more complex biology compared to *Ec*BPL. The *E. coli* enzyme biotinylates one biotin-dependent enzyme, ACC, and has one known target gene, *bioO*. Thus it is able to utilize biotin as well as synthesize it upon cellular demand. *Sa*BPL biotinylates two biotin-dependent enzymes (namely ACC and PC) and is proposed to regulate the expression of the biotin transporter gene *bioY* in addition to *bioO* (11). Hence, *Sa*BPL can control not only the synthesis but also the import of biotin into the bacteria. This extra layer of complexity may require more tightly regulated control of gene expression, subsequently allowing *S. aureus* to sample and respond quickly to different environments. This function may allow *S. aureus* to adapt to fluctuating biotin availability, which is especially important during infection. A recent study has highlighted the importance of biotin in nutritional immunity in the Gram-negative bacteria *Francisella*

tularensis. The protein FTN_0818, which has previously been shown to be essential in virulence, also plays a key role in biotin biosynthesis and rapid escape from the *Francisella*-containing phagosome. Addition of biotin rescued an attenuated FTN_0818 mutant *in vitro* and *in vivo*, supporting the proposal that biotin may be a limiting factor during infection (12). Similarly, *de novo* biotin synthesis has also been shown to be essential for *M. tuberculosis* to establish and maintain a chronic infection in a murine model of tuberculosis (13). Understanding how bacteria adapt their metabolism to their habitat will be critical for extending our understanding of bacterial pathogenesis.

The strength of the dimers formed by Class II BPLs also varies depending on the ligand involved. In *Ec*BPL, formation of biotinyl-5´-AMP is a pre-requisite for stable dimerization in solution. Equilibrium sedimentation studies show that the binding of the intermediate increases the stability of the dimer by 3.7 kcal/mol relative to biotin alone (14). In this thesis, sedimentation velocity experiments carried out on *Sa*BPL have shown that biotin alone does not shift the equilibrium towards dimer formation compared to the apo enzyme (Chapter 5). This was explained by the fast on and off-rates observed with biotin binding to *Sa*BPL (Chapter 3). Variable dissociation constants for biotin have been documented for *Ec*BPL $(4.5 \times 10^{-8} M)$ (15), *Aa*BPL $(3.5 \times 10^{-6} M)$ (2) and *Mt*BPL $(\sim 1 \times 10^{-6} M)$ (1) despite the high degree of conservation of amino acids within the biotin pocket. However, when a tight binding biotin analogue was used, the K_D for *Sa*BPL dimerization was 6-fold tighter compared to apo and biotin-bound forms of the enzyme (Chapter 5). Our hypothesis is that a long lived enzyme: ligand complex is required to strengthen dimer formation and clamp down on the DNA. This would lead to a functional switch of *Sa*BPL from acting as a ligase to a transcriptional repressor. Class I monofunctional BPLs have been shown to have lower affinities for biotinyl-5´-AMP compared to *Ec*BPL (1). Tight binding of ligands may be required for Class II BPLs to perform the repressor function.

Apart from oligomerization, the order of substrate binding also differs between BPLs. In this study, surface plasmon resonance was employed to determine that biotin binds to *Sa*BPL first, followed by ATP binding (Chapter 2) (16). This ordered substrate binding has previously been observed in *Ec*BPL (17) and *Mt*BPL (1) and is related to the disordered-to-ordered transition of the biotin and adenylate-binding loops (18). Structural data supports this mechanism since the ATP site is formed as a consequence of ordering of specific loops triggered by biotin binding. On the other hand, *Aa*BPL (2) and *Ph*BPL (4)

can bind ATP in the absence of biotin, although in *Aa*BPL the process is co-operative. Here the loops are pre-organized in the ligand-free form for both these enzymes, resulting in a well-defined ATP-binding pocket. Thermophile proteins have been shown to have less flexibility compared to their mesophile homologues (19). Natural selection could have resulted in these proteins adopting more ordered structures in order to survive and function at higher temperatures, thus increasing their stability.

As mentioned previously, the biotin-binding loop is highly conserved due to its essential role in heterodimerization and/or biotin transfer. Two residues found in this loop were examined in this work: Arg122 and Phe123. The arginine at position 122 in *Sa*BPL is absolutely conserved in all BPLs. Mutation of this amino acid to a glycine resulted in unaltered K_m values for biotin and MgATP, which is also observed with the equivalent mutant in *Mt*BPL (20). This is in contrast to what is observed in *Ec*BPL, where the equivalent mutation (R118G) resulted in a decrease in the affinity for biotin by 100-fold (21). Not surprisingly, the catalytic efficiency of *Sa*BPL-R122G was severely compromised, highlighting the critical role of this residue in the reaction mechanism. Like *Ec*BPL (21), *Sa*BPL-R122G also has the ability to biotinylate non-target proteins in a non-specific manner (Chapter 4). The equivalent mutant in the Class I *Aa*BPL, R40G, can also biotinylate non-specifically but to a lesser extent than *Ec*BPL-R118G and *Sa*BPL-R122G (2). This is likely to be a consequence of the elevated temperature of the reaction with the thermostable enzymes as biotinylation with biotinyl-5′-AMP is proximity-dependent (21). Thus, the lifetime of AMP mixed anhydrides in aqueous solution will be significantly shorter at 65° C, reducing the amount of intermediate left to modify another protein (20). The mutation of the equivalent residue in Class I *Mt*BPL, Arg69, to an alanine resulted in a protein that was unable to biotinylate non-specifically (20). This was reasoned to be due to a loss of enzyme activity and ATP binding upon mutation.

The second amino acid examined in *Sa*BPL was Phe123, which is the position of most variability in the biotin-binding loop. The equivalent residue in *Ec*BPL, Arg119, has been shown to play a key role in dimerization but has no involvement in biotin or MgATP binding (15). Mutation of Phe123 to a glycine or arginine, the equivalent residue in *Ec*BPL, abolished the ability of *Sa*BPL to dimerize (Chapter 5). The mutants retained 10% of the catalytic efficiency of the wild-type enzyme and biotin affinity decreased by 3-fold,

while ATP binding remained the same. The reduction in activity due to the inability to dimerize may suggest a role for the dimer in catalysis. Oligomerization has been shown to increase thermal stability and optimization of enzyme catalysis by reducing flexibility (22,23). Interestingly, Phe123 plays a role in the selective binding of biotin acetylene to *Sa*BPL. The arginine mutation increased the K_i value by >20-fold, resulting in an inhibition constant similar to that obtained for wild-type *Ec*BPL. The reverse effect was observed when the arginine residue in *Ec*BPL was replaced by a phenylalanine, demonstrating the importance of this residue in ligand affinity. Thus, Phe123 plays a dual role in *Sa*BPL which has not been observed in other BPLs.

The mutagenic work described so far has focused on the first partial reaction, i.e., binding of biotin and ATP. Another area of interest is the second partial reaction involving the transient protein: protein interaction with the biotin domain substrate. Mutational studies have helped provide insights into the molecular basis of the genetic disorder multiple carboxylase deficiency. This disease is linked to a number of mutations in *Hs*BPL, including the commonly occurring Arg508 to tryptophan mutation, which maps to Arg122 of *Sa*BPL. Apart from mutations in the catalytic domain, mutations in the N-terminal domain have also been linked to the disease. The N-terminal domain is completely distinct to that found in Class II BPLs. While the removal of the first 57 residues of the human BPL resulted in no differences in substrate binding or catalytic efficiency (7), deletion of the first 159 N-terminal amino acids resulted in attenuated enzymatic activity and implicated the involvement of these residues in making contacts with the biotin domain (24). In this thesis, mutations in the N-terminal domain identified in MCD patients resulted in a >15-fold increase in dissociation rate from the biotin domain substrate compared to wild-type *Hs*BPL (Chapter 7) (25). It is proposed that this enhanced dissociation rate is too fast to allow the biotinyl-transferase reaction to proceed, resulting in non-biotinylated enzymes. Together, these data suggest a previously unknown function for the N-terminal extension in stabilizing the enzyme: substrate complex during catalysis. It is proposed that the N-terminal region may also possess 'proof-reading activity' that allows it to differentiate between the five human carboxylases. In biotin starvation conditions, only some of these enzymes may be maintained. These studies have elucidated a distinct function of Class III BPLs not present in Class I and II BPLs.

8.1.2 Inhibitor design

Antibacterial drug targets that have a closely related human homologue, such as BPL, represent a new frontier in antibiotic discovery. One of the main objectives of this thesis was to provide proof of concept that *Sa*BPL could be selectively targeted over the human homologue. One of the targets of *Sa*BPL is ACC, which catalyzes the first committed step in the fatty acid biosynthetic pathway. This pathway is essential in Gram-negative bacteria due to the requirement for β-hydroxy-fatty acids to assemble the lipid A core structure of outer membrane polysaccharides (26). Supplementation of exogenous β-hydroxy-fatty acids is ineffective in replacing *de novo* fatty acid biosynthesis highlighting its essential function (27). However, there has been some debate lately on the effectiveness of targeting the fatty acid biosynthetic pathway in Gram-positive bacteria (26,28-31). There has been evidence to suggest that inhibition of this pathway *in Streptococcus agalactiae* can be suppressed by the uptake of fatty acids from exogenous sources both *in vitro* and *in vivo* (28). It has also been reported that *S. aureus* can incorporate exogenous fatty acids into membranes (30). However, Balemans *et al.* showed that serum fatty acids could not overcome the effect of fatty acid biosynthesis inhibitors in *S. aureus* (29). Recently, Parsons *et al.* concluded that while *S. aureus* can uptake exogenous fatty acids, this can only support 50% of the phospholipid synthesis (31). To further support this, there have been a number of reports highlighting the efficacy of fatty acid synthesis inhibitors in *S. aureus* infection models in mice (32-36). One of these studies included the discovery of inhibitors of biotin carboxylase, a subunit of ACC, using whole-bacterial cell screen of a library of pyridopyrimidines, derived from a eukaryotic tyrosine protein kinase inhibitor pharmacophore (36). This differential ability in the incorporation of exogenous fatty acids between Gram-positive bacteria highlights important differences in this metabolic pathway. For example, *S. aureus* synthesizes branched chain, saturated fatty acids which are vital for membrane function, but are not found in mammals and therefore unlikely to circumvent *de novo* synthesis (26). All this evidence supports the idea that targeting fatty acid synthesis by inhibiting BPL can result in the development of novel antibacterial therapeutics against *S. aureus*.

Since *Sa*BPL has an ordered reaction mechanism with biotin binding first, two strategies were employed in this thesis to develop novel inhibitors of this enzyme: 1) Target the biotin pocket only and 2) Perform a fragment-based approach to target both the biotin and

nucleotide pockets. Chapter 3 describes a series of chemical analogues based on biotin that were designed and tested for enzyme inhibition and antimicrobial activities against clinically relevant strains of *S. aureus*. This approach resulted in highly potent compounds ($K_{i <}$ 100 nM) with antibacterial activity against methicillin resistant strains (MIC = 2 - 16 µg/mL). However, only moderate selectivity over the human enzyme (10 - 20 fold) was observed (37). A series of azide and alkyne derivatives of biotin have been previously screened against a number of BPLs and were shown to act as substrates for BPLs from *P. horikoshii* and *S. cerevisiae* only (Figure 8.1) (38). These studies highlight the difficulties in altering the biotin structure so that the resulting molecule can still be accommodated in the biotin pocket of BPLs.

Species of biotin ligase	Probes Tested							
	1	2	3	4	5	6	7	8
Human	+	–	–	–	–	–	–	–
S. cerevisiae (yBL)	+	–	+	–	–	–	–	–
B. subtilis	+	–	–	–	–	–	–	–
P. acnes	+	–	–	–	–	–	–	–
L. mesenteroides	+	–	–	–	–	–	–	–
T. cruzi	+	–	–	–	–	–	–	–
M. jannaschii	+	–	–	–	–	–	–	–
P. horikoshii (PhBL)	+	+	+	–	–	–	–	–
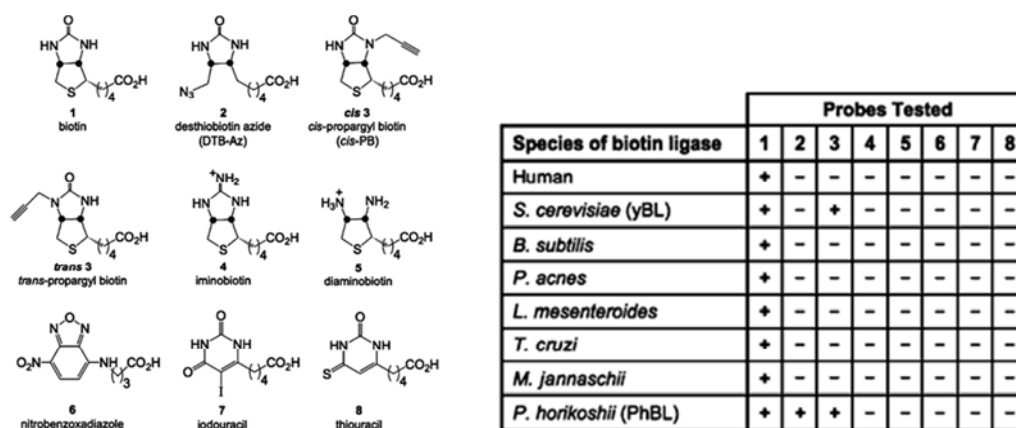
Figure 8.1: *Biotin analogues screened against a range of BPLs for their potential to be substrates. Formation of product is indicated by a '+'. Figure adapted from Slavoff et al. 2008 (38).*

Developing analogues of the intermediate biotinyl-5´-AMP could provide a means to achieve selectivity by exploiting the more variable nucleotide pocket. Not surprisingly, the non-hydrolyzable analogue of the reaction intermediate, biotinol-5´-AMP, has been shown to be a pan inhibitor. A bi-substrate inhibitor of *M. tuberculosis* BPL has recently been characterized, where the highly labile phosphodiester bond was replaced by a more stable sulphonamide linker. This compound displayed sub-nanomolar enzyme inhibition and had antibacterial activity against a range of multi-drug resistant *M. tuberculosis* strains (39), although it also showed some toxicity against cultured mammalian cells. Chapter 2 describes a novel class of 1,2,3 biotin triazoles that were identified by targeting both biotin and ATP-binding pockets, which show cytotoxicity against *S. aureus* but not cultured

mammalian cells (16). The most potent inhibitor from the biotin-triazole series (K_i = 90 nM) displayed >1100-fold selectivity for the *S. aureus* BPL over the human homologue (16). The molecular basis for the selectivity was identified using mutagenesis studies. A key arginine residue in the biotin-binding loop was identified as being necessary for the selective binding of the triazole linker (Chapter 2). Furthermore, the mutation of all seven non-conserved amino acids in the ATP-binding site of *Sa*BPL to those found in the equivalent positions in *Hs*BPL, resulted in a chimeric protein that is no longer inhibited by our lead compound (Chapter 6). These studies opened the doors for alternative bioisosteres to the phosphodiester in biotinyl-5´-AMP to be further investigated.

Since a class of triazole molecules has been identified as selective inhibitors of *Sa*BPL, we reasoned that this enzyme would provide an ideal candidate for performing *in situ* click chemistry. Novel ways of improving the *in situ* click approach so it can be more widely used have recently been published (40-44). A novel avenue for generating agonists and antagonists for ligand-gated ion channels has been proposed using a subunit interface binding region of the multi-subunit protein acetylcholine binding proteins as template surrogates for nicotinic acetylcholine receptors (43,44). The use of iterative *in situ* click chemistry and the one-bead-one-compound method for the creation of a peptide library have enabled the fragment-based assembly of selective high-affinity, tri-ligand capture agents against carbonic anhydrase II (40). This approach has been extended to synthesize a high specificity branched tri-ligand capture agent/inhibitor against Akt kinase by developing two novel strategies: 1) Use of a pre-inhibited form of the protein to allow screening of an allosteric site inhibitor, 2) Development of a quantitative PCR-based method to detect the amount of product formed from iterative on-bead *in situ* click chemistry (41). The direct detection of products in crude samples has resulted in the identification of new inhibitors against glucocerebrosidase (42). In this work, a novel method for improving the detection of triazole products generated was employed by using the 'leaky' mutant *Sa*BPL-R122G, which results in a 40-fold increase in the rate of product formation relative to the wild-type enzyme (Chapter 4). This enabled our target enzyme to selectively form detectable levels of the most potent binder from a library of building blocks in a single reaction mixture. This is only the second example of an enzyme that can perform a multi-component *in situ* click reaction, thus demonstrating the potential wider applicability of this approach to drug discovery.

From our SAR series, some conclusions can be drawn about which features are necessary for designing inhibitors of *Sa*BPL.

1. Bulky substituents are not tolerated on the bicyclic ring of the biotin structure. The valeric acid tail, however, that binds between three hydrophobic β-sheets and the hydrophobic portion of the biotin-binding loop, is amenable to derivatization.
2. The triazole linker provides selectivity between *Sa*BPL and *Hs*BPL due to a key hydrogen bond interaction with a non-conserved Arg125 in *Sa*BPL.
3. A 1, 4 triazole linkage between the biotin and the secondary site analogue is favoured over a 1, 5 linkage.
4. The optimum tether length between the biotin and the triazole is 5 carbons.
5. The ribose ring on the adenosine has been shown to be dispensable.
6. The adenine ring can be replaced with groups that structurally do not resemble ATP, resulting in improved potency.

The aim now is to optimize the biotin-triazole scaffold represented by pharmacophore X (Figure 8.2). Pharmacophore X has been identified as a key lead structure in order to produce potent and selective inhibitors of *Sa*BPL, while offering significant advances in ease of synthesis and derivatization. Building up a chemically diverse library of molecules with this pharmacophore will help to overcome problems that might be encountered in the developmental process that could halt the progress of turning these hit compounds into lead structures.
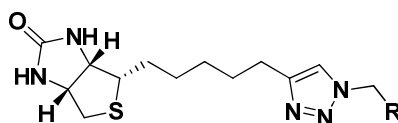

Figure 8.2: *Pharmacophore representing the biotin-triazole moiety.*

8.2 Future directions

8.2.1 In situ click chemistry

The *in situ* click approach has been shown to be feasible using the *Sa*BPL system. The enzyme can select a pair of fragments to form the most potent binder from five building blocks that are concurrently present in a single reaction mixture (Chapter 4). Interestingly, the triazole containing molecules do not inhibit *Hs*BPL at solubility limiting concentrations. As there are a number of commercially available azides, the next step would be to expand the library of compounds screened against *Sa*BPL. This work is now continuing.

Arg125 in *Sa*BPL has been found to make a hydrogen bonding interaction with the triazole linker which is important for selectivity (Chapter 2). This amino acid is variable amongst BPLs, although *Mt*BPL and some other bacteria also have an arginine at the equivalent position. Interestingly, a number of triazole molecules have recently been shown to inhibit BPL from *M. tuberculosis* with low micromolar potency (Miss A. Paparella, University of Adelaide, unpublished). These results suggest that target-catalysed *in situ* click chemistry may be used to identify high-affinity, selective inhibitors of *Mt*BPL and possibly of BPLs from other pathogens.

The *in situ* click approach could also be extended to other enzymes that employ an adenylated reaction intermediate, forming a linker between the carboxyl group of the organic acids and the alpha-phosphate of ATP. Examples include the t-RNA amino-acyl synthetases (45), indole-3-acetic acid synthetases (46) and lipoyl ligases (47), amongst others. Designing small molecule inhibitors of these enzymes by mimicking the adenylated intermediate, where the labile linker is replaced by a more stable isostere such as the triazole linker, could prove to be useful.

8.2.2 Discovering novel scaffolds to refine the biotin-triazole pharmacophore

The SAR series from the compounds described in Chapters 2 and 3 demonstrated that although alterations in the biotin fragment result in poor inhibitors, the ATP pocket of *Sa*BPL can accommodate fragments that do not resemble the nucleotide. The crystal

structures of holo *Sa*BPL as well as SPR experiments described in Chapter 2 demonstrate that the pre-formation of the enzyme and biotin complex enhances binding in the nucleotide pocket. This suggests that when screening for inhibitors of the secondary site, the biotin pocket must be filled first. One way to identify potential binders of the nucleotide pocket is to perform an *in silico* docking screen of a commercially available 'fragment' library. Constraints can be placed in the library to refine the screen. AMP can be used as a positive control for the docking studies. Candidates with calculated binding energies lower than the positive control can be short-listed, purchased and then be tested for binding using SPR. Biotin acetylene, which has been shown to be the tightest binding analogue (Chapter 3), can be added at a saturating concentration first to induce the formation of the nucleotide pocket. Results from this study could be employed to refine the docking and scoring functions to increase our hit rate before testing and purchasing a larger number of compounds. Multiple docking programmes should be employed to re-screen the compound library to allow a consensus score to be determined across all programmes and facilitate short listing of the most likely candidates. Related hit compounds can then be bundled into hit classes.

A pilot study has been conducted to show whether this approach can successfully be used to find fragments that are better binders than AMP. A library of 12,000 compounds from the ZINC library ($M_w \leq 300$ Da, rotatable bonds ≤ 3, $c$logP ≤ 3 (48)) was screened against *Sa*BPL using Autodock VINA (Assoc. Prof. G. Booker, University of Adelaide, unpublished). From the twelve compounds purchased, four resulted in a binding response at 100 µM (Figure 8.3). SPR binding assays showed that these four compounds have lower K_D values than AMP (Soares da Costa, unpublished). None of these fragments bound to the enzyme in the absence of biotin acetylene, further confirming the ordered substrate binding mechanism. For this to be an efficient lead identification approach, these fragments need to be appropriately linked to biotin.
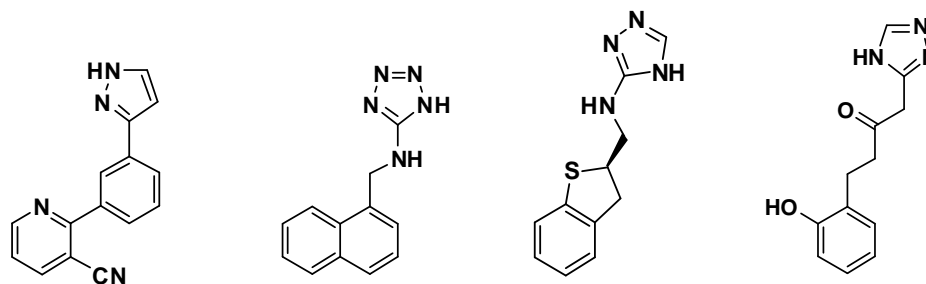
Figure 8.3: *Hit compounds identified using in silico docking and SPR from a 12,000 compound ZINC library.*

Another way of identifying novel scaffolds that can bind in the nucleotide pocket is by high-throughput screening. Natural products still present the best sourcing pool of novel drugs. Our collaborators from the Institute of Microbiology at the Chinese Academy of Sciences have created a library of 23,000 samples from fermentation products of various marine microbes. Thirty hits against *Ec*BPL have been identified that have antibacterial activity against *E. coli* in culture. The ability of these compounds to bind to *Sa*BPL has been analyzed using SPR. A 13% success rate against *Sa*BPL was observed, with four compounds being identified as binders in a biotin dependent manner (Soares da Costa, unpublished). They have been docked against the *Sa*BPL structure using Autodock VINA to predict a mode of binding and K_D values have been calculated using steady-state affinity (Figure 8.4) (Soares da Costa, unpublished). These natural products still need to be tested against cultured *S. aureus* cells. A BPL knock down strain of *S. aureus* would be useful to investigate off-target effects.

(A)   **(B)**

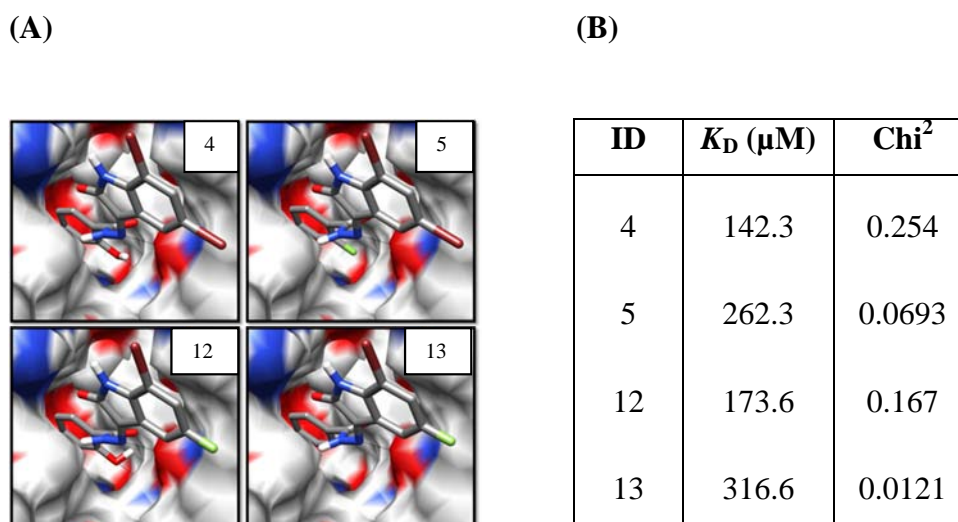| ID	K_D (µM)	Chi^2
4	142.3	0.254
5	262.3	0.0693
12	173.6	0.167
13	316.6	0.0121

Figure 8.4: *Hit compounds identified against SaBPL using a natural compound library screen. (A) Docking of hits to SaBPL structure using Autodock VINA, (B) K_D values of hits calculated using a steady state affinity model in the presence of saturating concentrations of a biotin analogue.*

8.2.3 Biotin transporter

A thorough understanding of the mechanism of uptake of the BPL inhibitors should aid our current drug design efforts. It is reasonable to propose that our biotin analogues cross the bacterial cell membrane via the biotin transporter. Surprisingly, little is known about the mechanisms behind biotin uptake. Although many bacteria, certain Archaea and plants can synthesize biotin from its precursors or metabolic intermediates, uptake from the environment is energetically favoured (49). Comparative genomics analysis suggested that *bioY* is most likely to encode the biotin transporter in bacteria and Archeons and it is often clustered with biotin metabolism genes. There has been great progress made in recent years to characterize the bioY protein. The bioY transporter belongs to the energy coupling factor (ECF) family and it actively moves biotin across the bacterial cell membrane in an ATP-dependent manner. It differs from the classical ABC transporters in terms of subunit architecture and mechanism (Figure 8.5) (50). BioY in the absence of the ECF module is a monomer, with high affinity for α-biotin but unable to transport the substrate on its own (51). Homologues for the *bioY* gene have not been identified in the genome sequences of many proteobacteria however, including *E. coli* (11). Active transport was observed for *E. coli* K12 over 30 years ago (52). The biotin transporter was specific for an intact ureido ring, where compounds with altered side chains or tetrahydrothiophene ring have little effect. It has been shown that biotinylated peptides with chain lengths up to 31 amino acids

178

can be taken up by *E. coli* and other Gram-negative bacteria (53). In mammalian cells, biotin is transported across the plasma membrane by a sodium-dependent multivitamin transporter and, in some tissues, by monocarboxylase transporter 1 (54). It is important that BPL inhibitors developed have the desirable chemical properties so that they can be recognized and imported by the transporters. Identifying the features in biotin that are important for recognition and/or interactions with the transporter are crucial. A way of improving MIC values for the compounds developed would be to find ways to up-regulate the *bioY* gene to ensure the biotin analogues can be taken in. Alternative transport proteins could also exist in *S. aureus*. The differences in biotin uptake mechanisms between various species could potentially be exploited to design biotin analogues with greater selectivity for pathogenic bacteria. Thus more work needs to be done in this area to probe the biochemical and physiological function of the transporter proteins in cells.
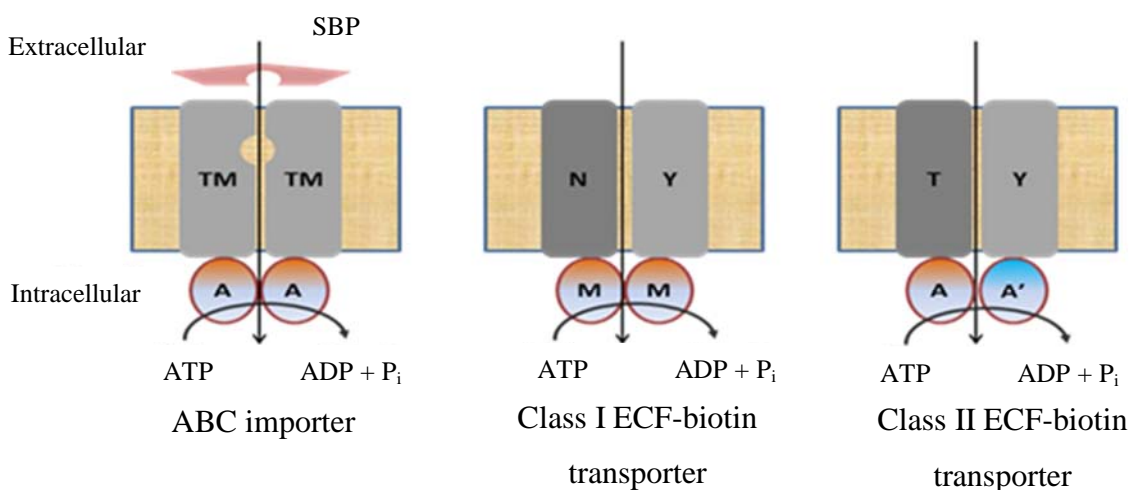
Figure 8.5: *Structures of ABC and ECF biotin transporters. The ABC importers consist of two transmembrane (TM) domains, two ATP-binding (A) proteins and one solute binding protein (SBP). The Class I ECF transporters for biotin contain two specific ATP-binding (M) proteins and two TM domains that determine their solute specificity (Y) and complex stability (N). Similar to the Class I ECF-biotin importers, the Class II ECF-biotin importers also have a substrate specificity TM (S component) but share their ECF (A, A´ and T) with other vitamin importers.*

8.2.4 *Transcriptional regulation*

As discussed in section 8.1.1, *Sa*BPL is proposed to control transcription of *bioY* and *bioO* in response to the supply and demand for cellular biotin (11,55). The functional switch between acting as a ligase or a repressor is somewhat controversial and has been proposed to result from two competing protein: protein interactions (55) or to be dependent on the cellular concentration of biotinyl-5´-AMP (56). Understanding the complex network of transcriptional regulation in *S. aureus* is important. Crystal structures of BPL in complex with DNA could provide us with important clues about *bioY* and *bioO* regulation, but these are yet to be reported. In order to increase the probabilities of obtaining co-crystal structures, super-repressor *Ec*BPL mutant strains have recently been isolated that retained normal activity for growth (56). Chromatin immunoprecipitation assays could be used to capture a snapshot of the DNA-BPL interaction in living cells by treating the cells with formaldehyde or other crosslinking reagents in order to stabilize the interactions for downstream purification and detection. These assays require an antibody against the target protein and PCR primers for the DNA sequence of interest. Reporter assays could also provide a real time *in vivo* read-out of translational activity for the promoters of *bioO* and *bioY*. Upon activation of the promoter, the reporter gene can code for a protein with detectable properties such as Renilla or firefly luciferase resulting in a colour change that can be spectroscopically monitored. The signal from the reporter gene is then used as an indirect determinant for the translation of endogenous proteins driven from the same promoter. Proteomics can also be used to provide insights into the changes in levels of protein expression once BPL forms a complex with DNA.

While *Sa*BPL has been proposed to regulate *bioY* and *bioO* transcription, no *in vivo* evidence has been presented to confirm this. With the use of microarray and subsequent validation techniques, not only can the regulation of *bioO* and *bioY* expression by BPL be confirmed, but other possible DNA targets of BPL transcriptional regulation can also be identified. By comparing mRNA levels from *S. aureus* with wild-type BPL and a transcriptional repressor deficient BPL in a microarray analysis, differences in gene expression due to the loss of transcriptional repression ability can be identified. Chromatin immunoprecipitation-PCR and quantitative real time PCR can then confirm the microarray results by identifying direct targets and the extent of transcriptional regulation by BPL, providing further understanding of gene regulation by this enzyme. Recent advances in

sequencing technologies also allow us to analyze entire transcriptomes within a population of cells via deep sequencing (57).

8.3 Conclusions

It is clear that there is an urgent need to replenish the antibiotic discovery pipeline as fast evolving bacteria are constantly becoming resistant to existing drugs. A detailed understanding of the target enzyme and function is essential for advancements in research and discovery of new medicines. This study provided new insights into *Sa*BPL and the first evidence that high-affinity and pathogen-specific bidentate BPL inhibitors can be identified. We envisage that these enabling technologies will allow the chemical optimization of a new class of antibiotics against the superbug *Staphylococcus aureus*.

8.4   References

1. Purushothaman, S., Gupta, G., Srivastava, R., Ramu, V. G., and Surolia, A. (2008) *PLoS One* **3**, e2320

2. Tron, C. M., McNae, I. W., Nutley, M., Clarke1, D. J., Cooper, A., Walkinshaw, M. D., Baxter, R. L., and Campopiano, D. J. (2009) *Journal of Molecular Biology* **387**, 129-146

3. Bagautdinov, B., Kuroishi, C., Sugahara, M., and Kunishima, N. (2005) *Journal of Molecular Biology* **353**, 322-333

4. Daniels, K. G., and Beckett, D. (2010) *Biochemistry* **49**, 5358-5365

5. Wood, Z. A., Weaver, L. H., Brown, P. H., Beckett, D., and Matthews, B. W. (2006) *Journal of Molecular Biology* **357**, 509-523

6. Polyak, S. W., Chapman-Smith, A., Brautigan, P. J., and Wallace, J. C. (1999) *Journal of Biological Chemistry* **274**, 32847-32854

7. Ingaramo, M., and Beckett, D. (2009) *Journal of Biological Chemistry* **284**, 30862-30870

8. Kwon, K., Streaker, E. D., Ruparelia, S., and Beckett, D. (2000) *Journal of Molecular Biology* **304**, 821-833

9. Zhao, H., and Beckett, D. (2008) *Journal of Molecular Biology* **380**, 223-236

10. Dams, T., Auerbach, G., Bader, G., Jacob, U., Ploom, T., Huber, R., and Jaenicke, R. (2000) *Journal of Molecular Biology* **297**, 659-672

11. Rodionov, D. A., Mironov, A. A., and Gelfand, M. S. (2002) *Genome Research* **12**, 1507-1516

12. Napier, B. A., Meyer, L., Bina, J. E., Miller, M. A., Sjostedt, A., and Weiss, D. S. (2012) *Proceedings of the National Academy of Sciences* **109**, 18084-18089

13. Woong Park, S., Klotzsche, M., Wilson, D. J., Boshoff, H. I., Eoh, H., Manjunatha, U., Blumenthal, A., Rhee, K., Barry, C. E., 3rd, Aldrich, C. C., Ehrt, S., and Schnappinger, D. (2011) *PLoS Pathogens* **7**, e1002264

14. Eisenstein, E., and Beckett, D. (1999) *Biochemistry* **38**, 9649-9656

15. Kwon, K., and Beckett, D. (2000) *Protein Science* **9**, 1530-1539

16. Soares da Costa, T. P., Tieu, W., Yap, M. Y., Pendini, N. R., Polyak, S. W., Sejer Pedersen, D., Morona, R., Turnidge, J. D., Wallace, J. C., Wilce, M. C., Booker, G. W., and Abell, A. D. (2012) *Journal of Biological Chemistry* **287**, 17823-17832

17. Xu, Y., and Beckett, D. (1994) *Biochemistry* **33**, 7354-7360

18.   Zhao, H., Naganathan, S., and Beckett, D. (2009) *Journal of Molecular Biology* **389**, 336-348

19.   Mamonova, T. B., Glyakina, A. V., Kurnikova, M. G., and Galzitskaya, O. V. (2010) *Journal of Bioinformatics and Computational Biology* **8**, 377-394

20.   Purushothaman, S., Annamalai, K., Tyagi, A. K., and Surolia, A. (2011) *PLoS One* **6**, e16850

21.   Choi-Rhee, E., Schulman, H., and Cronan Jr, J. E. (2004) *Protein Science* **13**, 3043-3050

22.   Griffin, M. D., Dobson, R. C., Gerrard, J. A., and Perugini, M. A. (2010) *Archives of Biochemistry and Biophysics* **494**, 58-63

23.   Pearce, F. G., Dobson, R. C., Jameson, G. B., Perugini, M. A., and Gerrard, J. A. (2011) *Biochimica et Biophysica Acta* **1814**, 1900-1909

24.   Lee, C. K., Cheong, C., and Jeon, Y. H. (2010) *FEBS Letters* **584**, 675-680

25.   Mayende, L., Swift, R. D., Bailey, L. M., Soares da Costa, T. P., Wallace, J. C., Booker, G. W., and Polyak, S. W. (2012) *Journal of Molecular Medicine* **90**, 81-88

26.   Parsons, J. B., and Rock, C. O. (2011) *Current Opinion in Microbiology* **14**, 544-549

27.   Raetz, C. R., Reynolds, C. M., Trent, M. S., and Bishop, R. E. (2007) *Annual Review of Biochemistry* **76**, 295-329

28.   Brinster, S., Lamberet, G., Staels, B., Trieu-Cuot, P., Gruss, A., and Poyart, C. (2009) *Nature* **458**, 83-86

29.   Balemans, W., Lounis, N., Gilissen, R., Guillemont, J., Simmen, K., Andries, K., and Koul, A. (2010) *Nature* **463**, E3

30.   Brinster, S., Lamberet, G., Staels, B., Trieu-Cuot, P., Gruss, A., and Poyart, C. (2010) *Nature* **463**, E4

31.   Parsons, J. B., Frank, M. W., Subramanian, C., Saenkham, P., and Rock, C. O. (2011) *Proceedings of the National Academy of Sciences* **108**, 15378-15383

32.   Payne, D. J., Miller, W. H., Berry, V., Brosky, J., Burgess, W. J., Chen, E., DeWolf Jr, W. E., Jr., Fosberry, A. P., Greenwood, R., Head, M. S., Heerding, D. A., Janson, C. A., Jaworski, D. D., Keller, P. M., Manley, P. J., Moore, T. D., Newlander, K. A., Pearson, S., Polizzi, B. J., Qiu, X., Rittenhouse, S. F., Slater-Radosti, C., Salyers, K. L., Seefeld, M. A., Smyth, M. G., Takata, D. T., Uzinskas, I. N., Vaidya, K., Wallis, N. G., Winram, S. B., Yuan, C. C., and Huffman, W. F. (2002) *Antimicrobial Agents and Chemotherapy* **46**, 3118-3124

183

33. Miller, W. H., Seefeld, M. A., Newlander, K. A., Uzinskas, I. N., Burgess, W. J., Heerding, D. A., Yuan, C. C., Head, M. S., Payne, D. J., Rittenhouse, S. F., Moore, T. D., Pearson, S. C., Berry, V., DeWolf, W. E., Jr., Keller, P. M., Polizzi, B. J., Qiu, X., Janson, C. A., and Huffman, W. F. (2002) *Journal of Medicinal Chemistry* **45**, 3246-3256

34. Wang, J., Soisson, S. M., Young, K., Shoop, W., Kodali, S., Galgoci, A., Painter, R., Parthasarathy, G., Tang, Y. S., Cummings, R., Ha, S., Dorso, K., Motyl, M., Jayasuriya, H., Ondeyka, J., Herath, K., Zhang, C., Hernandez, L., Allocco, J., Basilio, Á., Tormo, J. R., Genilloud, O., Vicente, F., Pelaez, F., Colwell, L., Lee, S. H., Michael, B., Felcetto, T., Gill, C., Silver, L. L., Hermes, J. D., Bartizal, K., Barrett, J., Schmatz, D., Becker, J. W., Cully, D., and Singh, S. B. (2006) *Nature* **441**, 358-361

35. Wang, J., Kodali, S., Lee, S. H., Galgoci, A., Painter, R., Dorso, K., Racine, F., Motyl, M., Hernandez, L., Tinney, E., Colletti, S. L., Herath, K., Cummings, R., Salazar, O., Gonzalez, I., Basilio, A., Vicente, F., Genilloud, O., Pelaez, F., Jayasuriya, H., Young, K., Cully, D. F., and Singh, S. B. (2007) *Proceedings of the National Academy of Sciences* **104**, 7612-7616

36. Miller, J. R., Dunham, S., Mochalkin, I., Banotai, C., Bowman, M., Buist, S., Dunkle, B., Hanna, D., Harwood, H. J., Huband, M. D., Karnovsky, A., Kuhn, M., Limberakis, C., Liu, J. Y., Mehrens, S., Mueller, W. T., Narasimhan, L., Ogden, A., Ohren, J., Prasad, J. V. N. V., Shelly, J. A., Skerlos, L., Sulavik, M., Thomas, V. H., VanderRoest, S., Wang, L., Wang, Z., , Whitton, A., Zhu, T. , and Stover, C. K. (2009) *Proceedings of the National Academy of Sciences* **106**, 1737– 1742

37. Soares da Costa, T. P., Tieu, W., Yap, M. Y., Zvarec, O., Bell, J. M., Turnidge, J. D., Wallace, J. C., Booker, G. W., Wilce, M. C. J., Abell, A. D., and Polyak, S. W. (2012) *ACS Medicinal Chemistry Letters* **3**, 509-514

38. Slavoff, S. A., Chen, I., Choi, Y. A., and Ting, A. Y. (2008) *Journal of American Chemical Society* **130**, 1160-1162

39. Duckworth, B. P., Geders, T. W., Tiwari, D., Boshoff, H. I., Sibbald, P. A., Barry, C. E., 3rd, Schnappinger, D., Finzel, B. C., and Aldrich, C. C. (2011) *Chemistry & Biology* **18**, 1432-1441

40. Agnew, H. D., Rohde, R. D., Millward, S. W., Nag, A., Yeo, W.-S., Hein, J. E., Pitram, S. M., Tariq, A. A., Burns, V. M., Krom, R. J., Fokin, V. V., Sharpless, K.

B., and Heath, J. R. (2009) *Angewandte Chemie International Edition* **48**, 4944-4948

41.   Millward, S. W., Henning, R. K., Kwong, G. A., Pitram, S., Agnew, H. D., Deyle, K. M., Nag, A., Hein, J., Lee, S. S., Lim, J., Pfeilsticker, J. A., Sharpless, K. B., and Heath, J. R. (2011) *Journal of American Chemical Society* **133**, 18280-18288

42.   Diaz, L., Casas, J., Bujons, J., Llebaria, A., and Delgado, A. (2011) *Journal of Medicinal Chemistry* **54**, 2069-2079

43.   Grimster, N. P., Stump, B., Fotsing, J. R., Weide, T., Talley, T. T., Yamauchi, J. G., Nemecz, Á., Kim, C., Ho, K.-Y., Sharpless, K. B., Taylor, P., and Fokin, V. V. (2012) *Journal of the American Chemical Society* **134**, 6732-6740

44.   Yamauchi, J. G., Gomez, K., Grimster, N., Dufouil, M., Nemecz, A., Fotsing, J. R., Ho, K. Y., Talley, T. T., Sharpless, K. B., Fokin, V. V., and Taylor, P. (2012) *Molecular Pharmacology* **82**, 687-699

45.   Gottlieb, A., Frenkel-Morgenstern, M., Safro, M., and Horn, D. (2011) *PLoS One* **6**, e20361

46.   Bottcher, C., Dennis, E. G., Booker, G. W., Polyak, S. W., Boss, P. K., and Davies, C. (2012) *PLoS One* **7**, e37632

47.   Cusack, S., Yaremchuk, A., and Tukalo, M. (1996) *Embo Journal* **15**, 6321-6334

48.   Irwin, J. J., Raushel, F. M., and Shoichet, B. K. (2005) *Biochemistry* **44**, 12316-12328

49.   Abdel-Hamid, A. M., and Cronan, J. E. (2007) *Chemistry & Biology* **14**, 1215-1220

50.   Rodionov, D. A., Hebbeln, P., Eudes, A., ter Beek, J., Rodionova, I. A., Erkens, G. B., Slotboom, D. J., Gelfand, M. S., Osterman, A. L., Hanson, A. D., and Eitinger, T. (2009) *Journal of Bacteriology* **191**, 42-51

51.   Berntsson, R. P., ter Beek, J., Majsnerowska, M., Duurkens, R. H., Puri, P., Poolman, B., and Slotboom, D. J. (2012) *Proceedings of the National Academy of Sciences* **109**, 13990-13995

52.   Prakash, O., and Eisenberg, M. A. (1974) *Journal of Bacteriology* **120**, 785-791

53.   Walker, J. R., and Altman, E. (2005) *Applied and Environmental Microbiology* **71**, 1850-1855

54.   Zempleni, J. (2005) *Annual Review of Nutrition* **25**, 175-196

55.   Beckett, D. (2007) *Annual Review of Genetics* **41**, 443-464

56.   Chakravartty, V., and Cronan, J. E. (2012) *Journal of Bacteriology* **194**, 1113-1126

57.   Wang, Z., Gerstein, M., and Snyder, M. (2009) *Nature Review Genetics* **10**, 57-63